Universidad
de Navarra

Departamento de Tecnología y Química Farmacéuticas
Facultad de Farmacia y Nutrición

Design, synthesis and biological evaluation of novel methylselenoesters as antiproliferative and cytotoxic agents

Nuria Díaz Argelich

Pamplona, 2018

Universidad
de Navarra

Departamento de Tecnología y Química Farmacéuticas
Facultad de Farmacia y Nutrición

Design, synthesis and biological evaluation of novel methylselenoesters as antiproliferative and cytotoxic agents

Memoria presentada por Dña. Nuria Díaz Argelich para aspirar al grado de Doctor por la Universidad de Navarra.

El presente trabajo ha sido realizado bajo nuestra dirección en el Departamento de Tecnología y Química Farmacéuticas y autorizamos su presentación ante el tribunal que lo ha de juzgar.

Pamplona, diciembre de 2018

Dra. Carmen Sanmartín Grijalba Dr. Juan Antonio Palop Cubillo

FUNDING

The research leading to these results has received funding from Plan de Investigación de la Universidad de Navarra, PIUNA (Ref 2014-26), “la Caixa” and “CAN” Foundations, The Swedish Cancer Society (Cancerfonden), Åke Wibergs stiftelse, Stockholm Cancer Society and Marianne and Marcus Wallenbergs foundation.

The Ph. D candidate received a grant from La Caixa Banking Foundation and the Asociación de Amigos de la Universidad de Navarra.

AGRADECIMIENTOS/ACKNOWLEDGEMENTS

Esta tesis no hubiera sido posible sin la participación y el apoyo de muchas personas.

Agradezco a la Universidad de Navarra, particularmente a la Facultad de Farmacia y Nutrición, la excelente formación recibida durante la carrera, el máster y la etapa doctoral. A la Asociación de Amigos de la Universidad de Navarra y a la “Obra Social La Caixa”, les agradezco la confianza depositada en mí y el apoyo económico, sin el cual este doctorado no hubiera sido posible.

A mis directores de tesis, la Dra. Carmen Sanmartín y el Dr. Juan Antonio Palop, por la oportunidad que me dieron de realizar el doctorado bajo su supervisión. Gracias por vuestra ayuda, dedicación y apoyo durante estos años de formación científica.

Al Dr. Ignacio Encío, por aceptarme en su laboratorio en la Universidad Pública de Navarra para la realización de los ensayos biológicos, por el tiempo dedicado a la interpretación de resultados, y en la supervisión del artículo.

Gracias a todos los que forman o han formado parte del Departamento de Química Orgánica: profesores, doctorandos y personal de apoyo, por estar siempre dispuestos a echar una mano. Gracias especialmente a la Dra. Elena González-Peñas, la Dra. Elena Lizarraga, Ángel Irigoyen y al Dr. Ángel Zamarreño (Biología Ambiental), por su ayuda con los masas y HRMS. Gracias al Dr. Daniel Plano y la Dra. María Font. Gracias a los pestuncios y demás doctorandos por los buenos momentos en el laboratorio. A Ronces, por estar siempre disponible para cualquier duda en el laboratorio. Gracias a Carmen Elizalde, Gorka y Iulen por los análisis y resonancias.

Thanks to Dr. Aristi Fernandes for the chance to do my research stay at Karolinska Institutet. Thank you for all your help and dedication, the time you spent to discuss and plan experiments and for the opportunity to participate in other projects. Thanks to Prajakta Khalkar, without your help many experiments could not have been done. Thanks for all the good and stressing moments we spent at the lab and outside. Thanks to all the Division of Biochemistry at MBB, specially to Yurika, Lucia and Renato for making my stay at KI such a great time.

Gracias a todos mis amigos, por animarme en los momentos duros y alegraros conmigo en los momentos buenos, en Pamplona o repartidos por el resto de España.

Gracias a mis padres y abuelos, que habéis confiado siempre en mí, me habéis apoyado y animado en todo momento, que os habéis involucrado en esta tesis como si fuera vuestra. Gracias Jacobo, Pilar, Inés, Javi, Miriam y Sofía, que habéis vivido esta tesis conmigo. Gracias Leticia y Alberto, por vuestro apoyo.

Gracias, Gon, por haber estado a mi lado en cada momento de esta tesis. Sin tu ayuda, apoyo, ánimos y comprensión, probablemente esta tesis no hubiera salido adelante.

INDEX

FUNDING ... v
AGRADECIMIENTOS/ACKNOWLEDGEMENTS ... vii
INDEX ... ix
ABBREVIATIONS ... x
INTRODUCTION ... 1
  1. CANCER ... 3
    1.1 Epidemiology ... 3
    1.2 Biochemical and molecular features of cancer ... 5
      1.2.1 Hallmarks of Cancer and their Relationship to the Tumor Microenvironment ... 6
      1.2.2 Types of Cell Death ... 10
      1.2.3 Importance of Adhesion Molecules in Tumor Progression ... 15
    1.3 Current treatments ... 19
      1.3.1 Surgery ... 19
      1.3.2 Radiotherapy ... 19
      1.3.3 Chemoterapy ... 19
      1.3.4 Immunotherapy ... 20
      1.3.5 Other Treatments ... 20
  2. SELENIUM ... 22
    2.1 Role of Selenium in health and disease ... 22
    2.2 Selenium and cancer ... 25
      2.2.1 Role of Selenoproteins in Cancer ... 28
BACKGROUND ... 29
  1. Selenium compounds and mechanism of action in cancer ... 31
    1.1 Methylselenol ... 32
  2. Background of the research group ... 35
HYPOTHESIS AND AIMS ... 37
RESULTS ... 43
  PAPER 1 ... 47
  PAPER 2 ... 89
  PAPER 3 ... 113
  PAPER 4 ... 129
DISCUSSION ... 145
CONCLUSIONS ... 157
REFERENCES ... 161
APPENDIX ... 177
  SYNTHESIZED COMPOUNDS ... 179

ABBREVIATIONS

AKT/PKB	protein kinase B
AML	acute myeloid leukemia
Ang-2	angiopoietin-2
APAF1	apoptotic protease activating factor 1
ATG	autophagic related proteins
ATP	adenosine triphosphate
Bcl-2	B-cell lymphoma 2 gene
Bid	BH-3 interacting-domain death agonist
c-FLIP	cellular FLICE-inhibitory protein
CAFs	cancer-associated fibroblasts
CatB	cathepsin B
CatD	cathepsin D
CDC42	Cell division control protein 42 homolog
CDK	cyclin-dependent kinases
CDKi	CDK inhibitor
CD29	β1-integrin
CICs	cell-in-cell structures
CIP/KIP	CDK interacting protein/Kinase inhibitory protein
COX	cyclooxygenase
DAB2	disabled homolog 2
DISC	death-inducing signaling complex
DIO	iodothyronine deiodinase
DMeT	demethyl transferases
DNA	deoxyribonucleic acid
E-cadherin	epithelial cadherin
ECM	extracellular matrix
EGFR	epidermal growth factor receptor
EMT	epithelial to mesenchymal transition
ER	endoplasmic reticulum
ERK	extracellular signal-regulated kinase
FADD	Fas-associated death domain
FAK	focal adhesion kinase
FGF	fibroblast growth factor
FGFR	fibroblast growth factor receptor
FIP200	focal adhesion kinase family integrating protein of 200 kDa
GCN5	general control nonrepressed protein 5
GPx	glutathione peroxidase
GTP	guanosine triphosphate
HDAC	histone deacetylases
HIF-1α	hypoxia-inducible factor 1-alpha
HIP1	huntingtin interacting protein
IARC	International Agency for Research on Cancer
IG-CAMs	immunoglobulin cell adhesion molecules
iNOS	inducible nitric oxide synthase
IL	interleukin
JNK	c-jun N-terminal kinases

KLF4	Krüppel-like factor 4
LC3	microtubule-associated protein 1 light chain 3
MAPK	mitogen-activated protein kinase
Mcl-1	myeloid cell leukemia 1
MCP-1	monocyte chemoattractant protein 1
MET	mesenchymal to epithelial transition
Met	methioninase
MeT	methyltransferases
MMP	metalloproteinase
MOMP	mitochondrial outermembrane permeabilization
MSA	methylseleninic acid
MSC	methylselenocysteine
mTOR	mechanistic target of rapamycin
NADH	nicotinamide adenine dinucleotide
NADPH	nicotinamide adenine dinucleotide phosphate
N-cadherin	neural cadherin
NPC	Nutritional Prevention of Cancer Trial
Nrf2	nuclear factor erythroid 2–related factor 2
PanIN	pancreatic intraepithelial neoplasia
PARP	DNA damage-responsive enzymes poly(ADP-ribose) polymerases (PARPs)
PDAC	Pancreatic ductal adenocarcinoma
PDGF	platelet-derived growth factor
PDGFR	platelet-derived growth factor receptor
PDL1	Programmed death-ligand 1
PI3K	phosphoinositide 3-kinase
PTEN	phosphatase and tensin homolog
RB	retinoblastoma
RIP1/RIP3	receptor-interacting protein 1 or 3
RNA	ribonucleic acid
ROCKI/II	Rho-kinase I and II
ROS	reactive oxygen species
SDC1	syndecan 1
Se	selenium
SeCys	selenocysteine
Sel	**s**elenoproteins
SELECT	Selenium and Vitamin E Cancer Prevention Trial
SMAC	second mitochondria-derived activator of caspases
SPS2	selenophosphate synthetase
TCA	tricarboxylic acid cycle (Krebbs cycle)
TERT	telomerase subunit reverse transcriptase
TGF-ß	transforming growth factor beta
TNF	tumor necrosis factor
TP53	tumor protein p53
ULK	unc-51 like autophagy activating kinase
VEGF	vascular endothelial growth factor

VEGFR	vascular endothelial growth factor receptor
VPS	vacuolar protein sorting-associated protein
WHO	World Health Organization
xCT	cystine/glutamate antiporter system
XIAP	X-linked inhibitor of apoptosis protein

INTRODUCTION

1. CANCER

1.1 EPIDEMIOLOGY

Cancer constitutes one of the leading causes of human morbidity and mortality worldwide. There are different regional patterns regarding incidence, mortality and tumor-type characteristics; thus, understanding cancer epidemiology is a crucial factor to improve and develop cancer control.

According to GLOBOCAN 2018, the most common cancers worldwide regarding incidence are lung (11.6%), breast (11.6%), colorectal (10.2%), prostate (7.1%) and stomach (5.7%) cancer. Trends in tumor type, however, vary among women and men and are shown in **Figure 1**.[1]

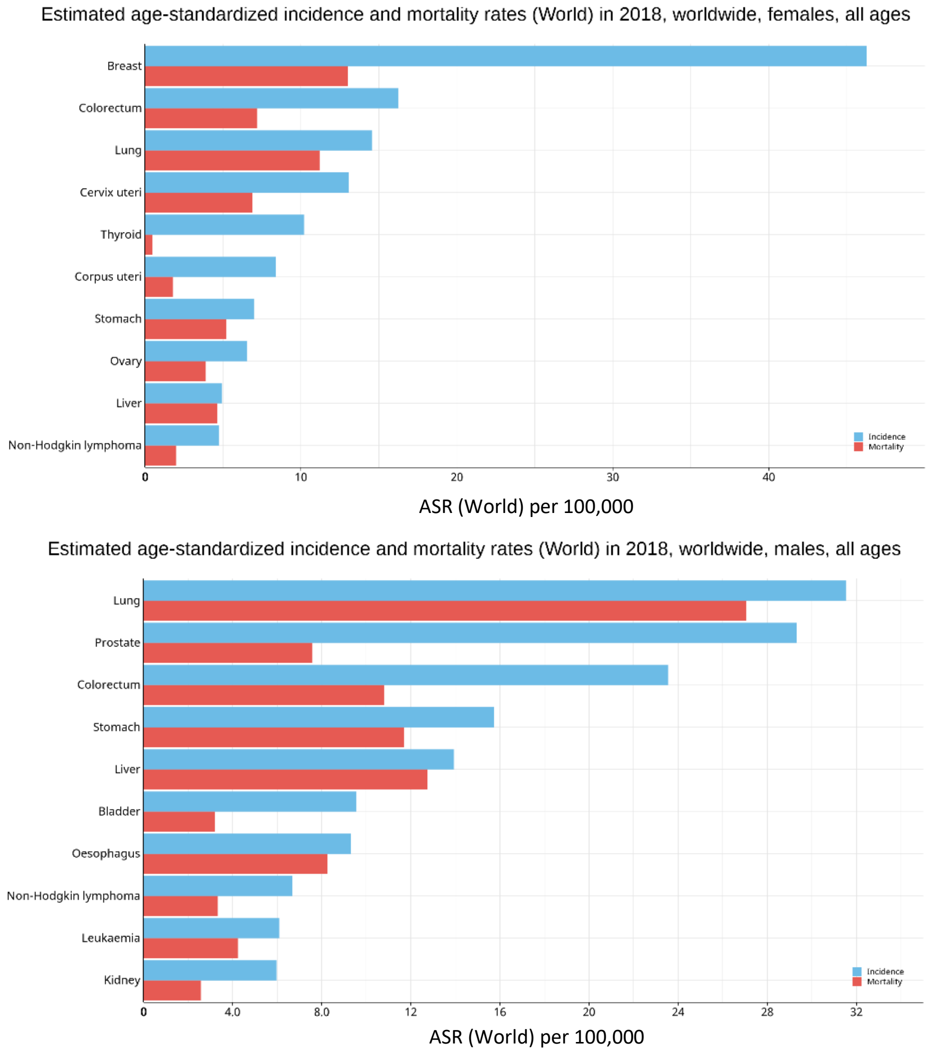

Figure 1. Incidence and mortality of the most common cancers worldwide. ASR (W) indicates age-standardized rate (per 100,000). From GLOBOCAN 2018. Global Cancer Observatory. International Agency for Research on Cancer. (IARC).

Geographically, Asia comprises almost half of the overall cancer incidence. Nearly 24% of cancer incidence belongs to Europe, and the remainder is divided between America (21%) and Africa (5.8%), Oceania representing only

1.4%. Regarding mortality, the economic development plays a key role in the disease outcome, as a decreased number of cases is found in more economically developed regions. Around 70% of cancer deaths occur in middle and low-income countries from Africa, Asia and Central and South America, mainly due to late or inaccessible diagnosis or unavailable treatments (**Figure 2**).[2]

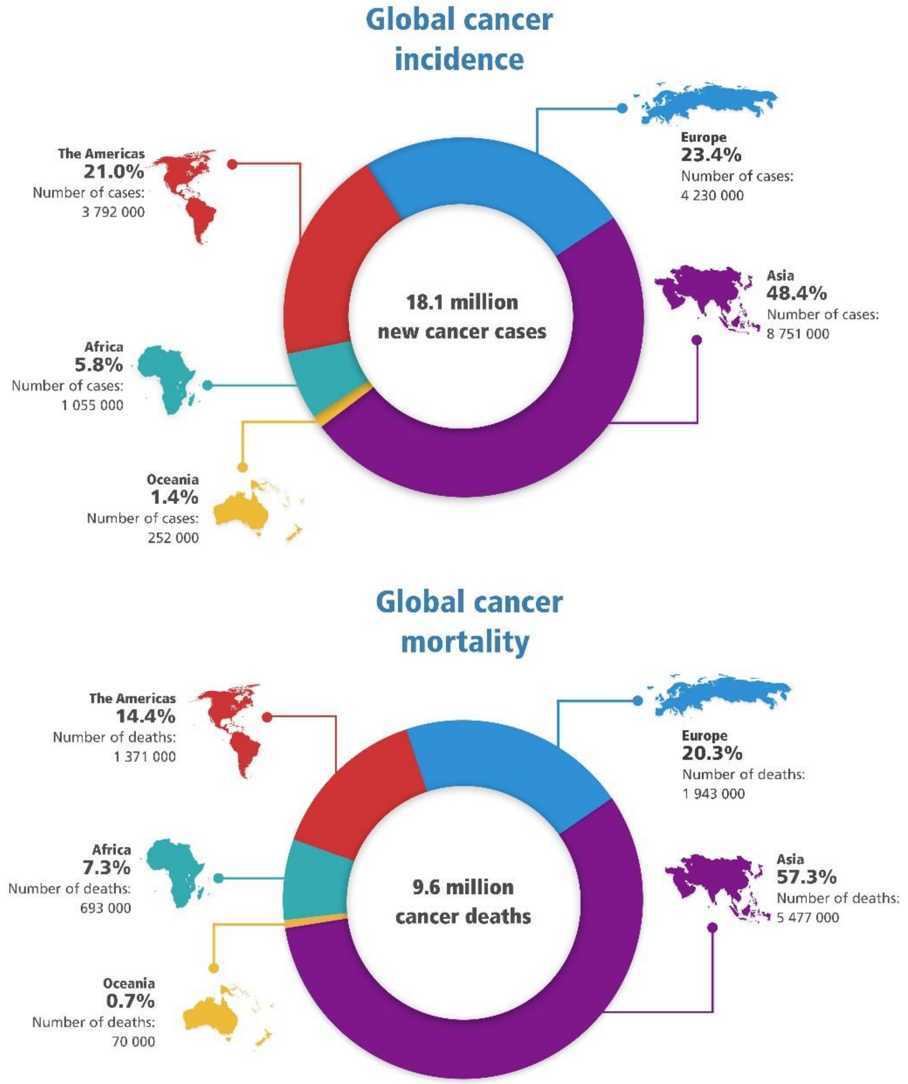

Figure 2. Estimated global cancer incidence and mortality in 2018, represented by major regions, in both sexes combined. From GLOBOCAN 2018.[2]

In 2018, 9.6 million deaths are estimated to be caused by cancer. This represents nearly 1 in 6 of all global deaths, a fact that turns cancer into the second leading cause of death worldwide. Moreover, cancer incidence is expected to grow by 70% in the next two decades.[3]

In Spain, according to REDECAN data, there were 247,771 new cancer cases in 2015. Among them, the most common diagnosed cancers were colorectal

(41,441 cases), prostate (33,370 cases), lung (28,347 cases), breast (27,747 cases) and bladder cancer (21,093 cases).

According to the Spanish Statistical Office, 27.5% of deaths in 2016 were tumor-related, accounting for 112,939 cases. The last report from the National Epidemiology Centre (Institute of Health Carlos III) claimed cancer as the first cause of death in men in our country in 2016, followed by cardiovascular and respiratory diseases. In women, on the other hand, cardiovascular diseases remain the first cause of death whereas cancer takes up the second place.[4]

According to the World Health Organization (WHO), between 30 and 50% of cancer deaths could be prevented by developing healthy lifestyles: avoiding tobacco, overweight and physical inactivity, reducing alcohol consumption and vaccinating against cancer-related infectious agents (i.e. human papilloma, hepatitis B and C viruses or *Helicobacter pylori*).[3]

Nevertheless, the left-over cases remain a burden for health systems. Actual treatments are not entirely satisfactory, mainly due to drug resistance and adverse effects, therefore making the search for new treatments an urgent need.

1.2 BIOCHEMICAL AND MOLECULAR FEATURES OF CANCER

The generic term *cancer* encompasses a multitude of diseases, whose underlying characteristic is the accumulation of aberrant mutations in both protooncogenes and tumor suppressor genes that lead to uncontrolled growth of abnormal cells.

Cancer is the result of the interaction of human genetic factors with three possible causing agents: physical (ultraviolet and ionizing radiation), chemical (such as asbestos, components of tobacco smoke…) or biological agents (certain viruses, bacteria or parasites).

All cancer cells acquire a series of determined traits. Hanahan *et al.*[5] have recently revisited the hallmarks of cancer cells they compiled in 2000, adding some emerging features (**Figure 3**). Moreover, cancer research is changing from a tumor cell-centered view to a more holistic approach. Research in the last years has pinpointed the complexity of tumor biology, which not only involves cancer cells but the stroma: the extracellular matrix and "normal" recruited cells.[6] Not only cancer cells, but the active role of the tumor microenvironment determine the therapeutic outcome.[7]

This microenvironment co-evolves with cancer cells to an activated state that promotes cancer progression, facilitating the acquisition of cancer hallmarks, fostering the tumorigenic process and drug resistance. Inflammation and genome instability promote the achievement of these traits.

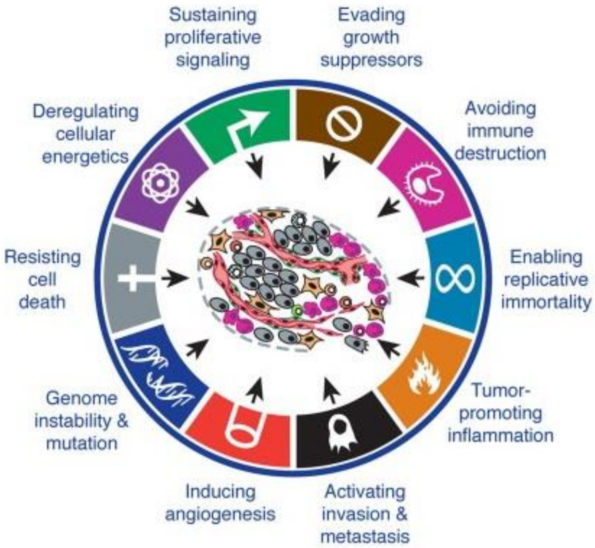
Sustaining proliferative signaling
Evading growth suppressors
Avoiding immune destruction
Enabling replicative immortality
Tumor-promoting inflammation
Activating invasion & metastasis
Inducing angiogenesis
Genome instability & mutation
Resisting cell death
Deregulating cellular energetics

Figure 3. Hallmarks of cancer cells. From Hanahan, D. *Cell* (2011).[5]

1.2.1 Hallmarks of Cancer and their Relationship to the Tumor Microenvironment

a. Sustained Proliferation

Proliferation signaling is mediated by mitogenic signaling within the cells and by growth factor signals, which are released by enzymes in the extracellular matrix (ECM) and pericellular space. Cancer cells can constitutively activate proliferation signaling pathways such as Raf/mitogen-activated protein kinase (Raf-MAPK) or phophoinositide-3-kinase/protein kinase B (PI3K-AKT/PKB). They can disrupt negative feedback mechanisms, as it occurs when Ras, the phosphatase and tensin homolog (PTEN) or the mechanistic target of rapamycin (mTOR) are mutated. Besides, they can produce growth factor ligands themselves or increase surface receptors to provide an increased response. Moreover, the tumor microenvironment contributes to tumor cell proliferation. Tumor cells can stimulate "normal" surrounding cells to produce growth factors. For instance, cancer-associated fibroblasts (CAFs) and pericytes release growth factors, hormones and cytokines that promote sustained proliferation.[6]

All pro-mitogenic signals converge in the executor machinery regulating the cell cycle. Normal cell division comprises four stages and progression through the cell cycle is driven by cyclin-dependent kinases (CDKs) and cyclins[8] (**Figure 4**):

G_1: In this phase, the cell is sensitive to positive or negative proliferation stimulus. The complexes cyclin D-CDK4, cyclin D-CDK6 and cyclin E-CDK2 elicit progress to the next phase. CDK4 and 6 phosphorylate the tumor suppressive retinoblastoma protein (RB), which allows a gene expression program coordinated by the E2F family of transcription factors.[9]

S: Cyclin A-CDK2 initiates this phase, controls DNA replication and further phosphorylates RB.

G_2: In this phase, the cell prepares the entry into mitosis and is driven by cyclin B-CDK2.

M: The cell divides into two daughter cells. CDK1 is the only CDK that can drive the mitosis onset.[9]

G_0 is an alternative phase in which the cell presents a reversible quiescent status and it is characteristic of most adult tissues.[9]

There are strict checkpoints between each phase that tightly regulate the cell cycle to avoid uncontrolled or mutant cell proliferation. When there are aberrant or incomplete cycles, CDK inhibitors (CDKIs) inhibit CDK activity. The Ink4 family inhibits CDK4 and CDK6 whereas CDK2 is targeted by the CDK interacting protein/Kinase inhibitory protein family (Cip/Kip), which includes p21, p27 and p57 (**Figure 4**). However, in cancer, deregulation of cell cycle leads to uncontrolled proliferation due to upregulation of CDKs and/or inactivation of CDKIs.[8]

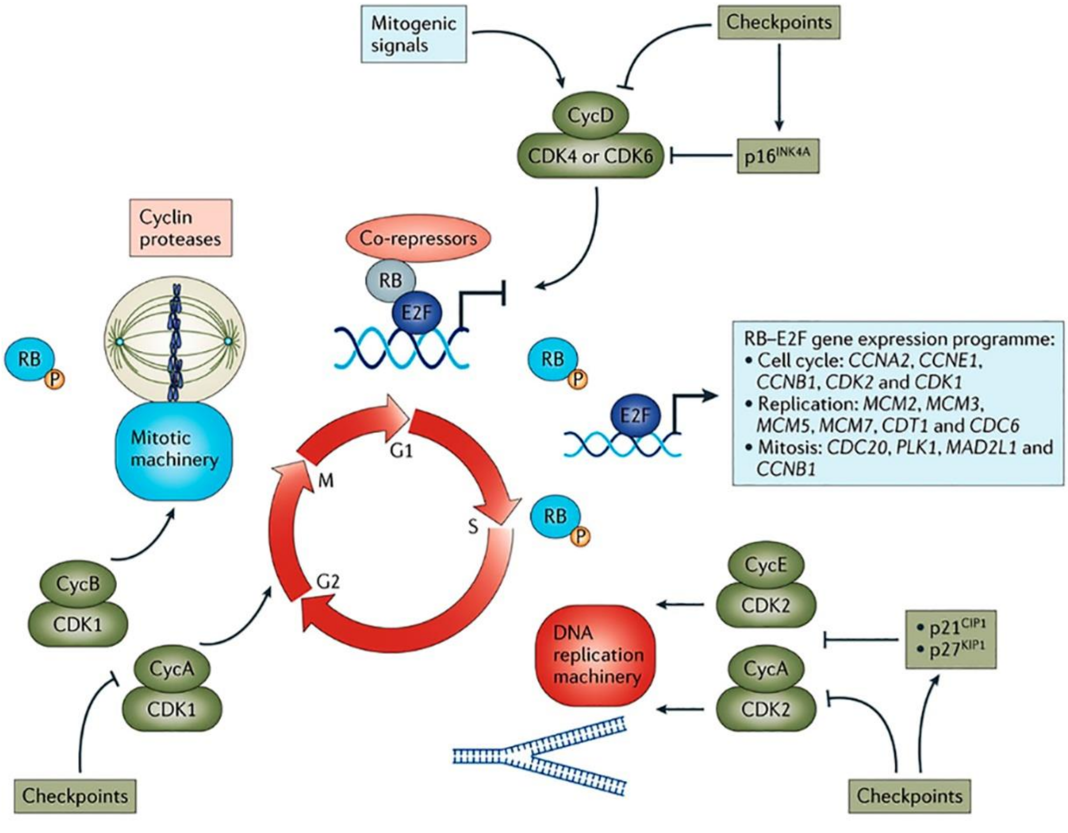
Mitogenic signals
Checkpoints
CycD
CDK4 or CDK6
p16^{INK4A}
Cyclin proteases
Co-repressors
RB
E2F
RB
P
Mitotic machinery
RB
P
E2F
RB–E2F gene expression programme:
• Cell cycle: *CCNA2, CCNE1, CCNB1, CDK2* and *CDK1*
• Replication: *MCM2, MCM3, MCM5, MCM7, CDT1* and *CDC6*
• Mitosis: *CDC20, PLK1, MAD2L1* and *CCNB1*
G1
M
S
G2
RB
P
CycB
CDK1
CycA
CDK1
CycE
CDK2
DNA replication machinery
CycA
CDK2
• p21^{CIP1}
• p27^{KIP1}
Checkpoints
Checkpoints

Nature Reviews | Drug Discovery

Figure 4. Overview of cell cycle regulation by cyclin-CDK complexes. From Asghar *et al.*, *Nat Rev Drug Discov* (2015).[9]

b. Evasion of growth suppression

Evasion of growth suppression can occur through different mechanisms. Mutations in tumor suppressor genes, like RB or the tumor protein p53 (TP53), lead to a loss of tumor-suppressor function. Besides, the loss of tumor suppressor function can be achieved by phosphorylation of RB by CDKs.[8] Mechanisms of pathway dysregulation are mutually exclusive and frequently, tumor type-specific. For example, small lung cancer is characterized by RB loss whereas glioblastoma commonly exhibits loss of p16^{INK4A}, a protein from the Ink4 CDK inhibitors family.[9]

Besides, cancer cells can manage to evade cell-cell contact inhibition or to corrupt ordinarily antiproliferative pathways. For instance, the corrupted transforming growth factor beta (TGF-ß) pathway aberrantly activates the epithelial-mesenchymal transition (EMT), promoting a metastatic phenotype.[10,11]

c. Death resistance

Cancer cells develop mechanisms to be more resistant to apoptosis, the most common type of programmed cell death (see TYPES OF CELL DEATH section). Among others, these mechanisms include loss of TP53, upregulation of antiapoptotic regulators or survival signals; and downregulation of proapoptotic proteins. Besides, other types of cell death might have a dark-side role in fostering the tumorigenic process: for instance, autophagy can promote cell survival by providing recycled nutrients or necrosis can release pro-inflammatory signals that recruit potential tumor active immune cells.[5]

Evasion of programmed cell death is as well supported by survival signals derived from the stromal compartment. In addition, CAFs and pericytes contribute to the remodeling of the ECM, which plays a crucial role in tumor progression. Tumor cell adhesion to ECM through integrins, for example, activates survival signaling pathways.[6]

d. Replicative immortality

Unlimited replication of cells is avoided through senescence (an irreversible non-proliferative but viable state) or crisis, which involves cell death. Senescence occurs when the end of the chromosomes is lost due to progressive shortening of the telomeres in each division. Cancer cells, however, manage to bypass cellular senescence and DNA damage-induced inhibitory signaling, mainly due to upregulated or reactivated telomerases.[12] These enzymes maintain the telomere length, thus permitting unlimited replication with short but stable telomeres.[13] In addition, an RNA component of telomerases, the reverse transcriptase (TERT) has other noncanonical functions related to transcriptional regulation and metabolic reprogramming, therefore contributing to tumorigenesis.[14]

e. Induced angiogenesis

In order to evolve, tumors develop tumor-associated neovasculature which supplies oxygen and nutrients to cancer cells. In contrast to the otherwise normally quiescent vasculature, an angiogenic switch fosters the formation of new vessels during tumorigenesis. The vascular endothelial growth factor and its receptor (VEGF/VEGFR), the hypoxia-inducible factor (HIF) and the fibroblast growth factor and its receptor (FGF/FGFR), among other factors, are implicated in this angiogenic switch.[15] CAFs also promote sustained angiogenesis releasing pro-angiogenic factors.[6]

However, the angiogenic pattern is dependent on the tumor type, ranging from largely avascular tumors to highly angiogenic ones.[5]

f. Invasion and metastasis activation

Cancer progression and metastasis are dependent on changes in cell adhesion properties and migration. After a multistep process transformation from the pre-cancerous lesions to the malignant phenotype, cancer cells acquire metastatic features that promote invasion into nearby tissues, cell dissemination through the bloodstream or lymphatic system, and colonization of distant organs. This process, called metastasis, is the primary cause of cancer-related death.

Changes in morphology and attachment, both to the ECM and neighbor cells, occur prior to and after the invasion. Cells undergo the EMT program, which provides them with invasion and dissemination capabilities, stem-like properties and resistance to apoptosis, a programmed cell death.[5] Moreover, some studies have highlighted the contribution of stromal cells in the process of invasion.[16]

The opposite process, called mesenchymal to epithelial transition (MET), comprises cancer cell re-differentiation and occurs when the colonization of distant organs takes place. However, recent evidence indicates that rather than a dichotomy between the epithelial and mesenchymal states, an intermediate state or partial EMT might occur in cancer biology.[17]

The activated tumor microenvironment also contributes to tumor progression in this stage. CAFs facilitate the acquisition of a malignant phenotype through ECM remodeling, providing protease activity and making ECM-adhering factors bioavailable. [6]

g. Dysregulation of Cellular Energetics

Cancer cells adjust their glucose metabolism to anaerobic glycolysis, favoring glycolysis over oxidative phosphorylation, even in the presence of oxygen. This effect is known as the Warburg effect. The low-efficiency adenosine triphosphate (ATP) production pathway is compensated with an increased glucose uptake.[18]

h. Avoidance of Immune Destruction

The concept of cancer surveillance has been long established and implicates the immune system identifying and eradicating evolving tumors. However, in the past few years, cancer surveillance was proved to be just one part of the process and the term "immunoediting" has been coined. Immunoediting is a dynamic process that includes tumor prevention as well as shaping the immunogenicity of cancer cells. This is achieved through a multi-step process including the elimination of cancer cells, the equilibrium with cancer cells and the escape of cancer cells. It is believed that tumors might arise from low immunogenic cancer cell clones which can escape from immune surveillance, while immunocompetent hosts destroy highly immunogenic cells.[5,19] However, this could be a simplified relationship between tumor and the host immune system, given that highly immunogenic cancer cell clones could also disable the immune system by secreting immunosuppressive factors.[19] Although the relationship between tumor microenvironment and host immune system is complex and still not fully understood, immunoevasion is considered a hallmark of cancer cells.[5]

1.2.2 Types of Cell Death

Achieving cancer cell death is one of the principal aims of anticancer drugs. There are several types of regulated cell death, which is characterized by programmed machinery that elicits controlled cell destruction. Some of the most common types, according to the Nomenclature Committee on Cell Death[20], are described below:

a. Apoptosis

Apoptosis was the first described class of regulated cell death. It is characterized by cytoplasmatic shrinkage, chromatin condensation, nuclear fragmentation, minimal alteration of cell organelles, cell blebbing and the formation of apoptotic bodies. Caspases are critical proteases in apoptosis and can be divided in initiator (caspases 1, 2, 4, 5, 8, 9, 10, 11 and 12) or executor caspases (caspases 3, 6, 7 and 14), depending on the cleaved substrate. Initiator caspases cleave executor caspases to activate them and the latter cleave different proteins leading to apoptosis.[21] Apoptosis can be triggered by two different pathways, depending on the nature of the apoptotic stimulus (**Figure 5**).

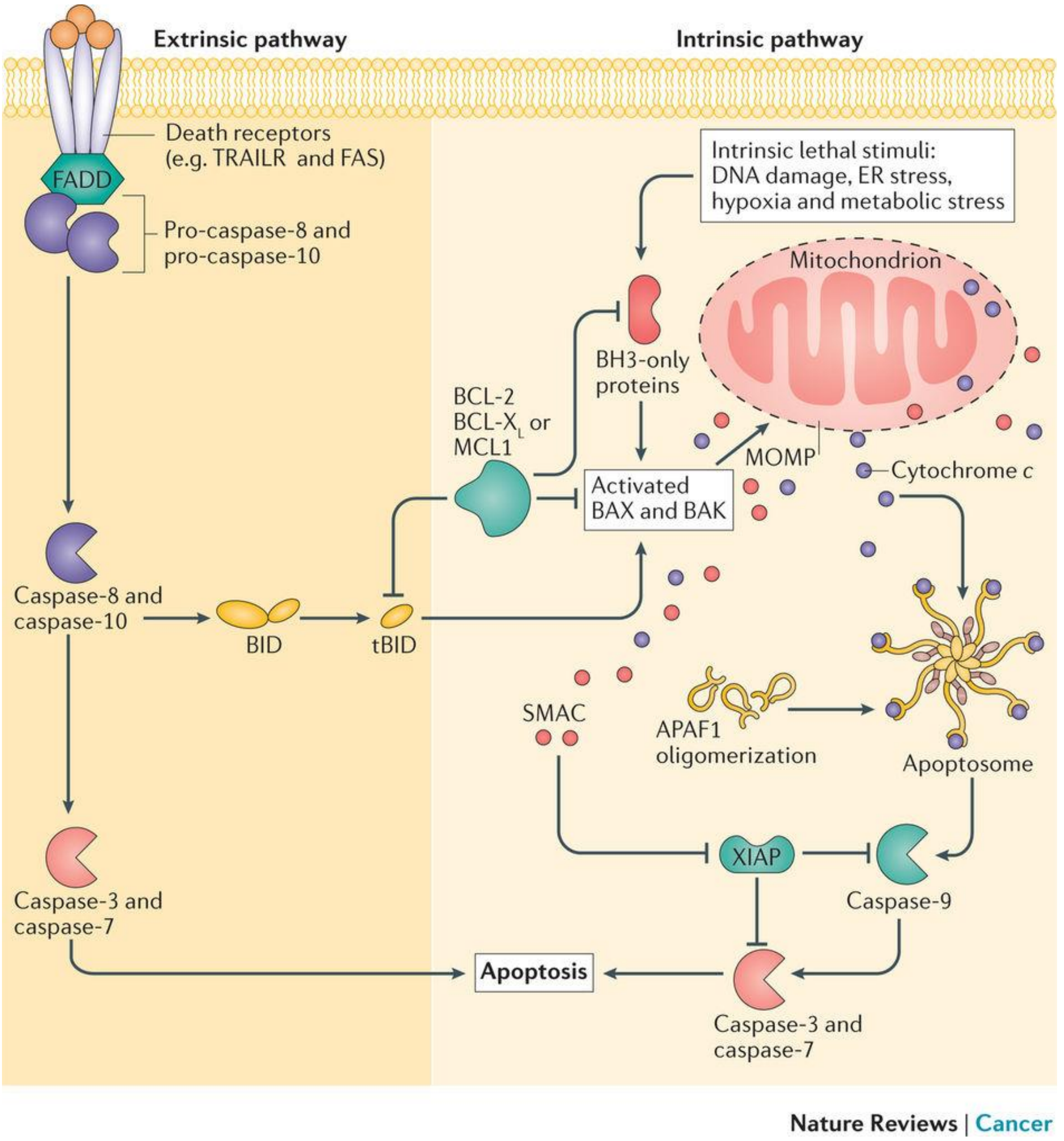
Extrinsic pathway
Intrinsic pathway
Death receptors (e.g. TRAILR and FAS)
FADD
Pro-caspase-8 and pro-caspase-10
Intrinsic lethal stimuli: DNA damage, ER stress, hypoxia and metabolic stress
Mitochondrion
BH3-only proteins
BCL-2 BCL-X$_L$ or MCL1
Activated BAX and BAK
MOMP
Cytochrome c
Caspase-8 and caspase-10
BID
tBID
SMAC
APAF1 oligomerization
Apoptosome
XIAP
Caspase-9
Caspase-3 and caspase-7
Apoptosis
Caspase-3 and caspase-7
Nature Reviews | Cancer

Figure 5. Extrinsic and intrinsic apoptotic pathways. From Ichim G., *Nat Rev Cancer* (2016).[22]

The extrinsic pathway involves an extracellular stimulus which activates death-cell receptors. Upon activation, the adaptor protein Fas-associated death domain (FADD) recruits caspase 8 and forms the death-inducing signaling complex (DISC), which in turn activates executioner caspases 3 and 7. Besides, caspase 8 can also activate the BH-3 interacting-domain death agonist (Bid), which is translocated to the mitochondria and activates the intrinsic way.[22,23]

Intrinsic apoptosis occurs in response to intracellular stimulus and involves BH3-only proteins (Bim, Bid and Bad), a series of stress sensor sentinels belonging to the B-cell lymphoma 2 (Bcl-2) family. When activated upon a stress signal, they trigger Bax or Bak aggregation. The mitochondrial death pathway is then induced.[24] After the permanent permeabilization of the outer mitochondrial membrane (MOMP), there is a release of some proteins, such as the second mitochondria-derived activator of caspases (SMAC), cytochrome c and the apoptotic protease activating factor 1 (APAF-1). The two latter form the apoptosome together with dATP and activate caspase 9, which in turn activates caspase 7 and caspase 3.[23] SMAC blocks the X-link inhibitor of apoptosis protein (XIAP) therefore contributing to apoptosis.[22]

b. Autophagy

Autophagy is a self-degradative lysosomal-dependent process where cell organelles and long-lived proteins are degraded in response to starvation stress. Autophagic death courses with massive cytoplasmatic vacuolization due to the formation of double-membraned autophagosomes within the cells and in the absence of chromatin condensation.[25,26] Both pro- and antimetastatic functions have been attributed to autophagy, depending on the tumor type and stage. Autophagy can promote tumor progression by recycling cellular structures into available nutrients but also has been reported to induce cell death. In early metastatic steps, autophagy is thought to be tumor suppressive whereas it turns into tumor promoter in advanced stages.[27] Autophagy is induced after ECM-detachment. In fact, a decrease in CD29 (ß1-integrin) is enough to induce autophagy, which promotes cell survival in this context by mediating anoikis-resistance (**Figure 6**).[28]

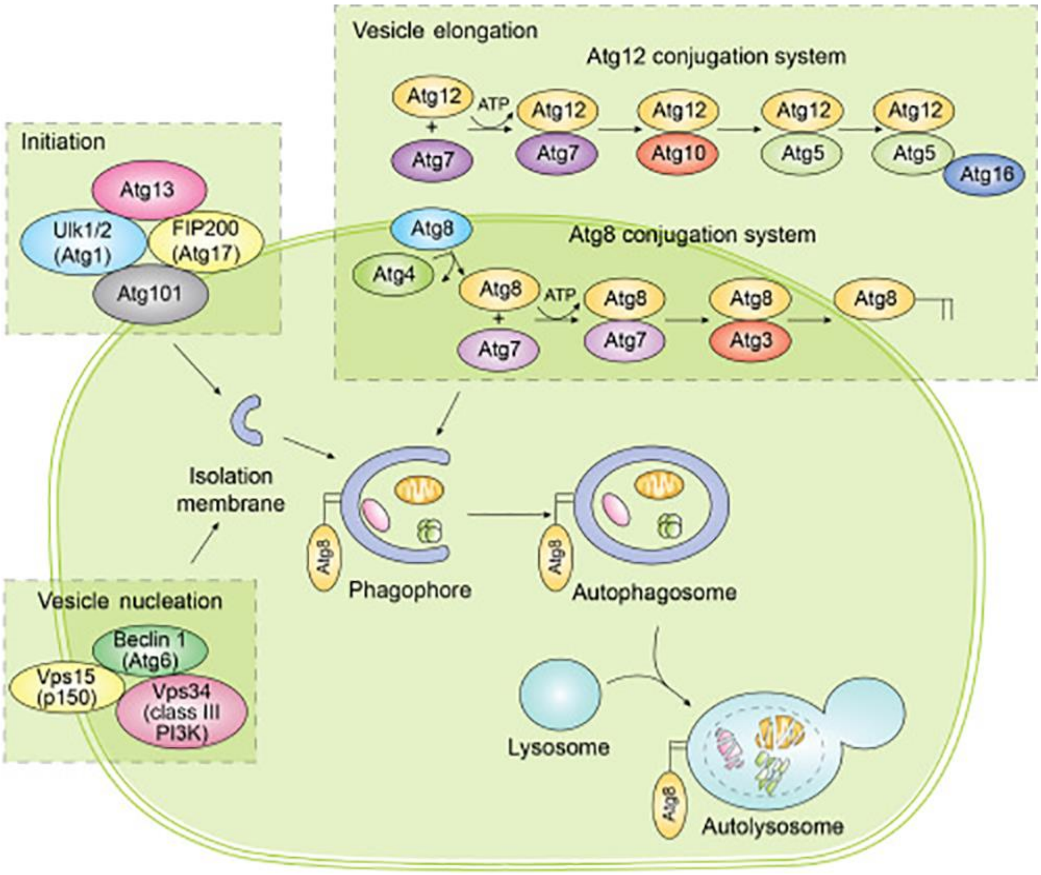
Vesicle elongation
Atg12 conjugation system
Atg12
ATP
Atg7
Atg10
Atg5
Atg16
Atg8 conjugation system
Atg8
Atg4
Atg3
Initiation
Atg13
Ulk1/2 (Atg1)
FIP200 (Atg17)
Atg101
Isolation membrane
Phagophore
Autophagosome
Vesicle nucleation
Beclin 1 (Atg6)
Vps15 (p150)
Vps34 (class III PI3K)
Lysosome
Autolysosome

Figure 6. Autophagic molecular pathways. From Anding, A., *Curr Top Dev Biol* (2015).[29]

The autophagosome is formed thanks to the coordinate action of the autophagic-related proteins (ATG) and it is targeted by lysosomes, which degrade the sequestered cargo. Specifically, in the phagophore –the isolation membrane– the UNC51-like (ULK) system (composed by ULK1 or ULK2 and ATG13, FAK family kinase interacting protein of 200 kDa (FIP200) and ATG101) is recruited to initiate the autophagosome formation. ULK targets a class III PI3K complex (consisting of beclin1, vacuolar sorting protein 15 (VPS15), VPS34 and ATG14) to produce phosphatidylinositol-3-phosphate. Finally, ATG12-ATG5-ATG16 in the autophagosome membrane facilitates the lipidation of microtubule-associated protein 1 light chain 3 (LC3) with phosphatidylethanolamine.[30]

c. *Entosis*

Entosis is a recently described phenomenon that refers to homotypic cell engulfment leading to the characteristic cell-in-cell structures (CICs) observed in tumor epithelial cells.[31] High CICs levels constitute a good prognosis feature in pancreatic cancer,[32] but not in head and neck cancer, where it is an adverse prognostic factor for survival.[33] Entosis differs from phagocytosis. Engulfed cells form epithelial adherens junctions with their neighbors through E-

cadherin and α-catenin and ultimately invade them, having an active role. The invasion is driven by controllers of cell tension Rho-GTPase, Rho-kinase I and II (ROCKI/II) and myosin.[34,35]
This internalization can result in a non-apoptotic cell death (entotic death), which is dependent on the autophagy machinery of the engulfing cell (Figure 7). Surprisingly, autophagy within internalized cells is thought to promote their survival.[34,36]

Entosis is mainly triggered by cell-ECM detachment, although it has also been described in attached cells.[37] Like many other processes, a dual-faced role has been proposed for entosis because it can also result in the release of the internalized cell, arguing for both tumor suppressive and tumor promoter roles, depending on the context. Anchorage-independent growth is a prerequisite for the metastatic process, supporting entosis as a tumor suppressor. On the other hand, entosis could be advantageous to the host cell by providing a nutrient recycling source during metabolic stress, therefore promoting tumor progression. In fact, glucose starvation has been described to induce entosis.[35]

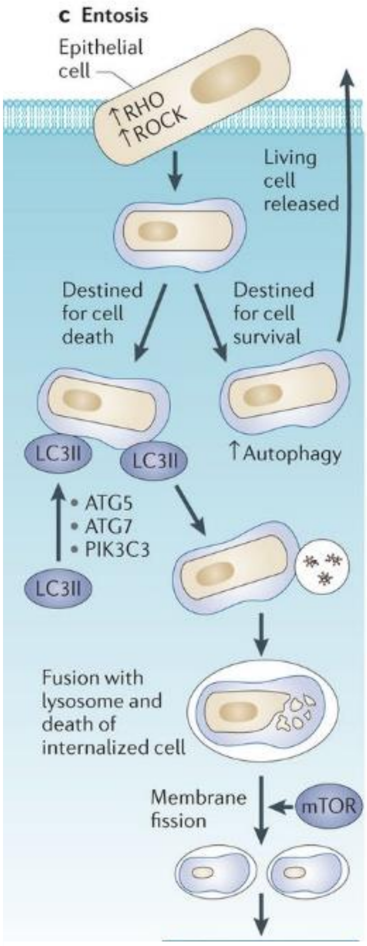
c Entosis
Epithelial cell
↑RHO
↑ROCK
Living cell released
Destined for cell death
Destined for cell survival
LC3II
LC3II
↑Autophagy
• ATG5
• ATG7
• PIK3C3
LC3II
Fusion with lysosome and death of internalized cell
Membrane fission
mTOR

Figure 7. Entosis process. Modified from Buchheit, C., *Nat Rev Cancer* (2014).

d. Mitotic catastrophe

Although previously considered a type of cell death caused by aberrant mitosis, mitotic catastrophe has been redefined recently.[20,38] It is considered a previous oncosuppressive step that triggers apoptosis, necrosis or senescence, depending on multiple proteins, to avoid genomic instability.[39]

e. Necroptosis

Necroptosis is a form of regulated necrosis triggered by ligands of death receptors in an apoptotic-deficient scenario. It courses with the activation of receptor-interacting protein 1 (RIP) 1 or RIP3.

f. Parthanatos

Parthanatos involves DNA damage-responsive enzymes poly(ADP-ribose) polymerases (PARPs). It is probably a caspase-independent regulated necrosis cell death, which plays a role in inflammation, neurodegeneration, diabetes and stroke.[20]

g. Pyroptosis

Pyroptosis encloses both apoptotic and/or necrotic morphological features and is a type of cell death mainly characterized by caspase-1 activation.[20] Although first described in macrophages presenting bacterial infection, it was later demonstrated neither to be exclusive of macrophages nor a death mechanism only caused by bacteria.[20]

1.2.3 Importance of Adhesion Molecules in Tumor Progression

Recent research is unveiling the importance of cell adhesion in regulating not only physiological cell survival and proliferation, but also crucial steps along the tumorigenic process.

Cell surface molecules not only mediate ECM or cell-cell attachment but transduce adhesive signals to downstream effectors and transcriptional programs that regulate cell behavior and tissue homeostasis. Deregulation of cell surface molecules in pathological circumstances can lead to abnormal proliferation and metastatic transformation.

1.2.3.1 Family of Adhesion Molecules

The most important families of adhesion molecules are described below:

I. Integrins

Integrins constitute the major family of cell-ECM contact mediators. These membrane proteins are α/ß heterodimers that, when activated, mechanically link the actin cytoskeleton to the ECM at the focal adhesions and transduce bidirectional signals that modulate cell behavior. There are 24 known functional integrins formed by the combination 18 α subunits and 8 ß subunits. A determined integrin can recognize one or more ECM components, such as laminin, collagen, vitronectin or fibronectin, and undergo a conformational change that leads to an activated or high avidity state.[40]

Under physiological conditions, integrins prevent anchorage-independent growth. Ligated integrins mediate signalling to different pathways, including PI3K/AKT, ERK, JNK or p38.[41,42] They can modulate the activity of several growth factors receptors, such as VEGFR, FGFR, PDGFR and EGFR, in a ligand-dependent or independent way;[40,43] increase Bcl-2 and FLIP levels or inactivate p53.[44] At the same time, integrins can transduce inside-out signals by affecting the affinity to the ligands.

Importantly, loss of cell-ECM adhesion or unligated integrins induces apoptosis, which is termed anoikis in this context (**Figure 8**). Anoikis ensures tissue homeostasis and avoids ectopic cell proliferation. In cancer progression, cells acquire a migrative phenotype allowing them to overcome detachment-induced cell death. Therefore, resistance to anoikis is emerging as a main feature of metastatic cells. Entosis and autophagy can, under certain circumstances, be mechanisms to circumvent anoikis.[45]

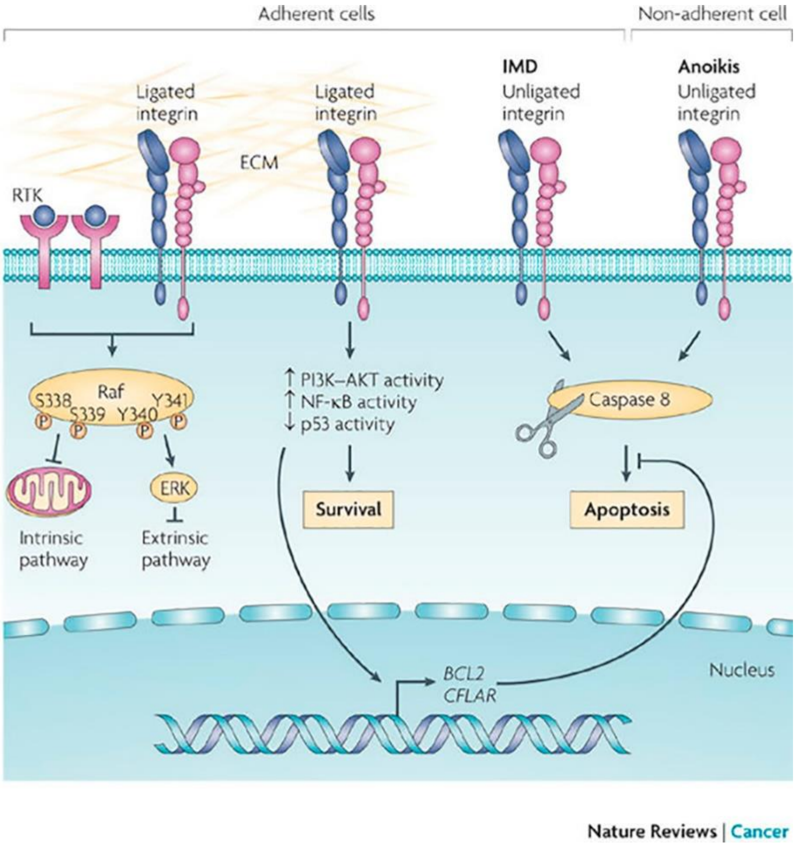
Adherent cells
Non-adherent cell
IMD
Anoikis
Ligated integrin
Ligated integrin
Unligated integrin
Unligated integrin
ECM
RTK
Raf
S338
S339
Y340
Y341
P
↑ PI3K–AKT activity
↑ NF-κB activity
↓ p53 activity
Caspase 8
ERK
Intrinsic pathway
Extrinsic pathway
Survival
Apoptosis
Nucleus
BCL2
CFLAR
Nature Reviews | Cancer

Figure 8. In a physiological context, integrins regulate both pro-survival and pro-apoptotic signals depending on their ligation state. From Desgrosellier, *Nat Rev Cancer* (2010).[44]

However, in cancer, deregulated integrin activity plays a central role in cell survival upon ECM detachment, allowing migration and metastasis. For instance, ß1 integrin promotes cells growing in suspension in prostate[46] and breast[47] cancer.

Different integrin patterns can recognize different ECM signatures, avoiding cell growth in ectopic sites. In cancer, specific tumor cells can disseminate to determined metastatic niches such as bone, lung or brain because of the specific recognition of cell- ECM signatures due to the cancer cell integrin repertoire.[40]

Besides, deregulated integrins might have a role in cell-adhesion mediated-drug resistance: ß1 integrin has been related to resistance to doxorubicin, lapatinib and trastuzumab in breast cancer[48,49] or to erlotinib in lung cancer.[50]

II. Cadherins

The cadherin superfamily are Ca^{2+}-dependent surface proteins that orchestrate cell-cell contacts forming adherens junctions through homotypic interactions. The formation of *cis* and *trans* dimers allow a zipper-like mechanism that clusters neighboring cells.[51] These mechanical linkages are dynamically regulated, allowing for a rapid disruption when needed. In addition to their adhesive function, cadherins are significant regulators of tissue homeostasis by transducing adhesive signals to a complex network of downstream effectors and transcriptional programs. Cadherins are formed by an extracellular domain, which mediates the adhesive function; a single-pass transmembrane domain and a cytoplasmatic domain embed to signaling and cytoskeletal proteins. The cytoplasmatic domain links to catenins (mainly ß, ɣ or p120catenin), which in turn are linked to actin via α-catenin.[52]

It has recently been reported that heterotypic cadherin adhesion mediates the crosstalk between cancer cells and CAFs leading to tumor progression.[16]

The most important cadherin are described below:

a. E-cadherin

The type I cadherin epithelial cadherin (E-cadherin), is the major component of the adherens junctions in epithelial tissues. E-cadherin establishes homotypic interactions between neighboring cells, linking their actin cytoskeletons, giving shape to the epithelium and ensuring cohesion.

E-cadherin is commonly considered a tumor suppressor. Loss of E-cadherin is observed many tumors and correlated with poor prognosis.[53–55] Decreased E-cadherin levels destabilize (or even suppress) cell-cell adhesion, which is a crucial step in EMT.[56]

Notwithstanding this tumor suppressor role in specific contexts, a dark side for E-cadherin as tumor promoter has been recently suggested in inflammatory breast carcinoma, ovarian cancer and glioma.[57,58]

b. N-cadherin

N-cadherin is a type I cadherin typically expressed in non-epithelial tissues, like the brain, where it plays a role in synaptogenesis; and heart, where it is the chief organizer of stress-resistant intercalated discs that connect heart muscle cells.[59]

In cancer, N-cadherin might have opposite roles depending on the tissue type. While its pro-metastatic role has been largely described in a variety of tumors such as breast,[60] prostate,[61] multiple myeloma,[62] melanoma[63] or ovarian[64] cancer, some studies have reported an antitumor effect in hepatocellular carcinoma[65] and neuroblastoma.[66] In addition to this tissue type-dependence, N-cadherin role might also be dependent on the tumor stage: a tumor suppressive role has been reported in pancreatic intraepithelial neoplasia (PanIN)[67] in contrast with a tumor promoter role in more advanced stages.[68]

Before cells metastasize, a cadherin switch occurs in epithelial cells leading to a more motile and invasive mesenchymal phenotype. This process is called EMT and courses with the up-regulation of N-cadherin and loss of E-cadherin expression.

III. Selectins

Selectins are adhesive molecules mediating transitory cell-cell interactions in the vasculature during inflammation, allowing lymphocyte extravasation.[41] The ligands of these molecules consist of a carrier protein or lipid that is modified by carbohydrates rather than protein-protein interactions as happens in other adhesion molecules. Three members belong to this family: E-selectin (present in endothelial cells), P-selectin (present both in platelets and endothelial) and L-selectins (in leucocytes).[43]

IV. Immunoglobulin cell adhesion molecules (IG-CAMs)

Ig-CAMs are a family of adhesion molecules presenting one or more Ig-like domains in the extracellular portion. They mediate homophilic or heterophilic cell-cell interactions. Besides, they can also bind to ECM components. Intracellularly, they bind to other components of the cytoskeleton as well as effectors of signal transduction pathways.[69]

1.2.3.2 Integrins-cadherin crosstalk

The Rho small GTPase family, comprising Rho, Rac1, and Cdc42, is a well-known regulator of cell-cell adhesion. Reciprocally, cell junctions can modulate Rho regulators localization and activity.[70] Besides, they are also downstream effectors of integrin engagement that affect cell polarity and migration due to rearrangements in the actin cytoskeleton,[56] indicating complex and important crosstalk among cadherins and integrins in cell behavior.[56,71] Forces at cell-cell and cell-ECM adhesions are intimately connected and reciprocally influenced. The composition and stiffness of the ECM can also affect the forces at cell-cell junctions.[72] In cancer, cells develop a more motile phenotype allowing migration. Coordinated cadherin-integrin crosstalk becomes especially relevant in this setting.

1.3 CURRENT TREATMENTS

Nowadays, the most common treatments for cancer include, usually in combination, the following.[73]

1.3.1 Surgery

It is used to remove solid and localized tumors or previous lesions that could evolve into malignant tumors, such as colon polyps. Also, it has a crucial role in diagnostic.

1.3.2 Radiotherapy

It uses high-energy particles or waves to destroy or damage cancer cells. Although it can damage nearby cells, it usually avoids systemic adverse effect given that is a localized treatment.

1.3.3 Chemoterapy

Chemotherapy is the use of drugs to treat cancer, alone or in combination among them or with other treatments, such as radiation or surgery. Some representative chemical structures are shown in **Figure 9**.

- *Alkylating agents*

Alkylating agents are the oldest class of anticancer drugs. The mechanism of action relies on the covalent bond between the alkyl residue and nucleophilic moieties of DNA. The alkylation impairs DNA processes such as replication or transcription.[74]

- *Antimetabolites*

The so-called antimetabolites are analogs of purine, pyrimidine, or folic acid. They interfere with different enzymes, substituting the genuine substrate and finally inducing cell death.

- *Mitotic inhibitors*

Usually derived from plants, these anticancer drugs inhibit cell division by binding to tubulin and thwarting the microtubule formation.

- *Topoisomerase inhibitors*

Topoisomerases inhibition impedes the uncoiling and recoiling of double DNA helixes during replication and transcription.

- ***Antibiotics***

Anticancer antibiotics have proven to kill cancer cells in addition to their antibacterial activity. They belong to the anthracyclines group (doxorubicin, daunorubicin), are alkylating agents (mitomycin C) or topoisomerase inhibitors (mitoxantrone).

- ***Hormone therapy***

Hormone therapy is used to treat hormone-dependent cancers. These drugs block or low the amount of hormones, thereby slowing or stopping cancer growth.

- ***Targeted therapies***

In the last years, cancer treatment has shifted from nonspecific cytotoxic drugs targeting all dividing cells into more specific therapies acting on a specific molecular target, thus reducing adverse side effects. The acquired knowledge about key signaling pathways has provided the tools for a specific target-based design. For instance, vemurafenib targets BRAF^{V600E}, a mutated form of the growth signaling protein BRAF. Imatinib mesylate blocks the protein product (a tyrosine kinase) of the BCR-ABL fusion oncogene, which drives leukemic cells growth.

1.3.4 Immunotherapy

Immunotherapy consists of either boosting the patient's immune system to promote cancer cell destruction or in directly providing immune system components. It includes monoclonal antibodies, immune checkpoints inhibitors, vaccines and other non-specific immunotherapies.[75]

Monoclonal antibodies recognize and link to a specific protein in the cell surface. They work by flagging the cell for immune destruction, blocking cell growth, preventing blood vessel growth (bevacizumab), blocking immune system inhibitors (nivolumab, ipilimumab, pembrolizumab), directly promoting cell destruction, delivering radiation or chemotherapy or by binding cancer and immune cells.

1.3.5 Other Treatments

Other treatments include stem cell transplant, hyperthermia, photodynamic therapy, blood transfusions or laser treatments.

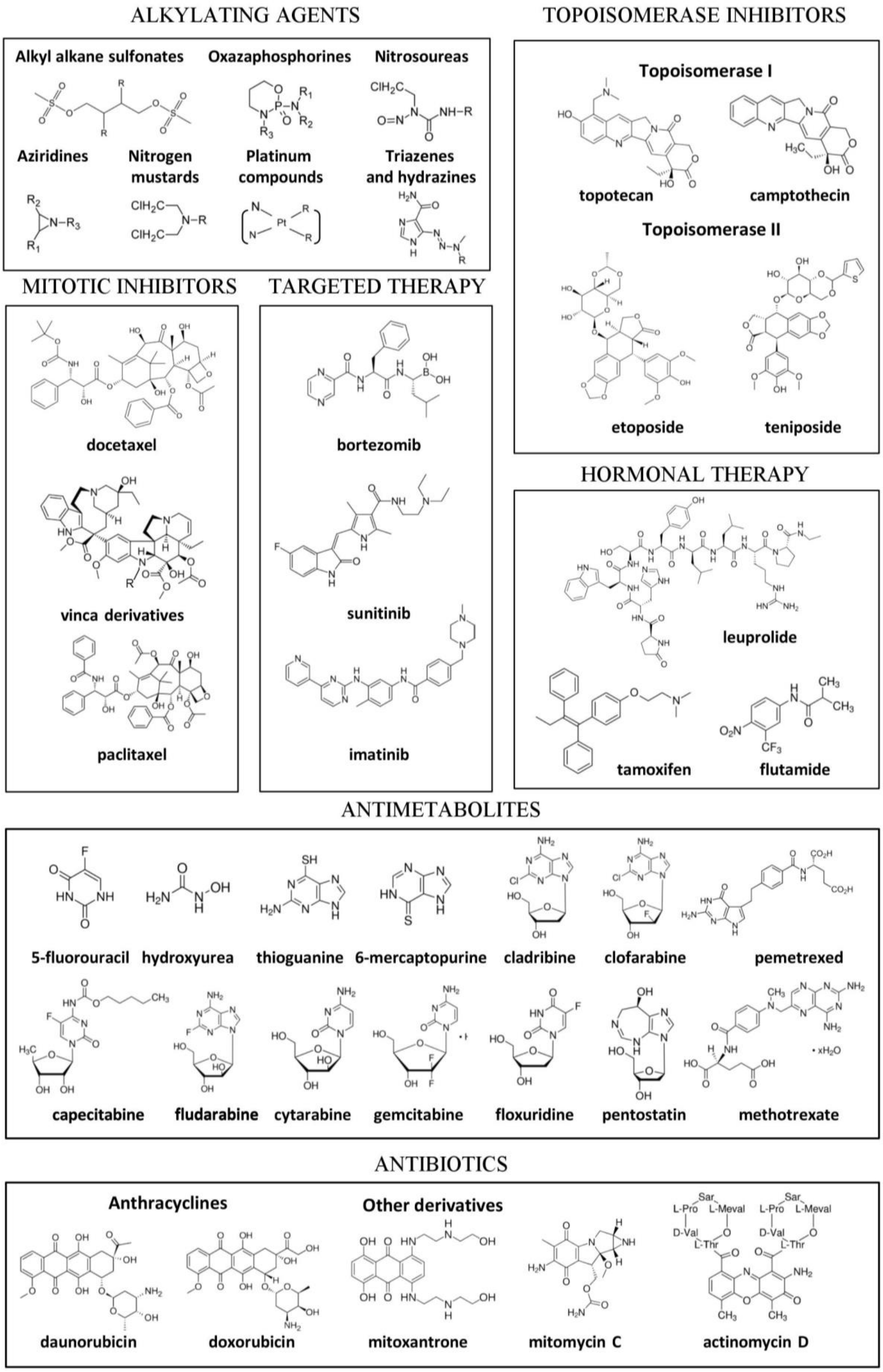
ALKYLATING AGENTS
Alkyl alkane sulfonates
Oxazaphosphorines
Nitrosoureas
Aziridines
Nitrogen mustards
Platinum compounds
Triazenes and hydrazines
TOPOISOMERASE INHIBITORS
Topoisomerase I
topotecan
camptothecin
Topoisomerase II
etoposide
teniposide
MITOTIC INHIBITORS
docetaxel
vinca derivatives
paclitaxel
TARGETED THERAPY
bortezomib
sunitinib
imatinib
HORMONAL THERAPY
leuprolide
tamoxifen
flutamide
ANTIMETABOLITES
5-fluorouracil
hydroxyurea
thioguanine
6-mercaptopurine
cladribine
clofarabine
pemetrexed
capecitabine
fludarabine
cytarabine
gemcitabine
floxuridine
pentostatin
methotrexate
ANTIBIOTICS
Anthracyclines
Other derivatives
daunorubicin
doxorubicin
mitoxantrone
mitomycin C
actinomycin D

Figure 9. Representative chemotherapeutic drugs.

2. SELENIUM

2.1 ROLE OF SELENIUM IN HEALTH AND DISEASE

Selenium (Se) was discovered in 1817 by the Swedish chemist Jöns Jacob Berzelius. Although it was first described as a toxin, the characterization of Se-deficiency-caused illnesses (i.e., Keshan disease) along with the breakthrough of mammalian selenoproteins, unveiled its role as an essential micronutrient.

Natural sources of Se are found in different foods and dietetic supplements providing the most common selenium compounds, which are detailed in **Figure 10**. Se intake worldwide varies and is highly dependent on Se concentration in soils where crops are grown. Recommended daily doses vary among agencies, ranging from 26 µg for women and 34 µg for men (WHO, 2004) to 50 µg for women and 70 µg for men (Panel on Dietetic Products, Nutrition and Allergies from the European Food Safety Authority; the Nordic Council of Ministers, Institute of Medicine Food and Nutrition Board).[76,77]

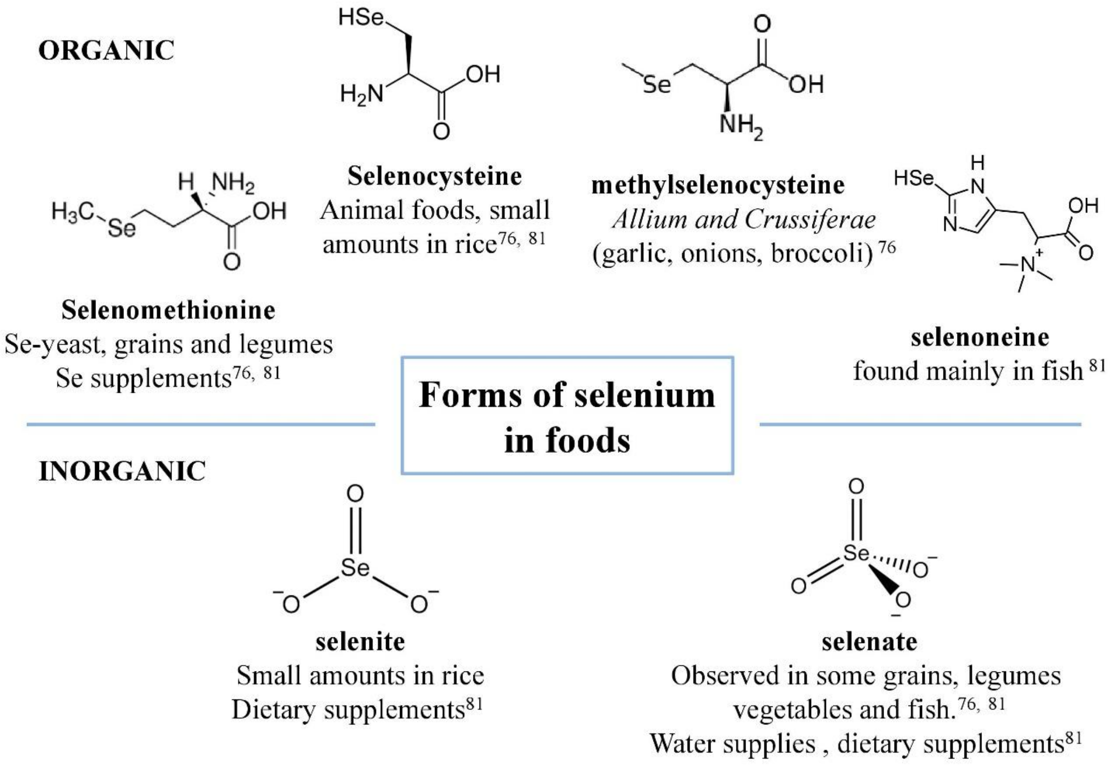
ORGANIC
HSe
H₂N
OH
O
Se
OH
NH₂
H NH₂
H₃C
Se
OH
O
Selenocysteine
Animal foods, small amounts in rice76, 81
methylselenocysteine
Allium and Crussiferae (garlic, onions, broccoli) 76
HSe
H
N
N
OH
O
N+
Selenomethionine
Se-yeast, grains and legumes
Se supplements76, 81
Forms of selenium in foods
selenoneine
found mainly in fish 81
INORGANIC
O
Se
O−
O−
selenite
Small amounts in rice
Dietary supplements81
O
Se
O
O−
O−
selenate
Observed in some grains, legumes vegetables and fish.76, 81
Water supplies , dietary supplements81

Figure 10. Most common dietary Se compounds.

At low doses, Se is considered to be a redox gatekeeper, and a detoxification, antioxidant, and cytoprotective agent.[78] Se exerts these physiological activities through incorporation into selenoproteins (Sel), mainly oxidoreductases, as the 21st aminoacid selenocysteine (SeCys). The SeCys residue is usually found at the enzyme active site, mastering catalytic redox reactions.[79] Among the 25 known

Sel (**Figure 11**), glutathione peroxidases (GPx), thioredoxin reductases (TrxR) and glutaredoxins (Grx) are the most important families. These Sel play a fundamental role in the defense against oxidative damage by scavenging reactive oxygen species (ROS) and other prooxidants. Oxidative damage can cause cell transformation as a first step in the carcinogenesis process and is also related to other illnesses outcome.

In addition to these redox functions, Sel serve other diverse biological roles. For instance, they modulate signaling proteins and transcription factors, control the cytoskeleton/actin assembly and supervise the structural disulfide bonds in proteins. Also, they are involved in hormone activation or inactivation in the iodine and thyroid hormone metabolism and are as well involved in calcium metabolism and the estrogen receptor stress response.[78,79] A deficient Se status impairs Se bioavailability, leading to reduced Sel levels.

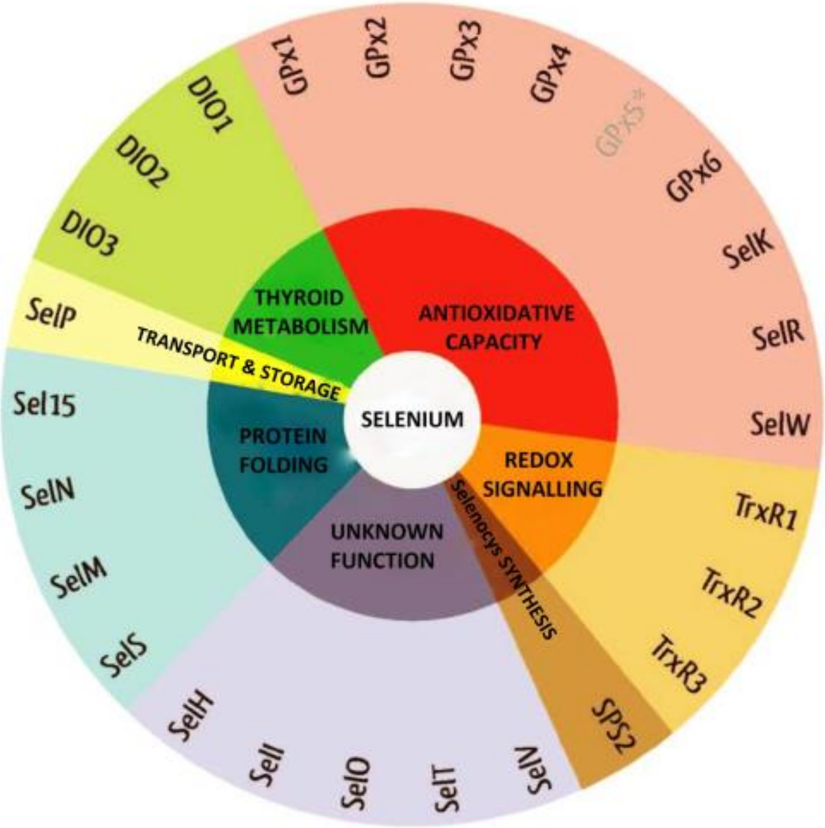
SELENIUM
ANTIOXIDATIVE CAPACITY
THYROID METABOLISM
TRANSPORT & STORAGE
PROTEIN FOLDING
UNKNOWN FUNCTION
REDOX SIGNALLING
Selenocys SYNTHESIS
GPx1
GPx2
GPx3
GPx4
GPx5*
GPx6
SelK
SelR
SelW
TrxR1
TrxR2
TrxR3
SPS2
SelV
SelT
SelO
SelI
SelH
SelS
SelM
SelN
Sel15
SelP
DIO3
DIO2
DIO1

Figure 11. Classification and function of selenoproteins. Modified from Benstoem *et al.*, *Nutrients* (2015).[80] Abbreviations: DIO iodothyronine deiodinase enzymes; GPx, glutathione peroxidase; Sel: selenoprotein; TrxR: thioredoxin reductase; SPS2 selenophosphate synthetase.

The narrow window between the needed physiological amount of Se and the toxic concentrations highlights its unique dual-faced role: both Se excess and deficiency originate human diseases (**Table 1**), although Se-deficiency pathologies are far more common.

Table 1. Role of Se in human health and disease

DISEASE	Se STATUS	SYMPTOMS
Selenosis	Excess	Garlic breath, hair and nail loss, disorders of the nervous system, poor dental health, paralysis.[81]
Keshan disease	Deficiency	Cardiomyopathy characterized by fibrosis, necrosis and myocytolysis.[82]
Kashin-Beck	Deficiency	Chronic osteochondral disease, characterized by articular cartilage deformities and arthralgia [83]
Myxedematous endemic cretinism	Deficiency (along with iodine deficiency)	Thyroid atrophy and mental retardation

Low Se status is linked to increased mortality risk, reduced immune function, and cognitive decline.[81] An adequate Se intake is needed for the proper function of many systems, as detailed below:

-Thyroid system

At least two families of Sel are involved in the thyroid hormone system: the DIO and GPx. DIO catalyze the activation via 5′-deiodination of the inactive precursor T_4 to the active T_3 hormone. Autoimmune thyroid disease such as Hashimoto's thyroiditis, improves with Se supplementation, mainly due to the optimization of endocrine-immune system interaction, given that the autoantibodies are lowered.[81,84] GPx degrade peroxides using glutathione as a reduction agent.

-Reproductive system

Se is necessary for testosterone biosynthesis and the proper formation and development of spermatozoa, which are protected from oxidative stress by GPx4. In women, miscarriage and preeclampsia have been related to lower serum Se concentration, although other studies did not found any correlation.[85]

-Cardiovascular system

Controversial results have been found regarding serum Se status and cardiovascular diseases. Deficient Se levels can lead to Keshan disease, a cardiomyopathy. However, whereas some studies correlated low Se levels with increased risk of myocardial infarction and death from cardiovascular disease, other revealed that high serum Se levels increased risk factors such as hypertension or serum lipid levels.[76]

-Immune system

Deficient Se status has been related to incidence, virulence and disease progression of viral infections, such as coxsackie and influenza viruses.[81] Adequate and supranutritional Se levels confer health benefits in case of HIV and influenza A infection.[86]

Se supplementation, even in patients with an adequate Se status increased the cytotoxic lymphocyte-mediated tumor cytotoxicity, the natural killer activity and fostered the proliferation of activated T cells. Sel are crucial for the proper function of activated-T cells, due to the sensitivity of these cells to oxidative stress.[81]

-Nervous system

Se plays an important role in the brain. Low Se status has been associated with a faster decline in the cognitive function,[87] Alzheimer disease,[88] higher prevalence of Parkinson and epileptic seizures.[81]

Noteworthy, the role of Sel in the nervous system has been reported by several studies. A mutated TrxR was associated with generalized genetic epilepsy[89] whereas other studies highlighted an impaired function of GPx in Parkinson and the possible role of Sel in preventing neurodegeneration in Alzheimer's disease.[90]

Importantly, different Se compounds offered promising results in alleviating some of these pathologies. Selenomethionine (SeMet)[91,92], ebselen[93] and sodium selenate[94] ameliorated Alzheimer's pathology in mice. Sodium selenate retarded epileptogenesis in rats[95] and diphenyl diselenide partially restored motor impairment in a Parkinson rat model[96] (**Figure 12**).

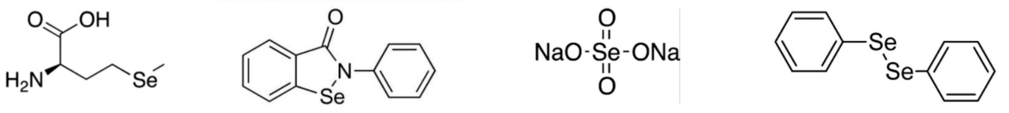

SeMet **Ebselen** **Sodium selenate** **Diphenyl diselenide**

Figure 12. Se compounds with promising results in preclinical models of Alzheimer, epilepsy or Parkinson diseases.

2.2 SELENIUM AND CANCER

The role of Se in cancer has gained the attention of several researchers in the last decades. An inverse relationship between Se status and cancer was supported by the identification of antioxidant Se-containing enzymes, extensive laboratory data and the first cohort studies. These facts fostered the development of randomized trials.[77]

Early clinical studies revealed that Se-yeast (mainly containing SeMet, but also other Se compounds) decreased the incidence risk of some types of cancers inChina.[97,98*] These studies encouraged the *Nutritional Prevention of Cancer Trial* (NPC), which revealed a decrease in lung, colon or prostate cancer risk upon daily supplementation with 200 μg Se-yeast.[99–103] However, further studies as the *Selenium and vitamin E Cancer Prevention Trial* (SELECT), which used SeMet, showed no risk decrease and was in fact prematurely discontinued.[104,105] Besides, an increase in type-2 diabetes risk was found in subjects with adequate Se status.

Subsequent analyses of these studies have revealed that both the plasma Se status of the studied subjects and the Se form were determinant for Se activity. Thus, the controversial results arise from not taking into account the strict dependency of Se activity on multiple factors. The complicated U-shaped relationship between Se status and disease incidence discourages Se supplementation in people with an adequate-to-high Se status.[81] Moreover, the chemical speciation, dose and tested model profoundly determine Se efficacy.

Vinceti *et al.* have recently recompiled and reviewed all the studies published from 2007 to 2017. Except for one study using inorganic Se, there is no evidence of a decreased overall cancer risk with organic Se supplementation, majorly in the form of SeMet. They conclude that Se intakes of 250 μg/day or above, have no effect on cancer risk and could, in fact, increase the risk for some cancers and other chronic diseases. However, they highlight that it is yet to be determined if Se intakes below these values may affect cancer risk.[77]

Whereas the utility of Se supplementation on cancer prevention in epidemiological studies remains elusive, the role of Se compounds as therapeutic agents in cancer is well-demonstrated.[76,78,106,107] The term *therapeutic* implies the efficacy of Se compounds to reduce cell proliferation or to kill cancer cells both *in vitro* or *in vivo*.

Their ability to induce cell death might be based on the fact that, at high doses, some Se compounds turn into pro-oxidants. It is known that cancer cells deal with increased levels of oxidative stress as a result of altered metabolism (Warburg effect) leading to an excess of ROS and reducing equivalents (NADH, NADPH…). The thioredoxin and glutathione systems are the main responsibles of maintaining the redox status of the cell. As a counteraction to avoid ROS-induced death, cancer cells overexpress their antioxidant systems to maximum levels, being therefore highly vulnerable to even small extra ROS production.[106]

Also, Se compounds present a selective uptake among cancer cells with respect to healthy cells. The uptake depends on the type of compound and includes ATPases for selenide[108] or the cystine/glutamate antiport system (the

---

[*] These studies were excluded from subsequent meta-analysis due to their poor methodological quality.[77,191,192]

xCT) along with the extracellular thiol status for selenite[109]. Besides, the ZIP8 divalent cation transporter has also been recently described for selenite.[110] However, the exact mechanism explaining the selective Se uptake is yet to be fully elucidated.[78,109]

The anticancer effects of Se compounds are exerted by their metabolites, given that these effects are achieved at substantially higher doses than those required for maximal Sel expression.[111]

Elucidating Se metabolism is thus crucial to understand Se activity, with metabolites and not original molecules ultimately exerting the biological effects. All Se compounds converge in two main metabolites: hydrogen selenide (H_2Se) and methylselenol (CH_3SeH). Besides, the activity of Se compounds mainly depends on where they enter the metabolic pathway: before or beyond the H_2Se pool.[112] Upstream of these molecular species, each compound has its pathway to be metabolized. Downstream, there are three possible pathways: methylation (preceding excretion), incorporation into Sel or selenosugars, being the latter excreted in urine (**Figure 13**).

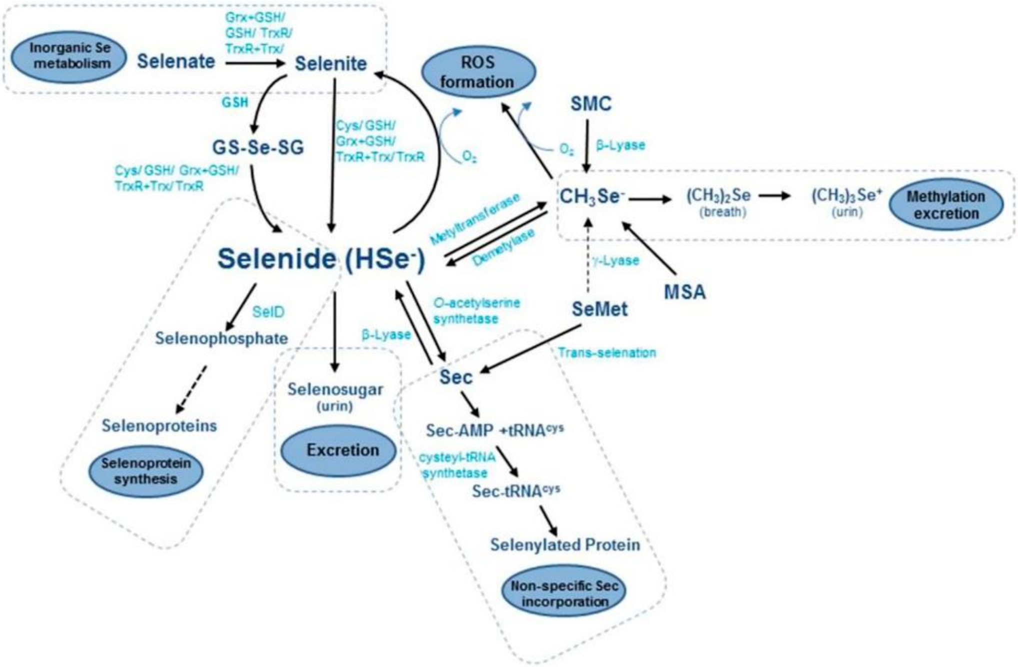
Inorganic Se metabolism
Selenate
Grx+GSH/ GSH/ TrxR/ TrxR+Trx/
Selenite
GSH
GS-Se-SG
Cys/ GSH/ Grx+GSH/ TrxR+Trx/ TrxR
Cys/ GSH/ Grx+GSH/ TrxR+Trx/ TrxR
O₂
ROS formation
SMC
O₂
β-Lyase
CH₃Se⁻
(CH₃)₂Se (breath)
(CH₃)₃Se⁺ (urin)
Methylation excretion
Metyltransferase
Demetylase
Selenide (HSe⁻)
γ-Lyase
MSA
SeMet
SelD
Selenophosphate
O-acetylserine synthetase
β-Lyase
Trans-selenation
Sec
Selenosugar (urin)
Excretion
Selenoproteins
Selenoprotein synthesis
Sec-AMP +tRNAᶜʸˢ
cysteyl-tRNA synthetase
Sec-tRNAᶜʸˢ
Selenylated Protein
Non-specific Sec incorporation

Figure 13. Metabolic pathways of dietary Se compounds. From Fernandes *et al.*, *Biochem BioPhys Acta.* (2015).[106] Abbreviations: DMeT, demethyltransferases; MeT, methyltransferases DeMeT, demethyltrans-ferases; MeT, methyltransferases; SPS, selenophosphate synthetase.

Even though methylated species of selenium are thought to be less toxic, Ganther *et al.* demonstrated that the methylation degree was an essential factor determining the anticancerous activity of Se compounds.[113] In fact, they demonstrated that a monomethylated species was essential for Se cytotoxicity.[114,115] CH_3SeH is commonly accepted as one of the key executors of Se biological activities. However, due to its high reactivity and volatile nature, efficient precursors are required. Importantly, the rate of endogenous monomethylated Se production is a critical factor for Se activity.[114]

2.2.1 Role of Selenoproteins in Cancer

Sel have an antioxidant function that can delay cancer initiation by alleviating DNA damage resulting from oxidative stress. However, recent research has pinpointed the dual role of oxidative stress, which can either contribute or hinder tumorigenesis depending on cellular context.[116] In addition to their antioxidant function, selenoproteins participate in oncogenic and tumor-suppressive pathways. So rather than an overall contribution, the contribution of individual Sel must be taken into account as well as the tumor stage and cellular context. Knockout experiments in mice of Sel P revealed an increase in tumorigenesis. TrxR1 has been suggested as a possible therapeutic target due to its role in tumor progression.[117] Concerning GPx, they are highly tissue and context-specific. For instance, GPx1 is decreased in many tumor types[116], but GPx1 overexpression in a mouse model of skin cancer increased the tumor burden.[118] GPx2 is upregulated in most tumors in comparison to healthy tissue[119], but GPx2 knockdown had ambivalent effects.[116]

Gpx2 appears to contribute to tumor progression in already established tumors whereas it develops an anticancer activity in inflammation-driven carcinogenesis.

GPx3 usually has a tumor-suppressive role although it might be dependent on p53, as mutant p53 abrogates this effect.[120]

In conclusion, the role of Sel in cancer is highly diverse and tissue and stage-specific. Further research is needed to thoroughly dissect their exact contribution to cancer development as they can act both as oncosuppressors and promoters.[121]

BACKGROUND

1. SELENIUM COMPOUNDS AND MECHANISM OF ACTION IN CANCER

The antiproliferative and/or cytotoxic properties of Se compounds are the consequence of a multi-targeted effect in tumor cells, and this effect is highly dependent on the compound type, dose and model tested. Different Se compounds can trigger different cellular responses. In general trends, there are three main mechanisms of action: i. ROS production, which is linked to cell cycle arrest and immune response; ii. thiol modification of protein and/or low molecular weight compounds, which affect transcription factors, signal transduction and endoplasmic reticulum (ER) stress; and iii. Chromatin binding or modification, which interferes with angiogenesis, causes DNA damage and histone deacetylases (HDAC) inhibition.[106] In **Figure 14**, some of the most representative Se compounds are shown. Noteworthy, ebselen has largely been under study for multiple purposes, including cardiovascular disease, arthritis, cancer[122] and stroke,[123] showing a good safety profile. Recently, it has been tested successfully for the prevention of hear-loss.[124] Besides, sodium selenite and ethaselen are currently under phase I clinical trials.[125,126]

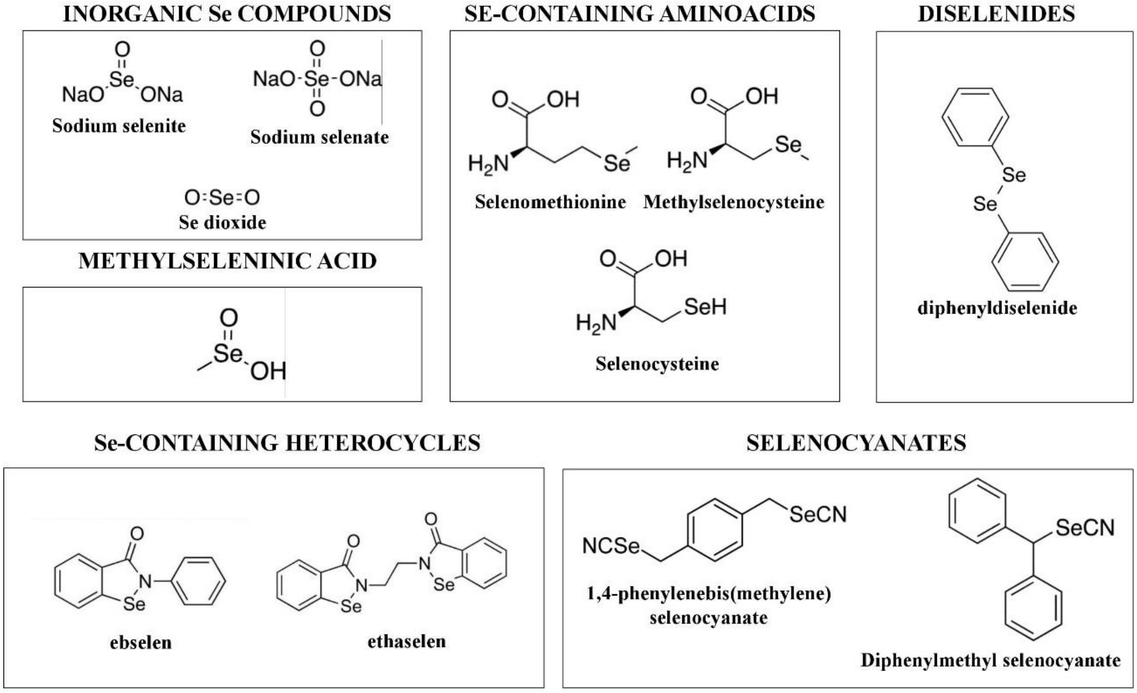
INORGANIC Se COMPOUNDS
Sodium selenite
Sodium selenate
Se dioxide
METHYLSELENINIC ACID
SE-CONTAINING AMINOACIDS
Selenomethionine
Methylselenocysteine
Selenocysteine
DISELENIDES
diphenyldiselenide
Se-CONTAINING HETEROCYCLES
ebselen
ethaselen
SELENOCYANATES
1,4-phenylenebis(methylene) selenocyanate
Diphenylmethyl selenocyanate

Figure 14. Representative Se compounds with antitumor properties.

1.1 Methylselenol

CH_3SeH is considered an essential metabolite in Se anticancerous activity. However, due to its high reactivity and volatility, it cannot be used *per se* and the *in situ* production or the use of precursors are required. In fact, CH_3SeH precursors are considered the next generation Se compounds.[127]

Three main CH_3SeH precursors have been extensively studied in the last decades. Methylselenocysteine (MSC) requires the action of a ß-lyase to release the metabolite, but it has shown especially *in vivo* some promising results.[106,128,129] The prodrug/enzyme system of SeMet/*L*-methioninase is considered to be less potent since they are quite inert and present lower redox activity.[76] Methylseleninic acid (MSA) is a synthetic molecule which has been broadly studied both *in vivo* and *in vitro*[130–132], and it is considered one of the best CH_3SeH precursors.[76]

CH_3SeH triggers a multi-targeted effect involving several pathways and functions. It counteracts almost all of the acquired cancer features described by Hannahan *et al.*, as summarized in **Figure 15**, where the most relevant mechanisms and the specific CH_3SeH precursor used are summarized.

Several studies have reported CH_3SeH to induce cell cycle arrest and cell death, both *in vitro* and *in vivo*.[133–136] Several proteins related to these two processes are modulated by CH_3SeH. It decreases c-Myc, E2F1 and cyclin D1[137]; and increases p21[135] and cyclin-dependent kinase inhibitor 1C (p57).[138] Besides, treatment with MSA suppressed the hyperphosphorylation of RB, through reduction of cyclin-CDK4 activity.[139]

Regarding cell death, it down-regulates anti-apoptotic proteins such as Bcl-XL, survivin, and c-FLIP[140] and upregulates pro-apoptotic Bad. MSA induced autophagy in some pancreatic cancer cell lines, but possibly as a drug-induced counteraction to promote cell survival.[133]

Besides, CH_3SeH might exert an antiangiogenic role, evidenced by the decrease of HIF-1α[141], VEGF[141,142], the platelet-derived growth factor (PDGF)[143] and angiopoietin-2 (Ang-2).[144] Moreover, it diminished the microvessel density and promoted the vessel maturation index.[143] MSA used at nutritional levels inhibited angiogenesis by downregulating integrin ß3 expression and its clustering in HUVEC cells. This led to inhibition of AKT/NF-κB phosphorylation, and consequently, inhibition of angiogenesis.[145] Integrin downregulation is also crucial in the migration process. CH_3SeH produced from SeMet/MET and MSC was able to disrupt adhesive properties to fibronectin and vitronectin by reducing integrin expression. *In vitro*, CH_3SeH affects cell adhesion causing detachment from the culture plate.[133,138,146–148]

In vivo, it reduced pulmonary metastasis from primary B10F16 melanoma.[149] Other *in vitro* assays treating fibrosarcoma HT1080 cells, revealed that CH_3SeH from SeMet/METase ameliorated the migrating and invasive potential.[150]

Besides, MSA reduces matrix metalloproteinase-2 (MMP-2) levels and its gelatinolytic activity in endothelial cells[151] as well as MMP-9 plasma levels in mice.[152] Metalloproteinases degrade the ECM, master the extracellular tissue signaling network and are involved in many physiological roles such as angiogenesis and migration.[149,151]

CH_3SeH has an additional role in boosting the immune system. CH_3SeH derived from MSA was shown to increase MHCI in melanoma cells[153] and different precursors or CH_3SeH were able to increase MICA/B, the ligands that trigger NKG2D receptors in lymphocytes.[154]

CH_3SeH from MSA reduced osteoblast-caused inflammation in breast-derived bone metastasis via inhibiting nuclear factor- κß (NF-κß). This led to a reduced expression of COX-1, interleukin-6 (IL-6), monocyte chemoattractant protein 1 (MCP-1) and inducible nitric oxide synthase (iNOS).[155] In MSA-treated mice, plasma TNFα/IL-6 levels were decreased with respect to untreated mice.[156]

A role as an epigenetic regulator has also been described for MSA. It was shown to modulate target genes through the inhibition of HDAC activity.[141] In human esophageal squamous cell carcinoma cells, it increased histone acetylation at H3K9 as a result of concomitant HDAC activity inhibition and the increase of general control non repressed protein 5 (GCN5). Besides it increased Krüppel-like factor 4 (KLF4), contributing to proliferation inhibition.[157]

MSA also affects cancer cell metabolism. It blocks the glycolytic activity, the tricarboxylic acid (TCA) cycle, the pentose phosphate pathway and the nucleotide biosynthesis in A549 cells.[158]

In addition to its own effects, CH_3SeH derived from MSA can act as a sensitizer agent. It enhances the cytotoxic activity of other drugs[159] like paclitaxel[160,161], etoposide[162], carboplatin[163] or cisplatin[132,164], but it surprisingly antagonizes bortezomib-induced apoptosis in mantle cell lymphoma.[165] The synergistic effect could be due to the inhibition of ß-catenin, which has been related to poor prognosis and chemoresistance.[166]

CH_3SeH can act as a chemopreventive agent through different mechanisms: it can increase the expression of antioxidant and phase II detoxification enzymes through the activation of Keap/Nrf2 pathway[167,168] or it can strengthen cancer progression barriers, such as p53-senescence.[169]

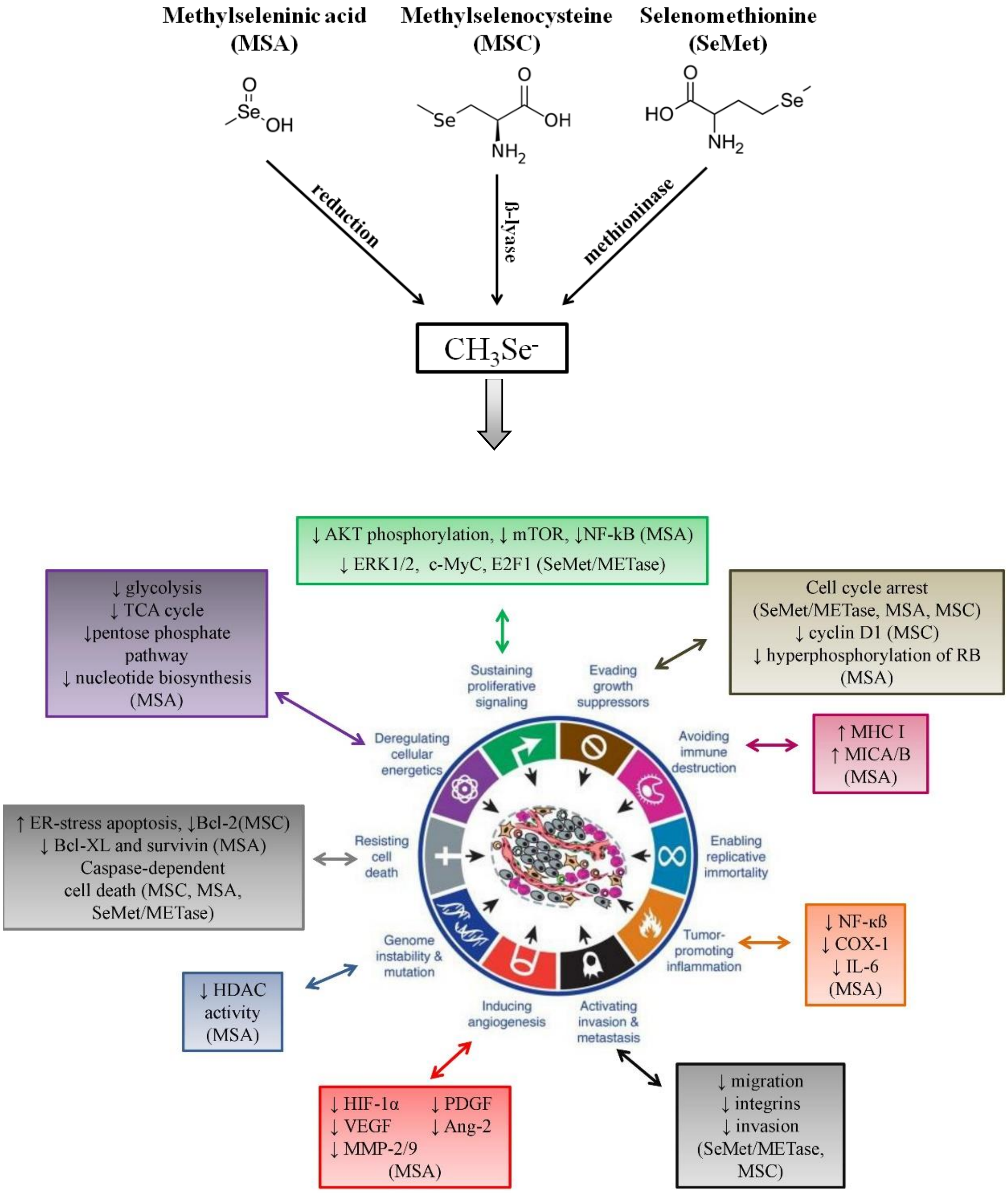
Methylseleninic acid (MSA)
Methylselenocysteine (MSC)
Selenomethionine (SeMet)
O
Se
OH
Se
O
OH
NH2
O
HO
Se
NH2
reduction
β-lyase
methioninase
CH3Se-
↓ AKT phosphorylation, ↓ mTOR, ↓NF-kB (MSA)
↓ ERK1/2, c-MyC, E2F1 (SeMet/METase)
↓ glycolysis
↓ TCA cycle
↓pentose phosphate pathway
↓ nucleotide biosynthesis
(MSA)
Cell cycle arrest
(SeMet/METase, MSA, MSC)
↓ cyclin D1 (MSC)
↓ hyperphosphorylation of RB
(MSA)
Sustaining proliferative signaling
Evading growth suppressors
Deregulating cellular energetics
Avoiding immune destruction
↑ MHC I
↑ MICA/B
(MSA)
↑ ER-stress apoptosis, ↓Bcl-2(MSC)
↓ Bcl-XL and survivin (MSA)
Caspase-dependent
cell death (MSC, MSA,
SeMet/METase)
Resisting cell death
Enabling replicative immortality
Genome instability & mutation
Tumor-promoting inflammation
↓ NF-κß
↓ COX-1
↓ IL-6
(MSA)
↓ HDAC
activity
(MSA)
Inducing angiogenesis
Activating invasion & metastasis
↓ HIF-1α
↓ PDGF
↓ VEGF
↓ Ang-2
↓ MMP-2/9
(MSA)
↓ migration
↓ integrins
↓ invasion
(SeMet/METase,
MSC)

Figure 15. Antagonizing effects of methylselenol on cancer hallmarks. Modified from Hanahan *et al.*, *Cell* (2011).[5]

2. BACKGROUND OF THE RESEARCH GROUP

During the last decade, our group has focused on the design, synthesis and biological evaluation of organic Se derivatives as potential anticancer drugs. Se derivatives induce distinct cellular responses affecting different targets, depending on the chemical speciation, dose and model tested as well as the followed metabolic route. Given this strict dependency of biological activity on speciation, different Se functionalizations have been explored[170–176], some of which are summarized in **Figure 16**.

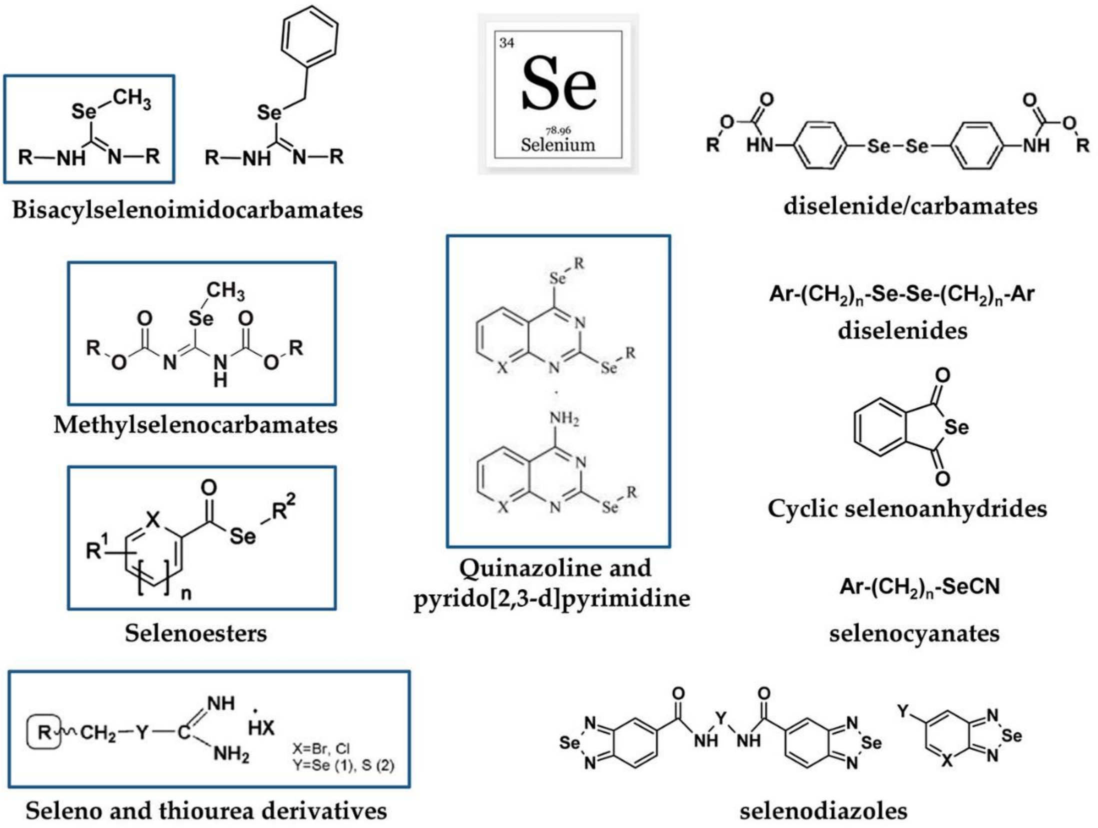
Bisacylselenoimidocarbamates
34
Se
78.96
Selenium
diselenide/carbamates
Methylselenocarbamates
Ar-(CH2)n-Se-Se-(CH2)n-Ar
diselenides
Quinazoline and
pyrido[2,3-d]pyrimidine
Cyclic selenoanhydrides
Selenoesters
Ar-(CH2)n-SeCN
selenocyanates
X=Br, Cl
Y=Se (1), S (2)
Seleno and thiourea derivatives
selenodiazoles

Figure 16. Scaffolds of previously synthesized Se derivatives. Highlighted general structures are the ones containing a methylseleno moiety in at least one compound of the series.

Mounting evidence highlights CH_3SeH as a key metabolite in Se anticancer activity. Interestingly, it triggers a multi-targeted effect, which might decrease the chance of drug-resistance. Accordingly with this hypothesis, our group has evaluated several methylseleno derivatives during the last years.[170,173,177–179] Those compounds exhibited significant anticancer activity compared to other alkyl derivatives against a broad spectrum of cancer cells both *in vitro* and *in vivo*. Moreover, we demonstrated that *Se*-methylselenourea derivatives were able to release CH_3SeH in aqueous systems.[180]

Recently, we identified a novel series of selenoester derivatives in which the presence of a methylselenoester moiety substantially improved the antiproliferative activity of the corresponding selenoglycolic acids.[172] To widen current knowledge about novel CH_3SeH precursors, a new series of molecules bearing the methylselenoester functionality was designed for this Ph.D. project.

HYPOTHESIS AND AIMS

HYPOTHESIS AND AIMS

CH_3SeH has been described as a critical mediator of the biological activity. However, the high reactivity and volatility of this molecule limits its use as a therapeutic agent, therefore arguing for the *in-situ* production or the use of precursors.

Significantly, the CH_3SeH delivery rate appears as a compelling process to evaluate, as it could determine the cytotoxic activity of compounds. Different molecules can be metabolized to CH_3SeH. Among them, we will focus on molecules already carrying a methylseleno moiety. Aiming to release CH_3SeH in a modulated way, the following facts will determine the design of the new precursors:

1. The ester entity can be easily attacked by a nucleophile such as water. Consequently, the introduction of a methylselenoester moiety might render CH_3SeH in an aqueous environment as one possible mechanism to release this essential metabolite.

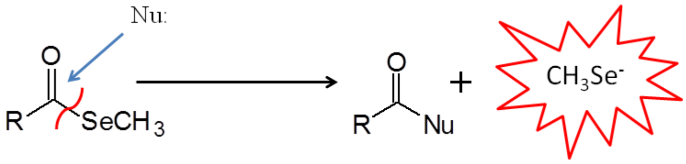
Nu:
O
R
SeCH3
O
R
Nu
+
CH3Se-

2. On account of a fragment-based design, we selected cytotoxic-reported heteroaromatic and carboaromatic rings as carriers of the selenoester group, aiming to improve the activity of CH_3SeH through synergy with these cytotoxic moieties. Besides, the chemical diversity of these substituents might modulate the carbonyl-selenium bond strength and either hinder or facilitate the nucleophilic attack, and therefore the release of CH_3SeH.

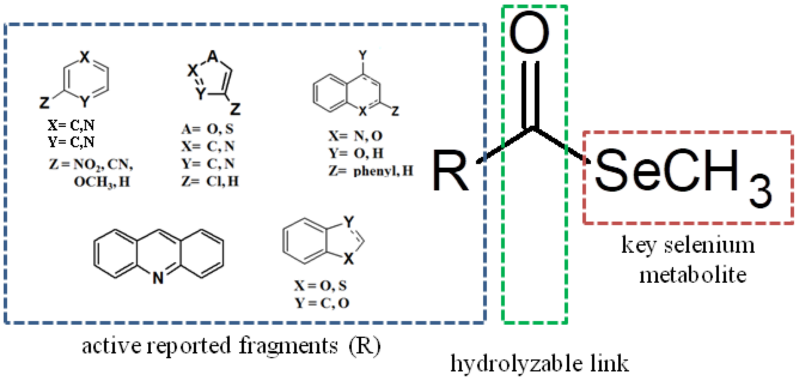
X= C,N
Y= C,N
Z= NO2, CN, OCH3, H
A= O, S
X= C, N
Y= C, N
Z= Cl, H
X= N, O
Y= O, H
Z= phenyl, H
X= O, S
Y= C, O
R
O
SeCH3
key selenium metabolite
active reported fragments (R)
hydrolyzable link

3. The bifunctionalization with two methylselenoester moieties might increase the potency of those compounds.

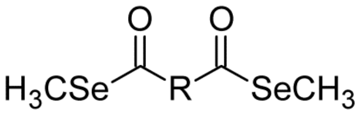
O
O
H3CSe
R
SeCH3

In summary, this Ph.D. project will target CH_3SeH precursors, due to their promising prospective as antitumor agents.[127] The main purpose will be the design, synthesis and biological evaluation of novel methylselenoesters as potential antiproliferative and/or cytotoxic agents.

On the other hand, the specific objectives of this thesis are outlined below:

1. Synthesis and purification of an innovative series of methylated selenium derivatives mono- or bi-functionalized with the chemical form methylselenoester and hybridized with heteroaromatic or carboaromatic rings present in cytotoxic-reported molecules.

Note: The obtained biological results required the additional synthesis of ethyl, pentyl and benzylselenoesters to verify a determined mechanism of action, although these structures were not an initial aim of this work.

2. Characterization of the novel compounds through infrared (IR) spectroscopy, ^1H and ^{13}C NMR spectroscopy, elemental analysis, mass spectrometry (MS) and high-resolution mass spectrometry (HRMS).

3. Determination if hydrolysis in aqueous environment renders CH_3SeH release and if the chemical molecular features determine the release rate.

4. Evaluation of the novel compounds against a panel of cancer cell lines to determine their cytostatic or cytotoxic activity.

5. Evaluation of the selectivity against two nonmalignant cell lines, MSA being the reference control.

6. Selection of the leader compounds and elucidation of their possible mechanism of action, including, among others:
    a. Evaluation against 3D in contrast to 2D cultures.
    b. Cell cycle evaluation in a dose and time-dependent manner.
    c. Cell death quantification and assessment of cell death type.
    d. Analysis of altered signaling pathways upon treatment.
    e. Evaluation of the compounds as possible substrates for different Se-related enzymes.

7. Evaluation of the antioxidant profile of the new compounds. Se compounds can behave as chemopreventive molecules if they have antioxidant properties. To this aim, their ability to reduce the DPPH radical will be measured and further confirmed with the ABTS assay for the most promising compounds.

All these objectives, claiming to verify our initial hypothesis, are developed in Papers 1 and 2 presented in the Results section.

In addition, the research stay at the Karolinska Institutet (Stockholm, Sweden) allowed for participation in two Se-related projects that have resulted in two published papers (Paper 3 and 4), which are also included in the Results section.

RESULTS

RESULTS

PAPER 1: NOVEL METHYLSELENOESTERS AS ANTIPROLIFERATIVE AGENTS

PAPER 2: NOVEL METHYLSELENOESTERS INDUCE PROGRAMED CELL DEATH VIA ENTOSIS IN PANCREATIC CANCER CELLS

PAPER 3: SELENITE AND METHYLSELENINIC ACID EPIGENETICALLY AFFECTS DISTINCT GENE SETS IN MYELOID LEUKEMIA: A GENOME WIDE EPIGENETIC ANALYSIS.

PAPER 4: METHYLSELENINIC ACID SENSITIZES OVARIAN CANCER CELLS TO T-CELL MEDIATED KILLING BY DECREASING PDL1 AND VEGF LEVELS

molecules

Article

Novel Methylselenoesters as Antiproliferative Agents

Nuria Díaz-Argelich [1,2,3], Ignacio Encío [4], Daniel Plano [1,2], Aristi P. Fernandes [3],
Juan Antonio Palop [1,2] and Carmen Sanmartín [1,2,*]

PUBLISHED

Molecules 2017 Aug 2;22(8)

PAPER 1

molecules

MDPI

Article

Novel Methylselenoesters as Antiproliferative Agents

Nuria Díaz-Argelich [1,2,3], Ignacio Encío [4], Daniel Plano [1,2], Aristi P. Fernandes [3], Juan Antonio Palop [1,2] and Carmen Sanmartín [1,2,*]

[1] Department of Organic and Pharmaceutical Chemistry, Faculty of Pharmacy and Nutrition, University of Navarra, Irunlarrea 1, E-31008 Pamplona, Spain; ndiaz@alumni.unav.es (N.D.-A.); dplano@unav.es (D.P.); jpalop@unav.es (J.A.P.)
[2] Oncology and Hematology Section, IdiSNA, Navarra Institute for Health Research, Irunlarrea 3, E-31008 Pamplona, Spain
[3] Division of Biochemistry, Department of Medical Biochemistry and Biophysics (MBB), Karolinska Institutet, SE-171 77 Stockholm, Sweden; Aristi.Fernandes@ki.se
[4] Department of Health Sciences, Public University of Navarra, Avda. Barañain s/n, E-31008 Pamplona, Spain; ignacio.encio@unavarra.es
* Correspondence: sanmartin@unav.es; Tel.: +34-948-425-600

Received: 29 June 2017; Accepted: 28 July 2017; Published: 2 August 2017

Abstract: Selenium (Se) compounds are potential therapeutic agents in cancer. Importantly, the biological effects of Se compounds are exerted by their metabolites, with methylselenol (CH_3SeH) being one of the key executors. In this study, we developed a new series of methylselenoesters with different scaffolds aiming to modulate the release of CH_3SeH. The fifteen compounds follow Lipinski's Rule of Five and with exception of compounds **1** and **14**, present better drug-likeness values than the positive control methylseleninic acid. The compounds were evaluated to determine their radical scavenging activity. Compound **11** reduced both DPPH and ABTS radicals. The cytotoxicity of the compounds was evaluated in a panel of five cancer cell lines (prostate, colon and lung carcinoma, mammary adenocarcinoma and chronic myelogenous leukemia) and two non-malignant (lung and mammary epithelial) cell lines. Ten compounds had GI_{50} values below 10 μM at 72 h in four cancer cell lines. Compounds **5** and **15** were chosen for further characterization of their mechanism of action in the mammary adenocarcinoma cell line due to their similarity with methylseleninic acid. Both compounds induced G_2/M arrest whereas cell death was partially executed by caspases. The reduction and metabolism were also investigated, and both compounds were shown to be substrates for redox active enzyme thioredoxin reductase.

Keywords: methylselenoester; methylselenol release; cytotoxicity; cell cycle arrest; cell death; thioredoxin reductase

1. Introduction

Cancer is one of the leading causes of mortality and morbidity worldwide. Current chemotherapy is not completely satisfactory [1] and the development of new drugs is an urgent need. In the last few years, scientific evidence has backed the rationale for studying the mechanism of selenium-containing compounds as cancer therapeutic agents [2]. The role of Se is highly versatile due to multiple factors that determine its activity. It has been described both as a chemopreventive and cytotoxic agent [2–4] on account of the dual role as antioxidant and pro-oxidant, which is highly dependent on dose, chemical species and the redox state of the cell. Chemotherapeutic activity of Se compounds is mainly based in a multi-targeting effect which triggers complex cascades of death signaling and inhibits tumor formation and metastasis in animal models [2,5–7]. Because of this, the utility of Se compounds for the treatment of tumoral diseases and even drug-resistant cancers offers an interesting pursuit.

Molecules **2017**, *22*, 1288; doi:10.3390/molecules22081288

However, Se activity relies in multiple factors such as chemical form, dose and metabolism. Results from in vitro studies, animal experiments and clinical trials suggest that the biological activities of Se are dependent on the type and the nature of metabolites derived from the Se derivative [8,9]. Metabolites, and not original molecules, seem to be the ultimate executors of Se biological activity for some Se compounds. Thus, understanding the metabolic routes of Se compounds is highly necessary [10,11]. Se biochemistry encompasses a complex net of interrelated intermediates that converge in two main metabolites: methylselenol (CH_3SeH) and hydrogen selenide (H_2Se). Among all Se metabolites, it is largely accepted that CH_3SeH stands out as a key executor for Se anticancer activity [3].

The volatile nature and high reactivity of CH_3SeH obliges to the use of precursors with the ability to release it through hydrolysis, chemical reactions or cellular metabolism. Different approaches have been investigated. Methylselenocysteine requires the action of a ß-lyase to release the metabolite, but it has shown some promising results, especially in vivo [2,12,13]. The prodrug/enzyme system of selenomethionine/L-methioninase is considered to be less potent since they are quite inert and present lower redox activity [14]. Methylseleninic acid (MSA) is a synthetic molecule which has been broadly studied both in vivo and in vitro [15–17] and it is considered one of the best CH_3SeH precursors [14].

In addition to these classical precursors, our group has been synthesizing during the last decade several methylseleno derivatives [18–22]. These compounds exhibited significant anticancer activity compared to other alkyl derivatives against a broad spectrum of cancer cells both in vitro and in vivo. Moreover, we demonstrated that *Se*-methylselenourea derivatives were able to release CH_3SeH in aqueous systems [23]. Recently, we identified a novel series of selenoester derivatives in which the presence of a methylselenoester moiety substantially improved the antiproliferative activity of the corresponding selenoglycolic acids [24]. Continuing with this work, herein we propose an extended series of molecules bearing this functionality. The methylselenoester entity can be easily attacked by a nucleophile such as water, as one possible mechanism to deliver CH_3SeH. The release of the key metabolite in aqueous medium could therefore be modulated through the chemical features of the core of the molecule.

Using a fragment-based approach, different aromatic or heteroaromatic rings were selected to ensure enough chemical diversity to either hinder or facilitate the hydrolysis. In addition, we chose fragments that are present in compounds which have been reported active as anticancer agents by our group [19] and the literature: thienyl [25,26], isoxazolyl [27,28], furyl [29], chromonyl [30,31], pyrazinyl [32], pyridyl [33], thiazolyl [34], benzo[*b*]thienyl [35], quinolyl and phenylquinolyl [36–38] or acridinyl [39,40] as well as substituted aromatic rings (Figure 1).

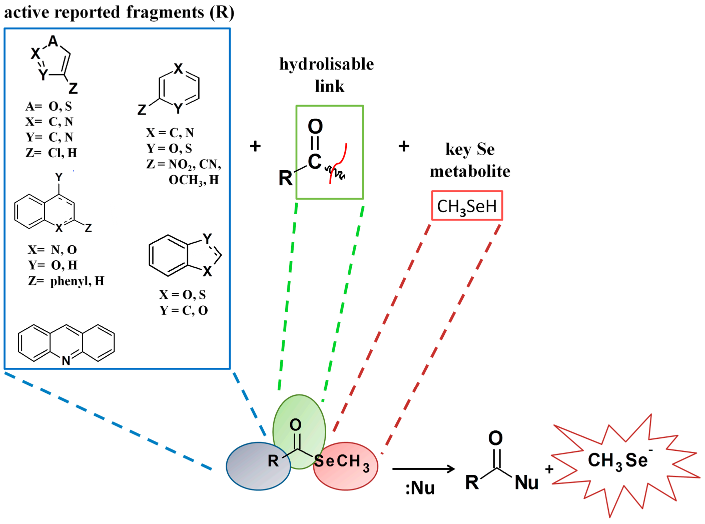

Figure 1. Fragment-based design of the novel methylselenoesters.

Fifteen new compounds were synthesized and their ability to release CH_3SeH in a modulated way was investigated. In addition, given the redox-modulating properties of Se compounds and based on previous antioxidant results of our work [24,41], the radical scavenging activity was also evaluated. All the compounds were screened against a panel of five cancer cell lines and two non-malignant cell lines. Moreover, two compounds were chosen to further perform mechanistic studies, including modulation of cell cycle, cell death evaluation and interaction with redox active enzymes.

2. Results and Discussion

2.1. Chemistry

Based on our previous research, we designed a new series of methylselenoesters. The selenoester moiety was chosen to facilitate a nucleophilic attack (i.e., water) resulting in the release of the key metabolite CH_3SeH. Diverse active aromatic and heteroaromatic fragments were linked to the methylselenoester in order to provide different hydrolysis modulation, by hindering or facilitating the reaction. Bifunctionalized molecules bearing two methylselenoester groups were also synthesized to analyze if the cytotoxicity could be enhanced.

A novel series of methylselenoesters was synthesized according to previously reported synthetic routes with few modifications [24,42,43]. The reaction of selenium powder and sodium borohydride in water (for compounds **4**, **6**, **8**, **9**, **11**, **14** and **15**) or ethanol (for compounds **1–3**, **5**, **7**, **10**, **12** and **13**) yielded sodium hydrogen selenide, which acts as a nucleophile. Substitution of the corresponding acyl chloride led to the sodium aroyl or heteroaroyl selenide, which was further methylated by an excess of methyl iodide (Scheme 1). Structures of the newly synthesized compounds are shown in Table 1.

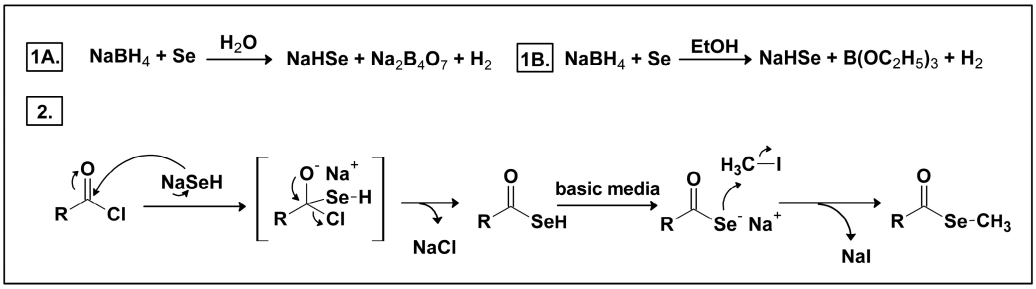
1A.
$NaBH_4 + Se \xrightarrow{H_2O} NaHSe + Na_2B_4O_7 + H_2$
1B.
$NaBH_4 + Se \xrightarrow{EtOH} NaHSe + B(OC_2H_5)_3 + H_2$
2.
NaSeH
NaCl
basic media
H_3C—I
NaI
R Se-CH3

Scheme 1. Synthesis of the methylselenoesters. Synthetic procedure and proposed reaction mechanism for the formation of the methylselenoesters.

Even though acyl chlorides are usually hydrolyzed in aqueous solvents, the compounds might be formed in water due to the fact that NaHSe is a superior nucleophile compared to water and reacts faster. Compounds **1–3**, **5**, **7**, **10**, **12** and **13**, however, could not be obtained in these conditions. Changing the solvent to absolute ethanol not only improved the solubility of the acyl chlorides, but enabled the formation of these compounds. For example, hydrolysis of extremely reactive acyl chlorides before reacting with NaHSe (i.e., the 4-nitrophenyl derivative) might be avoided in absolute ethanol. In addition, ethanol is less polar than water resulting in enhanced nucleophility of NaHSe, thus facilitating the nucleophilic substitution in more deactivated molecules, for instance in those with electron donors (i.e., the 4-methoxyphenyl derivative).

The purity of the newly synthesized compounds was assessed by thin layer chromatography (TLC) and elemental analysis. The compounds were purified mainly by recrystallization in different solvents or by column chromatography using methylene chloride as the eluent. Compounds **3**, **8**, **10** and **12** presented a troublesome purification with poor yields (<20%).

Structures were confirmed by infrared spectroscopy (IR), ^{1}H-NMR, ^{13}C-NMR and mass spectrometry (MS). Regarding IR, a characteristic strong peak corresponding to the carbonyl group appeared at 1620–1681 cm^{-1} whereas peaks corresponding to the methyl group (C–H$_{\text{aliph}}$) appeared at

2918–2981 cm^{-1}. In ^{1}H-NMR, two microsatellites showing coupling of ^{77}Se with ^{1}H ($J_{\text{Se–H}}$ = 5.2–5.6) were characteristic of the methyl group, whose chemical shift appeared at δ 2.28–2.64 ppm. MS data revealed that the base peak in almost all the molecules was the ion resulting from a 95-weight fragment loss, corresponding to CH_3SeH. Interestingly, the base peak of the quinoline derivatives **9** and **10** had also lost the carbonyl group, even though compound **10** had an almost equal abundant ion (96%) which conserved it. For compound **13**, the two ions with and without the carbonyl group coexisted at almost the same abundance (100% and 92%). Compound **11** was the only molecule where the base peak did not correspond to the loss of CH_3SeH but to a more fragmented ion. Compound **15** showed an interesting behavior. The base peak corresponded to the ion resulting from losing only one CH_3SeH group. This did not happen with the other bifunctionalized molecule, compound **14**, whose more stable ion had lost both CH_3SeH moieties in addition to the cyano group.

Table 1. Structure of the novel synthesized methylselenoesters.

General Structure

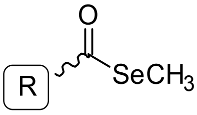

Ref. [a]	**R**	**Solvent** [b]	**Ref.**	**R**	**Solvent**
1	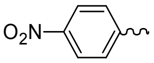	EtOH	**8**	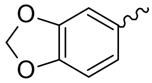	H_2O
2	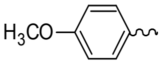	EtOH	**9**	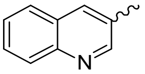	H_2O
3	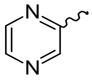	EtOH	**10**	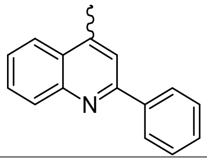	EtOH
4	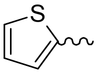	H_2O			
5	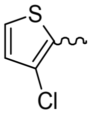	EtOH	**11**	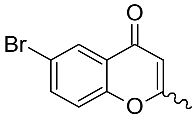	H_2O
6	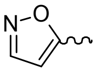	H_2O	**12**	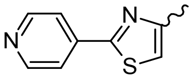	EtOH
7	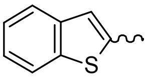	EtOH	**13**	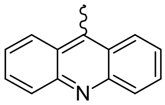	EtOH

General structure

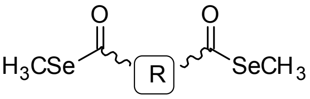

Ref.	**R**	**Solvent**	**Ref.**	**R**	**Solvent**
14	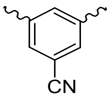	H_2O	**15**	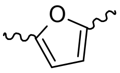	H_2O

The wavy bond indicates the attachment position for the methylselenoester moiety. [a] Compound reference; [b] Solvent used as reaction medium.

2.2. Methylselenol Release Studies

The new compounds were designed as CH_3SeH precursors. The chemical features of the selenoester functional group facilitate a nucleophilic attack (i.e., with water) which would deliver the CH_3SeH residue. In order to verify if CH_3SeH could be released from the molecules by hydrolysis and if the rate differed among the compounds, the reaction of CH_3SeH with 5,5′-dithiobis(2-nitrobenzoic acid) (DTNB or Ellman's reagent) in aqueous environment was monitored [23,44]. Briefly, when the disulfide bridge of DTNB reacts with thiols or selenols, 2-nitro-5-thiobenzoate (TNB^{2-}) is released and the mixed disulfide or selenylsulfide is formed. Each released CH_3SeH produces one yellow TNB^{2-} species, whose absorbance can be quantified at 412 nm (Figure 2A).

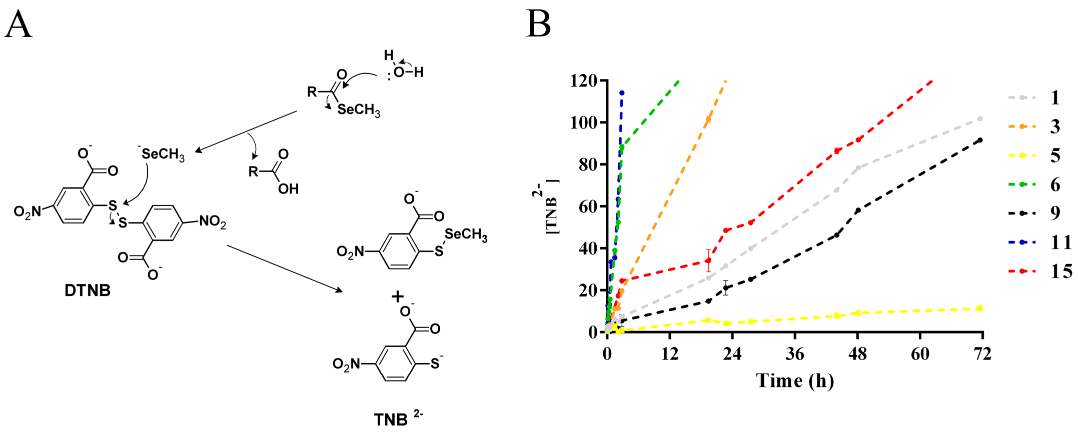

Figure 2. CH_3SeH release rates are dependent on the chemical features of the molecule. Released CH_3SeH was quantified through reaction with Ellman's reagent (DTNB). (**A**) Proposed reaction between CH_3SeH and DTNB; (**B**) Quantification of TNB^{2-} at different times. The compounds were tested at 100 μM in 200 μL of 100 mM phosphate buffer (1 mM EDTA, pH = 8). DTNB concentration was also 100 μM. Absorbance was followed at 412 nm over 72 h. A cysteine standard curve (7.5–150 μM) was used to calculate the concentration of TNB^{2-} over time. Compounds showing less than 15% hydrolysis at 72 h are not included, except for compound **5** as example. Error bars indicate SD of triplicates.

Results showed that the hydrolysis rate in these conditions varied among the compounds, as intended in the design of the molecules (Figure 2B). A fast release was observed for compounds **6** and **11**, which were completely hydrolyzed within the first two hours of incubation. CH_3SeH was completely released from compound **3** at 24 h whereas a more sustained release corresponded, in this order, to compounds **15**, **1**, and **9**. However, the remaining compounds were hardly hydrolyzed (<15%) at 72 h. Unfortunately, compound **12** could not be tested due to reproducibility issues caused by lack of solubility in the assay conditions.

Results from this assay might not be predictive of the behavior of the compounds in other biological matrixes due to different testing conditions. In addition, other mechanisms rather than hydrolysis could lead to the release of methylselenol in the cell culture. However, we demonstrate that the chemical features are diverse enough to differentially modulate the lability of the carbonyl-selenium bond in this particular setting.

2.3. Theoretical Calculations of Molecular Properties

In order to provide a theoretical prediction of the drug-likeness properties of the new methylselenoesters, the freely accessible Molinspiration and Osiris DataWarrior programs were employed.

2.3.1. Molinspiration Calculations

Molinspiration calculations predict large values of logP, fitting all the compounds the recommended range of $0 \leq \log P \leq 5$ (Table 2). In fact, most of the derivatives present a logP value around the mean value of this range, which can be considered as the optimal relation between hydrophilicity and lypophilicity. Also, the theoretical values obtained are in accordance with the expected fact that structures with 3 aromatic rings (compounds **10** and **13**) should be the most lypophilic derivatives, showing higher logP values.

Table 2. Theoretical calculations of molecular properties based in Molinspiration calculations.

	Molinspiration Calculations							
Compound	**milogP** [a]	**PSA** [b]	**MW** [c]	**nON** [d]	**nOHNH** [e]	**nViolations** [f]	**Nrotb** [g]	**Volume**
1	2.39	62.90	244.11	4	0	0	3	166.41
2	2.48	26.30	229.14	2	0	0	3	168.62
3	0.96	42.85	201.09	3	0	0	2	134.77
4	2.33	17.07	205.14	1	0	0	2	133.79
5	2.93	17.07	239.59	1	0	0	2	147.33
6	1.15	43.10	190.09	3	0	0	2	120.49
7	3.63	17.07	255.20	1	0	0	2	177.78
8	2.32	35.54	243.12	3	0	0	2	167.01
9	2.41	29.96	250.16	2	0	0	2	182.91
10	4.55	29.96	326.26	2	0	0	3	254.32
11	3.33	47.28	346.04	3	0	0	2	205.51
12	2.23	42.85	283.21	3	0	0	3	196.89
13	4.19	29.96	300.22	2	0	0	2	226.91
14	2.60	57.93	345.12	3	0	0	4	218.97
15	2.41	47.28	310.07	3	0	0	4	183.68
MSA	0.60	37.30	127.00	2	1	0	0	68.78

[a] Octanol/water partition coefficient; [b] Molecular Polar Surface Area; [c] Molecular weight; [d] H-bond acceptors; [e] H-bond donors; [f] Number of violations of Lipinski's Rule of Five; [g] Number of rotatable bonds.

Furthermore, polar surface area (PSA) values equal to or greater than 140 are expected to exhibit poor intestinal absorption. All the values predicted are significatively below this threshold, pointing towards excellent intestinal absorption (Table 2).

To summarize, each of the fifteen selenoesters obtained shows good to excellent values for the calculated molecular descriptors and fulfills every facet of the Lipinski's Rule of Five. This fact suggests that these CH_3SeH precursors may show bioavailability, metabolic stability and transport properties comparable to known drugs.

2.3.2. Osiris DataWarrior Calculations

Toxicity risks predicted by using Osiris-based calculations are shown in Table 3. Nine out of the fifteen compounds showed no toxicity for the four toxic parameters predicted. However, although the drug-likeness scores are low for all of the compounds, we hypothesized that this might be due to the presence of the Se atom, which is treated by the program as a hazardous element. Nevertheless, a wide range for this drug-likeness score can be found among the Se compounds synthesized. Noteworthy, thirteen compounds exhibit better drug-likeness values than the reference MSA. Compounds **12**, **4**, **7**, **15** and **5**, in this order, present the five highest values predicted.

Table 3. Predicted toxicity of the compounds according to Osiris DataWarrior-based calculations.

Compound	Toxicity Level				Osiris Calculations
	Mutagenic	Tumorigenic	Irritant	RE [a]	DL [b]
1	🟩	🟥	🟩	🟩	−10.80
2	🟩	🟥	🟩	🟩	−5.34
3	🟩	🟩	🟩	🟩	−5.25
4	🟩	🟩	🟩	🟩	−1.96
5	🟩	🟩	🟩	🟩	−2.77
6	🟩	🟥	🟩	🟩	−5.52
7	🟩	🟩	🟩	🟩	−2.67
8	🟩	🟩	🟩	🟩	−2.91
9	🟩	🟩	🟩	🟩	−5.25
10	🟩	🟩	🟩	🟩	−5.25
11	🟥	🟩	🟩	🟩	−4.86
12	🟩	🟩	🟩	🟩	−0.85
13	🟧	🟧	🟩	🟩	−5.25
14	🟩	🟥	🟩	🟩	−9.53
15	🟩	🟩	🟩	🟩	−2.76
MSA	🟥	🟩	🟩	🟩	−5.69

[a] Reproductive effects; [b] Drug-likeness. 🟥 High risk; 🟧 Mild risk; 🟩 No risk.

2.4. Biological Studies

2.4.1. Radical Scavenging Activity of the New Methylselenoesters

Se compounds have a dual role as pro-oxidant and antioxidant, depending on the dose and the chemical species. In fact, the chemopreventive activity of Se is believed to be due to its antioxidant features through incorporation into selenoproteins. Aiming to have a first approach on the redox properties, we analyzed the radical scavenging capability of the novel methylselenoesters. First, the reduction of 1,1-diphenyl-2-picrylhydrazyl (DPPH) was measured. Compounds were tested at 100 µM up to 3 h and ascorbic acid was included as a positive control. Except for compound **11**, which showed similar activity to ascorbic acid after 1 h incubation, none of the compounds demonstrated radical scavenging properties (Figure 3A,B). To validate the antioxidant properties of compound **11**, the reduction of another radical, 2,2-azinobis(3-ethylbenzothiazoline-6-sulphonic acid) ($ABTS^{+\cdot}$), was also tested. The radical scavenging activity of compound **11** towards this radical was similar to ascorbic acid at 100 µM (Figure 3C) but at lower concentrations, ascorbic acid demonstrated greater antioxidant properties than compound **11**.

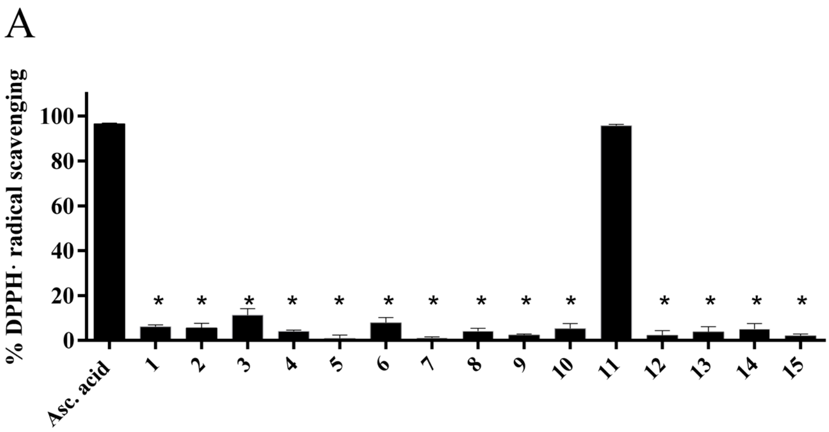

Figure 3. *Cont.*

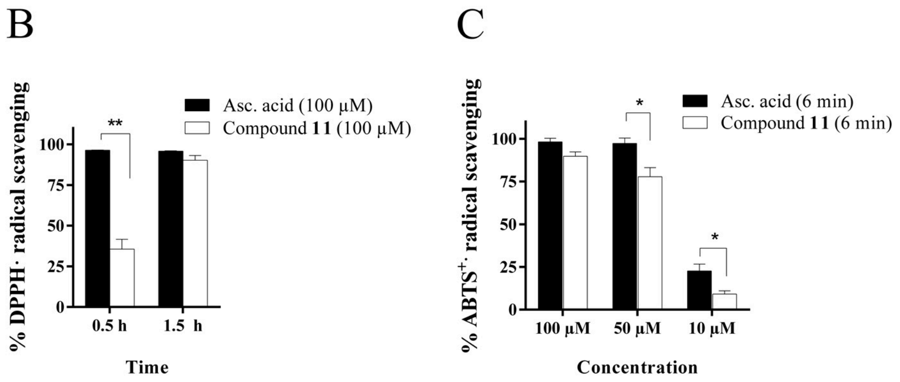

Figure 3. Compound **11** shows radical scavenging activity against DPPH· and ABTS+· radicals. (**A**) DPPH· radical scavenging activity of the methylselenoesters and ascorbic acid (Asc. acid) (100 µM) after 3 h incubation. Results represent the mean ± SEM of at least three independent assays performed in triplicate; (**B**) DPPH· radical scavenging activity of compound **11** at different times. Results represent the mean ± SEM of at least three independent assays performed in triplicate; (**C**) ABTS+· radical scavenging activity of compound **11** at different concentrations after 6 min incubation. Results represent the mean ± SD of quadruplicates. * $p < 0.05$, ** $p < 0.01$ with respect to ascorbic acid.

2.4.2. Cytotoxic Activity of the Novel Methylselenoesters

The novel compounds were tested against a panel of different cancer lines: PC-3 (prostate adenocarcinoma), MCF7 (mammary adenocarcinoma), HTB-54 (lung carcinoma), K-562 (chronic myelogenous leukemia) and HT-29 (colorectal adenocarcinoma). Two non-malignant cell lines, BEAS-2B (bronchial epithelial) and 184B5 (mammary epithelial) were also included to evaluate the toxicity of the novel synthesized compounds. The antiproliferative activity was measured with the [3-(4,5-dimethylthiazol-2-yl)-2,5-diphenyltetrazolium bromide] (MTT) assay after 72 h treatment. Six concentrations ranging from 0.1 to 100 µM were tested. MSA is largely known as the main CH_3SeH putative precursor and was therefore included as positive control. The following parameters were calculated: GI_{50} (concentration which reduces the growth by 50%), TGI (concentration completely inhibiting growth) and LC_{50} (concentration that kills 50% of the cells). Results are summarized in Table 4.

Table 4. Cytotoxic activity of the novel methylselenoesters at 72 h. Average GI_{50}, TGI and LC_{50} ± SD values are expressed in µM.

	Cell Line								
No.	**PC-3** [a]			**MCF7** [b]			**184B5** [c]		
	GI_{50}	**TGI**	**LC_{50}**	**GI_{50}**	**TGI**	**LC_{50}**	**GI_{50}**	**TGI**	**LC_{50}**
1	5.8 ± 0.7	10.4 ± 2.3	75.7 ± 3.3	4.1 ± 0.5	7.9 ± 0.9	45.0 ± 4.6	3.4 ± 0.4	6.4 ± 1.1	9.3 ± 0.6
2	7.3 ± 1.7	45.1 ± 4.5	>100	4.1 ± 0.8	9.3 ± 4.1	74.8 ± 4.0	3.7 ± 0.8	6.4 ± 1.5	9.0 ± 2.1
3	5.4 ± 1.1	15.3 ± 1.7	60.5 ± 4.3	3.5 ± 0.8	7.2 ± 1.0	40.1 ± 4.4	3.1 ± 0.5	6.6 ± 0.9	17.6 ± 4.4
4	5.2 ± 0.9	19.4 ± 3.6	62.0 ± 4.9	5.3 ± 1.4	22.8 ± 3.8	89.6 ± 4.1	3.6 ± 0.8	7.2 ± 1.4	27.9 ± 4.6
5	8.6 ± 1.7	47.7 ± 2.9	91.6 ± 3.9	3.1 ± 0.9	6.9 ± 1.1	35.9 ± 4.4	3.5 ± 0.4	5.9 ± 0.3	8.3 ± 0.2
6	4.5 ± 1.3	7.7 ± 0.1	61.5 ± 14.0	3.5 ± 1.0	8.8 ± 0.7	71.9 ± 3.2	2.7 ± 0.2	6.0 ± 0.4	9.3 ± 2.0
7	18.4 ± 4.5	47.8 ± 3.9	77.3 ± 4.5	6.9 ± 1.4	61.6 ± 4.1	>100	3.9 ± 1.2	6.9 ± 1.7	9.9 ± 0.8
8	5.7 ± 1.6	11.0 ± 3.1	96.0 ± 4.7	4.6 ± 0.5	9.2 ± 1.3	68.7 ± 2.5	3.7 ± 0.3	6.4 ± 0.2	9.0 ± 0.4
9	5.9 ± 0.5	10.0 ± 1.9	84.1 ± 8.9	4.4 ± 0.8	8.1 ± 1.2	48.0 ± 7.5	3.7 ± 0.5	6.2 ± 0.4	8.6 ± 0.4
10	4.4 ± 1.3	9.9 ± 4.7	70.9 ± 5.2	5.6 ± 1.3	51.3 ± 3.7	>100	3.9 ± 0.7	6.3 ± 0.5	8.7 ± 0.4
11	5.3 ± 1.1	17.1 ± 5.0	66.2 ± 2.4	4.2 ± 0.7	8.2 ± 1.1	>100	3.3 ± 0.1	6.7 ± 0.9	14.5 ± 4.5
12	16.9 ± 4.1	50.9 ± 4.9	85.0 ± 4.7	4.4 ± 1.0	8.1 ± 1.7	56.2 ± 9.6	3.4 ± 0.3	6.5 ± 0.8	9.6 ± 2.8
13	39.7 ± 5.1	>100	>100	4.2 ± 1.8	35.4 ± 4.7	83.4 ± 4.1	6.6 ± 1.2	26.8 ± 1.0	65.0 ± 4.5
14	7.2 ± 3.5	32.3 ± 3.7	68.7 ± 3.0	4.9 ± 0.8	8.4 ± 1.1	54.4 ± 2.7	3.8 ± 0.7	6.5 ± 0.6	9.3 ± 0.7
15	4.8 ± 0.8	8.4 ± 0.6	47.8 ± 4.4	1.8 ± 0.9	7.2 ± 1.9	57.0 ± 4.0	3.5 ± 1.1	6.4 ± 0.5	9.2 ± 0.9
MSA	4.4 ± 1.1	8.5 ± 2.4	47.6 ± 4.6	1.5 ± 0.5	5.4 ± 0.5	9.4 ± 1.0	5.3 ± 1.2	9.2 ± 1.3	13.1 ± 1.3

Table 4. *Cont.*

	Cell Line											
No.	**K-562** [d]			**HT-29** [e]			**HTB-54** [f]			**BEAS-2B** [g]		
	GI$_{50}$	**TGI**	**LC$_{50}$**	**GI$_{50}$**	**TGI**	**LC$_{50}$**	**GI$_{50}$**	**TGI**	**LC$_{50}$**	**GI$_{50}$**	**TGI**	**LC$_{50}$**
1	50.1 ± 2.3	85.3 ± 4.9	>100	5.0 ± 0.7	9.3 ± 1.4	87.2 ± 5.0	22.5 ± 4.5	50.5 ± 5.1	78.6 ± 2.9	3.8 ± 0.3	6.4 ± 0.4	9.0 ± 0.7
2	40.8 ± 4.8	70.6 ± 5.9	>100	4.1 ± 0.1	7.5 ± 1.1	50.0 ± 2.4	6.8 ± 1.7	29.7 ± 4.3	70.0 ± 2.9	3.2 ± 0.5	5.8 ± 0.6	8.4 ± 1.0
3	30.2 ± 2.2	59.1 ± 2.1	87.9 ± 2.0	4.7 ± 0.6	9.1 ± 0.8	>100	6.2 ± 1.5	21.1 ±4.1	71.1 ± 3.8	3.6 ± 0.6	6.1 ± 0.5	8.6 ± 0.5
4	40.6 ± 4.5	74.6 ± 4.9	>100	3.4 ± 0.2	7.2 ± 1.2	47.5 ± 3.2	8.5 ± 3.1	39.0 ± 3.1	73.9 ± 4.1	2.9 ± 0.3	5.8 ± 0.7	8.7 ± 2.1
5	38.7 ± 2.1	67.0 ± 1.9	95.2 ± 2.2	3.6 ± 0.3	6.3 ± 0.2	8.9 ± 0.2	4.9 ± 0.2	9.3 ± 2.7	61.5 ± 3.2	2.7 ± 0.5	5.3 ± 0.7	8.0 ± 1.0
6	18.5 ± 7.1	58.3 ± 3.5	98.1 ± 0.7	5.0 ± 0.8	15.1 ± 6.7	90.8 ± 15.0	9.0 ± 2.8	43.9 ± 3.9	82.0 ± 1.3	3.0 ± 0.9	5.6 ± 0.7	8.2 ± 0.5
7	29.2 ± 4.4	58.8 ± 1.5	88.3 ± 3.3	3.7 ± 0.2	7.4 ± 0.9	41.8 ± 4.5	17.5 ± 4.2	55.4 ± 4.4	93.4 ± 4.8	3.9 ± 0.6	6.8 ± 0.8	9.8 ± 1.1
8	29.7 ± 4.7	62.6 ± 3.9	95.4 ± 4.9	5.9 ± 0.8	27.7 ± 4.5	81.1 ± 4.0	6.0 ± 0.9	23.2 ± 2.6	77.1 ± 4.9	3.1 ± 0.3	5.6 ± 0.6	8.0 ± 1.1
9	39.5 ± 3.1	72.6 ± 4.1	>100	3.4 ± 0.2	7.0 ± 0.2	37.2 ± 5.0	7.8 ± 1.2	33.0 ± 4.5	69.2 ± 2.7	4.1 ± 1.0	7.1 ± 4.5	15.3 ± 9.1
10	9.7 ± 4.9	59.1 ± 3.5	>100	4.1 ± 0.3	7.5 ± 0.7	35.0 ± 2.4	5.9 ± 1.1	16.7 ± 2.3	64.4 ± 4.2	3.1 ± 0.5	5.5 ± 0.4	7.8 ± 0.5
11	81.9 ± 4.0	>100	>100	4.9 ± 0.7	9.6 ± 3	74.4 ± 4.2	9.4 ± 3.5	52.3 ± 2.9	>100	2.4 ± 0.9	5.0 ± 0.8	7.6 ± 0.7
12	82.0 ± 4.4	>100	>100	5.1 ± 0.1	14.2 ± 6.6	>100	9.8 ± 5.1	44.9 ± 3.7	80.5 ± 3.5	3.7 ± 1.3	6.4 ± 1.3	9.2 ± 1.0
13	n.a. [h]	n.a.	n.a.	6.0 ± 0.5	16.5 ± 1.9	66.6 ± 0.1	n.a.	n.a.	n.a.	3.8 ± 0.1	6.4 ± 0.2	8.9 ± 0.4
14	29.9 ± 0.6	54.7 ± 0.7	79.5 ± 0.7	3.8 ± 0.1	7.9 ± 0.7	>100	3.8 ± 0.6	7.7 ± 1.0	66.5 ± 4.5	3.2 ± 0.7	5.5 ± 0.5	7.8 ± 0.3
15	42.0 ± 3.8	70.6 ± 3.4	99.2 ± 5.3	3.0 ± 0.5	6.6 ± 0.4	35.8 ± 5.0	15.6 ± 4.3	46.0 ± 3.0	76.3 ± 1.1	2.6 ± 0.8	5.6 ± 0.9	8.6 ± 1.2
MSA	n.a.	n.a.	n.a.	n.a.	n.a.	n.a.	3.5 ± 0.1	6.9 ± 0.2	19.9 ± 1.2	3.7 ± 0.7	6.2 ± 1.2	8.7 ± 1.8

[a] Prostate adenocarcinoma; [b] Mammary adenocarcinoma; [c] Non-malignant mammary epithelium; [d] Chronic myelogenous leukemia; [e] Colorectal adenocarcinoma; [f] Lung carcinoma; [g] Non-malignant bronchial epithelial; [h] Data not available.

As shown in the table, every compound was able to inhibit proliferation, with compounds **2–6**, **8–11** and **14** presenting GI_{50} values below 10 µM in PC-3, MCF7, HT-29 and HTB-54, and greater than 10 µM in K-562, which was the most resistant cell line. GI_{50} values greater than 10 µM were also found for compounds **7**, **12** and **13** towards the prostate cancer cell line, and for compounds **1**, **7** and **15** against the lung cancer cell line, indicating that a higher dose of these compounds was needed to inhibit proliferation. When comparing compounds **4** and **5**, we found that the inclusion of an electron-withdrawing atom in the thiophene ring (compound 5) improved the activity in MCF7 (LC_{50} = 89.6 µM, LC_{50} = 35.9 µM, respectively) and HT-29 (LC_{50} = 47.5 µM, LC_{50} = 8.9 µM, respectively) but not in PC-3 or HTB-54. However, the presence of two methylseleno moieties did not particularly enhance potency, as neither compound **14** nor **15** had significantly lower GI_{50}, TGI or LC_{50} values than the monofunctionalized molecules. Regarding TGI, higher values were generally found in HTB-54 and PC-3 cell lines than in MCF7 and HT-29. On the contrary, low TGI values (<10 µM) were found for compounds **5** and **14** in HTB-54 and for compounds **6**, **10**, and **15** in PC-3. Finally, when considering the LC_{50} parameter, all the compounds exhibited similar moderate potencies. In fact, the compounds were more cytostatic than cytotoxic due to high LC_{50} values (>30 µM).

The similar behavior of the compounds might support a shared mechanism of action for all of them. This led us to consider CH_3SeH as the ultimate effector of the biological activity. However, we could not establish a clear correlation between CH_3SeH release rates due to hydrolysis in the Ellmans's assay and biological activity at the tested time period. The different conditions of both experiments could be an explanation for this fact. Besides, cell culture could modify the release rates: in addition to hydrolysis, other factors might be taking place, such as cell uptake before the molecules are hydrolyzed; cell metabolism leading to release of methylselenol; or concomitant reactions of the molecules with medium components. In fact, to evaluate if the acidic residue contributed to the activity in case of hydrolysis in the cell culture, we tested the corresponding acids. Given that CH_3SeH has been largely characterized in mammary carcinoma [45,46], we chose this cell line (MCF7) for further studies. Although the residues had been selected according to an active fragment-based approach, the acidic forms were not toxic at 72 h (GI_{50} > 100 µM), thus supporting CH_3SeH as the effector of the toxic activity.

Regarding the non-malignant cell lines, the positive control MSA was found to be toxic. Consistently, the new CH_3SeH precursors were also toxic for BEAS-2B and 184B5. Their toxicity, however, was in the same range as MSA, which has been broadly studied both in vitro and in vivo [7,47].

Taking into account all the data, and on the basis of similarity to MSA kinetic parameters in both tumor MCF7 and non-malignant 184B5 cell lines, compounds **5** and **15** exhibited the most similar profile. In addition, compounds **5** and **15** did not violate Lipinski's Rule of Five, presented good drug-likeness parameters and were among the five best compounds according to Osiris DataWarrior predictions. For these reasons, compounds **5** and **15** were selected for further characterization of their mechanism of action on the MCF7 cell line.

2.4.3. Compounds **5** and **15** Lead to Cell Cycle Arrest in G_2/M Phase

Cell cycle arrest is the target of many anticancer drugs, as it is the first step to decrease cell proliferation. To gain a better understanding of the mechanism of these compounds, the effect of compounds **5** and **15** on cell cycle distribution was analyzed. MCF7 cells were treated with increasing concentrations of both compounds for 24 h or with 15 µM **5** or 30 µM **15** for different times. The negative control was treated with vehicle, and camptothecin (6 µM) was used as a positive control. Samples were stained with propidium iodide using the Apo-Direct kit (BD Pharmingen, Madrid, Spain) and processed by flow cytometry.

As shown in Figure 4, treatment with compounds **5** and **15** increased the percentage of cells in G_2/M phase. This increase was dose-dependent at 24 h and evident for compound **15** when cells were treated with 7 µM or higher concentrations whereas it was observed for compound **5** only from 15 µM treatment. In the time-course analysis, we found an increase in G_2/M phase after 8 h treatment for both compounds that was correlated with a significant decrease in the G_0/G_1 phase at 8 h for compound **5** and 16 h for compound **15**. We conclude that these results indicate a cell cycle blockage in G_2/M phase.

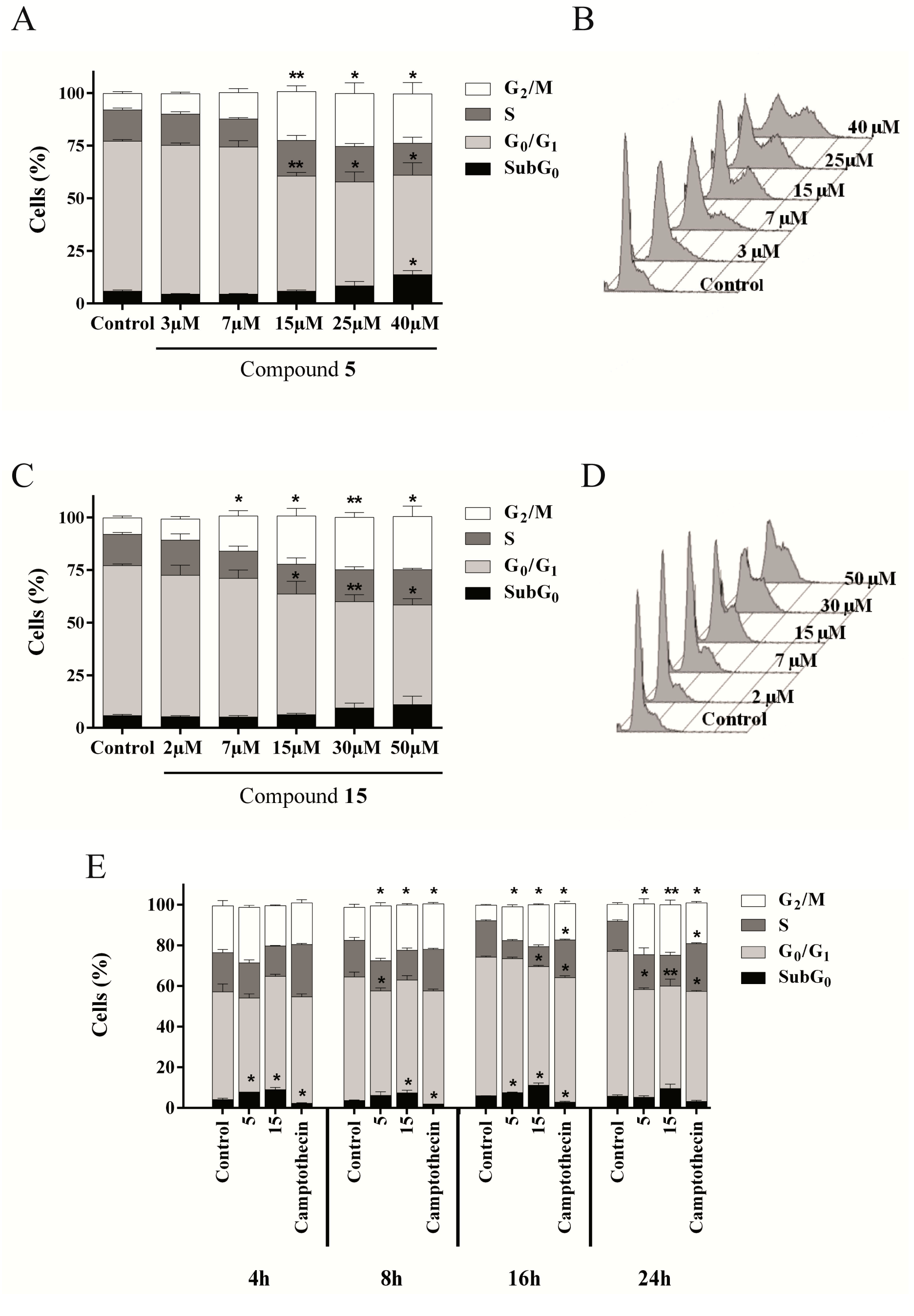

Figure 4. Compounds **5** and **15** induce cell cycle arrest in G_2/M phase in MCF7. MCF7 cells were treated with different concentrations of compound **5**, **15** or vehicle (control) for 24 h or for different time periods. Cells were stained with propidium iodide with the Apo-Direct kit and analyzed by flow cytometry. (**A**) Quantification of cell cycle distribution after 24 h treatment with increasing concentrations of compound **5**; (**B**) Representative experiment of A; (**C**) Quantification of cell cycle distribution after 24 h treatment with increasing concentrations of compound **15**; (**D**) Representative experiment of C; (**E**) Cell cycle distribution after treatment with vehicle, 15 μM of compound **5** or 30 μM of compound **15** for different times. Results represent the mean ± SEM of at least three independent experiments performed in duplicate. * $p < 0.05$, ** $p < 0.01$.

2.4.4. Evaluation of Cell Death Mechanism Induced by Compounds **5** and **15**

Induction of cell death is the major aim of antitumor drugs. We analyzed cell death progression using the TUNEL technique (in the Apo-Direct kit), which is based on DNA fragmentation. MCF7 cells were treated with increasing concentrations of compounds **5** and **15** for 24 h or with 30 µM of compound **15** or 15 µM of compound **5** for different times. The negative control was treated with vehicle, and camptothecin (6 µM) was included as a positive control.

Both compounds exhibited a dose-dependent effect at 24 h (Figure 5A), but only compound **15** caused cell death in a time-dependent manner (Figure 5B). Cell death was evident from only 4 h treatment for both compounds. However, whereas cell death induced by compound **15** rose from 20% of dead cells at 4 h up to 80% at 48 h, the highest values of cell death for compound **5** were observed after 4 h treatment.

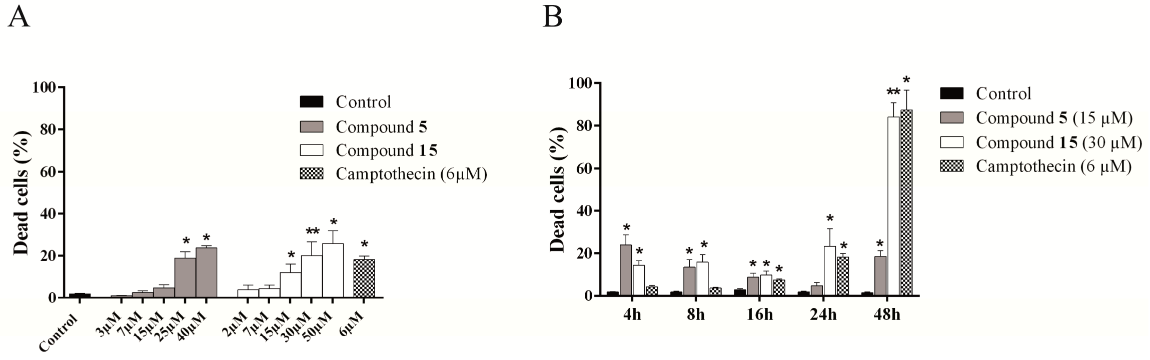

Figure 5. Cell death induction is dose and time-dependent for compound **15** in MCF7. MCF7 cells were treated with vehicle (control) or increasing doses of compound **5** or **15** for 24 h. For the time-course experiment, MCF7 cells were treated with vehicle (control), compound **5** (15 µM) or compound **15** (30 µM) for different times. Camptothecin (6 µM) was included as positive control. Cells were stained with the Apo-Direct kit (TUNEL assay) and analyzed by flow cytometry. (**A**) Dose-dependent cell death at 24 h; (**B**) Time-course analysis of cell death. Results show the mean ± SEM of at least three independent experiments performed in duplicate. * $p < 0.05$, ** $p < 0.01$.

Se compounds induce different types of cell death, among which apoptosis and autophagy are the most common. To further elucidate the pathway through which compounds **5** and **15** trigger cell death, we used Z-VAD-FMK, a pan-caspase inhibitor and wortmannin, a PI3K inhibitor which blocks autophagy. MCF7 cells were pre-incubated for 1 h with 50 µM of Z-VAD-FMK or 100 nM wortmannin and co-incubated with compound **5** (25 µM), compound **15** (30 µM) or vehicle (control) for 48 h. Treated cells without inhibitors were also included.

As shown in Figure 6, cell death induced by the novel methylselenoesters was not altered in the presence of wortmannin, ruling out autophagy as a mechanism of action. On the other hand, cell death was partially prevented when cells were treated in the presence of the pan-caspase inhibitor. Cell death induced by compound **5** was decreased by 36%, whereas the total number of dead cells was decreased by 14% in case of compound **15**. These results indicate that caspases are at least partially implicated in the cell death mechanism of these compounds. In fact, CH_3SeH has been described to induce caspase-mediated cell death [47,48].

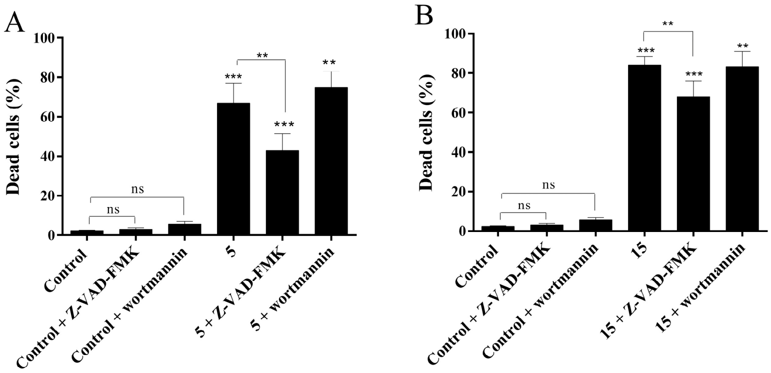

Figure 6. Cell death induced by compounds **5** and **15** involves the caspases pathway. MCF7 cells were pre-incubated with 50 μM of Z-VAD-FMK or 100 nM wortmannin for 1 h before treating cells with compound **5** (25 μM), compound **15** (30 μM) or vehicle (control) for 48 h. Cells were stained with the Apo-Direct kit (TUNEL assay) and analyzed by flow cytometry. (**A**) Cell death induced by compound **5** in the presence and absence of the inhibitors; (**B**) Cell death induced by compound **15** in the presence and absence of the inhibitors. Results show the mean ± SEM of at least three independent experiments performed in duplicate, ** $p < 0.01$, *** $p < 0.001$.

2.4.5. Compounds **5** and **15** are Substrates for Thioredoxin Reductase But not for the Glutathione-Glutaredoxin System

Metabolism is crucial for Se compounds, as the biological activity is mainly exerted through their metabolites. It has been described that Se compounds can be metabolized by redox active enzymes [49,50]. Thus, in an attempt to refine possible metabolic pathways, we examined whether compounds **5** and **15** interacted with thioredoxin reductase (TrxR) and/or the gluthatione-glutaredoxin (GSH-Grx) system. We used MSA as control, as it is known to be reduced by both GSH and TrxR [51,52].

Our results indicated that, while MSA was consistently reduced by both TrxR1 and GSH in accordance with previous studies, compounds **5** and **15** were substrates only for TrxR1 (Figure 7). The reduction by TrxR1 is considerably more efficient compared the spontaneous hydrolysis, indicating that this would facilitate the release of the active CH_3SeH metabolite intracellularly.

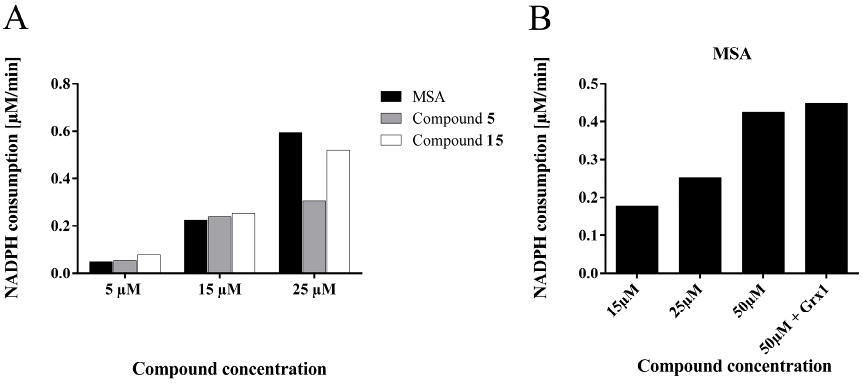

Figure 7. Compounds **5** and **15** are substrates for thioredoxin reductase but not for the glutathione-glutaredoxin system. (**A**) NADPH consumption indicating reduction of compounds **5**, **15** or MSA as control by thioredoxin reductase. The reaction mixture contained 100 nM TrxR1, 227 μM NADPH and the corresponding amount of compound in TE buffer (20 mM Tris, 2 mM EDTA pH = 8); (**B**) NADPH consumption indicating reduction of MSA by glutathione in the presence or absence of glutaredoxin. The reaction mixture contained the corresponding amount of compound, 0.1 M Tris, 2 mM EDTA pH = 8, 0.1 mg/mL BSA, 1 mM GSH, 200 μM NADPH, 0.008 OD/mL yeast GR and 1 μM hGrx1 when required. Only results for MSA are shown, as compounds **5** and **15** were not reduced.

3. Material and Methods

3.1. General Information

Melting points (m.p.) were determined with a FP82 + FP80 apparatus (Mettler, Greifensee, Switzerland). The NMR spectra (^{1}H/400 MHz and ^{13}C/100 MHz, Supplementary Materials) were recorded on a Ultrashield^{TM} 400 spectrometer (Bruker, Rheinstetten, Germany). The samples were dissolved in DMSO-d_6 or $CDCl_3$ and TMS was used as internal standard. IR spectra were obtained on a FT-IR Nexus spectrophotometer (Thermo Nicolet, Madison, WI, USA) using KBr pellets for solids or NaCl plates for oil compounds. Elemental analysis was performed on a CHN-900 Elemental Analyzer (LECO, Saint Joseph, MI, USA). HRMS were recorded using an Accurate-Mass TOF LC/MS 6220 (Agilent Technologies, Santa Clara, CA, USA). Only data from compounds **3**, **9**, **10**, **12** and **13** could be obtained due to poor volatilization of the remaining compounds. For TLC assays, Alugram SIL G7UV254 sheets (Macherey-Nagel; Düren, Germany) were used. Column chromatography was performed with silica gel 60 (Merck, Darmstadt, Germany). Chemicals were purchased from E. Merck, Panreac Química S.A. (Montcada i Reixac, Barcelona, Spain), Sigma-Aldrich Quimica, S.A. (Madrid, Spain) and Acros Organics (Janssen Pharmaceuticalaan, Geel, Belgium).

3.2. Chemistry

3.2.1. General Procedure

Following a described procedure [24,42,43] with a few modifications, sodium borohydride was slowly added to a suspension of selenium powder in water at room temperature or in ethanol, N_2 atmosphere and 0 °C, and stirred until the formation of the typical colorless solution of NaHSe. Then, the corresponding aroyl or heteroaroyl chloride was added. Temperature and time of reaction varied depending on the compounds. Methylation was achieved through the addition of methyl iodide (in excess). Purification was performed by several washings, recrystallization in different solvents or column chromatography. In those cases where the acyl chloride was not available, it was formed by the reaction of the corresponding carboxylic acid with $SOCl_2$ for 1–8 h at reflux. Solvent was removed under vacuum by rotatory evaporation, and the product was then washed three times with dry toluene, which was also eliminated by rotatory evaporation.

3.2.2. General Procedure for Compounds **4**, **6**, **8**, **9**, **11**, **14** and **15**

Sodium borohydride (4.15 mmol) was added to a suspension of powdered selenium (2 mmol) in water at room temperature. Discoloration to a colorless solution indicated the formation of sodium hydrogen selenide. Then, a solution of the acyl or heteroaroyl chloride in chloroform was added (2 mmol) and the mixture was stirred at 50 °C for 1 h, unless stated otherwise. For the bifunctionalized molecules (compounds **14** and **15**), 8.3 mmol of sodium borohydride, 4 mmol of powdered selenium and 2 mmol of the acyl chloride were used. Reaction was followed by TLC or IR. After filtering insoluble salts, an excess of methyl iodide (1.5 mL) was added and the reaction was heated at the same temperature (1 h, unless stated otherwise) until precipitation of the product or discoloration of the aqueous phase. The solid was filtered or extracted with methylene chloride, washed with slightly basic water and dried over Na_2SO_4. The solvent was eliminated under rotatory evaporation. Compounds were purified through recrystallization in appropriate solvents or column chromatography using methylene chloride as eluent (mobile phase).

Methyl 2-thiophencarboselenoate (**4**). From 2-thiophencarbonyl chloride. A yellow oil was obtained which was further purified by column chromatography. Yield: 26%. ^{1}H-NMR ($CDCl_3$): δ 2.42 (s, 3H, $–SeCH_3$), 7.15 (dd, 1H, H_4, $J_{4–3}$ = 3.9, $J_{4–5}$ = 4.9 Hz), 7.68 (dd, 1H, H_5, $J_{5–3}$ = 1.2 Hz, $J_{5–4}$ = 4.9 Hz), 7.82 ppm (dd, 1H, H_3, $J_{3–4}$ = 3.9, $J_{3–5}$ = 1.2 Hz). ^{13}C-NMR ($CDCl_3$): δ 5.7 ($–SeCH_3$), 128.3 (C_4), 131.8 (C_5), 133.3 (C_3), 144.3 (C_2), 185.5 ppm (–C=O). IR (KBr): ν 3102 (w, $C–H_{arom}$), 2932 ($C–H_{aliph}$), 1662 cm^{-1}

(–C=O). MS [*m*/*z* (% abundance)]: 206 ($M^{+\bullet}$ +1, 6), 111 (100), 83 (11). Elemental analysis calculated for C_6H_6OSSe (%): C: 35.13, H: 2.95; found: C: 35.20, H: 2.77.

Methyl 5-isoxazolecarboselenoate (**6**). From 5-isoxazolecarbonyl chloride. A brownish solid was obtained. Yield: 49%; m.p.: 41–42 °C. ^{1}H-NMR (DMSO-d_6): δ 2.42 (s, 3H, –$SeCH_3$), 7.40 (d, 1H, H_4, $J_{4–3}$ = 2.0 Hz), 8.92 ppm (d, 1H, H_3, $J_{3–4}$ = 2.0 Hz). ^{13}C-NMR (DMSO-d_6): δ 6.0 (–$SeCH_3$), 107.0 (C_4), 153.3 (C_5), 165.8 (C_3), 183.2 ppm (–C=O). IR (KBr): ν 3158–3101 (w, C–H_{arom}), 2931 (w, C–H_{aliph}), 1693 (s, –CN), 1649 cm^{-1} (s, –C=O). MS [*m*/*z* (% abundance)]: 191 ($M^{+\bullet}$ +1, 15), 96 (100), 68 (63) 113 (46), 40 (57). Elemental analysis calculated for $C_5H_5NO_2Se$ (%): C: 31.60, H: 2.65, N: 7.37; found: C: 31.45, H: 3.03, N: 7.27.

Methyl 1,3-benzodioxole-5-carboselenoate (**8**). From 1,3-benzodioxole-5-carboxylic acid. A yellow solid was obtained, which was purified through recrystallization from diethyl ether:hexane (1:1). Yield: 15%; m.p.: 48–49 °C. ^{1}H-NMR ($CDCl_3$): δ 2.36 (s, 3H, –$SeCH_3$), 6.05 (s, 2H, –CH_2–), 6.84 (d, 1H, H_7, $J_{7–6}$ = 8.2 Hz), 7.35 (s, 1H, H_4), 7.55 ppm (d, 1H, H_6, $J_{6–7}$ = 8.2 Hz). ^{13}C-NMR ($CDCl_3$): δ 4.9 (–$SeCH_3$), 101.7 (C_2), 106.5 (C_7), 107.8 (C_4), 123.2 (C_6), 133.2 (C_5), 147.8 (C_{3a}), 151.8 (C_{7a}), 192.3 ppm (–C=O). IR (KBr): ν 2918 (w, C–H_{aliph}), 1655 (s, –C=O), 1036 (s, C–O–C sym) 925 cm^{-1} (s, C–O–C as). MS [*m*/*z* (% abundance)]: 149 (100), 121 (35), 65 (28), 91 (10). Elemental analysis calculated for $C_9H_8O_3Se$ (%): C: 44.46, H: 3.32; found: C: 44.17, H: 3.91.

Methyl 3-quinolinecarboselenoate (**9**). From 3-quinolinecarboxylic acid. Conditions: 15 min reaction with methyl iodide. A brown solid was obtained. Yield: 43%; m.p.: 74–75 °C. ^{1}H-NMR ($CDCl_3$): δ 2.48 (s, 3H, –$SeCH_3$), 7.66 (dd, 1H, H_6, $J_{6–5}$ = $J_{6–7}$ = 7.5 Hz), 7.87 (dd, 1H, H_7, $J_{7–6}$ = 7.5 Hz, $J_{7–8}$ = 7.7 Hz), 7.99 (d, 1H, H_5, $J_{5–6}$ = 7.5 Hz), 8.21 (d, 1H, H_8, $J_{8–7}$ = 7.7 Hz), 8.72 (s, 1H, H_4), 9.35 ppm (s, 1H, H_2). ^{13}C-NMR ($CDCl_3$): δ 6.0 (–$SeCH_3$), 127.4 (C_6), 128.5 (C_{4a}), 129.5 (C_3), 129.8 (C_5), 132.0 (C_8), 132.9 (C_7), 136.9 (C_4), 147.5 (C_2), 149.9 (C_{8a}), 193.5 ppm (–C=O). IR (KBr): ν 3027 (w, C–H_{arom}), 2955 (w, C–H_{aliph}), 1671 (s, –C=O), 1616 cm^{-1} (s, –C=N). MS [*m*/*z* (% abundance)]: 156 (88), 128 (100), 101 (55), 75 (35). Elemental analysis calculated for $C_{11}H_9NOSe$ (%): C: 52.81, H: 3.63, N: 5.60; found: C: 53.01, H: 3.93, N: 5.39. HRMS calculated for $C_{11}H_{10}NOSe^+$ $[M + H]^+$: 251.9922; found: 251.9978.

Methyl 6-bromochromone-2-carboselenoate (**11**). From 6-bromochromone-2-carboxylic acid. The solid was purified through column chromatography. A yellow solid was obtained. Yield: 27%; m.p.: 156–157 °C. ^{1}H-NMR ($CDCl_3$): δ 2.46 (s, 3H, –$SeCH_3$), 6.93 (s, 1H, H_3), 7.52 (d, 1H, H_8, $J_{8–7}$ = 8.9), 7.86 (dd, 1H, H_7, $J_{7–5}$ = 2.4, $J_{7–8}$ = 8.9), 8.33–8.35 ppm (m, 1H, H_5). ^{13}C-NMR ($CDCl_3$): δ 5.7 (–$SeCH_3$), 101.0 (C_3), 120.2 (C_6), 120.9 (C_8), 126.3 (C_{4a}), 129.0 (C_5), 138.2 (C_7), 154.6 (C_{8a}), 157.1 (C_2), 177.2 (C_4), 190.6 ppm (–C=O). IR (KBr): ν 3039 (w, C–H_{arom}), 2928 (w, C–H_{aliph}), 1676 (s, –C=O), 1645 cm^{-1} (s, –COSe). MS [*m*/*z* (% abundance)]: 346 ($M^{+\bullet}$, 30), 251 (69), 282 (24), 223 (36), 169 (100), 88 (41), 69 (57). Elemental analysis calculated (%) for $C_{11}H_7BrO_3Se$: C: 38.18, H: 2.04; found: C: 37.87, H: 2.21.

Dimethyl 5-cyano-1,3-benzenedicarboselenoate (**14**). From 5-cyano-1,3-benzenedicarboxylic acid. Conditions: 1.5 h reaction with NaHSe and 4 h reaction with methyl iodide. The solid was purified through column chromatography. A pink solid was obtained. Yield: 26%; m.p.: 167–168 °C. ^{1}H-NMR ($CDCl_3$): δ 2.51 (s, 6H, –$SeCH_3$), 8.36 (d, 2H, H_4 + H_6, $J_{4–2}$ = $J_{6–2}$ = 2.7), 8.57 ppm (d, 1H, H_2, $J_{2–4}$ = $J_{2–6}$ = 2.7). ^{13}C-NMR ($CDCl_3$): δ 6.6 (–$SeCH_3$), 114.7 (C_5), 117.1 (–CN), 129.1 (C_4), 134.5 (C_2), 141.0 (C_1 + C_3), 192.9 ppm (–C=O). IR (KBr): ν 3073 (w, C–H_{arom}), 2935 (w, C–H_{aliph}), 2229 (s, –CN), 1670 cm^{-1} (s, –C=O). MS [*m*/*z* (% abundance)]: 252 (59), 129 (100), 101 (84). Elemental analysis calculated for $C_{11}H_9O_2Se_2N$ (%): C: 38.26, H: 2.61, N: 4.05; found: C: 38.36, H: 3.04, N: 3.98.

Dimethyl 2,5-furandicarboselenoate (**15**). From 2,5-furandicarboxylic acid. Conditions: 1.5 h reaction with NaHSe and 3 h reaction with methyl iodide. The solid was purified through column chromatography. A yellow solid was obtained. Yield: 30%; m.p.: 155–157 °C. ^{1}H-NMR ($CDCl_3$): δ 2.43 (s, 6H, –$SeCH_3$), 7.21 ppm (s, 2H, H_3 + H_4). ^{13}C-NMR ($CDCl_3$): δ 5.0 (–$SeCH_3$), 115.0 (C_3 + C_4), 153.7 (C_2 + C_5), 183.6 ppm (–C=O). IR (KBr): ν 2924 (w, C–H_{aliph}), 1643 cm^{-1} (s, –C=O). MS [*m*/*z* (% abundance)]: 312

(179, $M^{+\bullet}$ +2), 217 (100), 189 (42), 133 (54), 94 (62), 66 (68). Elemental analysis calculated for $C_8H_8O_3Se_2$ (%): C: 30.97, H: 2.58; found: C: 31.09, H: 2.86.

3.2.3. General Procedure for Compounds **1–3**, **5**, **7**, **10**, **12** and **13**

Under N_2 atmosphere, absolute ethanol (10 mL) was added to a mixture of $NaBH_4$ (2.15 mmol) and selenium (2 mmol) cooled by an ice bath, with magnetic stirring. Although reaction of these species occurs 1:1, a little excess of $NaBH_4$ was added, due to the slow rate of decomposition of $NaBH_4$ in this solvent reported by Klayman et al. [42] When the typical colorless solution of NaHSe was achieved, the ice bath was removed and the following reactions were carried out at room temperature. The acyl chloride was added and stirred for different amounts of time, depending on the reagents. Reaction was followed by TLC or IR. Before adding an excess of methyl iodide (1.5 mL), the mixture was filtered. After discoloration (20 min–1 h), the mixture was filtered, and ethanol was eliminated with rotatory evaporation or the product was precipitated with water. Compounds were purified through recrystallization from different solvents or column chromatography.

Methyl 4-nitrobenzoselenoate (**1**). From 4-nitrobenzoyl chloride. Conditions: 10 min reaction with NaHSe and 20 min reaction with methyl iodide. The compound was recrystallized from methylene chloride. A yellow powder was obtained. Yield: 28%; m.p.: 78–79 °C. ^{1}H-NMR ($CDCl_3$): δ 2.48 (s, 3H, $–SeCH_3$), 8.07 (d, 2H, $H_2 + H_6$, $J_{2–3} = J_{6–5} = 8.9$ Hz), 8.33 ppm (d, 2H, $H_3 + H_5$, $J_{3–2} = J_{5–6} = 8.9$ Hz). ^{13}C-NMR ($CDCl_3$): δ 6.0 ($–SeCH_3$), 124.1 ($C_3 + C_5$), 127.9 ($C_2 + C_6$), 143.3 (C_1), 150.5 (C_4), 193.7 ppm (–C=O). IR (KBr) ν 1665 (s, –C=O), 1518, 1348, 850 cm^{-1} ($–NO_2$ arom). MS [*m/z* (% abundance)]: 245 (15, $M^{+\bullet}$ +1), 150 (100), 120 (24), 104 (94), 92 (45), 76 (61). Elemental analysis calculated for $C_8H_7NO_3Se$ (%): C: 39.36, H: 2.89, N: 5.74; found: C: 39.40, H: 3.17, N: 5.86.

Methyl 4-methoxybenzoselenoate (**2**). From 4-methoxybenzoyl chloride. Conditions: 1 h reaction with NaHSe and 20 min with methyl iodide. The compound was recrystallized from methylene chloride. A grayish powder was obtained. Yield: 23%; m.p.: 36–37 °C. ^{1}H-NMR ($CDCl_3$): δ 2.38 (s, 3H, $–SeCH_3$), 3.88 (s, 3H, $–OCH_3$), 6.94 (d, 2H, $H_3 + H_5$, $J_{3–2} = J_{5–6} = 8.9$ Hz), 7.91 ppm (d, 2H, $H_2 + H_6$, $J_{2–3} = J_{6–5} = 8.9$ Hz). ^{13}C-NMR ($CDCl_3$): δ 5.0 ($–SeCH_3$), 55.6 ($–OCH_3$), 114.0 ($C_3 + C_5$), 129.4 ($C_2 + C_6$), 132.0 (C_1), 164.0 (C_4), 193.0 ppm (–C=O). IR (KBr): ν 2933–2839 (w, $C–H_{aliph}$), 1652 (–C=O), 1264–1025 cm^{-1} ($–OCH_3$). MS [*m/z* (% abundance)]: 230 ($M^{+\bullet}$ +1, 4), 135 (100), 107 (14), 92 (38), 77 (39), 63 (25). Elemental analysis calculated for $C_9H_{10}O_2Se$ (%): C: 47.18, H: 4.40; found: C: 47.38, H: 4.63.

Methyl pyrazinecarboselenoate (**3**). From pyrazinecarboxylic acid. Conditions: 30 min reaction with NaHSe and 30 min reaction with methyl iodide. The compound was recrystallized from hexane:methylene chloride (1:1). A yellow solid was obtained. Yield: 14%; m.p.: 48–49 °C. ^{1}H-NMR (DMSO-d_6): δ 2.28 (s, 3H, $–SeCH_3$), 8.84 (dd, 1H, H_5, $J_{5–6} = 2.4$, $J_{5–3} = 1.5$ Hz), 9.01 (d, 1H, H_6, $J_{6–5} = 2.4$), 9.03 ppm (d, 1H, H_3, $J_{3–5} = 1.5$ Hz). ^{13}C-NMR (DMSO-d_6): δ 4.9 ($–CH_3$), 140.0 (C_2), 145.8 (C_6), 147.2 (C_5), 150.9 (C_3), 198.0 ppm (–C=O). IR (KBr): ν 2922 (w, $C–H_{aliph}$), 1681 cm^{-1} (s, –C=O). MS [*m/z* (% abundance)]: 202 ($M^{+\bullet}$ +1, 37), 191 (45), 121 (61), 107 (100), 99 (95), 79 (80), 69 (61). Elemental analysis calculated for $C_6H_6N_2OSe$ (%): C: 35.84, H: 3.01, N: 13.93; found: C: 36.02, H: 3.31, N: 13.61. HRMS calculated for $C_6H_7N_2OSe^+$ $[M + H]^+$: 202.9718; found: 202.9778.

Methyl 3-chlorothiophen-2-carboselenoate (**5**). From 3-chlorothiophen-2-carboxylic acid. Conditions: 20 min reaction with NaHSe and 20 min reaction with methyl iodide. The compound was recrystallized from methylene chloride. A brownish powder was obtained. Yield: 31%; m.p.: 35–36 °C. ^{1}H-NMR (DMSO-d_6): δ 2.35 (s, 3H, $–SeCH_3$), 7.33 (d, 1H, H_4, $J_{4–5} = 5.45$ Hz), 8.10 ppm (d, 1H, H_5, $J_{5–4} = 5.45$ Hz). ^{13}C-NMR (DMSO-d_6): δ 6.9 ($–SeCH_3$), 127.9 (C_4), 131.6C_2), 134.7 (C_5), 137.2 (C_3), 184.3 ppm (–C=O). IR (KBr): ν 3096 (w, $C–H_{arom}$), 2938 (w, $C–H_{aliph}$), 1620 cm^{-1} (s, –C=O). MS [*m/z* (% abundance)]: 240 ($M^{+\bullet}$ +1, 5), 211 (31), 145 (100), 43 (35). Elemental analysis calculated for $C_6H_5ClOSSe$ (%): C: 30.08, H: 2.10; found: C: 30.35, H: 2.22.

Methyl benzo[b]thiophene-2-carboselenoate (**7**). From benzo[*b*]thiophene-2-carboxylic acid. Conditions: 30 min reaction with NaHSe and 20 min reaction with methyl iodide. The compound was precipitated with water and recrystallized from methylene chloride. Yield: 35%; m.p.: 65–67 °C. ^{1}H-NMR (DMSO-d_6): δ 2.41 (s, 3H, –SeCH$_3$), 7.50 (ddd, 1H, H_6, $J_{6–7}$ = 8.0, $J_{6–4}$ = 0.7 Hz), 7.57 (ddd, 1H, H_5, $J_{5–4}$ = 8.0, $J_{5–7}$ = 1.2 Hz), 8.08 (d, 1H, H_4, $J_{4–6}$ = 0.7 Hz, $J_{4–5}$ = 8.0), 8.09 (d, 1H, H_7, $J_{7–5}$ = 1.2 Hz), 8.41 ppm (s, 1H, H_3). ^{13}C-NMR (DMSO-d_6): δ 6.3(–SeCH$_3$), 124.1 (C_7), 126.4 (C_5), 127.4 (C_4), 128.9 (C_6), 130.6 (C_3), 139.3 (C_{3a}), 141.8 (C_{7a}), 143.0 (C_2), 187.6 ppm (–C=O). IR (KBr): ν 3064 (w, C–H_{arom}), 2925 (w, C–H_{aliph}), 1657 cm^{-1} (–C=O). MS [*m/z* (% abundance)]: 256 ($M^{+\bullet}$ +1, 6), 161 (100), 133 (42), 89 (65). Elemental analysis calculated for $C_{10}H_8OSSe$ (%): C: 47.06, H: 3.16; found: C: 47.32, H: 3.19.

Methyl 2-phenyl-4-quinolinecarboselenoate (**10**). From 2-phenyl-4-quinolinecarboxylic acid. Conditions: 45 minute reaction with NaHSe cooled in the ice bath and 1 h reaction with methyl iodide at room temperature. The compound was precipitated with water and purified through column chromatography using methylene chloride as eluent. A white solid was obtained. Yield: 11%; m.p.: 119–120 °C. ^{1}H-NMR (CDCl$_3$): δ 2.57 (s, 3H, –SeCH$_3$), 7.54–7.68 (m, 4H, $H_{2'}$ + $H_{3'}$ + $H_{5'}$ + $H_{6'}$), 7.84 (t, 1H, $H_{4'}$, $J_{4'–3'}$ = $J_{4'–5'}$ = 7.7 Hz), 8.23–8.25 (m, 2H, H_6 + H_7), 8.24 (s, 1H, H_3), 8.33–8.41 ppm (m, 2H, H_5 + H_8). ^{13}C-NMR (CDCl$_3$): δ 7.3 (–SeCH$_3$), 117.9 (C_3), 121.4 (C_6), 125.3 (C_5), 128.2 ($C_{2'}$ + $C_{6'}$), 128.8 ($C_{3'}$ + $C_{5'}$), 129.5 ($C_{4'}$), 129.8 (C_{4a}), 130.7 (C_8), 131.3 (C_7), 138.2 ($C_{1'}$), 146.3 (C_4), 148.7 (C_{8a}), 157.3 (C_2), 197.1 ppm (–C=O). IR (KBr): ν 3056 (w, C–H_{arom}), 2922 (w, C–H_{aliph}), 1685 cm^{-1} (s, –C=O). MS [*m/z* (% abundance)]: 327 ($M^{+\bullet}$ +1, 5), 232 (96), 204 (100), 75 (33). Elemental analysis calculated for $C_{17}H_{13}NOSe$ (%): C: 62.58, H: 4.02, N: 4.29; found: C: 62.58, H: 3.89, N: 4.28. HRMS calculated for $C_{17}H_{14}NOSe^+$ $[M + H]^+$: 328.0235; found: 328.0251.

Methyl 2-(4-pyridyl)thiazole-4-carboselenoate (**12**). From 2-(4-pyridyl)thiazole-4-carboxylic acid. Conditions: 30 minute reaction with NaHSe cooled on an ice bath and 30 minute reaction with methyl iodide at room temperature. The compound was recrystallized from methylene chloride and diethyl ether (1:1). A white solid was obtained. Yield: 20%. ^{1}H-NMR (CDCl$_3$): δ 2.40 (s, 3H, –SeCH$_3$), 8.00 (d, 2H, $H_{2'}$ + $H_{6'}$, $J_{2'–3'}$ = $J_{6'–5'}$ = 6.2 Hz), 8.20 (s, 1H, H_5), 8.82 ppm (d, 2H, $H_{3'}$ + $H_{5'}$, $J_{3'–2'}$ = $J_{5'–6'}$ = 6.2 Hz). ^{13}C-NMR (CDCl$_3$): δ 5.3 (–SeCH$_3$), 121.4 ($C_{2'}$ + $C_{6'}$), 122.7 (C_5), 141.1 ($C_{1'}$), 149.6 ($C_{3'}$ + $C_{5'}$), 156.5 (C_4), 164.9 (C_2), 189.7 ppm (–C=O). IR (KBr): ν 3134 (w, C–H_{arom}), 2919 (w, C–H_{aliph}), 1665 (s, C=O), 1132 cm^{-1} (s, thiazole ring vibration). MS [*m/z* (% abundance)]: 284 ($M^{+\bullet}$ +1, 21), 189 (84), 156 (100), 128 (77), 57 (91), 69 (59). Elemental analysis calculated for $C_{10}H_8N_2OSSe$: C: 42.41, H: 2.85, N: 9.89; found: C: 42.14, H: 3.34, N: 9.84. HRMS calculated for $C_{10}H_9N_2OSSe^+$ $[M + H]^+$: 284.9595; found: 284.9578.

Methyl 9-acridinecarboselenoate (**13**). From 9-acridinecarboxylic acid. Before adding the chloride to the reaction, it was dissolved in dry chloroform, treated with triethylamine (1:1) for 20 min to eliminate the hydrochloride and then used for reaction without further treatment. Conditions: 25 min reaction with NaHSe and 25 min reaction with methyl iodide. The compound was recrystallized from hexane. An orange solid was obtained. Yield: 23%; m.p.: 132–134 °C. ^{1}H-NMR (CDCl$_3$): δ 2.64 (s, 3H, –SeCH$_3$), 7.58–7.63 ppm (dd, 2H, H_2 + H_7, $J_{2–3}$ = $J_{7–6}$ = 7.7, $J_{2–1}$ = $J_{7–8}$ = 8.7), 7.79–7.85 (dd, 2H, H_3 + H_6, $J_{3–2}$ = $J_{6–7}$ = 7.7; $J_{3–4}$ = $J_{6–5}$ = 8.8), 8.09 (d, 2H, H_1 + H_8, $J_{1–2}$ = $J_{8–7}$ = 8.7), 8.31 ppm (d, 2H, H_4 + H_5, $J_{4–3}$ = $J_{5–6}$ = 8.8). ^{13}C-NMR (CDCl$_3$): δ 6.9 (–SeCH$_3$), 120.2 (C_{8a} + C_{9a}), 120.2 (C_1 + C_8), 124.6 (C_2 + C_7), 126.9 (C_4 + C_5), 129.2 (C_3 + C_6), 130.7 (C_9), 148.1 (C_{4a} + C_{10a}), 198.4 ppm (–C=O). IR (KBr): ν 2971–2925 (w, C–H_{aliph}), 1673 cm^{-1} (s, –C=O). MS [*m/z* (% abundance)]: 301 ($M^{+\bullet}$ +1, 4), 206 (100), 178 (93), 151 (31). Elemental analysis calculated for $C_{15}H_{11}NOSe$ (%): C: 60.01, H: 3.69; N: 4.67; found: C: 59.83, H: 3.97, N: 4.38. HRMS calculated for $C_{15}H_{12}NOSe^+$ $[M + H]^+$: 302.0078; found: 302.0091.

3.3. Methylselenol Release

A stock solution of the compounds was prepared in anhydrous DMSO (10 mM). The compounds were placed in a 96-well plate in a final concentration of 100 µM. Reaction started after adding 200 µL of an aqueous 100 mM Na_2HPO_4 buffer (1 mM EDTA, pH = 8), containing 100 µM of DTNB from a freshly prepared 10 mM ethanolic stock, which were added just before starting the reaction. The DTNB concentration was quantified with a cysteine standard curve (7.5–100 µM). Blanks for the compounds in the absence of DTNB were also included as well as a blank to measure the slow but spontaneous hydrolysis of DTNB, which was further subtracted from all the values. Absorbance was read at 412 nm in a FLUOstar Omega microplate reader (BMG LabTech, Ortenberg, Germany). Results represent means of triplicate values ± SD.

3.4. Theoretical Calculations of Molecular Properties

The drug-likeness score along with the TPSA values and the properties described in Lipinski's Rule of Five [molecular weight (MW) $\leq$ 500 Da, logP $\leq$ 5, H-bond donors (nOHNH) $\leq$ 5 and H-bond acceptors (nON) $\leq$ 10] were calculated using the freely download version of Osiris DataWarrior v.4.5.2 [53] and the online available Molinspiration [54] property calculation programs, respectively. Likewise, the toxicity risks (mutagenic, tumorigenic, irritant and reproductive effects) were obtained by Osiris DataWarrior program and are labeled in different colours (green for no risk, orange for mild risk and red for high risk).

3.5. Biology

3.5.1. Radical Scavenging Assays

DPPH assay

The assay was performed following a described protocol [41], with few modifications. Briefly, a stock solution of DPPH$^{\cdot}$ (2,2-diphenyl-1-picrylhydrazyl, Sigma Aldrich, Madrid, Spain) in methanol (0.04 mg/mL) was freshly prepared. Absorbance of the stock solution was adjusted at 0.8 ± 0.02 at 516 nm for each experiment. Due to solubility issues in methanol, a stock solution of each compound (10 mM) was prepared in DMSO. Compounds were tested at a final concentration of 100 µM. The negative control contained the same amount of DMSO to avoid interferences. The reaction was incubated in a 2 mL microtube in the dark and 300 µL were seeded in a 96-well plate at the determined times, to avoid erratic measures due to methanol evaporation if incubated all the time in the plate. Discolouration to the yellowish reduced form was followed at 516 nm in a FLUOstar Omega (BMG LabTech) plate reader. Ascorbic acid was used as a positive control.

Percentage of scavenged DPPH$^{\cdot}$ was calculated as follows:

$$\%\, of\ scavenged\ DPPH^{\cdot} = 100\ \times\ \frac{\mathrm{A_{control}} - \mathrm{A_{sample}}}{\mathrm{A_{control}}}$$

with $\mathrm{A_{control}}$ being the absorbance of the negative control (only DMSO) and $\mathrm{A_{sample}}$ the absorbance of each tested compound. The experiment was performed three times in quadruplicate.

ABTS assay

ABTS assay was performed with a colorimetric assay [55]. Briefly, ABTS was dissolved (1 mg/mL) in a 2.45 mM potassium persulfate solution and kept overnight in the dark at room temperature to generate the radical ABTS$^{+\cdot}$. For the reaction, the mixture was diluted with 50% ethanol to an absorbance of 0.700 ± 0.02 at 741 nm. The compounds were dissolved in DMSO and tested at different concentrations. The negative control had the same amount of DMSO. Ascorbic acid was used as a positive control. The reaction was started after adding 180 µL of the solution. Absorbance was read with a FLUOstar Omega (BMG LabTech) plate reader after 6 min incubation in the dark. The percentage of scavenged ABTS$^{+\cdot}$ was calculated with the following formula:

$$\%\, of\ scavenged\ ABTS^{+\cdot} = 100\ \times\ \frac{\mathrm{A_{control}} - \mathrm{A_{sample}}}{\mathrm{A_{control}}}$$

where $A_{control}$ corresponds to the absorbance of the negative control (DMSO only) and A_{sample} is the absorbance of the tested compounds. The experiment was performed in quadruplicate.

3.5.2. Cell Culture

All cells were purchased from the American Type Culture Collection (ATCC, Barcelona, Spain). HT-29 (colorectal adenocarcinoma), HTB-54 (grade III lung carcinoma), MCF7 (mammary adenocarcinoma), PC-3 (grade IV prostate adenocarcinoma) and K-562 (chronic myelogenous leukemia) were cultured in RPMI (Gibco, Madrid, Spain), 10% FBS (Gibco), 100 units/mL penicillin and 100 µg/mL streptomycin (Gibco). BEAS-2B cell line (normal epithelial lung) was cultured in DMEM (Gibco), 10% FBS, 100 units/mL penicillin and 100 µg/mL streptomycin. 184B5 (normal mammary gland) cell line was cultured in DMEM:F12 supplemented with 5% FBS, 1 × ITS (Lonza, Barcelona, Spain), 100 nM hydrocortisone (Sigma-Aldrich), 2 mM sodium pyruvate (Lonza), 20 ng/mL EGF (Sigma-Aldrich), 0.3 nM *trans*-retinoic acid (Sigma-Aldrich), 100 units/mL penicillin and 100 µg/mL streptomycin. Cells were cultured at 37 °C under 5% CO_2.

3.5.3. Viability Assay

Cell viability after treatment was assessed by the well-known 3-(4,5-dimethyl-thiazol-2-yl)-2,5-diphenyltetrazolium bromide (MTT, Sigma-Aldrich) assay [21]. Briefly, 10,000 cells were seeded in 96-well plates, treated and incubated for 72 h. Dilutions of the compounds in cell medium were freshly prepared from a 0.01 M stock in DMSO. After treatment, 50 µL of MTT solution in PBS (2 mg/mL) were added and cells were incubated for 4 h. Medium was removed and 150 µL of DMSO was added to dissolve the formed formazan crystals. Absorbance was read at 550 nm in a microplate absorbance reader (Sunrise, Tecan, Männedorf, Switzerland).

3.5.4. Cell Cycle and Cell Death Analysis

3×10^6 or 2×10^6 MCF7 cells were seeded in 25 cm^2 flasks for treatments up to 24 h or 48 h, respectively. DMSO (vehicle) or the dissolved compounds were added 24 h after seeding and cells were incubated for different times at 37 °C under 5% CO_2. Cell cycle and cell death were analyzed simultaneously with the Apo-Direct kit (BD Pharmingen, Madrid, Spain), following the manufacturer's protocol. Briefly, cells were fixed in 1% paraformaldehyde for 45 min at 0 °C, washed with PBS and incubated for at least 30 min in 70% ethanol on ice. Cells were then stained both with FITC-dUTP (1 h, 37 °C) and propidium iodide (30 min, room temperature) and analyzed by flow cytometry using a Coulter Epics XL cytometer (Beckman Coulter, Brea, CA, USA).

3.5.5. Caspase and Autophagy Inhibitors Assay

2×10^6 MCF7 cells were seeded in 25 cm^2 flasks. After 24 h, cells were pre-treated with 50 µM of the pan-caspase inhibitor Z-VAD-FMK (BD Pharmingen) or 100 nM wortmannin (Santa Cruz Biotechnology, Heidelberg, Germany) for 1 h before co-incubating them with 25 µM of compound **5**, 30 µM of compound **15** or vehicle (maximum amount of DMSO used in the treatments) for 48 h. Cells were collected and processed with the Apo-Direct kit as described previously.

3.5.6. Enzymatic Assays

Thioredoxin Reductase Activity Assay

The assay was performed as previously described [56], but in a final volume of 200 µL in a 96-well plate. Reaction started after addition of 133 µL of TE buffer (20 mM Tris, 2 mM EDTA, pH = 8), 0.227 mM NADPH (freshly prepared) to different concentrations of compounds solved in DMSO and TrxR1 (final concentration 100 nM). NADPH consumption was followed measuring absorbance decrease at 340 nm in a VersaMax microplate reader (Molecular Devices, Sunnyvale, CA, USA) over

45 min. A background sample with DMSO without the compounds was included and subtracted from the values.

Glutaredoxin/Glutathione Assay

The assay was performed as previously described [57], with minor modifications and adapted for a 96-well plate. A mixture of 0.1 M Tris pH 8, 2 mM EDTA pH = 8, 0.1 mg/mL BSA, 1 mM GSH, 200 µM NADPH, and 0.008 OD/mL yeast GR was prepared (all reagents were purchased from Sigma-Aldrich). Reactions were performed with 1 µM hGrx1 (IMCO Corporation, Stockholm, Sweden) when corresponding and different concentrations of the compounds. A 100 µL mixture was added, and the final volume was adjusted to 110 µL per well. Consumption of NADPH was monitored at A_{340} on a VersaMax microplate reader (Molecular Devices) for 45 min.

3.5.7. Statistics

The statistical analyses were performed with a Mann-Whitney test or a Wilcoxon test for the inhibitors assay. Statistical significance was calculated using GraphPad Prism 6.01. (* $p < 0.05$, ** $p < 0.01$, *** $p < 0.001$).

4. Conclusions

A novel series of 15 methylselenoesters has been synthesized. Differences in the hydrolytic release of CH_3SeH in aqueous medium indicated that the chemical features of the core of the molecule modulated the lability of the carbonyl-Se bond. In the preliminary assessment of redox properties, only compound **11** presented radical scavenging activity. The compounds were able to inhibit proliferation in different cancer cell lines and their toxicity towards non-malignant cell lines was in the same range as MSA. Compounds **5** and **15** arrested cell cycle in G_2/M phase in MCF7 cell line. Although both compounds induced cell death in a dose-dependent manner, only compound 15 was time-dependent. Pre-treatment of the cells with a pan-caspase inhibitor partially prevented cell death, suggesting that the caspase pathway is implicated in their mechanism. Even though further research is needed, results suggest that these compounds might be good precursors of CH_3SeH, one of the key metabolites in Se anticancerous activity and might be of great interest as potential antitumor agents.

Supplementary Materials: Supplementary materials are available online. ^{1}H- and ^{13}C-NMR of all the new synthesized compounds.

Acknowledgments: The authors express their gratitude to the Plan de Investigación de la Universidad de Navarra, PIUNA (Ref 2014−26), “la Caixa” and “CAN” Foundations for financial support for the project. The research leading to these results has also received funding from “la Caixa” Banking Foundation and from the Asociación de Amigos de la Universidad de Navarra, to whom Nuria Díaz-Argelich wishes to expresses her gratitude. We thank Elena González-Peñas and Ángel Irigoyen for technical support with the HRMS experiments.

Author Contributions: Carmen Sanmartín, Ignacio Encío and Juan Antonio Palop conceived and designed the experiments; Aristi P. Fernandes conceived and designed the enzyme kinetics experiment, contributed with the material and analyzed the data; Nuria Díaz-Argelich performed the experiments; Daniel Plano performed the theoretical calculations and wrote that section; Carmen Sanmartín, Ignacio Encío, Juan Antonio Palop and Nuria Díaz-Argelich analyzed the data; Nuria Díaz-Argelich wrote the paper and all the authors read, commented and approved the final manuscript.

Conflicts of Interest: The authors declare no conflict of interest.

References

1. Miller, K.D.; Siegel, R.L.; Lin, C.C.; Mariotto, A.B.; Kramer, J.L.; Rowland, J.H.; Stein, K.D.; Alteri, R.; Jemal, A. Cancer treatment and survivorship statistics, 2016. *CA. Cancer J. Clin.* **2016**, *66*, 271–289. [CrossRef] [PubMed]
2. Fernandes, A.P.; Gandin, V. Selenium compounds as therapeutic agents in cancer. *Biochim. Biophys. Acta Gen. Subj.* **2015**, *1850*, 1642–1660. [CrossRef] [PubMed]
3. Lü, J.; Zhang, J.; Jiang, C.; Deng, Y.; Özten, N.; Bosland, M.C. Cancer chemoprevention research with selenium in the post-SELECT era: Promises and challenges. *Nutr. Cancer* **2016**, *68*, 1–17. [CrossRef] [PubMed]

4. Lipinski, B. Redox-active Selenium in Health and Disease: A Conceptual Review. *Mini Rev. Med. Chem.* **2016**. [CrossRef]
5. Wallenberg, M.; Misra, S.; Björnstedt, M. Selenium cytotoxicity in cancer. *Basic Clin. Pharmacol. Toxicol.* **2014**, *114*, 377–386. [CrossRef] [PubMed]
6. Misra, S.; Boylan, M.; Selvam, A.; Spallholz, J.E.; Björnstedt, M. Redox-active selenium compounds—From toxicity and cell death to cancer treatment. *Nutrients* **2015**, *7*, 3536–3556. [CrossRef] [PubMed]
7. Yan, L.; Combs, G.F. Consumption of a high-fat diet abrogates inhibitory effects of methylseleninic acid on spontaneous metastasis of Lewis lung carcinoma in mice. *Carcinogenesis* **2014**, *35*, 2308–2313. [CrossRef] [PubMed]
8. Hagemann-Jensen, M.; Uhlenbrock, F.; Kehlet, S.; Andresen, L.; Gabel-Jensen, C.; Ellgaard, L.; Gammelgaard, B.; Skov, S. The selenium metabolite methylselenol regulates the expression of ligands that trigger immune activation through the lymphocyte receptor NKG2D. *J. Biol. Chem.* **2014**, *289*, 31576–31590. [CrossRef] [PubMed]
9. Marschall, T.A.; Bornhorst, J.; Kuehnelt, D.; Schwerdtle, T. Differing cytotoxicity and bioavailability of selenite, methylselenocysteine, selenomethionine, selenosugar 1 and trimethylselenonium ion and their underlying metabolic transformations in human cells. *Mol. Nutr. Food Res.* **2016**, 2622–2632. [CrossRef] [PubMed]
10. Rayman, M.P. Selenium in cancer prevention: A review of the evidence and mechanism of action. *Proc. Nutr. Soc.* **2005**, *64*, 527–542. [CrossRef] [PubMed]
11. Roman, M.; Jitaru, P.; Barbante, C. Selenium biochemistry and its role for human health. *Metallomics* **2014**, *6*, 25–54. [CrossRef] [PubMed]
12. Liu, Y.; Liu, X.; Guo, Y.; Liang, Z.; Tian, Y.; Lu, L.; Zhao, X.; Sun, Y.; Zhao, X.; Zhang, H.; Dong, Y. Methylselenocysteine preventing castration-resistant progression of prostate cancer. *Prostate* **2015**, *75*, 1001–1008. [CrossRef] [PubMed]
13. Cao, S.; Durrani, F.A.; Tóth, K.; Rustum, Y.M. Se-methylselenocysteine offers selective protection against toxicity and potentiates the antitumour activity of anticancer drugs in preclinical animal models. *Br. J. Cancer* **2014**, *110*, 1733–1743. [CrossRef] [PubMed]
14. Weekley, C.M.; Harris, H.H. Which form is that? The importance of selenium speciation and metabolism in the prevention and treatment of disease. *Chem. Soc. Rev.* **2013**, *42*, 8870–8894. [CrossRef] [PubMed]
15. Wang, L.; Guo, X.; Wang, J.; Jiang, C.; Bosland, M.C.; Lü, J.; Deng, Y. Methylseleninic acid superactivates p53-senescence cancer progression barrier in prostate lesions of pten-knockout mouse. *Cancer Prev. Res.* **2016**, *9*, 35–42. [CrossRef] [PubMed]
16. Park, J.-M.; Kim, D.-H.; Na, H.-K.; Surh, Y.-J. Methylseleninic acid induces NAD(P)H: Quinone oxidoreductase-1 expression through activation of NF-E2-related factor 2 in Chang liver cells. *Oncotarget* **2016**. [CrossRef] [PubMed]
17. Tarrado-Castellarnau, M.; Cortés, R.; Zanuy, M.; Tarragó-Celada, J.; Polat, I.H.; Hill, R.; Fan, T.W. M.; Link, W.; Cascante, M. Methylseleninic acid promotes antitumour effects via nuclear FOXO3a translocation through Akt inhibition. *Pharmacol. Res.* **2015**, *102*, 218–234. [CrossRef] [PubMed]
18. Plano, D.; Sanmartín, C.; Moreno, E.; Prior, C.; Calvo, A.; Palop, J.A. Novel potent organoselenium compounds as cytotoxic agents in prostate cancer cells. *Bioorg. Med. Chem. Lett.* **2007**, *17*, 6853–6859. [CrossRef] [PubMed]
19. Ibáñez, E.; Plano, D.; Font, M.; Calvo, A.; Prior, C.; Palop, J.A.; Sanmartín, C. Synthesis and antiproliferative activity of novel symmetrical alkylthio- and alkylseleno-imidocarbamates. *Eur. J. Med. Chem.* **2011**, *46*, 265–274. [CrossRef] [PubMed]
20. Ibáñez, E.; Agliano, A.; Prior, C.; Nguewa, P.; Redrado, M.; González-Zubeldia, I.; Plano, D.; Palop, J.A.; Sanmartín, C.; Calvo, A. The quinoline imidoselenocarbamate EI201 blocks the AKT/mTOR pathway and targets cancer stem cells leading to a strong antitumor activity. *Curr. Med. Chem.* **2012**, *19*, 3031–3043. [CrossRef] [PubMed]
21. Lamberto, I.; Plano, D.; Moreno, E.; Font, M.; Palop, J.A.; Sanmartin, C.; Encio, I. Bisacylimidoselenocarbamates cause G2/M arrest associated with the modulation of CDK1 and Chk2 in human breast cancer MCF-7 cells. *Curr. Med. Chem.* **2013**, *20*, 1609–1619. [CrossRef] [PubMed]
22. Romano, B.; Font, M.; Encío, I.; Palop, J.A.; Sanmartín, C. Synthesis and antiproliferative activity of novel methylselenocarbamates. *Eur. J. Med. Chem.* **2014**, *83*, 674–684. [CrossRef] [PubMed]

23. Zuazo, A.; Plano, D.; Ansó, E.; Lizarraga, E.; Font, M.; Martínez Irujo, J.J. Cytotoxic and proapototic activities of imidoselenocarbamate derivatives are dependent on the release of methylselenol. *Chem. Res. Toxicol.* **2012**, *25*, 2479–2489. [CrossRef] [PubMed]
24. Domínguez-Álvarez, E.; Plano, D.; Font, M.; Calvo, A.; Prior, C.; Jacob, C.; Palop, J.A.; Sanmartín, C. Synthesis and antiproliferative activity of novel selenoester derivatives. *Eur. J. Med. Chem.* **2014**, *73*, 153–166. [CrossRef] [PubMed]
25. Kaushik, N.K.; Kim, H.S.; Chae, Y.J.; Lee, Y.N.; Kwon, G.C.; Choi, E.H.; Kim, I.T. Synthesis and anticancer activity of di(3-thienyl)methanol and di(3-thienyl)methane. *Molecules* **2012**, *17*, 11456–11468. [CrossRef] [PubMed]
26. Racané, L.; Sedić, M.; Ilić, N.; Aleksić, M.; Pavelić, S.K.; Karminski-Zamola, G. Novel 2-Thienyl- and 2-Benzothienyl-Substituted 6-(2-Imidazolinyl)Benzothiazoles: Synthesis; in vitro Evaluation of Antitumor Effects and Assessment of Mitochondrial Toxicity. *Anti-Cancer Agents Med. Chem.* **2017**, *17*, 57–66. [CrossRef] [PubMed]
27. Im, D.; Jung, K.; Yang, S.; Aman, W.; Hah, J.M. Discovery of 4-arylamido 3-methyl isoxazole derivatives as novel FMS kinase inhibitors. *Eur. J. Med. Chem.* **2015**, *102*, 600–610. [CrossRef] [PubMed]
28. Ananda, H.; Kumar, K.S. S.; Hegde, M.; Rangappa, K.S. Induction of apoptosis and downregulation of ERα in DMBA-induced mammary gland tumors in Sprague–Dawley rats by synthetic 3,5-disubstituted isoxazole derivatives. *Mol. Cell. Biochem.* **2016**, *420*, 141–150. [CrossRef] [PubMed]
29. Alnabulsi, S.; Santina, E.; Russo, I.; Hussein, B.; Kadirvel, M.; Chadwick, A.; Bichenkova, E.V.; Bryce, R.A.; Nolan, K.; Demonacos, C.; et al. Non-symmetrical furan-amidines as novel leads for the treatment of cancer and malaria. *Eur. J. Med. Chem.* **2016**, *111*, 33–45. [CrossRef] [PubMed]
30. Do, A.; Pires, R.A.; Lecerf-Schmidt, F.; Guragossian, N.; Pazinato, J.; Gozzi, G.J.; Winter, E.; Valdameri, G.; Veale, A.; Ene Boumendjel, A.; et al. New, highly potent and non-toxic, chromone inhibitors of the human breast cancer resistance protein ABCG2. *Eur. J. Med. Chem.* **2016**, *122*, 291–301. [CrossRef]
31. Valdameri, G.; Genoux-Bastide, E.; Peres, B.; Gauthier, C.; Guitton, J.; Terreux, R.; Winnischofer, S.M.B.; Rocha, M.E.M.; Boumendjel, A.; Di Pietro, A. Substituted chromones as highly potent nontoxic inhibitors, specific for the breast cancer resistance protein. *J. Med. Chem.* **2012**, *55*, 966–970. [CrossRef] [PubMed]
32. Jia, H.; Dai, G.; Weng, J.; Zhang, Z.; Wang, Q.; Zhou, F.; Jiao, L.; Cui, Y.; Ren, Y.; Fan, S.; et al. Discovery of (*S*)-1-(1-(Imidazo[1,2-*a*]pyridin-6-yl)ethyl)-6-(1-methyl-1*H*-pyrazol-4-yl)-1*H*-[1,2,3]triazolo[4,5-*b*]pyrazine (volitinib) as a highly potent and selective mesenchymal-epithelial transition factor (*c*-Met) inhibitor in clinical development for tre. *J. Med. Chem.* **2014**, *57*, 7577–7589. [CrossRef] [PubMed]
33. Clausen, D.J.; Smith, W.B.; Haines, B.E.; Wiest, O.; Bradner, J.E.; Williams, R.M. Modular synthesis and biological activity of pyridyl-based analogs of the potent Class i Histone Deacetylase Inhibitor Largazole. *Bioorg. Med. Chem.* **2015**, *23*, 5061–5074. [CrossRef] [PubMed]
34. Zheng, S.; Zhong, Q.; Xi, Y.; Mottamal, M.; Zhang, Q.; Schroeder, R.L.; Sridhar, J.; He, L.; McFerrin, H.; Wang, G. Modification and biological evaluation of thiazole derivatives as novel inhibitors of metastatic cancer cell migration and invasion. *J. Med. Chem.* **2014**, *57*, 6653–6667. [CrossRef] [PubMed]
35. Romagnoli, R.; Baraldi, P.G.; Lopez-Cara, C.; Preti, D.; Aghazadeh Tabrizi, M.; Balzarini, J.; Bassetto, M.; Brancale, A.; Fu, X.-H.; Gao, Y.; et al. Concise synthesis and biological evaluation of 2-Aroyl-5-amino benzo[b]thiophene derivatives as a novel class of potent antimitotic agents. *J. Med. Chem.* **2013**, *56*, 9296–9309. [CrossRef] [PubMed]
36. Chao, M.; Huang, H.; Huangfu, W.; Hsu, K.; Liu, Y.; Liou, P.; Teng, C.; Yang, C. An oral quinoline derivative, MPT0B392, causes leukemic cells mitotic arrest and overcomes drug resistant cancer cells. *Oncotarget* **2017**, 1–14.
37. Hussaini, S.M. A. Therapeutic significance of quinolines: A patent review (2013–2015). *Expert Opin. Ther. Pat.* **2016**, *26*, 1–21. [CrossRef] [PubMed]
38. Richard, D.J.; Lena, R.; Bannister, T.; Blake, N.; Pierceall, W.E.; Carlson, N.E.; Keller, C.E.; Koenig, M.; He, Y.; Minond, D.; et al. Hydroxyquinoline-derived compounds and analoguing of selective Mcl-1 inhibitors using a functional biomarker. *Bioorg. Med. Chem.* **2013**, *21*, 6642–6649. [CrossRef] [PubMed]
39. Zhang, W.; Zhang, B.; Zhang, W.; Yang, T.; Wang, N.; Gao, C.; Tan, C.; Liu, H.; Jiang, Y. Synthesis and antiproliferative activity of 9-benzylamino-6-chloro-2-methoxy-acridine derivatives as potent DNA-binding ligands and topoisomerase II inhibitors. *Eur. J. Med. Chem.* **2016**, *116*, 59–70. [CrossRef] [PubMed]

40. Jiang, D.; Tam, A.B.; Alagappan, M.; Hay, M.P.; Gupta, A.; Kozak, M.M.; Solow-Cordero, D.E.; Lum, P.Y.; Denko, N.C.; Giaccia, A.J.; et al. Acridine Derivatives as Inhibitors of the IRE1 -XBP1 Pathway Are Cytotoxic to Human Multiple Myeloma. *Mol. Cancer Ther.* **2016**, *15*, 2055–2065. [CrossRef] [PubMed]
41. Romano, B.; Plano, D.; Encío, I.; Palop, J.A.; Sanmartín, C. In vitro radical scavenging and cytotoxic activities of novel hybrid selenocarbamates. *Bioorg. Med. Chem.* **2015**, *23*, 1716–1727. [CrossRef] [PubMed]
42. Klayman, D.L.; Griffin, T.S. Reaction of Selenium with Sodium Borohydride in Protic Solvents. A Facile Method for the Introduction of Selenium into Organic Molecules. *J. Am. Chem. Soc.* **1973**, *2*, 197–199. [CrossRef]
43. Athayde-Filho, P.F. De Synthesis and characterization of three new organo-selenium compounds. A convenient synthesis of aroylselenoglycolic acids. *Arkivoc* **2004**, *2004*, 22–26. [CrossRef]
44. Ellman, G.L. A colorimetric method for determining low concentrations of mercaptans. *Arch. Biochem. Biophys.* **1958**, *74*, 443–450. [CrossRef]
45. Ip, C.; Thompson, H.J.; Zhu, Z.; Ganther, H.E. In vitro and in vivo studies of methylseleninic acid: Evidence that a monomethylated selenium metabolite is critical for cancer chemoprevention. *Cancer Res.* **2000**, *60*, 2882–2886. [CrossRef] [PubMed]
46. Wu, X.; Zhang, Y.; Pei, Z.; Chen, S.; Yang, X.; Chen, Y.; Lin, D.; Ma, R.Z. Methylseleninic acid restricts tumor growth in nude mice model of metastatic breast cancer probably via inhibiting angiopoietin-2. *BMC Cancer* **2012**, *12*, 192–200. [CrossRef] [PubMed]
47. Zeng, H.; Wu, M. The Inhibitory Efficacy of Methylseleninic Acid Against Colon Cancer Xenografts in C57BL/6 Mice. *Nutr. Cancer* **2015**, *67*, 831–838. [CrossRef] [PubMed]
48. Zeng, H.; Wu, M.; Botnen, J.H. Methylselenol, a selenium metabolite, induces cell cycle arrest in G1 phase and apoptosis via the extracellular-regulated kinase 1/2 pathway and other cancer signaling genes. *J. Nutr.* **2009**, *139*, 1613–1618. [CrossRef] [PubMed]
49. Jackson, M.I.; Combs, G.F. Selenium and anticarcinogenesis: Underlying mechanisms. *Curr. Opin. Clin. Nutr. Metab. Care* **2008**, *11*, 718–726. [CrossRef] [PubMed]
50. Wallenberg, M.; Olm, E.; Hebert, C.; Björnstedt, M.; Fernandes, A.P. Selenium compounds are substrates for glutaredoxins: A novel pathway for selenium metabolism and a potential mechanism for selenium-mediated cytotoxicity. *Biochem. J.* **2010**, *429*, 85–93. [CrossRef] [PubMed]
51. Liu, C.; Liu, H.; Li, Y.; Wu, Z.; Zhu, Y.; Wang, T.; Gao, A.C.; Chen, J.; Zhou, Q. Intracellular glutathione content influences the sensitivity of lung cancer cell lines to methylseleninic acid. *Mol. Carcinog.* **2012**, *51*, 303–314. [CrossRef] [PubMed]
52. Gromer, S.; Gross, J.H. Methylseleninate is a substrate rather than an inhibitor of mammalian thioredoxin reductase. Implications for the antitumor effects of selenium. *J. Biol. Chem.* **2002**, *277*, 9701–9706. [CrossRef] [PubMed]
53. Agnihotri, S.; Narula, R.; Joshi, K.; Rana, S.; Singh, M. In silico modeling of ligand molecule for non structural 3 (NS3) protein target of flaviviruses. *Bioinformation* **2012**, *8*, 123–127.
54. Sander, T.; Freyss, J.; von Korff, M.; Reich, J.R.; Rufener, C. OSIRIS, an entirely inhouse developed drug discovery informatics system. *J. Chem. Inf. Model.* **2009**, *49*, 232–246. [CrossRef] [PubMed]
55. García-Herreros, C.; García-Iñiguez, M.; Astiasarán, I.; Ansorena, D. Antioxidant activity and phenolic content of water extracts of borago officinalis l.: Influence of plant part and cooking procedure. *Ital. J. Food Sci.* **2010**, *22*, 156–164.
56. Arnér, E.S.J.; Holmgren, A. Measurement of thioredoxin and thioredoxin reductase. In *Current Protocols in Toxicology/Editorial Board, Mahin D. Maines*; John Wiley & Sons, Inc.: Hoboken, NJ, USA, 2001.
57. Holmgren, A.; Aslund, F. Glutaredoxin. *Methods Enzym.* **1995**, *252*, 283–292.

Sample Availability: Samples of the compounds **1**–**15** reported in this paper are available from the authors.

© 2017 by the authors. Licensee MDPI, Basel, Switzerland. This article is an open access article distributed under the terms and conditions of the Creative Commons Attribution (CC BY) license (http://creativecommons.org/licenses/by/4.0/).

Supplementary material

Novel methylselenoesters as antiproliferative agents

Nuria Díaz-Argelich[1, 2, 3], Ignacio Encío[4], Daniel Plano[1, 2], Aristi P. Fernandes[3], Juan Antonio Palop[1, 2], Carmen Sanmartín[1, 2*]

1) University of Navarra. Faculty of Pharmacy and Nutrition. Department of Organic and Pharmaceutical Chemistry, Irunlarrea 1, 3E-1008 Pamplona, Spain
2) Oncology and Hematology Section, IdiSNA, Navarra Institute for Health Research, Irunlarrea 3, E-31008, Pamplona, Spain
3) Division of Biochemistry, Department of Medical Biochemistry and Biophysics (MBB), Karolinska Institutet, SE-171 77 Stockholm, Sweden
4) Department of Health Sciences, Public University of Navarra, Avda. Barañain s/n, E-31008 Pamplona, Spain

Contents:
Representative spectra (^{1}H and ^{13}C NMR) of the methylselenoesters

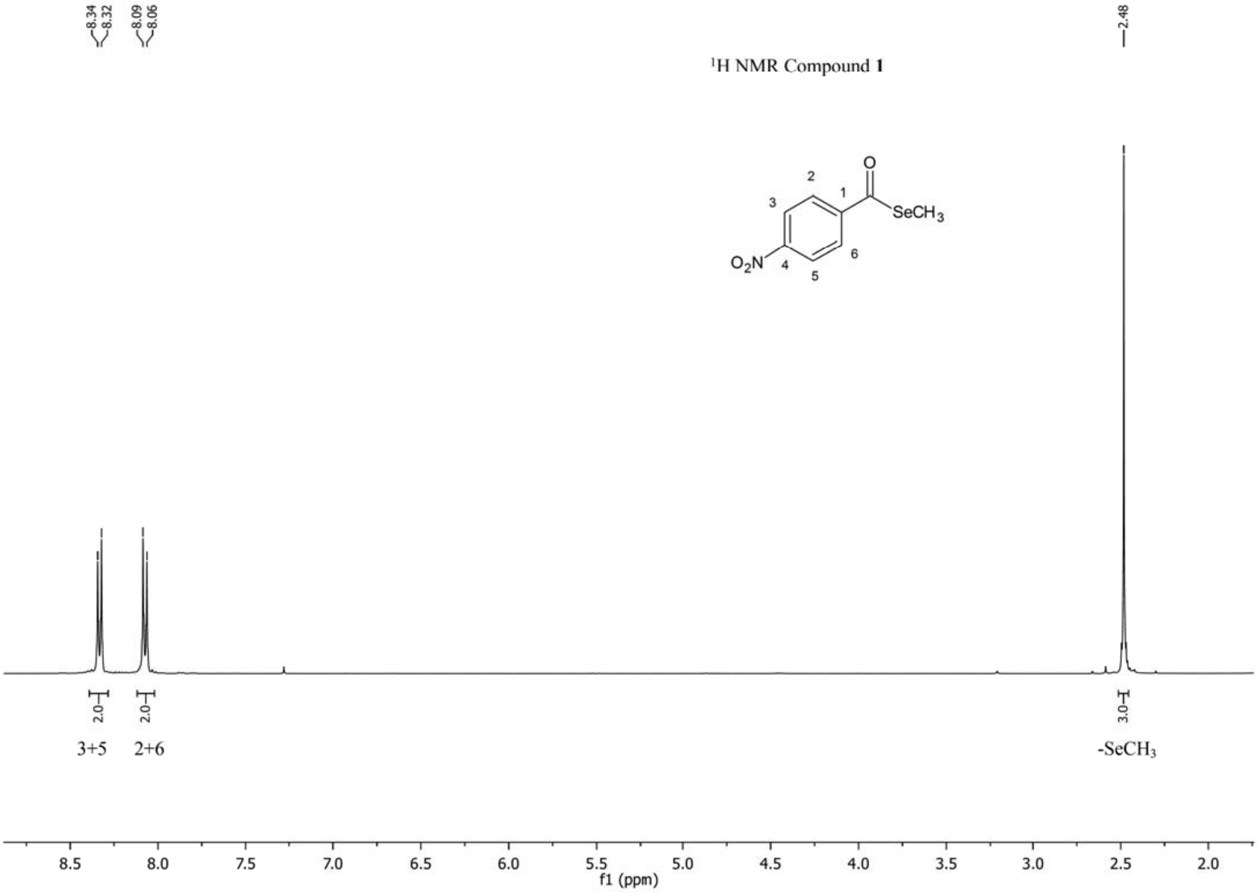
8.34
8.32
8.09
8.06
2.48
^{1}H NMR Compound **1**
O
SeCH$_3$
O$_2$N
1
2
3
4
5
6
2.0
2.0
3.0
3+5
2+6
-SeCH$_3$
8.5
8.0
7.5
7.0
6.5
6.0
5.5
5.0
4.5
4.0
3.5
3.0
2.5
2.0
f1 (ppm)

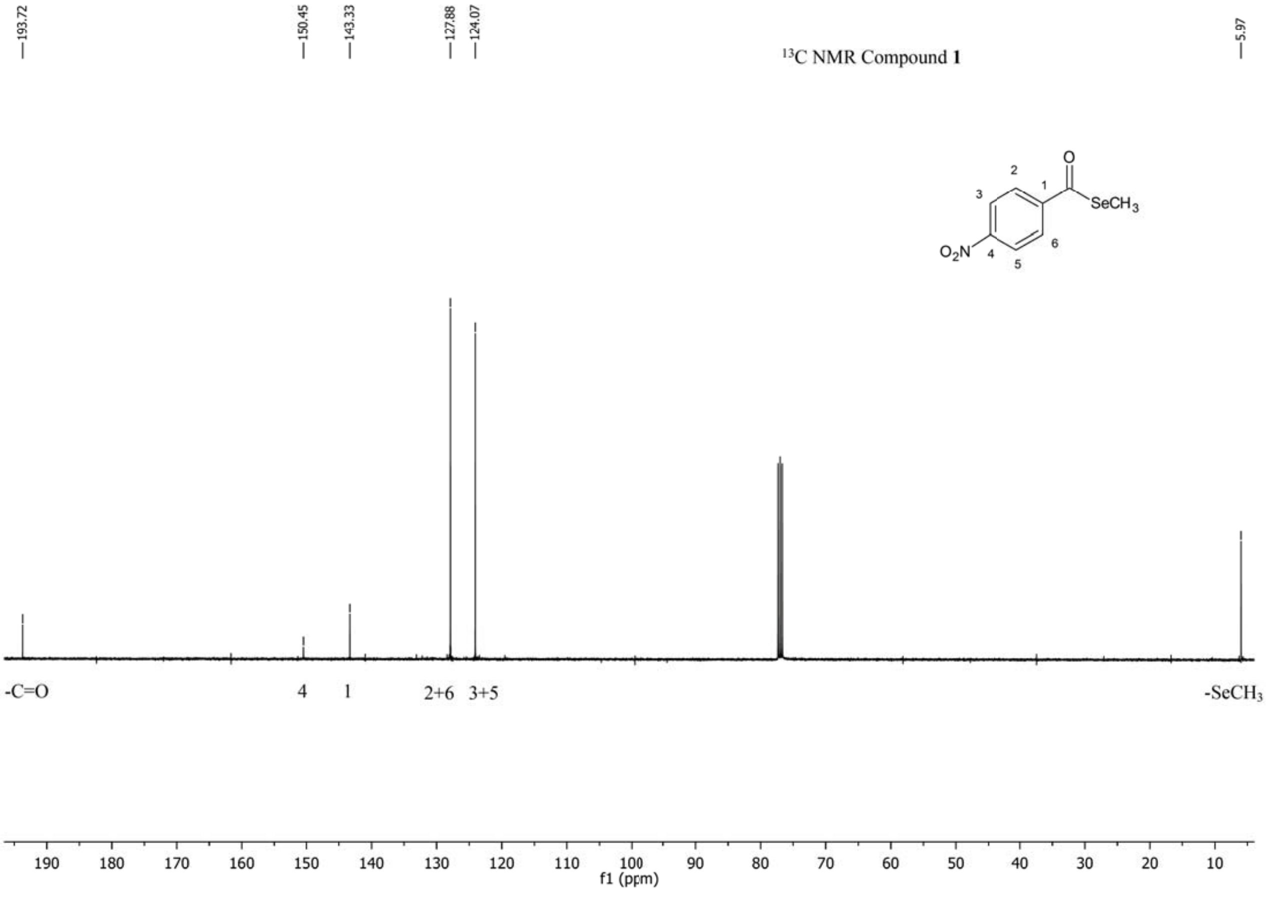
193.72
150.45
143.33
127.88
124.07
5.97
^{13}C NMR Compound **1**
O
SeCH$_3$
O$_2$N
1
2
3
4
5
6
-C=O
4
1
2+6
3+5
-SeCH$_3$
190
180
170
160
150
140
130
120
110
100
90
80
70
60
50
40
30
20
10
f1 (ppm)

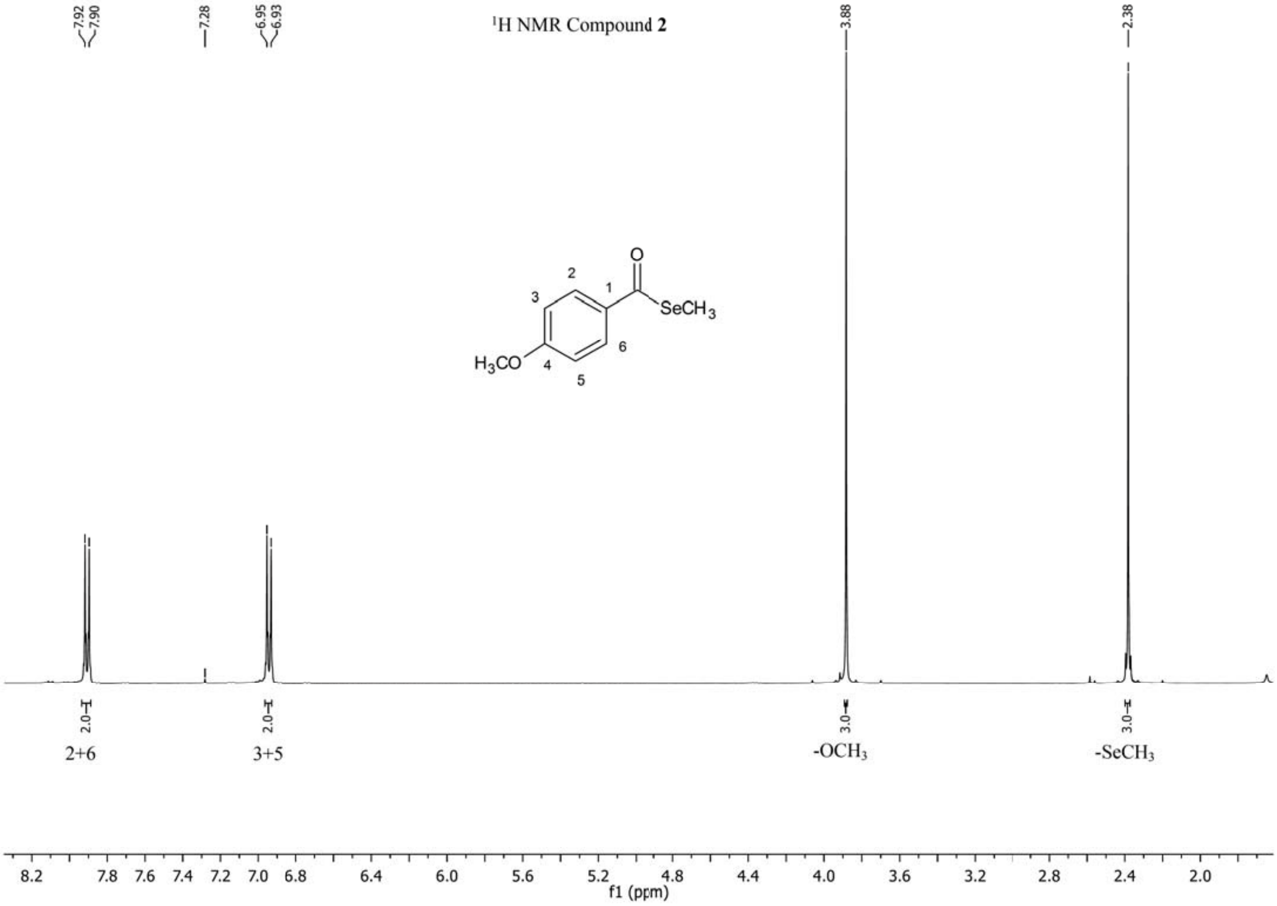
^{1}H NMR Compound **2**
7.92
7.90
7.28
6.95
6.93
3.88
2.38
O
SeCH$_3$
H$_3$CO
1
2
3
4
5
6
2.0
2.0
3.0
3.0
2+6
3+5
-OCH$_3$
-SeCH$_3$
8.2
7.8
7.6
7.4
7.2
7.0
6.8
6.4
6.0
5.6
5.2
4.8
4.4
4.0
3.6
3.2
2.8
2.4
2.0
f1 (ppm)

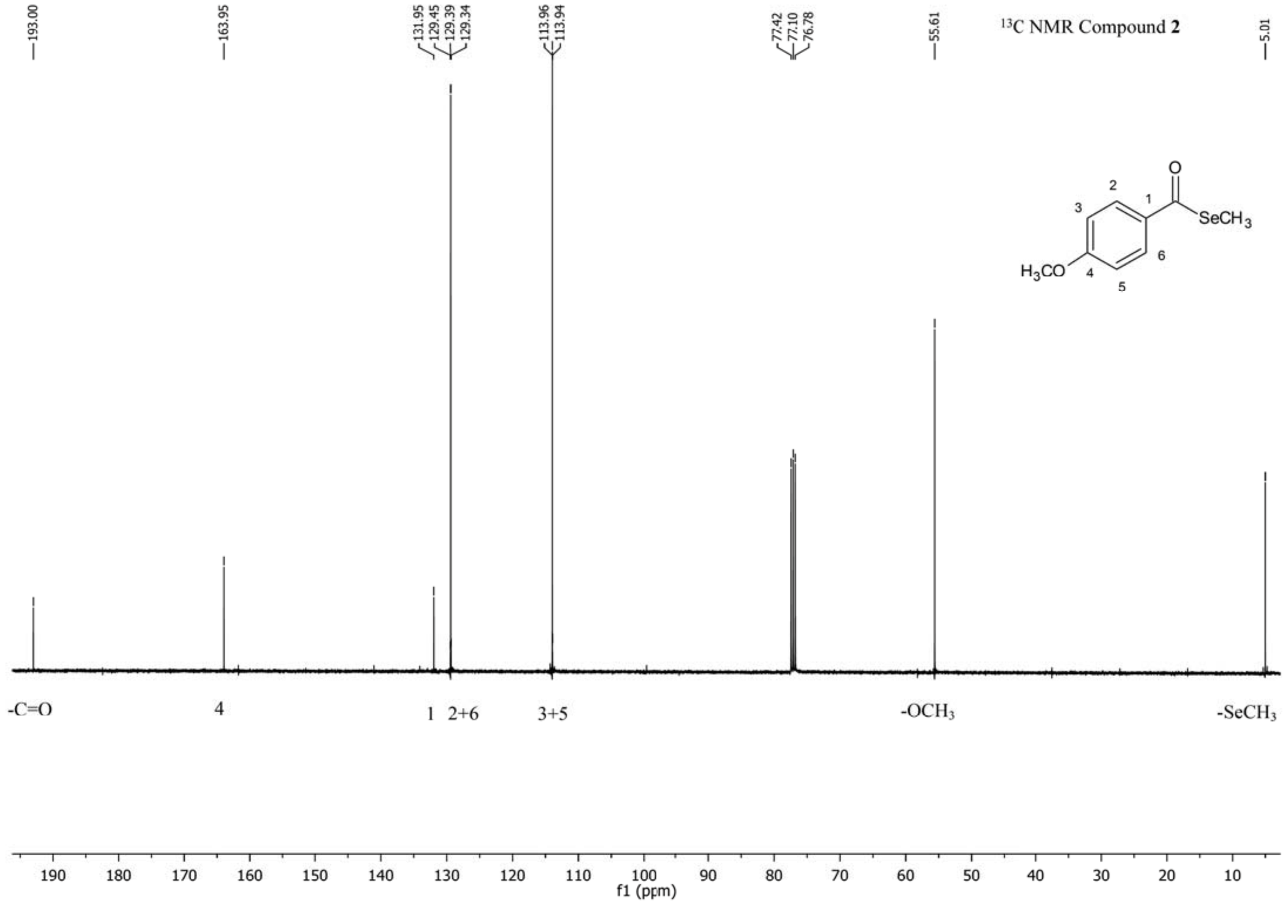
^{13}C NMR Compound **2**
193.00
163.95
131.95
129.45
129.39
129.34
113.96
113.94
77.42
77.10
76.78
55.61
5.01
O
SeCH$_3$
H$_3$CO
1
2
3
4
5
6
-C=O
4
1
2+6
3+5
-OCH$_3$
-SeCH$_3$
190
180
170
160
150
140
130
120
110
100
90
80
70
60
50
40
30
20
10
f1 (ppm)

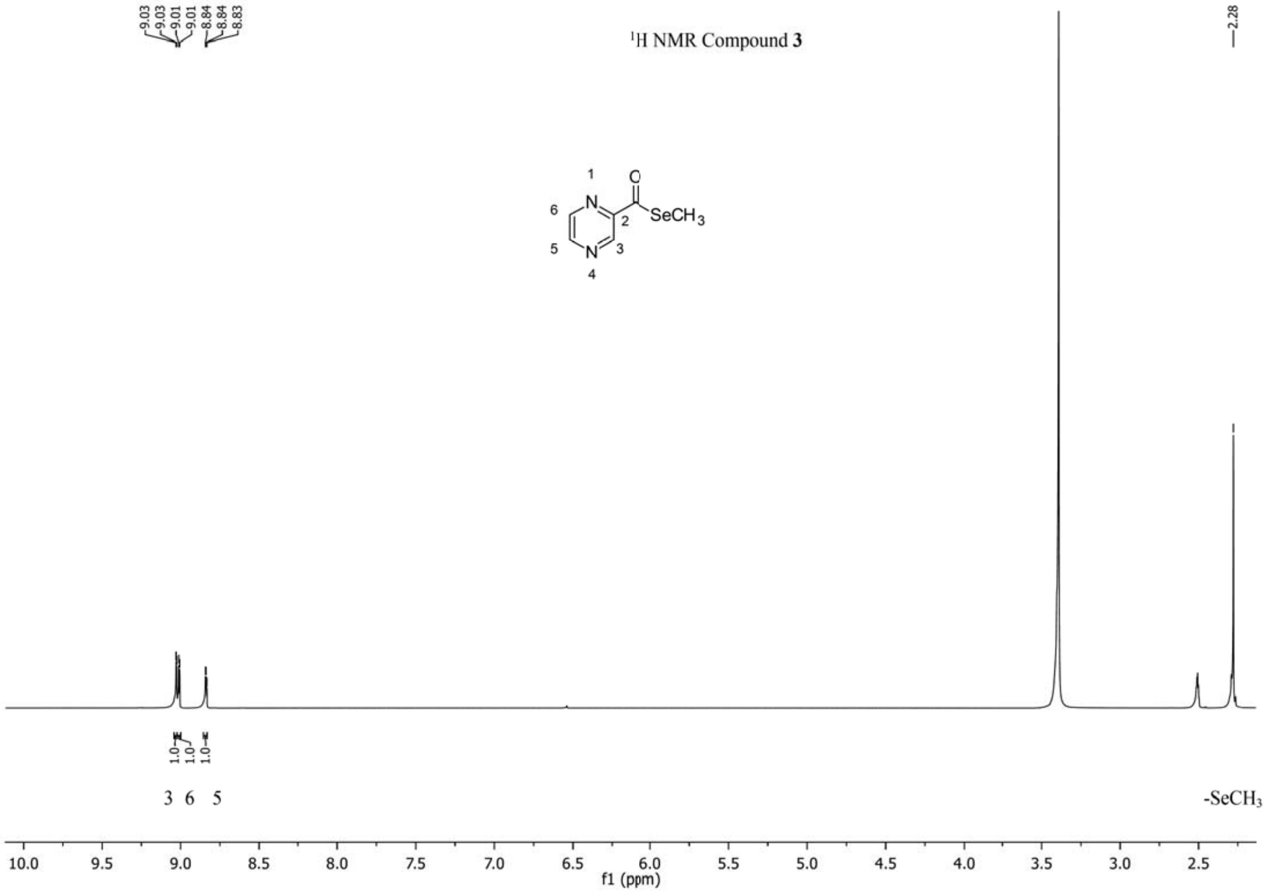
9.03
9.03
9.01
9.01
8.84
8.84
8.83
2.28
^{1}H NMR Compound **3**
1
6
2
5
3
4
N
N
O
SeCH$_3$
1.0
1.0
1.0
3 6 5
-SeCH$_3$
10.0
9.5
9.0
8.5
8.0
7.5
7.0
6.5
6.0
5.5
5.0
4.5
4.0
3.5
3.0
2.5
f1 (ppm)

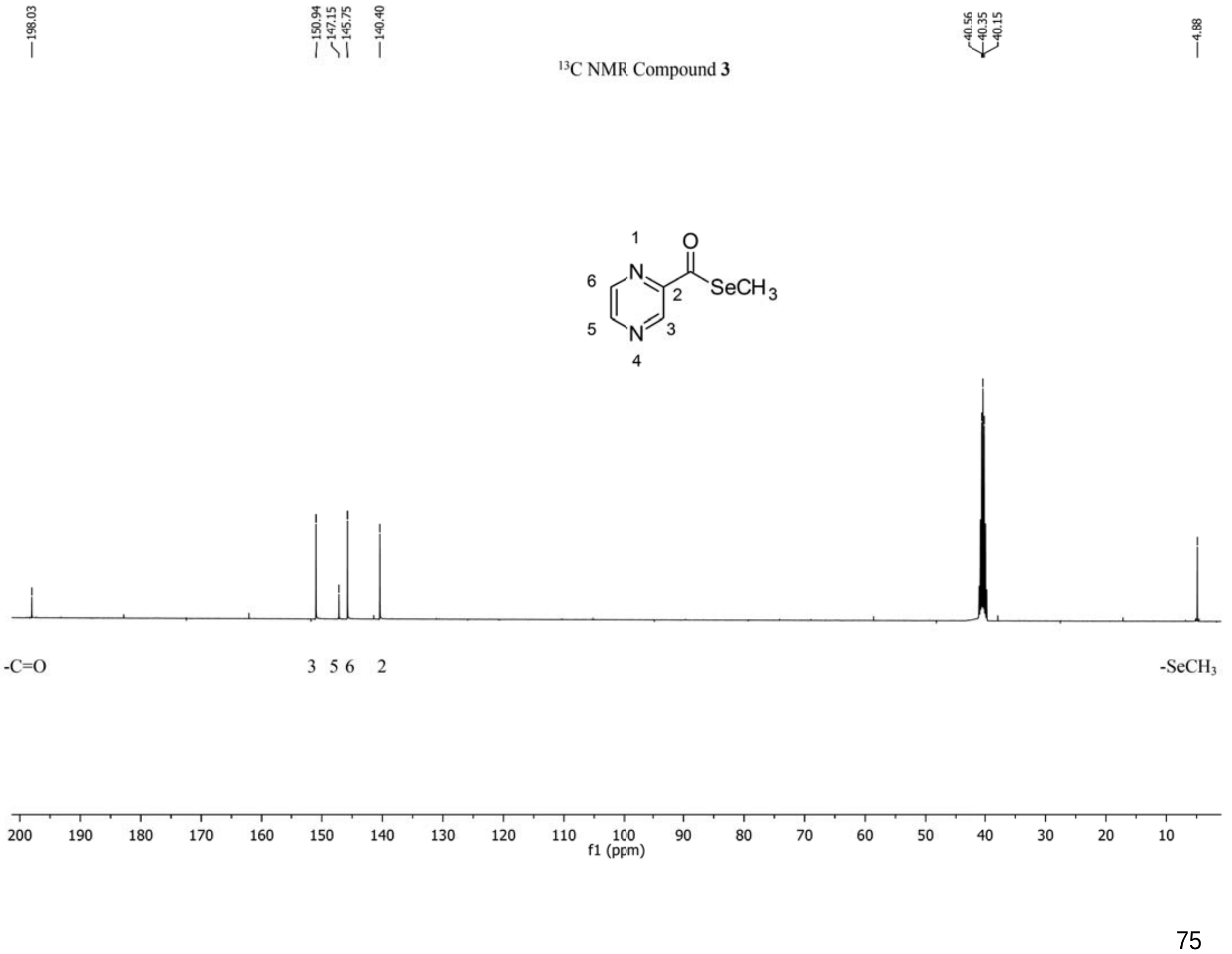
198.03
150.94
147.15
145.75
140.40
40.56
40.35
40.15
4.88
^{13}C NMR Compound **3**
1
6
2
5
3
4
N
N
O
SeCH$_3$
-C=O
3 5 6 2
-SeCH$_3$
200
190
180
170
160
150
140
130
120
110
100
90
80
70
60
50
40
30
20
10
f1 (ppm)

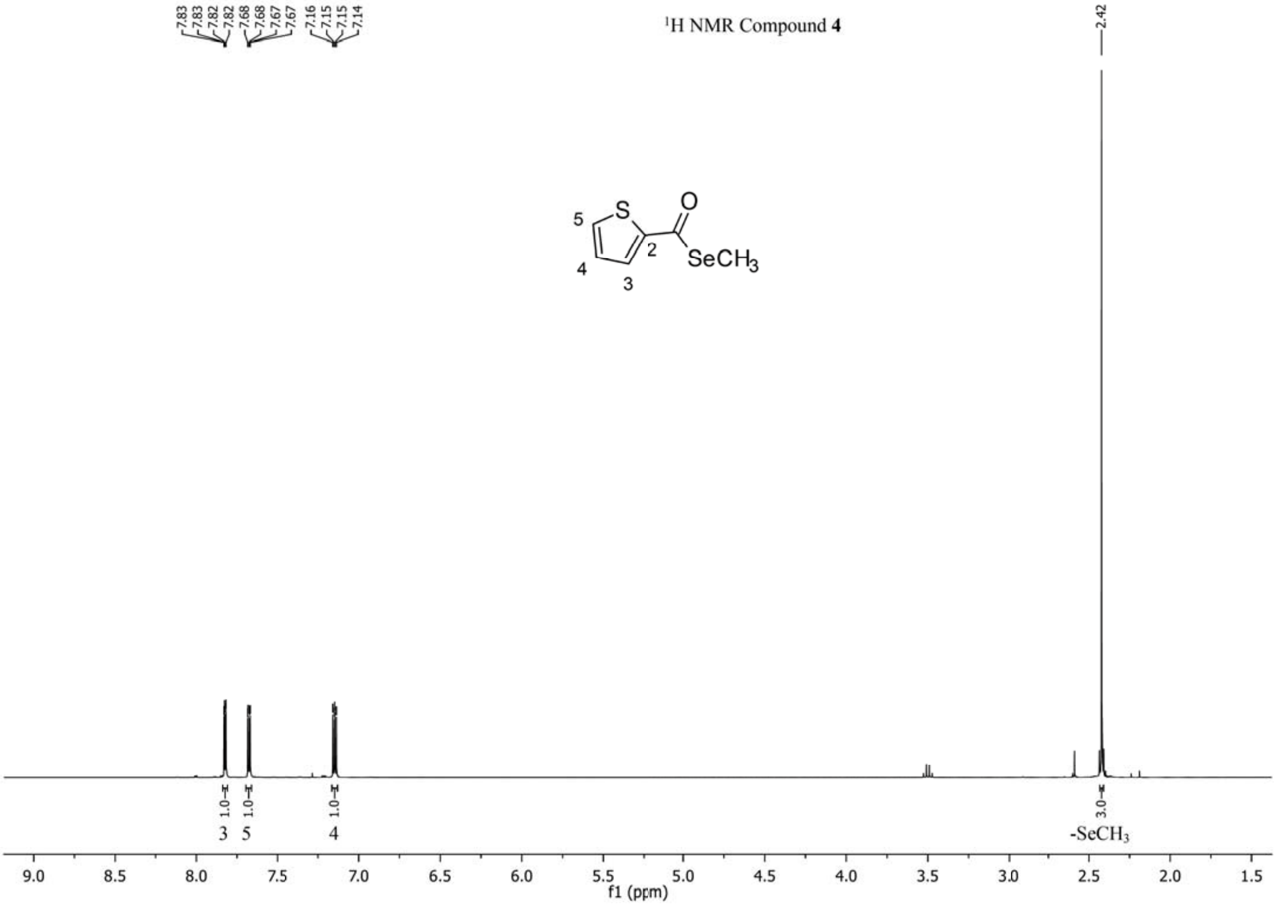
7.83
7.83
7.82
7.82
7.68
7.68
7.67
7.67
7.16
7.15
7.15
7.14
^{1}H NMR Compound **4**
2.42
5
S
O
2
SeCH$_3$
4
3
1.0
1.0
1.0
3.0
3 5
4
-SeCH$_3$
9.0
8.5
8.0
7.5
7.0
6.5
6.0
5.5
5.0
4.5
4.0
3.5
3.0
2.5
2.0
1.5
f1 (ppm)

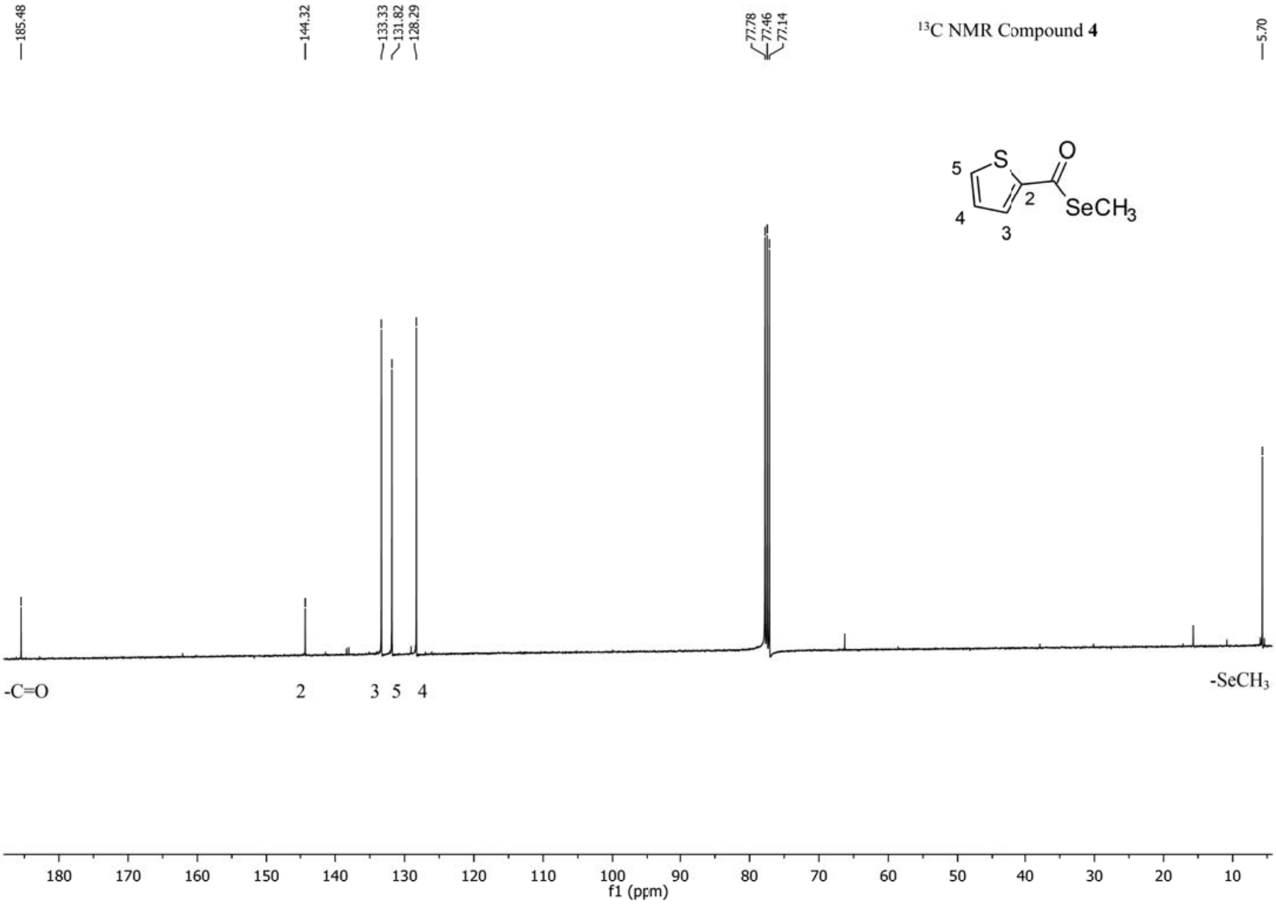
185.48
144.32
133.33
131.82
128.29
77.78
77.46
77.14
^{13}C NMR Compound **4**
5.70
5
S
O
2
SeCH$_3$
4
3
-C=O
2
3 5 4
-SeCH$_3$
180
170
160
150
140
130
120
110
100
90
80
70
60
50
40
30
20
10
f1 (ppm)

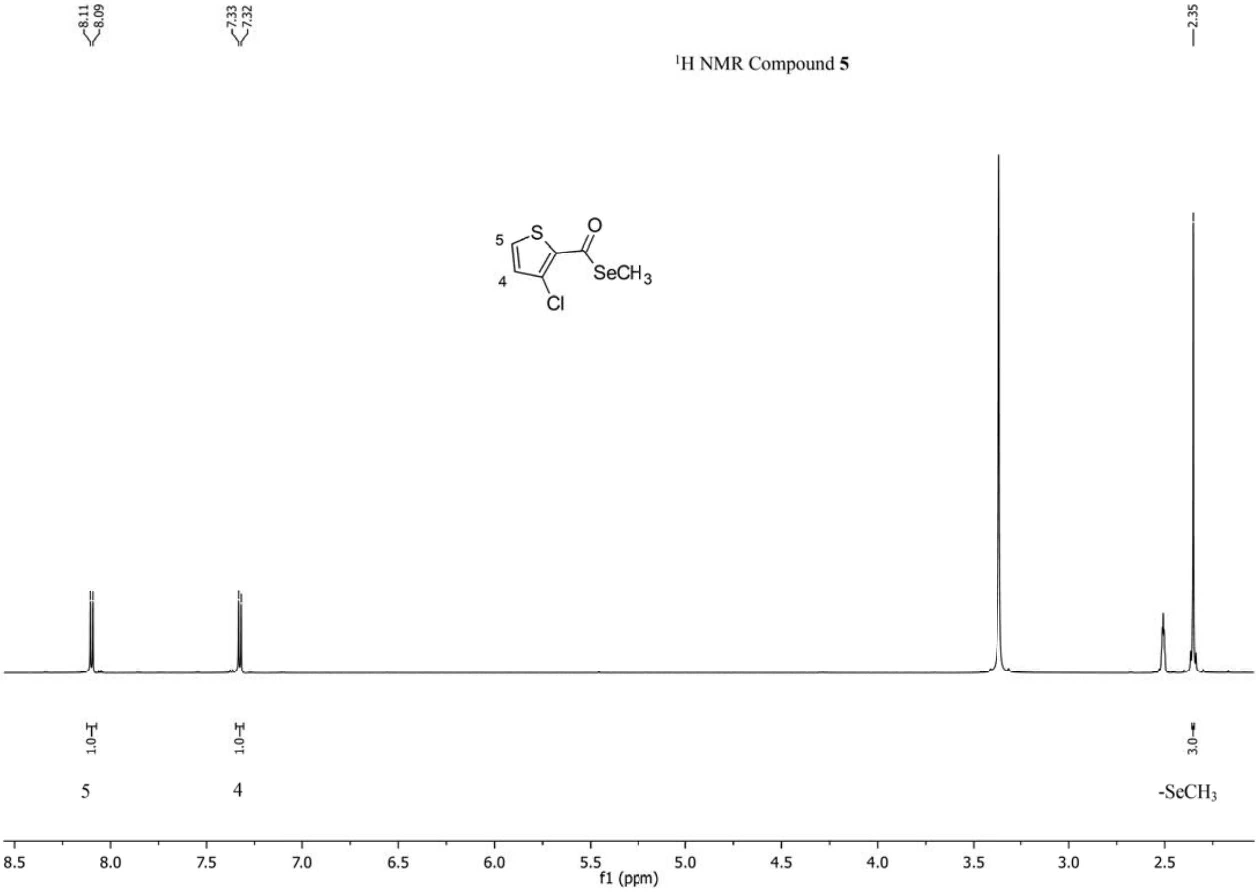
8.11
8.09
7.33
7.32
2.35
^{1}H NMR Compound **5**
5
S
O
SeCH3
4
Cl
1.0
1.0
3.0
5
4
-SeCH3
8.5
8.0
7.5
7.0
6.5
6.0
5.5
5.0
4.5
4.0
3.5
3.0
2.5
f1 (ppm)

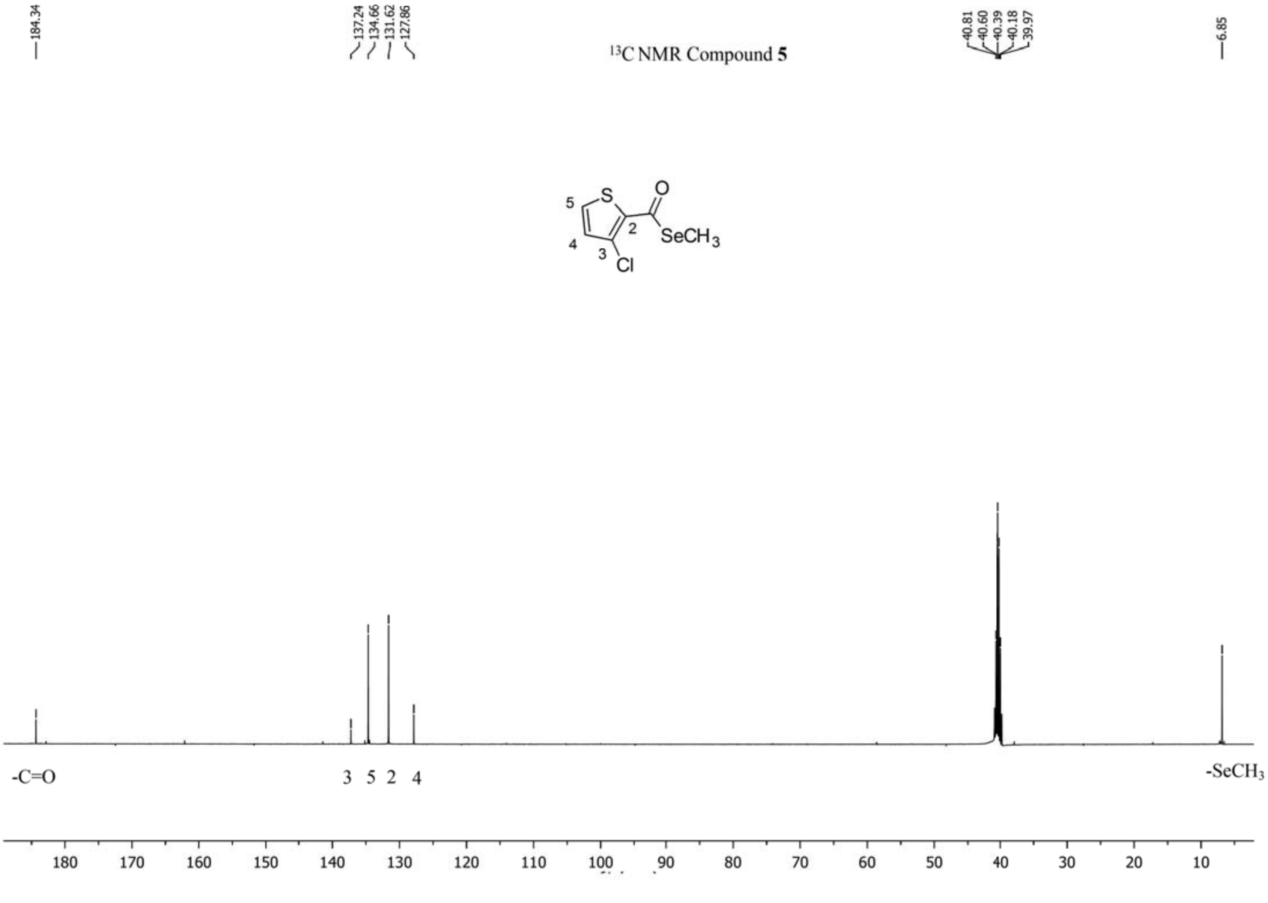
184.34
137.24
134.66
131.62
127.86
40.81
40.60
40.39
40.18
39.97
6.85
^{13}C NMR Compound **5**
5
S
O
2
SeCH3
4
3
Cl
-C=O
3 5 2 4
-SeCH3
180
170
160
150
140
130
120
110
100
90
80
70
60
50
40
30
20
10

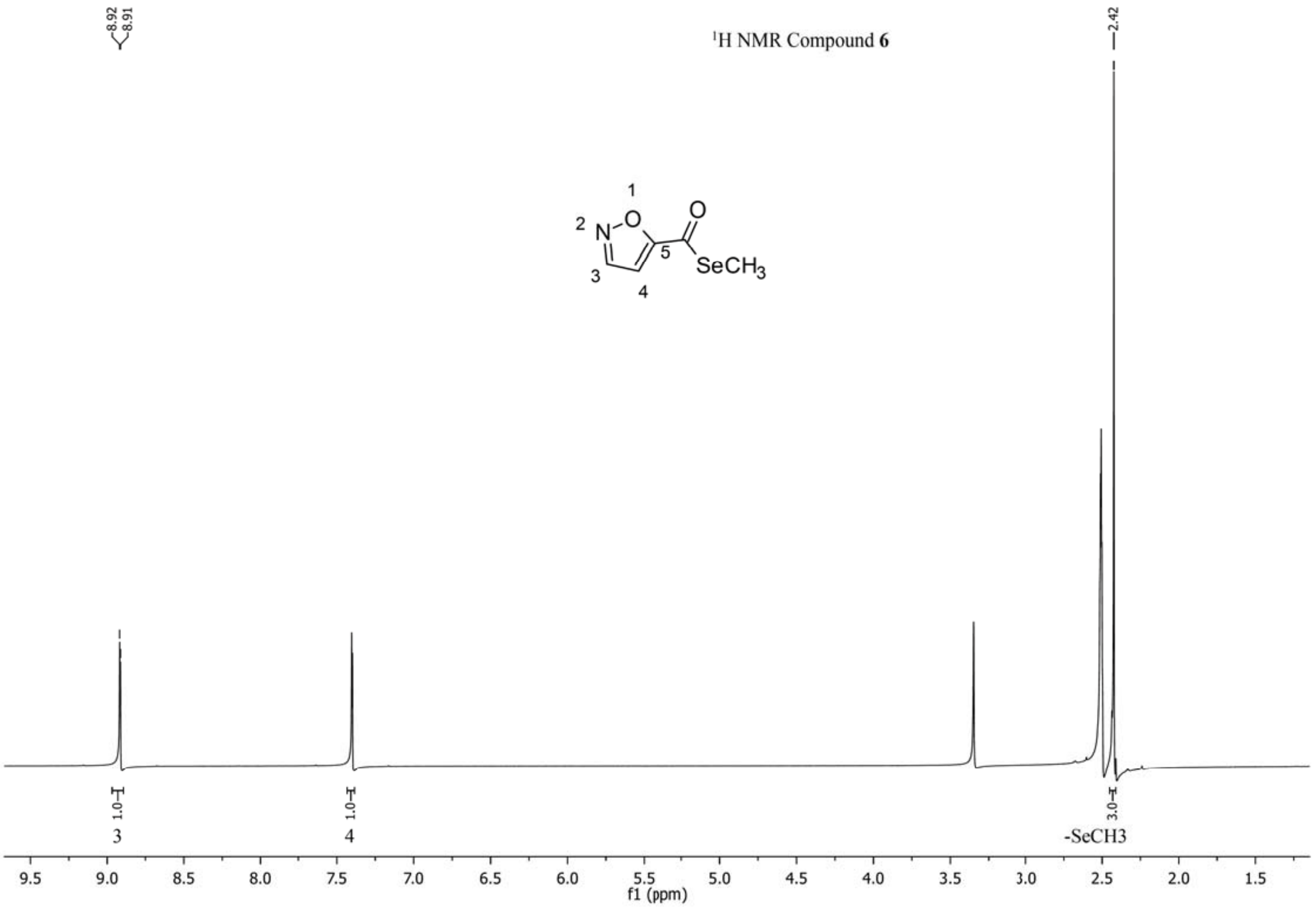
8.92
8.91
^{1}H NMR Compound **6**
2.42
1
2
N
O
O
5
SeCH$_3$
3
4
1.0
1.0
3.0
3
4
-SeCH3
9.5
9.0
8.5
8.0
7.5
7.0
6.5
6.0
5.5
5.0
4.5
4.0
3.5
3.0
2.5
2.0
1.5
f1 (ppm)

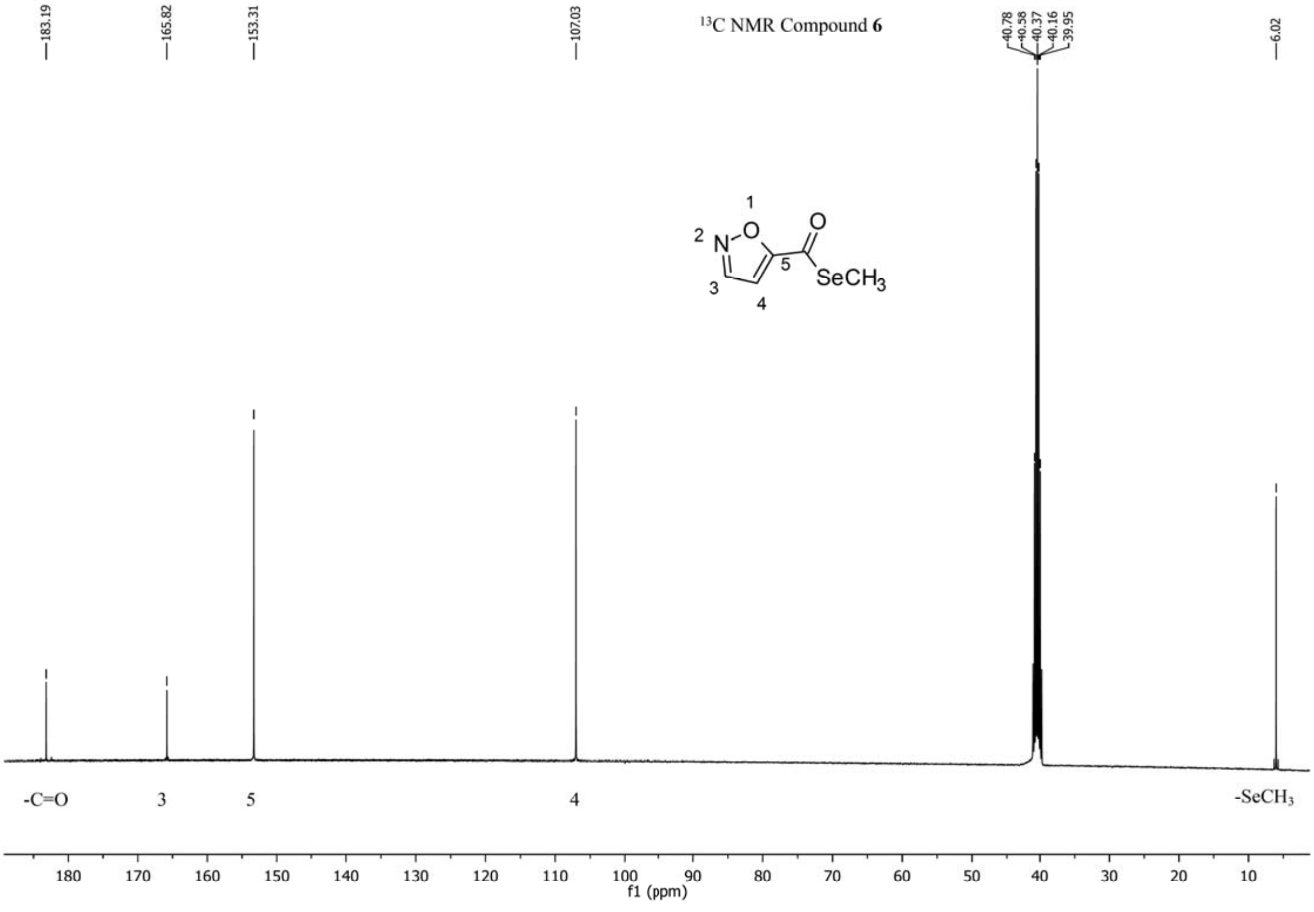
183.19
165.82
153.31
107.03
^{13}C NMR Compound **6**
40.78
40.58
40.37
40.16
39.95
6.02
1
2
N
O
O
5
SeCH$_3$
3
4
-C=O
3
5
4
-SeCH$_3$
180
170
160
150
140
130
120
110
100
90
80
70
60
50
40
30
20
10
f1 (ppm)

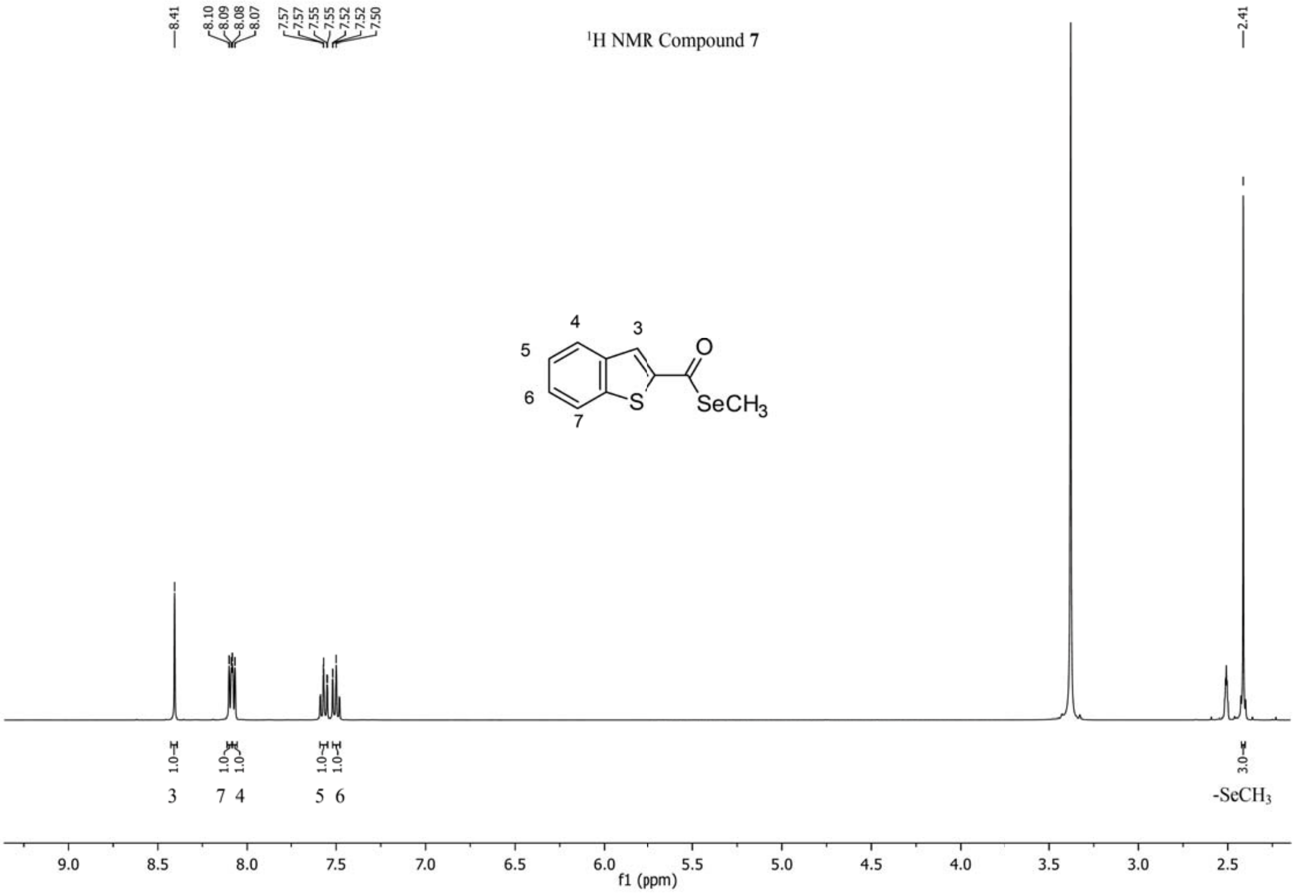
8.41
8.10
8.09
8.08
8.07
7.57
7.57
7.55
7.55
7.52
7.52
7.50
2.41
^{1}H NMR Compound 7
4
3
5
6
7
O
S
SeCH$_3$
1.0
1.0
1.0
1.0
1.0
3.0
3
7 4
5 6
-SeCH$_3$
9.0
8.5
8.0
7.5
7.0
6.5
6.0
5.5
5.0
4.5
4.0
3.5
3.0
2.5
f1 (ppm)

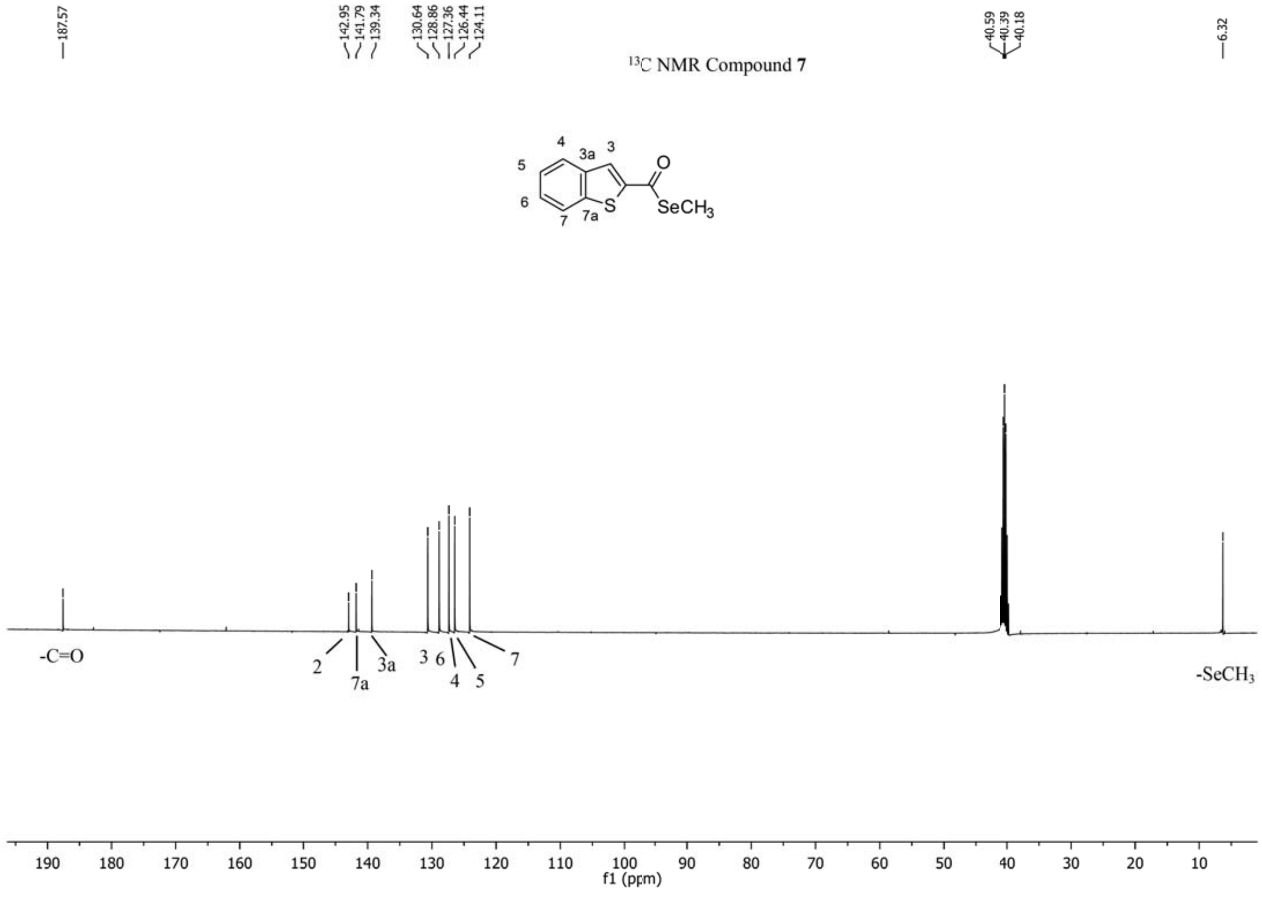
187.57
142.95
141.79
139.34
130.64
128.86
127.36
126.44
124.11
40.59
40.39
40.18
6.32
^{13}C NMR Compound 7
4
3a
3
5
6
7
7a
O
S
SeCH$_3$
-C=O
2
7a
3a
3 6
4 5
7
-SeCH$_3$
190
180
170
160
150
140
130
120
110
100
90
80
70
60
50
40
30
20
10
f1 (ppm)

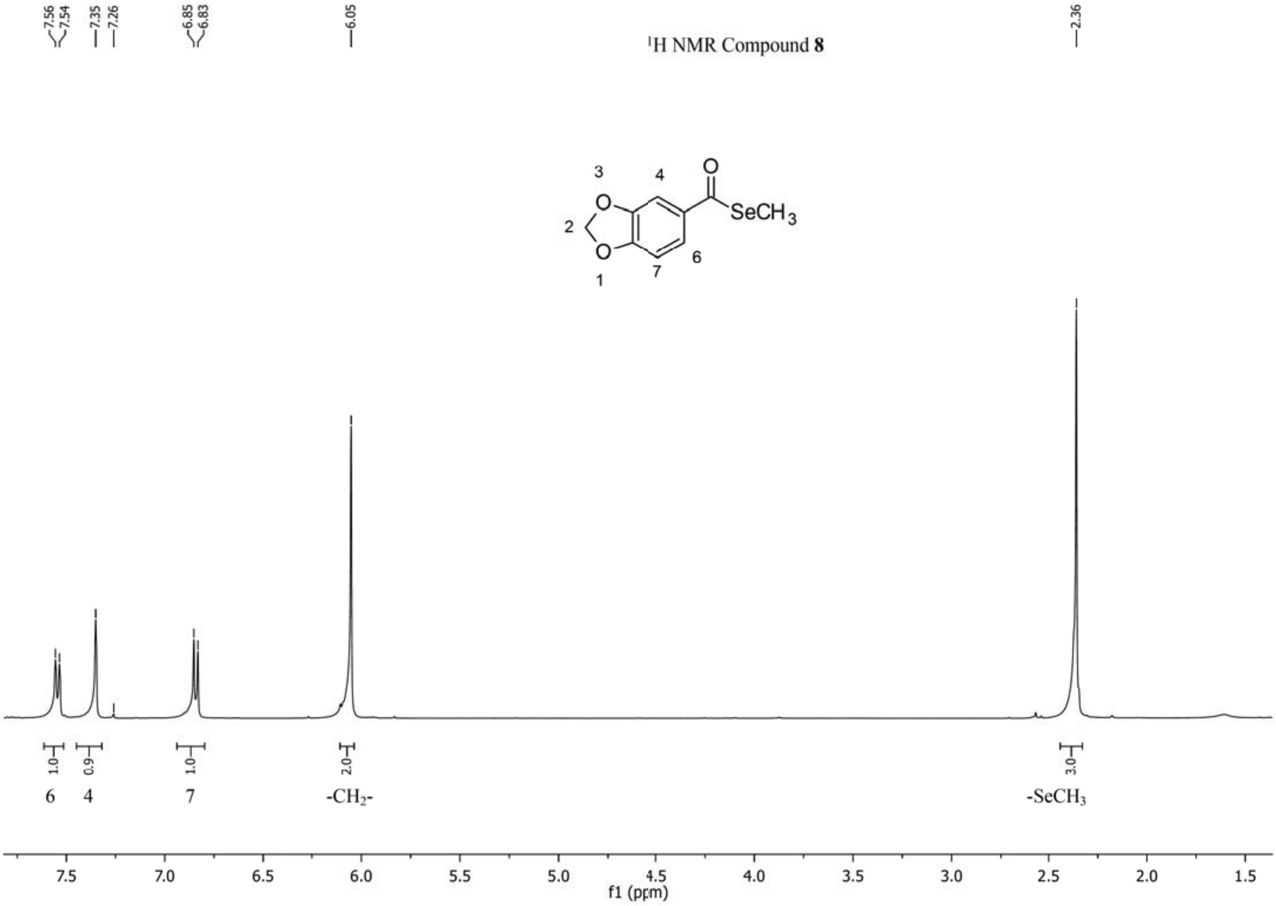
7.56
7.54
7.35
7.26
6.85
6.83
6.05
2.36
^{1}H NMR Compound 8
3
4
2
O
O
SeCH$_3$
1
7
6
1.0
0.9
1.0
2.0
3.0
6
4
7
-CH$_2$-
-SeCH$_3$
7.5
7.0
6.5
6.0
5.5
5.0
4.5
4.0
3.5
3.0
2.5
2.0
1.5
f1 (ppm)

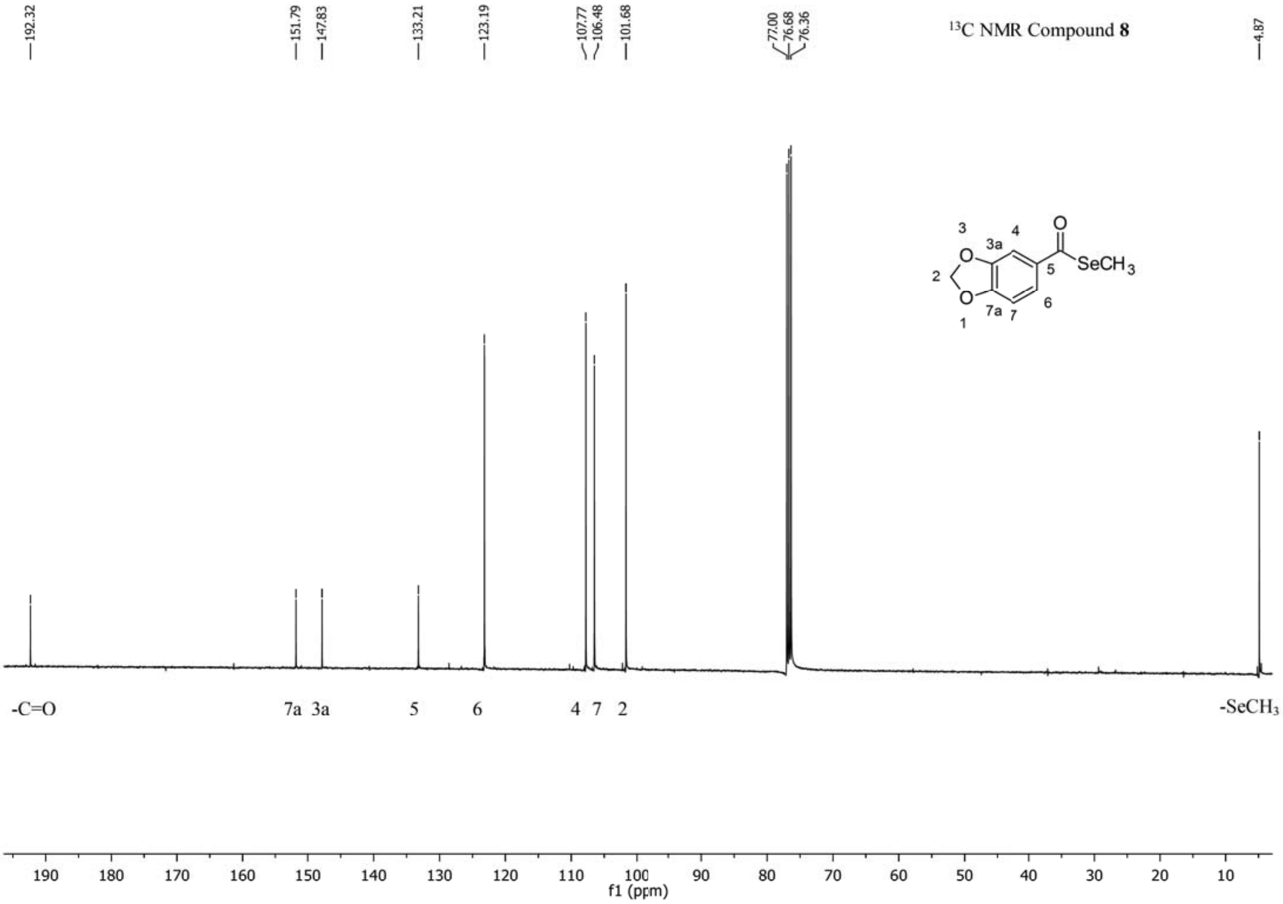
192.32
151.79
147.83
133.21
123.19
107.77
106.48
101.68
77.00
76.68
76.36
^{13}C NMR Compound 8
4.87
3
3a
4
2
5
O
SeCH$_3$
7a
7
6
1
-C=O
7a
3a
5
6
4
7
2
-SeCH$_3$
190
180
170
160
150
140
130
120
110
100
90
80
70
60
50
40
30
20
10
f1 (ppm)

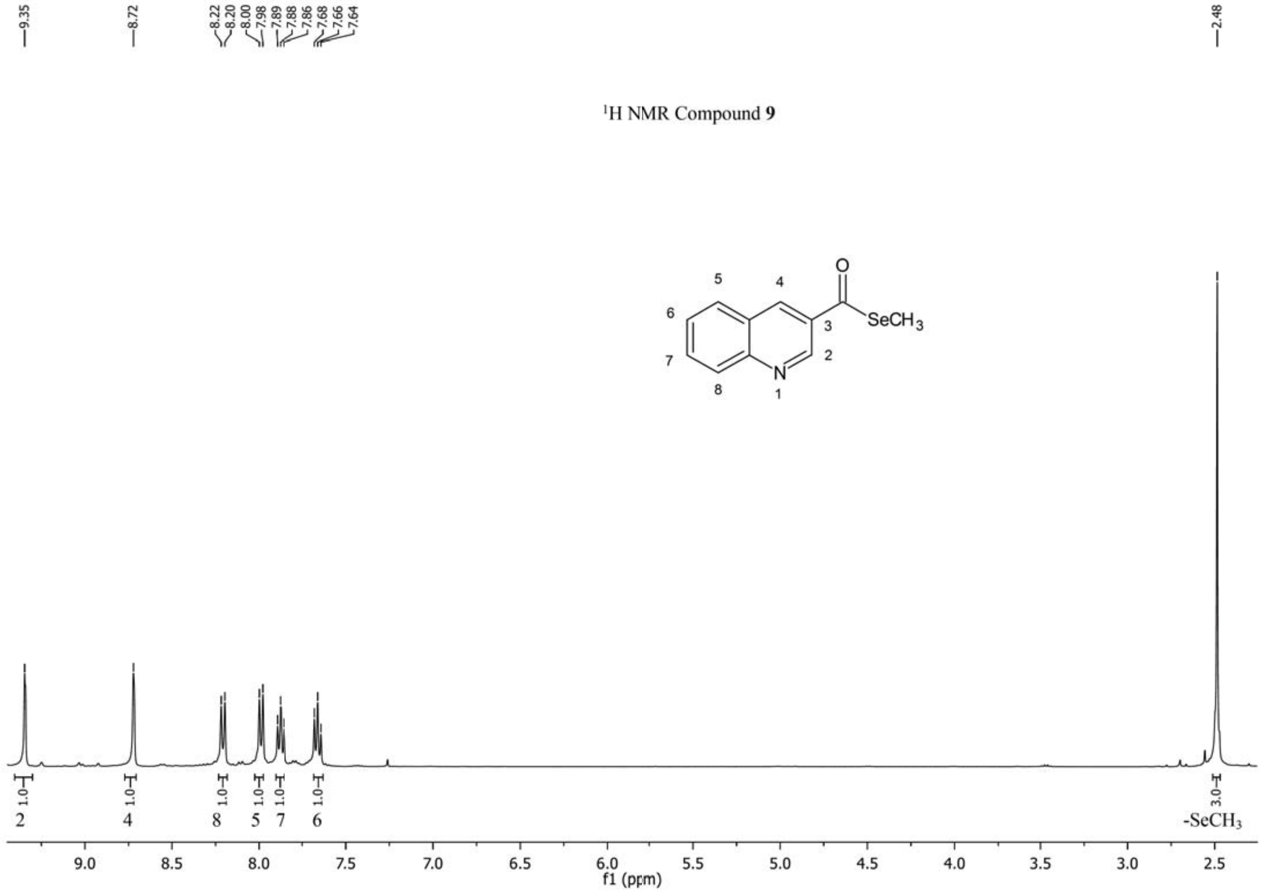

^{1}H NMR Compound **9**

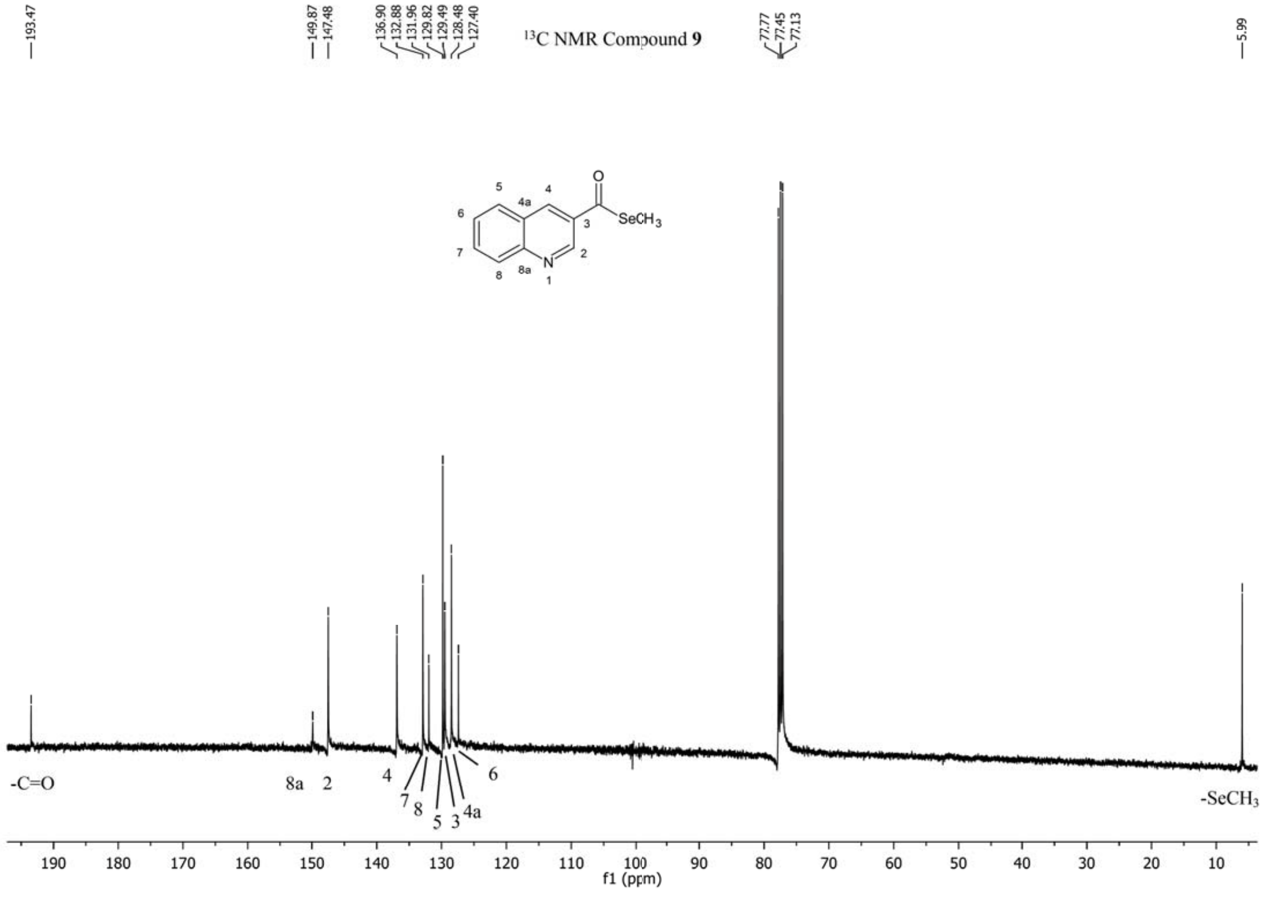

^{13}C NMR Compound **9**

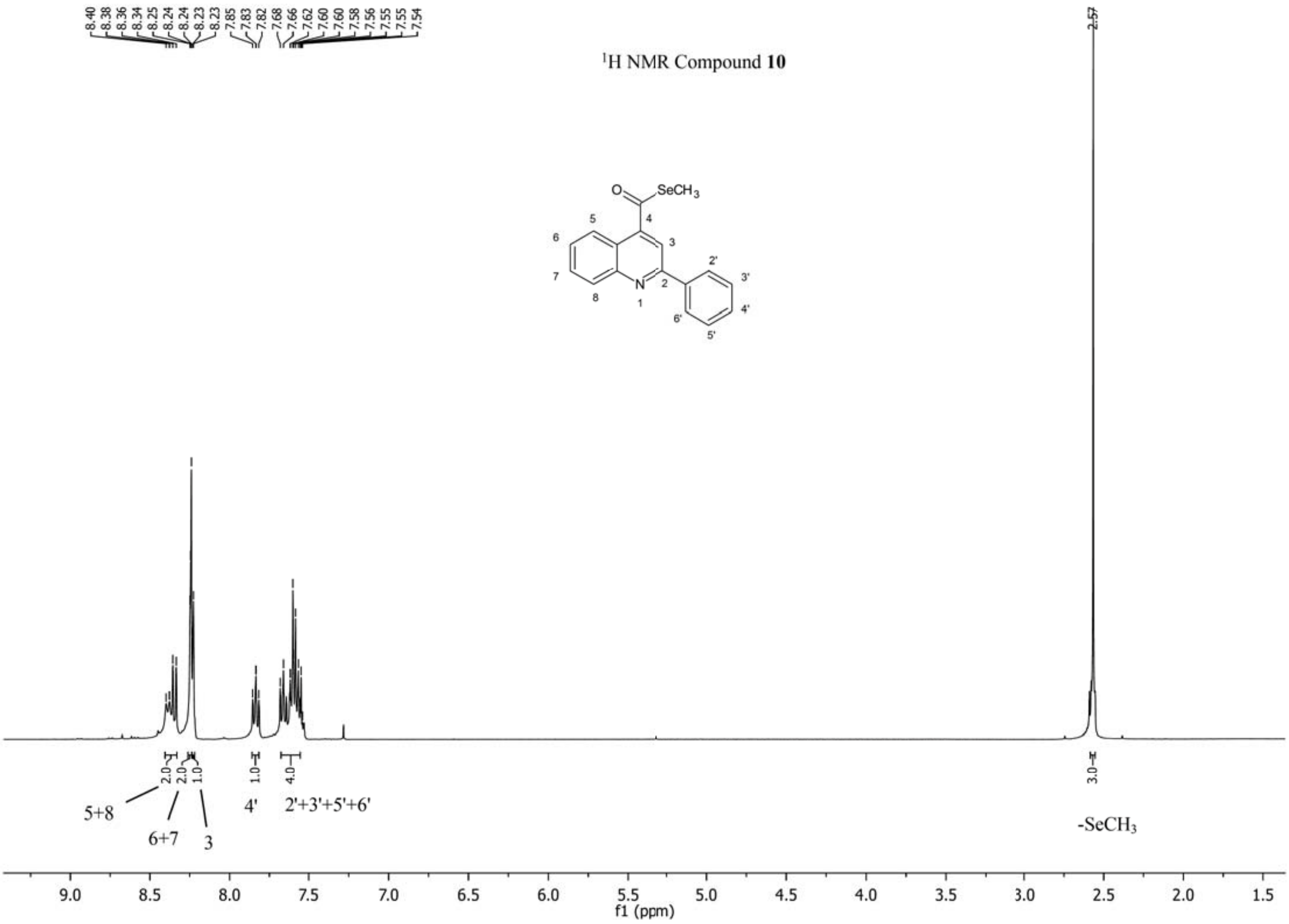
8.40
8.38
8.36
8.34
8.25
8.24
8.24
8.23
8.23
7.85
7.83
7.82
7.68
7.66
7.62
7.60
7.60
7.58
7.56
7.55
7.55
7.54
2.57
^{1}H NMR Compound **10**
O
SeCH$_3$
4
5
6
3
2'
7
N
2
3'
8
1
4'
6'
5'
2.0
2.0
1.0
1.0
4.0
3.0
5+8
6+7
3
4'
2'+3'+5'+6'
-SeCH$_3$
9.0
8.5
8.0
7.5
7.0
6.5
6.0
5.5
5.0
4.5
4.0
3.5
3.0
2.5
2.0
1.5
f1 (ppm)

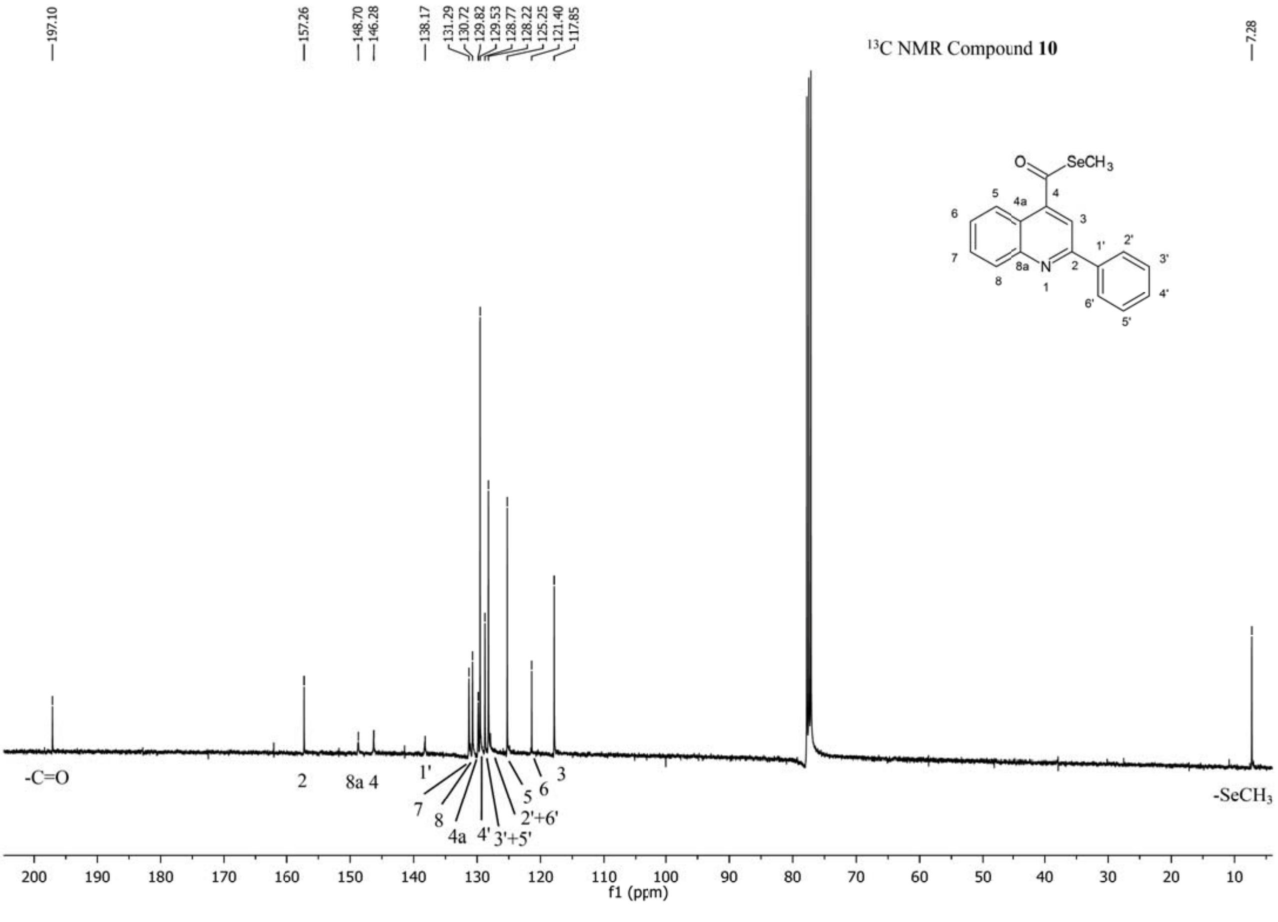
197.10
157.26
148.70
146.28
138.17
131.29
130.72
129.82
129.53
128.77
128.22
125.25
121.40
117.85
7.28
^{13}C NMR Compound **10**
O
SeCH$_3$
5
4a
4
6
3
1'
2'
7
8a
N
2
3'
8
1
4'
6'
5'
-C=O
2
8a 4
1'
7
8
4a
4'
3'+5'
5
6
3
2'+6'
-SeCH$_3$
200
190
180
170
160
150
140
130
120
110
100
90
80
70
60
50
40
30
20
10
f1 (ppm)

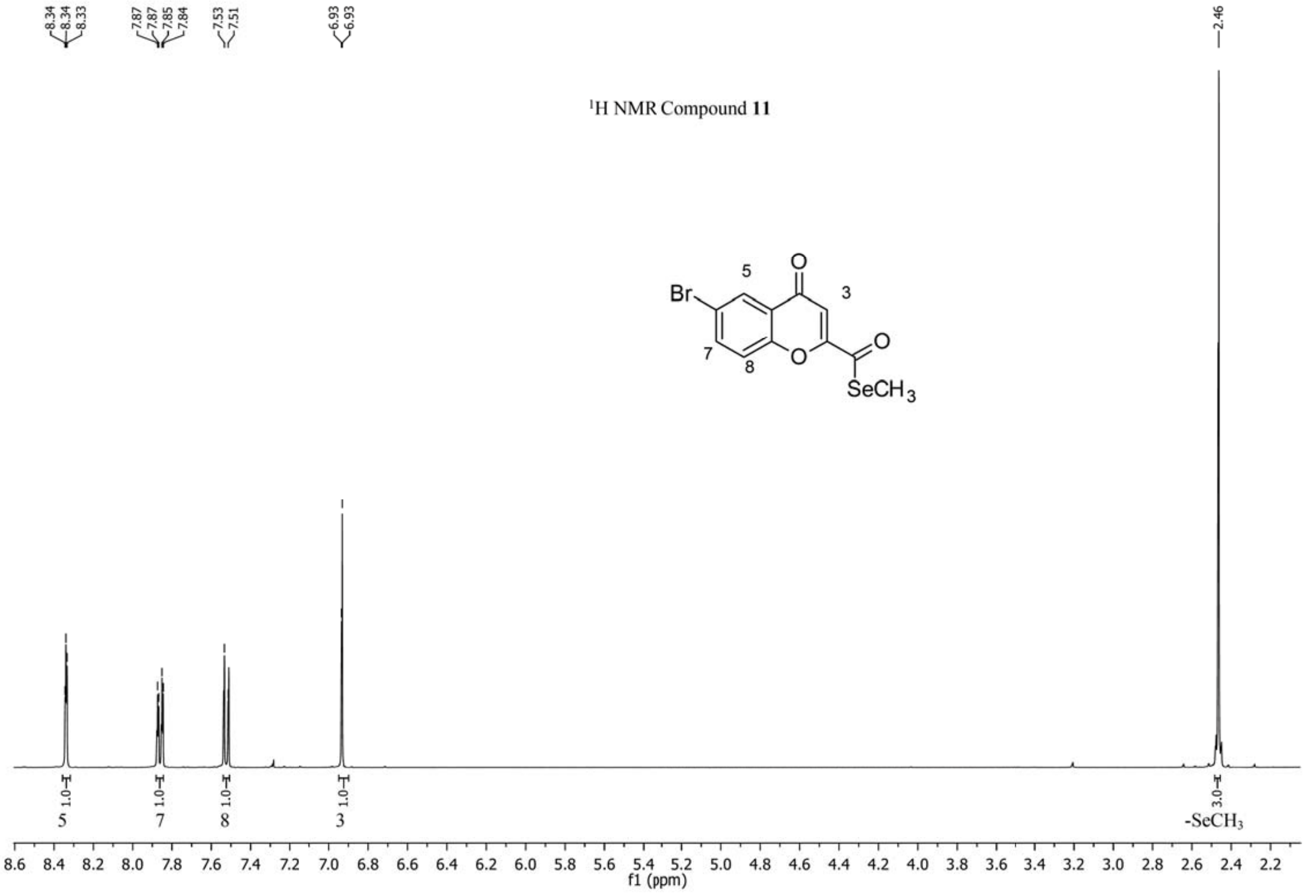
8.34
8.34
8.33
7.87
7.87
7.85
7.84
7.53
7.51
6.93
6.93
2.46
1H NMR Compound 11
Br
5
O
3
O
7
8
O
SeCH3
1.0
1.0
1.0
1.0
3.0
5
7
8
3
-SeCH3
8.6 8.4 8.2 8.0 7.8 7.6 7.4 7.2 7.0 6.8 6.6 6.4 6.2 6.0 5.8 5.6 5.4 5.2 5.0 4.8 4.6 4.4 4.2 4.0 3.8 3.6 3.4 3.2 3.0 2.8 2.6 2.4 2.2
f1 (ppm)

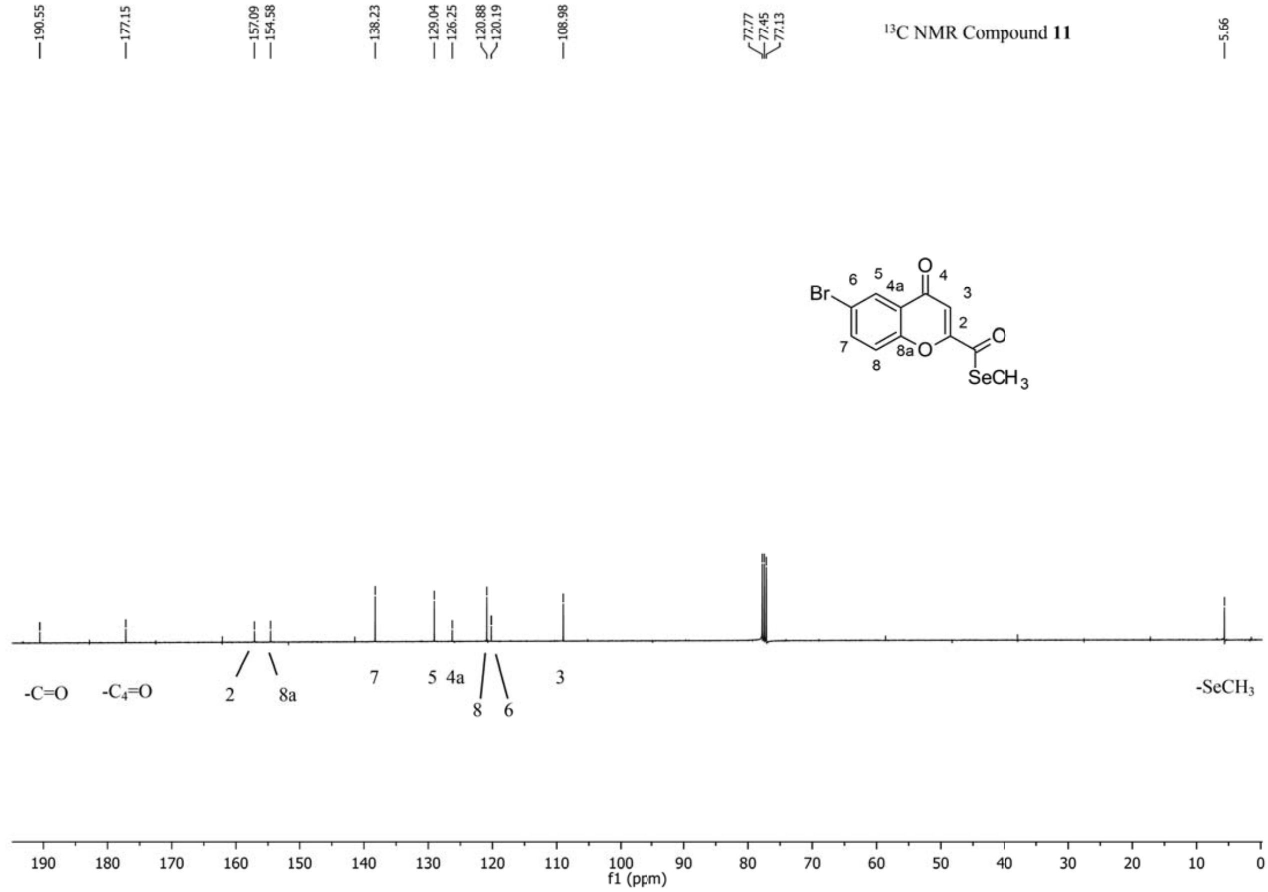
190.55
177.15
157.09
154.58
138.23
129.04
126.25
120.88
120.19
108.98
77.77
77.45
77.13
13C NMR Compound 11
5.66
Br
6
5
4a
O
4
3
2
O
7
8a
O
8
SeCH3
-C=O
-C4=O
2
8a
7
5
4a
8
6
3
-SeCH3
190 180 170 160 150 140 130 120 110 100 90 80 70 60 50 40 30 20 10 0
f1 (ppm)

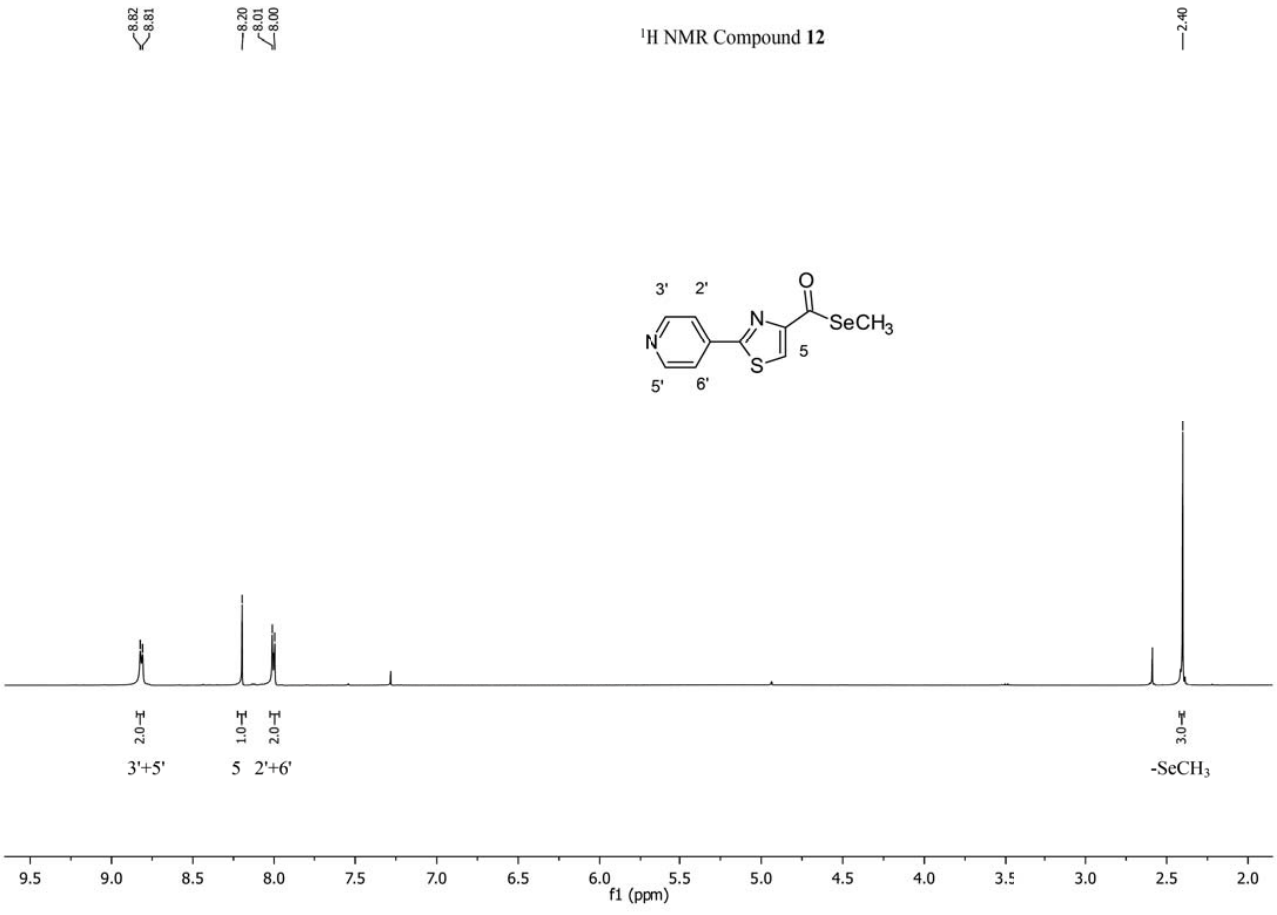
8.82
8.81
8.20
8.01
8.00
^{1}H NMR Compound **12**
2.40
3'
2'
N
N
O
SeCH$_3$
5
S
5'
6'
2.0
1.0
2.0
3.0
3'+5'
5
2'+6'
-SeCH$_3$
9.5
9.0
8.5
8.0
7.5
7.0
6.5
6.0
5.5
5.0
4.5
4.0
3.5
3.0
2.5
2.0
f1 (ppm)

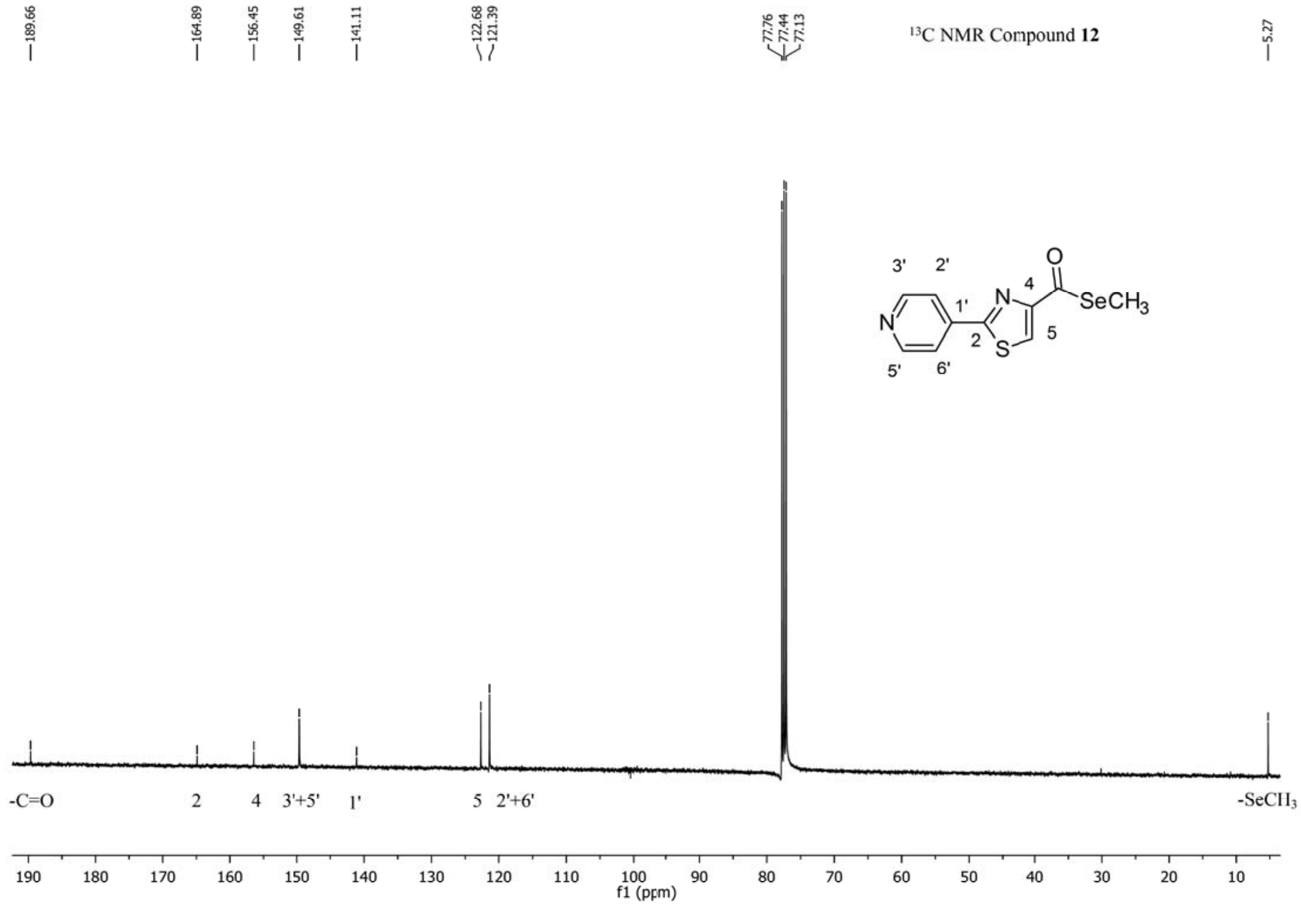
189.66
164.89
156.45
149.61
141.11
122.68
121.39
77.76
77.44
77.13
^{13}C NMR Compound **12**
5.27
3'
2'
1'
4
N
N
O
SeCH$_3$
2
S
5
5'
6'
-C=O
2
4
3'+5'
1'
5
2'+6'
-SeCH$_3$
190
180
170
160
150
140
130
120
110
100
90
80
70
60
50
40
30
20
10
f1 (ppm)

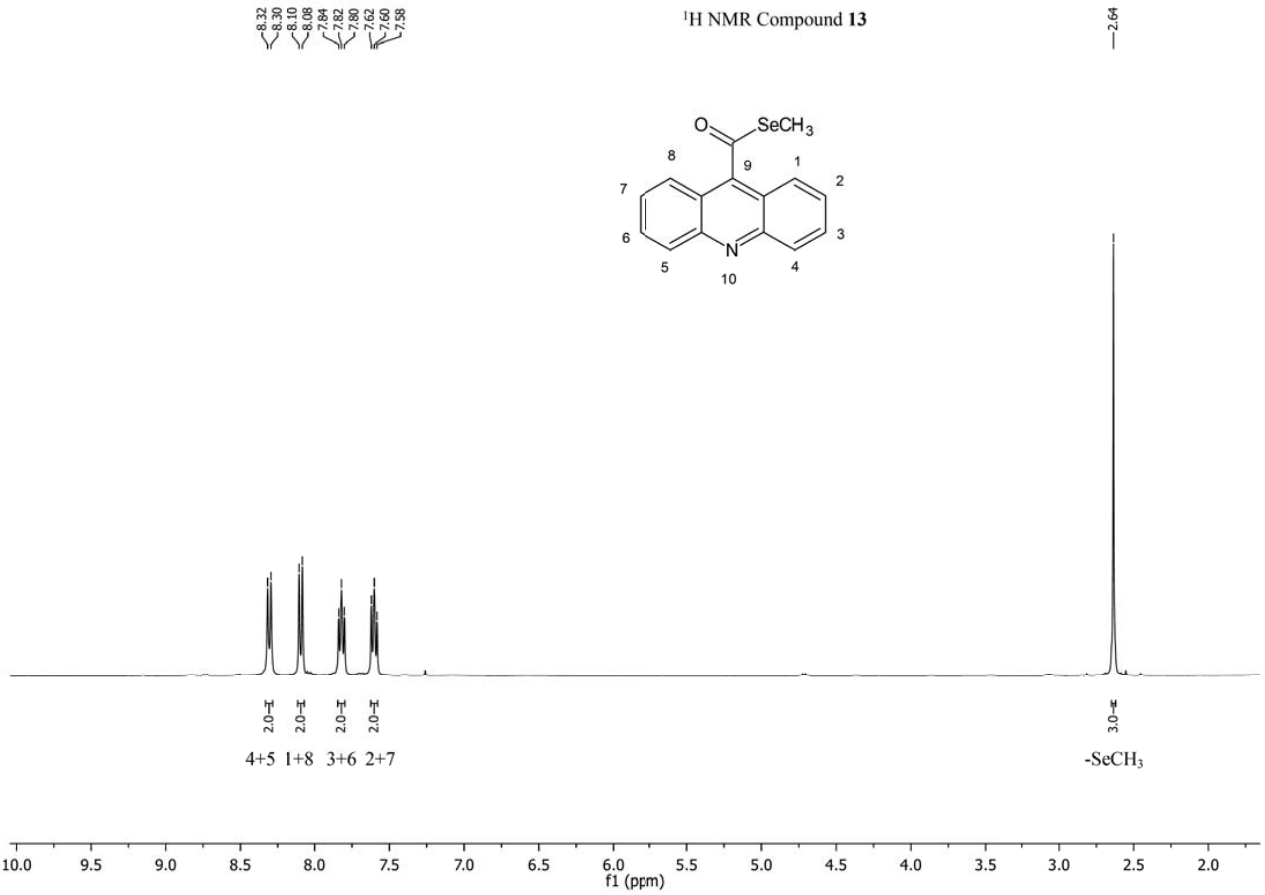
8.32
8.30
8.10
8.08
7.84
7.82
7.80
7.62
7.60
7.58
^{1}H NMR Compound **13**
2.64
O
SeCH$_3$
8
9
1
7
2
6
3
N
5
10
4
2.0
2.0
2.0
2.0
3.0
4+5 1+8 3+6 2+7
-SeCH$_3$
10.0
9.5
9.0
8.5
8.0
7.5
7.0
6.5
6.0
5.5
5.0
4.5
4.0
3.5
3.0
2.5
2.0
f1 (ppm)

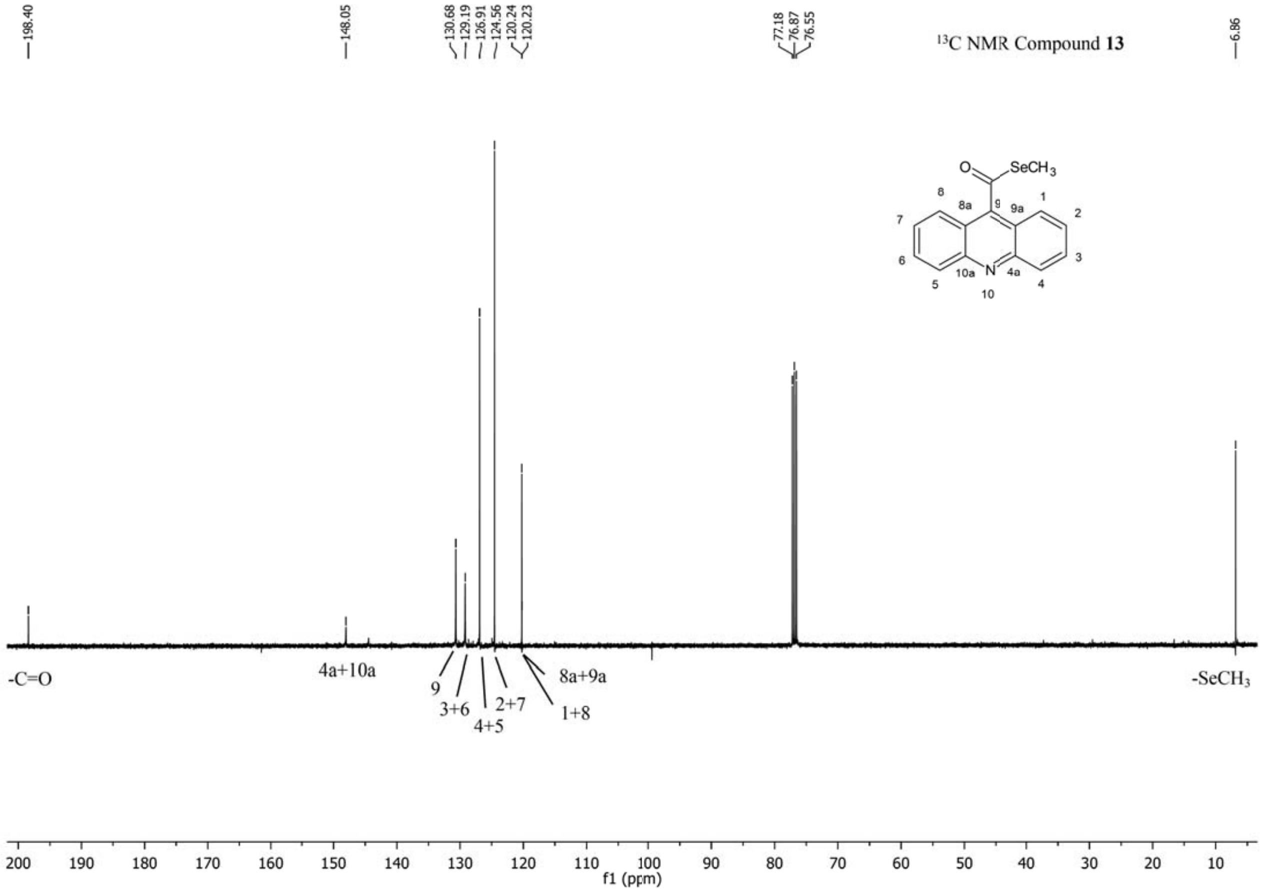
198.40
148.05
130.68
129.19
126.91
124.56
120.24
120.23
77.18
76.87
76.55
^{13}C NMR Compound **13**
6.86
O
SeCH$_3$
8
8a
9
9a
1
7
2
6
3
10a
N
4a
5
10
4
-C=O
4a+10a
9
3+6
4+5
2+7
8a+9a
1+8
-SeCH$_3$
200
190
180
170
160
150
140
130
120
110
100
90
80
70
60
50
40
30
20
10
f1 (ppm)

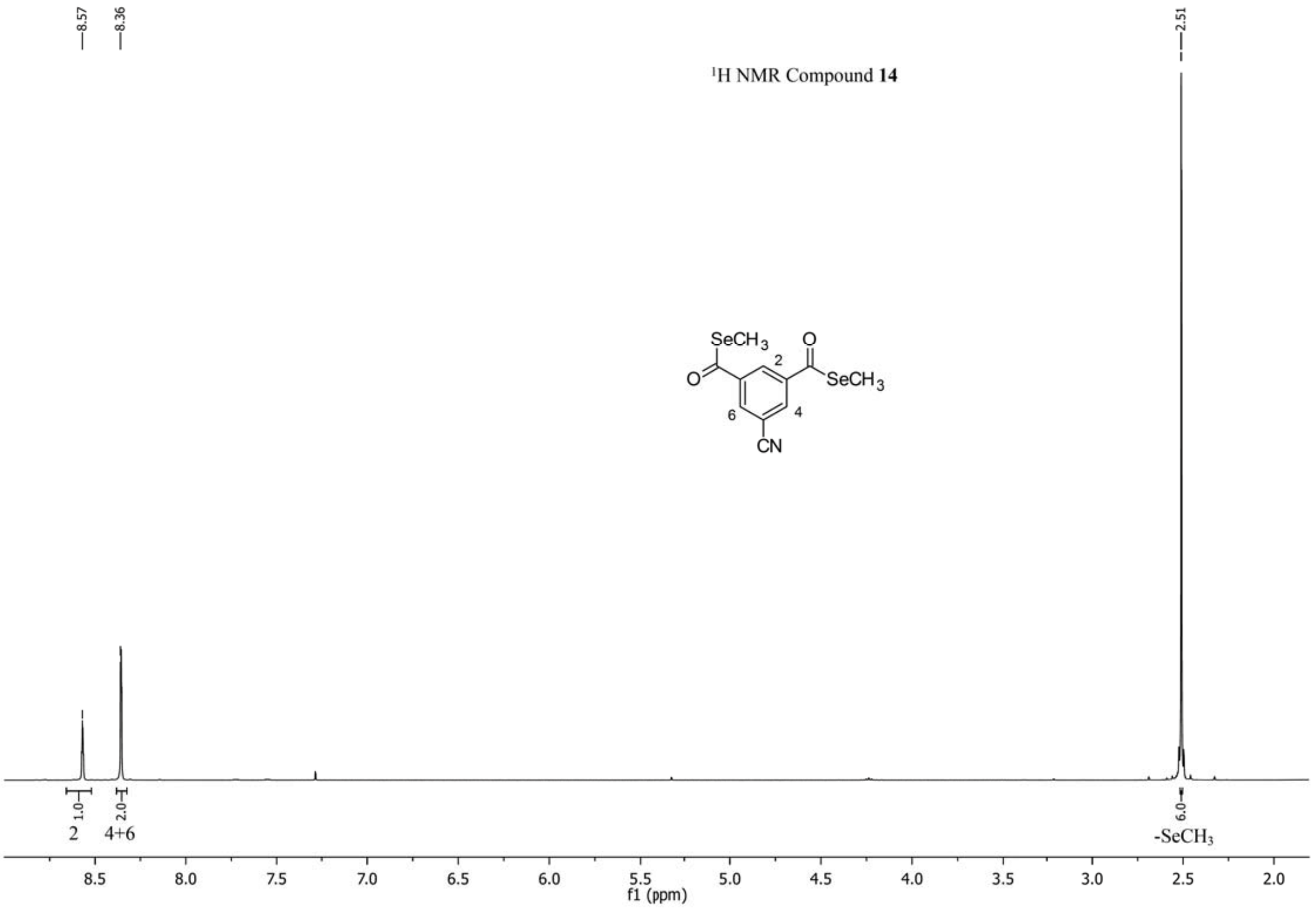
^{1}H NMR Compound **14**
8.57
8.36
2.51
SeCH3
O
2
SeCH3
6
4
CN
1.0
2.0
2
4+6
6.0
-SeCH3
8.5
8.0
7.5
7.0
6.5
6.0
5.5
5.0
4.5
4.0
3.5
3.0
2.5
2.0
f1 (ppm)

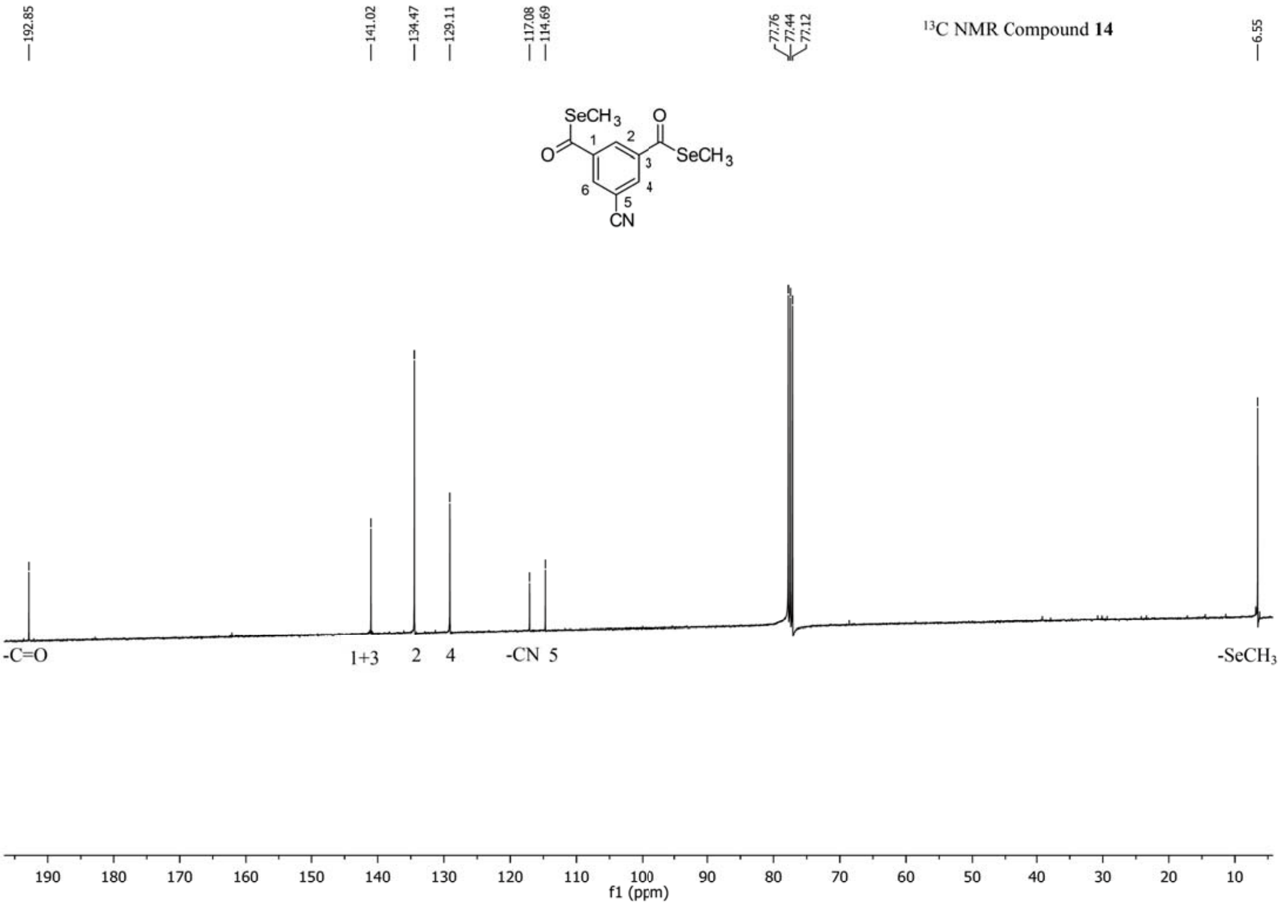
^{13}C NMR Compound **14**
192.85
141.02
134.47
129.11
117.08
114.69
77.76
77.44
77.12
6.55
SeCH3
1
2
3
SeCH3
6
5
4
CN
-C=O
1+3
2
4
-CN
5
-SeCH3
190
180
170
160
150
140
130
120
110
100
90
80
70
60
50
40
30
20
10
f1 (ppm)

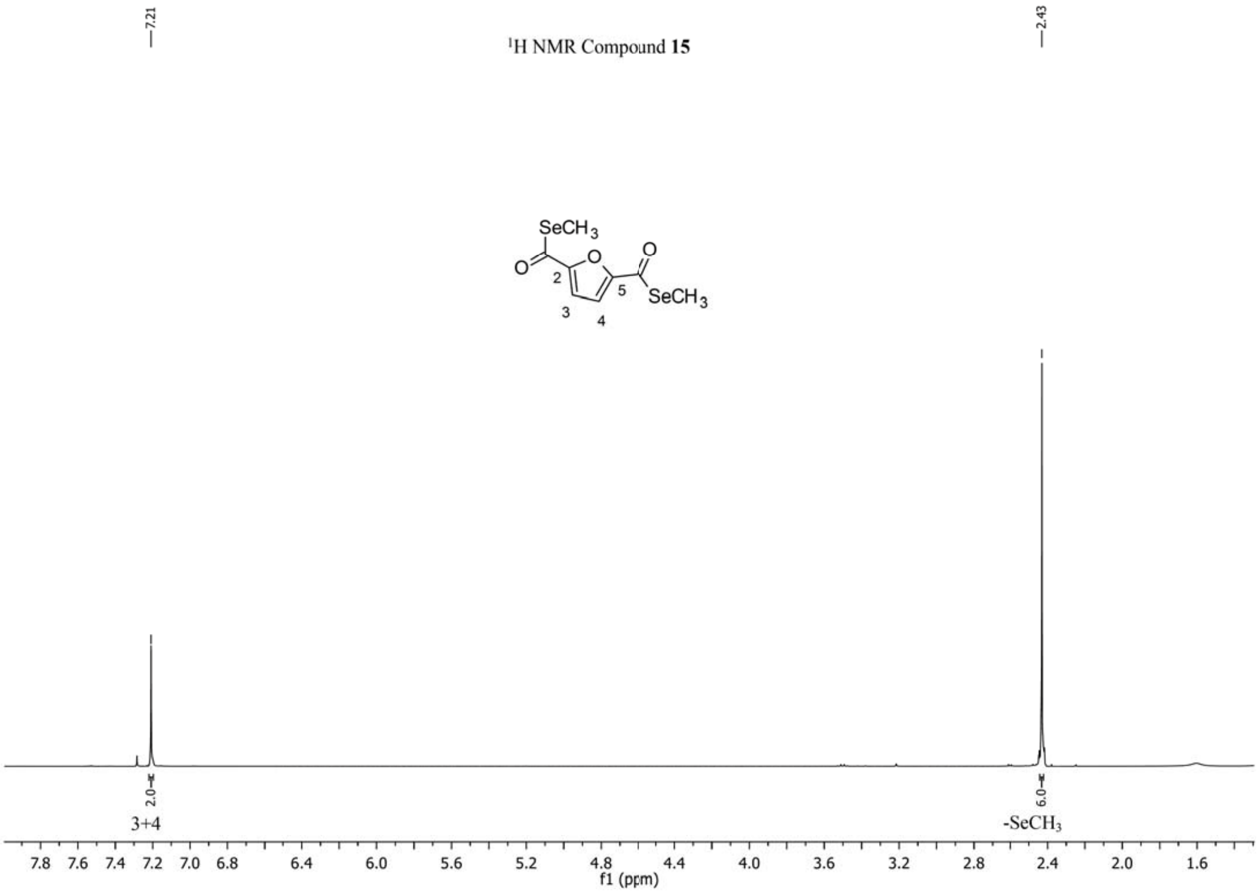
7.21
2.43
¹H NMR Compound **15**
SeCH3
O
2
O
5
SeCH3
O
3
4
2.0
3+4
6.0
-SeCH₃
7.8 7.6 7.4 7.2 7.0 6.8 6.4 6.0 5.6 5.2 4.8 4.4 4.0 3.6 3.2 2.8 2.4 2.0 1.6
f1 (ppm)

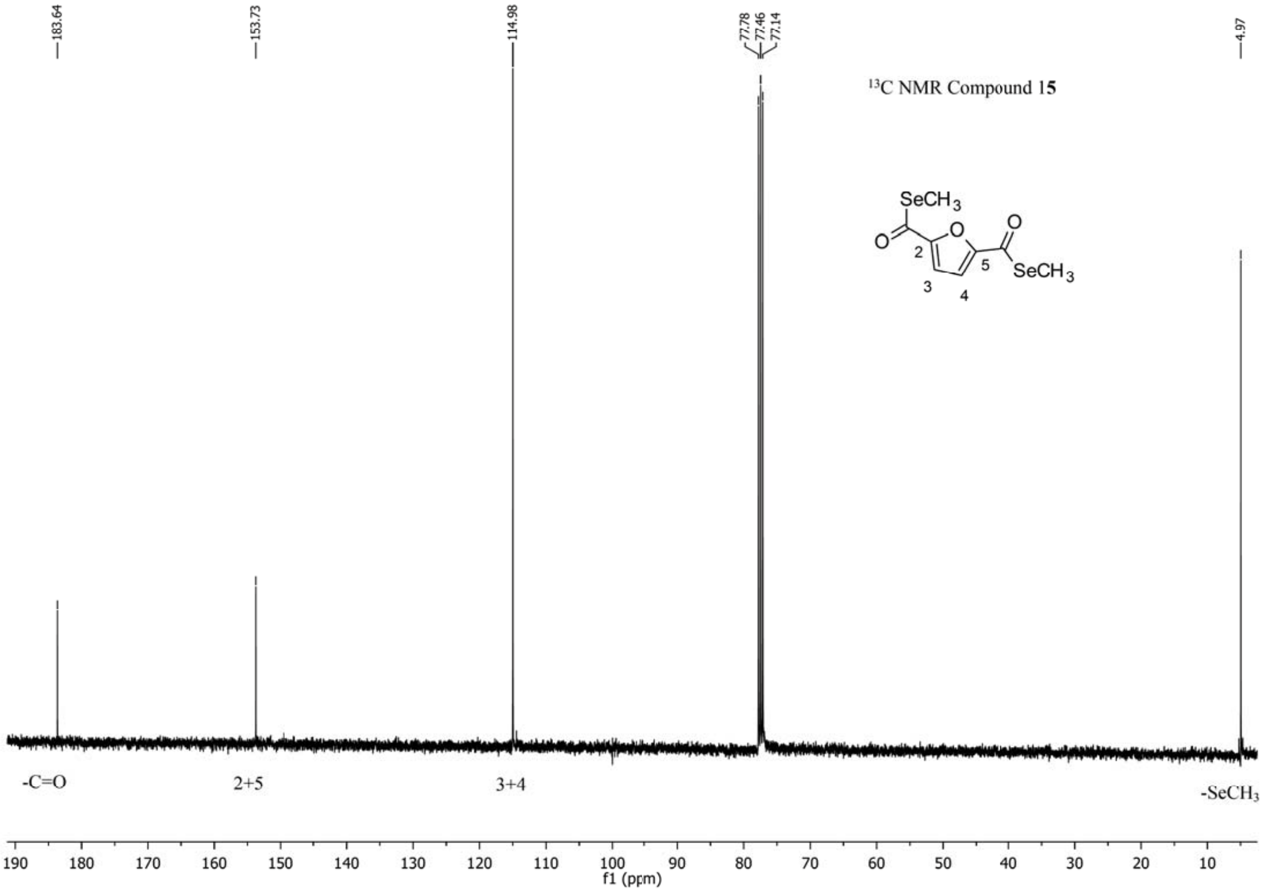
183.64
153.73
114.98
77.78
77.46
77.14
4.97
¹³C NMR Compound **15**
SeCH3
O
2
O
5
SeCH3
O
3
4
-C=O
2+5
3+4
-SeCH₃
190 180 170 160 150 140 130 120 110 100 90 80 70 60 50 40 30 20 10
f1 (ppm)

International Journal of
Molecular Sciences

MDPI

Article

Novel methylselenoesters induce programed cell death via entosis in pancreatic cancer cells.

Prajakta Khalkar [1, #*], Nuria Díaz-Argelich [1,2,3,#], Juan Antonio Palop [2,3], Carmen Sanmartín [2,3] and Aristi P. Fernandes [1]

# Authors have contributed equally

PUBLISHED

Int. J. Mol. Sci. 2018, 19, (10), 2849

PAPER 2

International Journal of
Molecular Sciences

MDPI

Article

Novel Methylselenoesters Induce Programed Cell Death via Entosis in Pancreatic Cancer Cells

Prajakta Khalkar [1,*,†], Nuria Díaz-Argelich [1,2,3,†], Juan Antonio Palop [2,3], Carmen Sanmartín [2,3] and Aristi P. Fernandes [1]

[1] Division of Biochemistry, Department of Medical Biochemistry and Biophysics (MBB), Karolinska Institutet, SE-171 77 Stockholm, Sweden; ndiaz@alumni.unav.es (N.D.-A.); Aristi.Fernandes@ki.se (A.P.F.)
[2] Department of Organic and Pharmaceutical Chemistry, Faculty of Pharmacy and Nutrition, University of Navarra, Irunlarrea 1, E-31008 Pamplona, Spain; japcubillo@gmail.com (J.A.P.); sanmartin@unav.es (C.S.)
[3] IdiSNA, Navarra Institute for Health Research, Irunlarrea 3, E-31008 Pamplona, Spain
* Correspondence: prajakta.khalkar@ki.se; Tel.: +46-8-52486990
† These authors contributed equally to this work.

Received: 27 August 2018; Accepted: 18 September 2018; Published: 20 September 2018

Abstract: Redox active selenium (Se) compounds have gained substantial attention in the last decade as potential cancer therapeutic agents. Several Se compounds have shown high selectivity and sensitivity against malignant cells. The cytotoxic effects are exerted by their biologically active metabolites, with methylselenol (CH_3SeH) being one of the key executors. In search of novel CH_3SeH precursors, we previously synthesized a series of methylselenoesters that were active (GI_{50} < 10 µM at 72 h) against a panel of cancer cell lines. Herein, we refined the mechanism of action of the two lead compounds with the additional synthesis of new analogs (ethyl, pentyl, and benzyl derivatives). A novel mechanism for the programmed cell death mechanism for Se-compounds was identified. Both methylseleninic acid and the novel CH_3SeH precursors induced entosis by cell detachment through downregulation of cell division control protein 42 homolog (CDC42) and its downstream effector β1-integrin (CD29). To our knowledge, this is the first time that Se compounds have been reported to induce this type of cell death and is of importance in the characterization of the anticancerogenic properties of these compounds.

Keywords: selenium; methylselenoesters; entosis; anticancer agent

1. Introduction

Pancreatic ductal adenocarcinoma is an extremely aggressive neoplasm and one of the cancers with the poorest prognosis, with a five-year survival of only 8% [1]. In addition, it is predicted to become the second leading cause of cancer-related death by 2030 [2]. Late diagnosis in advanced cancer stages due to a lack of prior symptomatology and the poor efficiency of actual therapeutics are the main causes. Drug resistance in pancreatic cancer is largely caused by an active stroma contributing to tumor progression [3]. Therefore, developing new therapeutic strategies has become an urgent need.

Modulation of redox homeostasis in cancer cells has emerged as a new opportunity for tumor intervention. Induction of reactive oxygen species (ROS) by these compounds may affect all the redox dependent pathways in the cell, which can be detrimental to cells. Antioxidant enzymes are often induced to eliminate elevated ROS production. Due to metabolic transformation, cancer cells have an increased and maximized antioxidant capacity in order to evade the ROS-induced cell death. For instance, the expression of mutant oncogenic KrasG12D is commonly present in pancreatic ductal adenocarcinoma (PDAC), resulting in an elevated basal state of the transcription factor, nuclear factor

E2-related factor 2 (NRF2) to mount an antioxidant response [4,5]. Therefore, even a slight additional ROS induction, using redox modulators, would lead to the killing of cancer cells [6,7], and provides an interesting therapeutic approach that has been established as a means of successful anti-cancer therapy [8–11].

Redox modulating selenium (Se) compounds have gained substantial attention in the last decade as potential cancer therapeutic agents [12]. Several Se compounds have shown high selectivity and sensitivity in malignant cells [13]. Depending on the compound use, they have been reported to induce different types of cell death, including apoptosis, autophagy, necrosis, or necroptosis.

Importantly, along with their active metabolites that execute their biological activity, the dosage and chemical form of Se compounds highly determine their efficacy [12]. Methylselenol (CH_3SeH) is considered a key metabolite in the anticancer activity of Se compounds. However, the in situ production or alternatively, the use of precursors, is required due to the high reactivity and volatility of this molecule.

In search of novel CH_3SeH precursors, we previously synthesized a series of methylselenoesters that were active ($GI_{50} < 10$ μM at 72 h) against a panel of cancer cell lines [14]. Herein, we studied the mechanism of action of the two lead compounds with the additional synthesis of new analogs (ethyl, pentyl, and benzyl derivatives) (Figure 1). This study uncovers a novel cell death mechanism for these Se-compounds as entosis inducers. Entosis was first described under anchorage-independent conditions and the loss of β1-integrin (CD29) signaling [15]. However, it has also been described in adherent cells [16–18] and recently, aberrant mitosis [16] and glucose deprivation [19] have been identified as other possible triggers.

During entosis, the stiffer cell (hereafter target cell) actively participates in its own internalization, via adherent junctions and the actin cytoskeleton that play a pivotal role in this process. Ultimately, the target cell is killed through lysosomal enzyme-mediated degradation, using the autophagy machinery, but independent of autophagosome formation [20]. The death subroutine might swift to apoptosis in the absence of autophagy-dependent nutrient recycling, or eventually, the internalized cell might divide or be released [21].

Methylseleninic acid (MSA) and the novel CH_3SeH precursors induce cell detachment through downregulation of cell division control protein 42 homolog (CDC42) and its downstream effector CD29 [22]. Cell-cell adhesion molecules such as N-cadherin were upregulated after treatment and facilitated cell clustering, which finally ended with cell-in-cell invasion and the degradation of the inner cell. To our knowledge, this is the first time that Se compounds have been reported to induce this type of cell death.

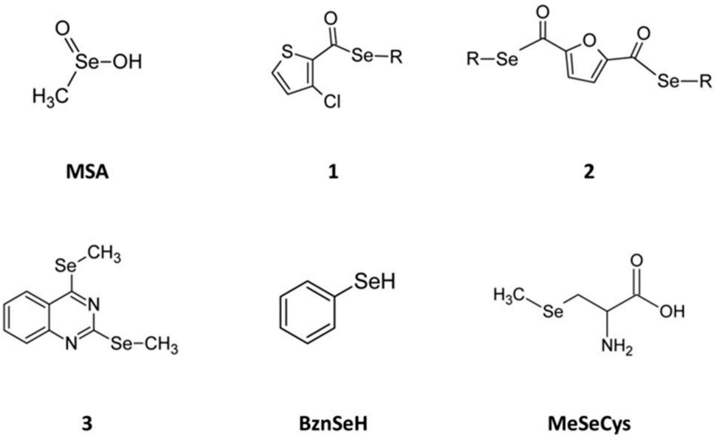

Compound	'R'
1	methyl
1a	ethyl
1b	pentyl
2	methyl
2a	ethyl
2c	benzyl

Figure 1. Chemical structures of the compounds. MSA, and compounds **1** and **2** were the primary focus of this study, whereas remaining compounds were used for comparative analysis in some experiments. MSA: methylseleninic acid; R: substituent; BznSeH: benzeneselenol; MeSeCys: methylselenocysteine.

2. Results

2.1. MSA, and Compounds **1** and **2** Reduce Panc-1 Cell Viability Both in 2D and 3D Cultures

Initial characterization of the compounds was performed through viability assays in 2D and 3D cultures of Panc-1 cells, given that 3D cultures have been demonstrated to mimic tumor behavior more efficiently than traditional monolayer (2D) cultures. Panc-1 cells were treated with increasing concentrations of MSA, and compounds **1** or **2** for 72 h. Cell viability was then determined. All three compounds were cytotoxic, with compound 2 being the most potent compound in 2D cultures. The compounds had IC50 values in the low micromolar range in 2D cultures (2.28, 3.31, and 1.43 µM for MSA, and compounds **1** and **2**, respectively). However, cells grown as spheroids (3D) were consistent with previously reported data [23], and more resistant and higher doses of the compounds were required to reduce cell proliferation and induce cell death (Figure 2A,B).

To further study the induced cell death in 3D cultures, spheroids were stained with Hoechst and propidium iodide (PI) after 72 h treatment. While Hoechst stains the nucleus of all cells, PI only penetrates and stains damaged membranes of dying cells. As shown in Figure 2C, the three compounds were not only able to induce cell death, but the cell death was observed in the core of the spheroid, suggesting that these compounds were able to reach to the core of the sphere.

The selenoester entity could be easily hydrolyzed by a nucleophile such as water, rendering the corresponding carboxylic acids and releasing CH_3SeH, which is believed to be a key molecule in Se activity (Figure 2D). To exclude the possibility that the toxicity was from the linked moieties, the analog carboxylic acids of compounds **1** (**1′**) and **2** (**2′**) were selectively tested as a proof-of-concept. As seen in Figure 2E, they did not induce any cell death compared to the Se-containing molecules.

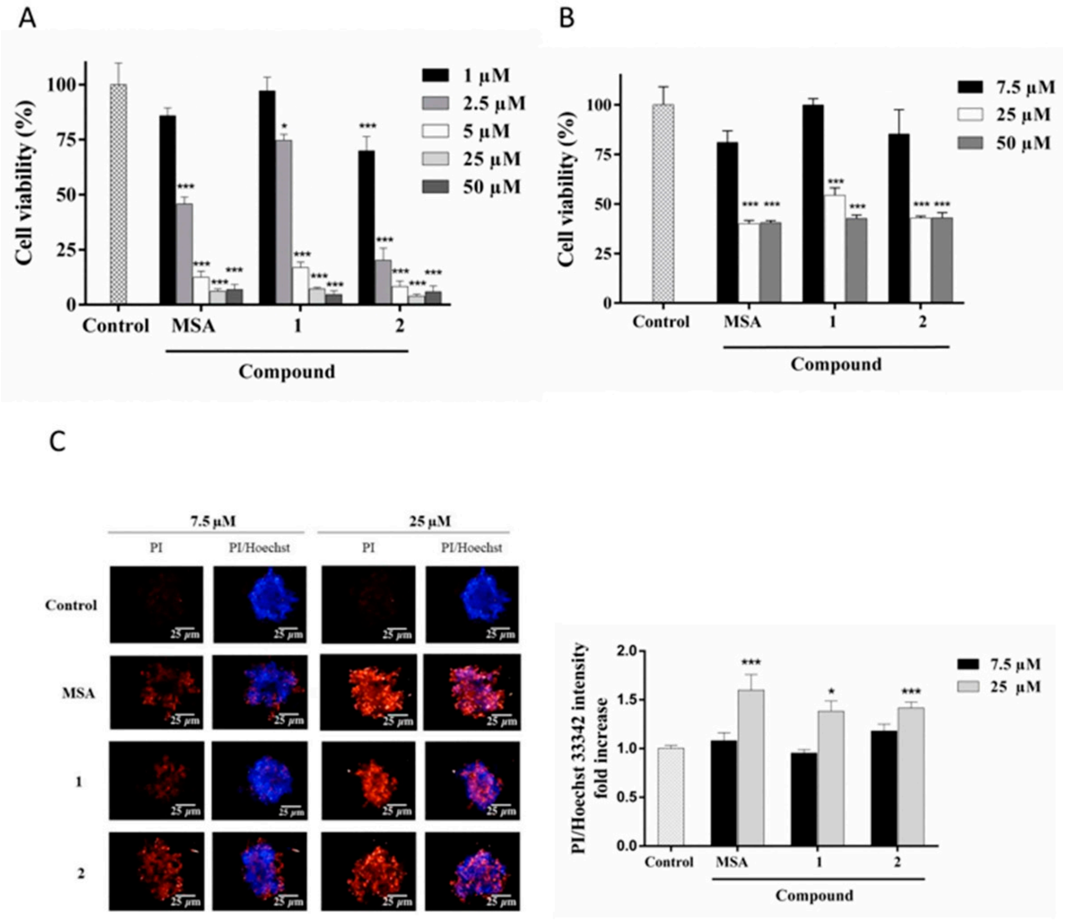

Figure 2. *Cont.*

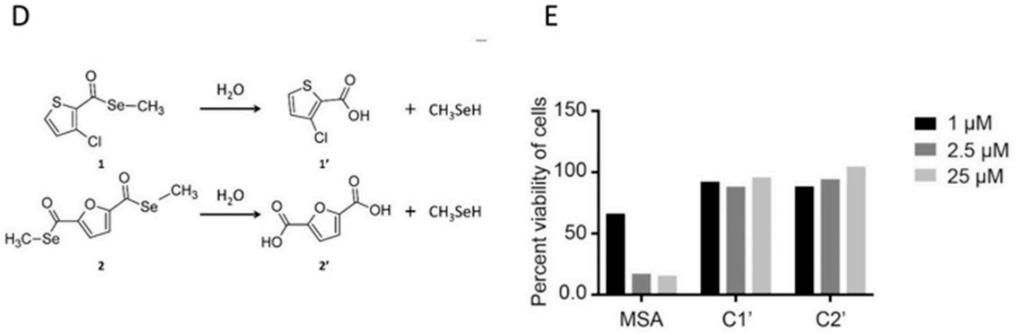

Figure 2. Compounds **1** and **2** and MSA decrease cell viability in 2D and 3D Panc-1 cultures. (**A**) Panc-1 cells (2D cultures) were treated with different concentrations of the compounds for 72 h followed by the determination of cell viability by the MTT (3-(4,5-Dimethylthiazol-2-yl)-2,5-Diphenyltetrazolium Bromide) assay. Results represent mean ± SEM of at least three independent experiments performed in quadruplicate. (**B**) Panc-1 spheroids (3D cultures) were treated with different concentrations of the compounds for 72 h, after which cell viability was determined using the acid phosphatase (APH) assay. Results represent mean ± SEM of at least three independent experiments performed in quadruplicate. (**C**) Representative confocal images of Panc-1 spheroids stained with Hoechst 33342 and PI after 72 h treatment with 7.5 μM and 25 μM of respective compounds. 10× objective magnification images were acquired from the Operetta® High-Content Imaging System and processed by Colombus™ analysis software. The adjacent graph represents a quantitative analysis of PI/Hoechst fluorescence. Results represent mean ± SEM (n = 4). (**D**) Potential hydrolysis reaction of compounds **1** and **2**. (**E**) 2D cell viability after treatment with the corresponding carboxylic acid for 72 h. Statistical significance compared to control: * $p < 0.05$, *** $p < 0.001$.

2.2. MSA, and Compounds **1** *and* **2** *Induce Cell Detachment and Compromise Reattachment Abilities by Promoting an Aberrant Adhesive Repertoire*

In order to study the early effects of this particular cell death, a concentration of 5 μM of respective compounds was chosen for further experiments in 2D cultures. Post 6 h treatment of Panc-1 cells, morphological changes like rounding of the cells and cellular detachment from culture flasks were observed. At 24 h, almost all the cells were detached, had acquired a refringent morphology, and were grouped in a grape-like manner (Figure 3A). Trypan blue exclusion, however, indicated that the floating cells were still alive at that particular time point (Figure 3B). To examine if the aberrant cellular detachment was irreversible, an adhesion assay was performed wherein the floating cells were washed to remove traces of the compounds and reseeded in fresh medium. The cells were then allowed to reattach to culture flasks for 3 h. Nevertheless, their reattachment abilities after treatment were observed to be compromised, with a clear loss of ability to re-adhere, especially in the case of compound **2** (Figure 3C).

As a next step, the effect of respective compounds on different cellular adhesion markers was analyzed. Post 24 h treatment, the expression of CD29, known to mediate adhesion to the extracellular matrix [24], was significantly reduced, as observed after flow cytometry analysis (Figure 3D), explaining the loss of cellular adhesion caused by these compounds. Moreover, the expression of N-cadherin, a cell-cell adhesion marker [25], showed a considerable increase after treatment with respective compounds, which explains the observed grape-like cellular clumping after detachment (Figure 3D).

In order to assess the fate of the detached cells, i.e., if they were able to recover or eventually go into the cell death mode, a clonogenic assay was performed. As illustrated in Figure 3E, post 24 h treatment with respective compounds, the cells displayed a significant decrease in colony formation compared to the control.

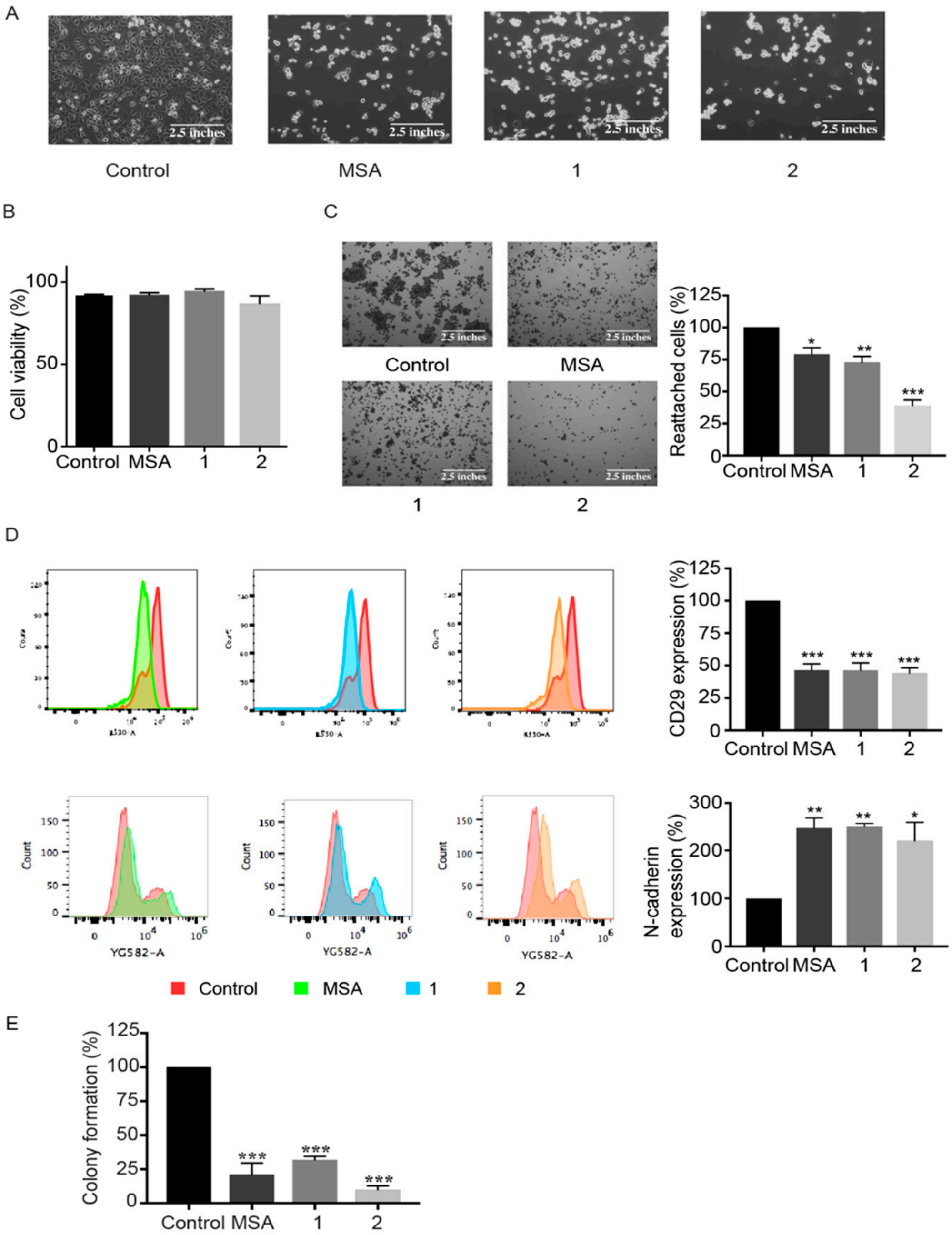

Figure 3. Compounds **1** and **2** and MSA induce loss of cellular adhesion prior to cell death and impair the colony forming ability. Panc-1 cells were treated with 5 µM of MSA, or compounds **1** or **2** for 24 h. (**A**) Representative phase-contrast images of treatment-induced cell detachment with respective compounds. (**B**) The viability of the floating cells was assessed using a trypan blue exclusion assay. (**C**) Adhesion assay. After 24 h of treatment with respective compounds, the non-adherent but viable cells, were collected and an adhesion assay was performed for 3 h, following which the adherent cells were stained with Coomassie Brilliant Blue. Representative phase-contrast microscopic images and graphical representation of percentage of non-adherent cells reattaching the tissue culture treated plates. Error bars indicate mean ± SEM of three biological replicates. (**D**) The expression levels of adhesion proteins, CD29, and N-Cadherin, post 24 h treatment with respective compounds as analyzed by flow cytometry and its graphical representation. Error bars indicate mean ± SEM of three biological replicates. (**E**) Clonogenic assay. Post 24 h treatment, with respective compounds, the non-adherent cells were collected and re-seeded in 24 well plates to check for the colony forming ability of these cells. Reduced colony forming ability indicates cell death. Error bars indicate mean ± SEM of three biological replicates. Statistical significance as compared to control * $p < 0.05$, ** $p < 0.01$, *** $p < 0.001$.

2.3. MSA, Compounds **1** *and* **2** *Induce Entosis.*

Two well described cell death pathways that have been reported to be initiated by the loss of cell adhesion are anoikis and entosis. Whereas anoikis is triggered exclusively upon adhesion loss and is coursed through caspase activation, entosis is characterized by active cell invasion, leading to endophagocytosis and the formation of cell-in-cell structures, and has been described both in suspension and adherent cells.

To distinguish the programmed cell death mode, we analyzed the expression of total poly (ADP-ribose) polymerase 1 (PARP) and cleaved PARP, wherein MSA and compounds **1** and **2** slightly increased the 89 kD cleaved fragment at 72 h (Supplementary Figure S1A). PARP has been reported to be cleaved by caspases, cathepsins, and calpains [26–29]. In order to rule out the possibility of apoptosis, the expression of caspase 9 and cleaved caspase 9 (upstream marker for apoptosis) was analyzed after 48 h treatment with these compounds. We observed no expression of cleaved caspase 9, suggesting that no activation of the caspase cascade was induced (Supplementary Figure S1A). Additionally, cells were treated with the broad pancaspase inhibitor z-VAD-fmk, along with respective compounds. Treatment with z-VAD-fmk did not prevent the cellular detachment, as well as cell death, induced by these compounds, as observed by brightfield microscopy and the trypan blue exclusion assay, respectively (Supplementary Figure S1B,C), suggesting a caspase-independent mechanism.

Furthermore, the expression of cathepsins, a structurally and catalytically distinguished class of proteases, was checked. A context-depending role has been described for cathepsins, with either tumor-promoting or suppressing activities. They have not only been reported to function as apoptotic mediators, but also to be related to entosis [15] and cell cannibalism [30].

Both cathepsin B (CatB) and cathepsin D (CatD) have been reported to play an important role in entosis [15,20,31]. Increased expression of CatB was observed, indicating that lysosomal degradation is implied in cell death induced by these compounds. Unexpectedly, CatD levels were downregulated (Figure 4A). Another family with a prominent role in entosis is the Rho family of GTPases, master regulators of the actin cytoskeleton. Therefore, the protein levels of CDC42 and RhoA were determined. Whereas CDC42 levels were decreased, RhoA levels remained unchanged (Figure 4A). To further confirm entosis, cell fate was tracked once detached. Cells were labeled with green or red fluorescent dyes, seeded, and treated with the compounds. Visualization by confocal microscopy revealed cell-in-cell internalization (Figure 4B). A time-lapse experiment also recorded live confirmed morphological changes during the formation of cell-in-cell structures and the ultimate degradation of the target cell (Supplementary videos 1–3).

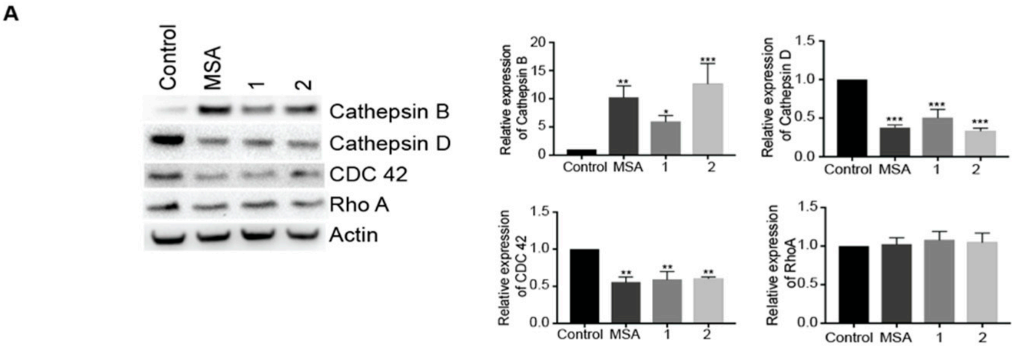

Figure 4. *Cont.*

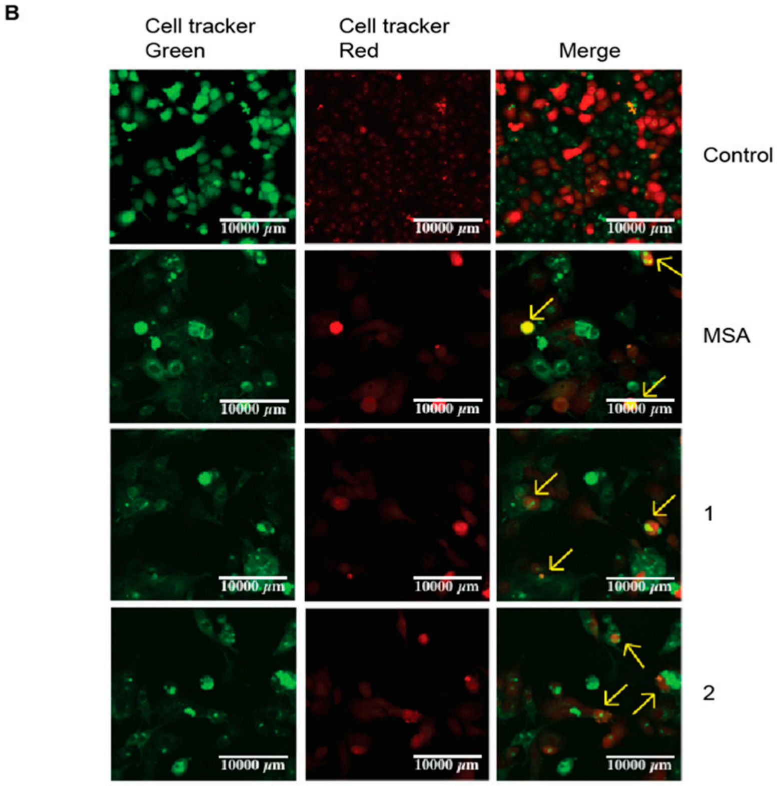

Figure 4. MSA, and compounds **1** and compound **2** induce entosis in Panc-1 cells. (**A**) Western blot analyses of Cathepsin B, Cathepsin D, CDC42, and Rho A upon treatment with MSA or compound **1** or compound **2** for 24 h. Beta actin was used as a loading control. The corresponding graphs display a quantitative analysis of western blots performed using the ImageJ program and GraphPad Prism software. Error bars indicate mean ± SEM of three biological replicates. (**B**) Panc-1 cells stained with CellTracker Red or Green and further mixed (1:1) were treated with MSA or compound **1** or compound **2** for 18 h, followed by live imaging using a confocal microscope, Zeiss LSM800. The arrows indicate cell-in-cell formations i.e., cells undergoing entosis. Statistical significance as compared to control * $p < 0.05$, ** $p < 0.01$, *** $p < 0.001$.

2.4. Cell Detachment Is Not Restricted to Selenomethylated Compounds and Does Not Correlate with the Cytotoxic Potential of the Compound

In order to distinguish the type of Se compound that could cause this phenomenon, other commercial Se derivatives together with other newly synthesized analogs of compounds **1** and **2** were analyzed. To evaluate if this effect was exclusive to methylated forms of Se or unrestricted to other alkyl or aromatic derivatives, the ethyl derivative for compounds **1** and **2** (**1a** and **2a**, respectively), the pentyl derivative for compound **1** (**1b**), and the benzyl analog for compound **2** (**2c**), were synthesized to cover different alkyl lengths and additional substituents. Methylselenocysteine (MeSeCys) was also selected as another CH_3SeH precursor and benzeneselenol (BznSeH) as an additional aromatic selenol for a comparative analysis. In addition, compound **3** was chosen, a previously synthesized selenide in our laboratory, as a proof-of-concept compound without a labile bond between the core of the molecule and the methylseleno residue [32], and therefore less prone to release it (Figure 1).

First, cell proliferation and cell death were evaluated. As illustrated in Figure 5A, all the compounds were able to reduce cell proliferation. However, a longer chain or the substitution with a benzyl residue impaired the cytostatic activity of the compounds. In general trends, and considering the 72 h time point, the potency to reduce proliferation decreased according to the following order: methyl > ethyl > pentyl or benzyl. Compound **2a** stopped proliferation at 24 h, while the methylated analog (**2**) achieved a reduction at 72 h. BznSeH and compound **3** had the highest cytostatic potential, with both of them inhibiting proliferation at 24 h of treatment.

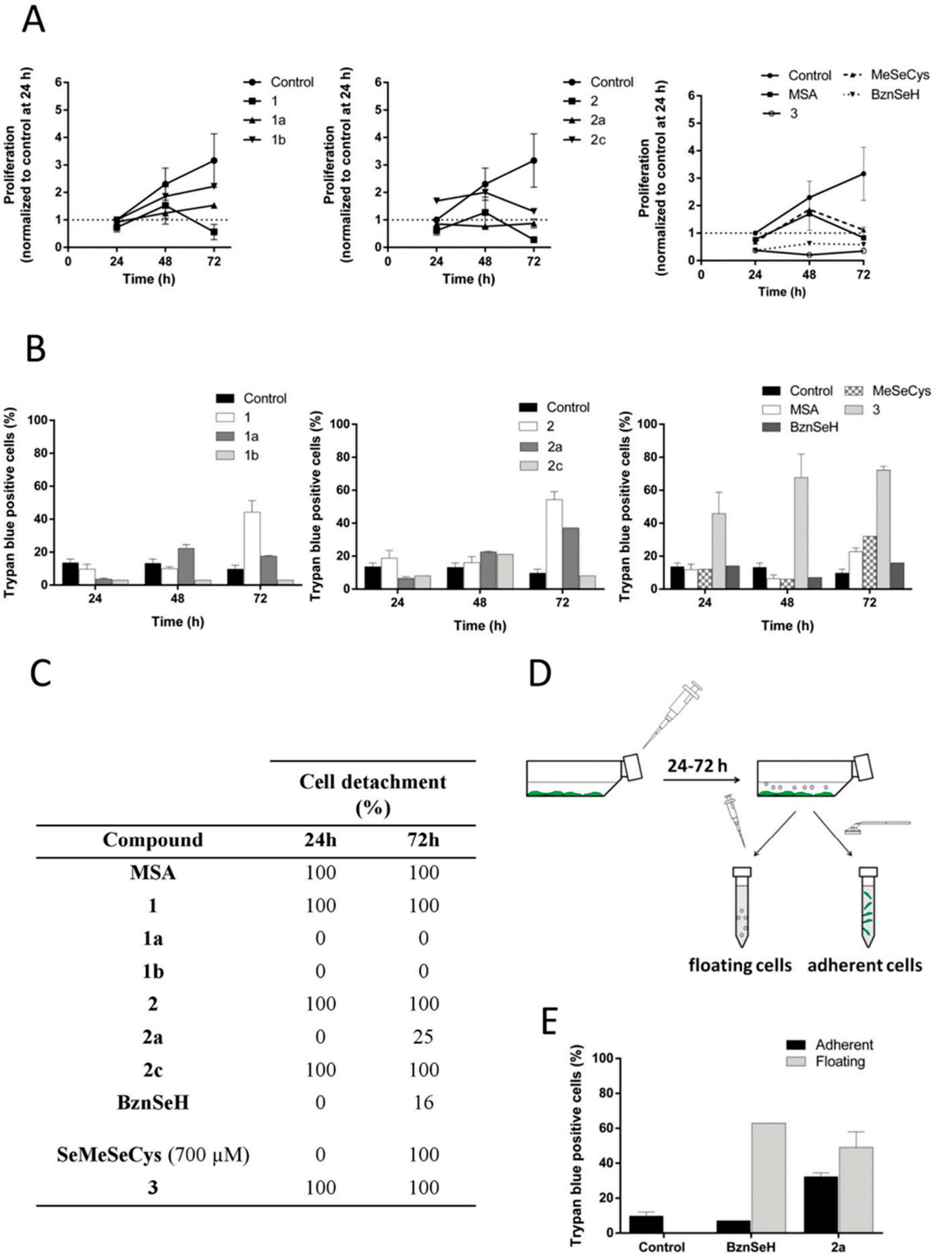

Compound	Cell detachment (%) 24h	72h
MSA	100	100
1	100	100
1a	0	0
1b	0	0
2	100	100
2a	0	25
2c	100	100
BznSeH	0	16
SeMeSeCys (700 µM)	0	100
3	100	100

Figure 5. Evaluation of the antiproliferative, cytotoxic, and de-adhesive properties of other Se analogs. Cells were seeded and incubated for 24 h before starting treatments with the compounds. Cell proliferation (**A**) and cell death based on Trypan blue exclusion (**B**) were analyzed after treatment with a 5 µM dose. For MeSeCys, a 700 µM dose was used. For BznSeH and compound **2a**, inducing a floating and attached population, proliferation, and cell death were calculated without taking into account the two populations in this case. (**C**) Cell detachment quantification after treatment. (**D**) Procedure scheme to evaluate the attached and floating population. Floating cells were collected with a pipette and remaining cells were considered as attached and slightly scrapped. (**E**) Cell death comparison in the floating and adherent populations induced by compound **2a** and BznSeH.

The methyl derivatives were more cytotoxic at 72 h than analogs with a longer alkyl chain or the benzyl moiety (Figure 5B). Almost all the compounds showed similar activity at 24 and 48 h, with the exception of compound **1b**, which was not cytotoxic. BznSeH, which was highly cytostatic, did not induce noteworthy cell death, with only 15% of dead cells at 72 h. MeSeCys, which has been reported to have a similar activity to MSA in vivo, required a considerably higher concentration to achieve similar cell death induction in vitro, due to the need of metabolic processing to release CH_3SeH, consistent with previous reports [33]. Compound **3**, on the other hand, was the most potent compound, inducing cell death at 24 h treatment.

In addition to cell proliferation and cell death, the ability of the compounds to induce cell detachment, and ultimately the same cell death mechanism as the methyl analogs, was analyzed. Most of the compounds completely detached the cells or completely remained ineffective, as illustrated in Figure 5C. However, some compounds induced two populations, and in this case, the procedure schematized in Figure 5D was followed. Compounds **1a** and **1b** were unable to detach cells. whereas compounds **2c** and **3** had detached all the cells at 24 h. MeSeCys detached all the cells at 72 h, and a concomitant increase in cell death was observed at that time point. However, cell detachment potential was not correlated with cell death induction in the case of compound **2c**, which was almost innocuous. BznSeH and compound **2a** induced mixed populations, with attached and floating cell fractions. (Figure 5D,E). Nevertheless, they had considerably less detachment potential than the methylated analogs, with only 16 and 24% of detached cells at 72 h, respectively.

3. Discussion

In this study, we demonstrate that MSA and two novel methylselenoesters induce entosis after provoking cell detachment in Panc-1 cells, revealing a new and unexplored cell death mechanism for Se compounds.

Compounds **1** and **2** and MSA reduced cell proliferation in both 2D and 3D cultures. Treatment with the compounds led to a unique phenotype, characterized by changes in morphology and cell detachment from the culture plate prior to cell death. Detached cells were alive at 24 h, but their reattachment capability and the colony forming ability had been dramatically compromised. We dismissed the possibility that the compounds were promoting anchorage-independent survival, and instead induced cellular death, as confirmed by the MTT assay and the expression of cleaved PARP in 2D cultures and PI staining in 3D spheroids.

Cell adhesion is gaining more attention due to its implication in cancer metastasis and progression, in addition to drug resistance. Importantly, these results are in accordance with recent investigations revealing that MSA targeted adhesion molecules in a leukemic cancer cell line, whereas inorganic selenite affected other gene sets, indicating an interesting type-dependent effect of Se compounds [34]. To further confirm the compound-induced adhesion disturbance, levels of different adhesion molecules were screened 24 h after treatment. We found that the expression of CD29 was significantly reduced. This integrin has been linked to gemcitabine resistance and a poor outcome in pancreatic cancer [35]. Moreover, its knockdown has been reported to inhibit cell adhesion, migration, proliferation, and metastasis of pancreatic cancer, unveiling CD29 as a potential therapeutic target [36].

The loss of CD29 signaling and consequent detachment from culture plate trigger entosis [16]. Entosis is primarily the engulfment of one live cell into another live cell. In our study, the detached cells post 24 h treatment were observed to be viable. Also, the formation of adherent junctions has been shown to be crucial for entosis initiation [15]. This kind of cell-cell contacts are mediated though cadherins, which are calcium-dependent molecules that play central roles in cancer progression. We found increased N-cadherin levels, which could explain cell clumping after detachment and the ultimate invasion of one cell into another. Although E-cadherin usually forms adherens junctions in epithelial cells, the coexpression of E- and N-cadherin has been reported in adherens junctions of endoderm-derived epithelial tissues and tumors, such as pancreatic ducts [37]. In addition, Panc-1 cells express very low basal levels of E-cadherin and, according to Cano et al. [38], it cannot be discarded that pancreatic homotypic cell-in-cell formation might rely on N-cadherin-mediated cell contacts. Although N-cadherin is usually linked to a more aggressive phenotype, it has been reported as a tumor suppressor in some types of cancers [39,40].

In addition, an upstream regulator of CD29 [22] and member of the Rho family of GTPases, CDC42, was also observed to be downregulated after treatment. CDC42 is overexpressed by 21% in pancreatic cancer [41] and the depletion of CDC42 enhances mitotic deadhesion and depends on Rho A activation in human bronchial epithelial cells [16]. Although it plays a crucial role in adherent entosis, it was reported to have no effect on suspension cells [16]. Consequently, treatment with the Se compounds affects CDC42 expression and mediates cell detachment through CD29 regulation.

Entotic cells mainly die through lysosomal-dependent pathways, although a swift to apoptosis can occur. In a floating population, different types of cell death have been reported to coexist [42].

Herein, we found that cell death induced by these Se compounds was caspase-independent, with a slight increase in PARP cleavage. We found increased levels of CatB in cell-in-cell structures undergoing entotic death, in concordance with previous reports [15]. By contrast, CatD, an interplayer between autophagy and apoptosis, was clearly downregulated. CatD can function as an anti-apoptotic mediator by increasing autophagy, revealing its two-faceted role [43]. In addition, CatD enhances anchorage-independent cell proliferation [44], and it is therefore quite interesting that it becomes down-regulated by compounds inducing cell detachment. Although cathepsins can mediate apoptosis, high levels of cathepsins have also been related to cancer progression. Pancreatic cancer patients, for instance, display a higher CatD concentration than healthy controls [45], and besides, elevated levels have been shown to promote cell dissemination in pancreatic cancer in vivo [46].

Cell detachment could be caused by CH_3SeH, one of the key metabolites in Se cytotoxicity, which has been reported to cause cell detachment in different cancer cell lines [47,48], along with a decrease in CD29 expression [48]. MSA is a penultimate precursor and compounds **1** and **2** bear this moiety. However, we ruled out that this effect was exclusive to the methylated form of Se, given that other compounds were able to induce the same phenotype. Lengthening the alkyl chain or the substitution over an arylselenol in general dramatically decreased the percentage of detached cells. However, the substitution of methyl for benzyl (compound **2c**) induced similar deadhesive effects. Intriguingly, despite induced cell detachment by this compound, it did not lead to cell death. The decreased cytotoxic effects are consistent with previous reports, showing the impaired cytotoxic activity of selenobenzyl derivatives with respect to their corresponding methylated analogs [49]. Hence, it is clear that detachment per se does not trigger death signaling, and it will be interesting to investigate the additional signaling pathways that the methyl and benzylseleno moieties are differentially able to activate, in order to avoid anchorange-independent cell growth.

In summary, we report a novel mechanism of action for MSA and two methylselenoesters: the induction of cell detachment through CDC42 and CD29 down-regulation leading to cell-in-cell formation (entosis) and death of the inner cell. However, these compounds need to be further evaluated in in vivo studies to gain an in-depth insight into their administration, hepatic metabolism for bioavailability and absorption, distribution, metabolism, and excretion properties. Additionally, the therapeutic potential of these compounds would be governed by the balance between their toxicity and efficacy profiles. Therefore, further research to fully dissect the relationship between structure, detachment abilities, and cell death induction of organic Se derivatives is required in order to understand the complex Se biochemistry.

4. Materials and Methods

4.1. Cell Culture

Panc-1 cells were obtained from the American Type Culture Collection (ATCC) and cultured in DMEM:F12 (Gibco™, ThermoFisher Scientific, Paisley, Scotland), 10% FBS (HyClone™, GE Healthcare Life Sciences, Logan, UT, USA), and 1% glutamine (Gibco) at 37 °C under 5% CO_2. The 3D spheroids were cultured following the protocol described by Longati et al. [23]. Briefly, phenol red-free DMEM:F12 (Gibco™, ThermoFisher Scientific, Paisley, Scotland), 10% FBS (HyClone™, GE Healthcare Life Sciences, Logan, UT, USA), and 0.24% methylcellulose were used. On day 0, 2500 Panc-1 cells in

50 µL volume were seeded in a low adherent 96-well round bottom microplate (Falcon™, ThermoFisher Scientific, Stockholm, Sweden). On day 4, treatments were added, diluted in 50 µL of medium.

4.2. 2D Viability Assay

Cell viability after treatment was assessed by the MTT (3-(4,5-dimethylthiazol-2-yl)-2,5-diphenyltetrazolium bromide) (Sigma Aldrich®, Stockholm, Sweden) assay. 6000 Panc-1 cells were seeded in 96-well plates. Cells were treated with increasing concentrations of the compounds. Dilutions of the compounds in cell medium were freshly prepared from a 0.01 M stock in DMSO. After 72 h treatment, 50 µL of MTT solution in PBS (2 mg/mL) was added and cells were incubated at 37 °C under 5% CO_2 for 4 h. Medium was removed and 150 µL of DMSO was added to dissolve the formazan crystals. Absorbance was read at 590 nm in a VersaMax microplate reader (Molecular Devices, San Jose, CA, USA). Viability is expressed as the percentage of untreated cells.

4.3. 3D Viability Assay

3D viability after 72 h treatment was analyzed with the acid phosphatase assay, following a previously described protocol [23]. Briefly, 70 µL of medium was carefully removed and 60 µL of PBS along with 100 µL APH buffer (1.5 M sodium acetate pH = 5.2, 0.1% TritonX-100) containing a final concentration of freshly prepared 2 mg/mL p-nitrophenyl phosphate were added. Cells were incubated for 5 h at 37 °C under 5% CO_2 and then 10 µL of NaOH 1M was added to stop the reaction. Absorbance was read at 405 nm in a VersaMax microplate reader (Molecular Devices, San Jose, CA, USA). Viability is expressed as the percentage of untreated cells.

4.4. Fluorescent Staining

Spheroid formation was developed in a Gravity Trap™ ULA plate (InSphero Europe GmbH, Waldshut, Germany), following the manufacturer's protocols. Briefly, on day 0, the plate was pre-wetted with 40 µL of medium before seeding 2000 Panc-1 cells in 75 µL phenol red-free DMEM:F12, 10% FBS, and 1% glutamine. The plate was centrifuged for 2 min at 250× *g*. On day 4, cells were treated, adding 25 µL of the corresponding compound in medium. Dilutions were freshly prepared from a 0.1 M DMSO stock. On day 7, cells were stained with 1 µM Hoechst 33342 (Molecular Probes®, Life Technologies™, Eugene, OR, USA) for 2 h, and 2 µM PI (Molecular Probes®, Life Technologies™, Eugene, OR, USA) for 1 h at 37 °C under 5% CO_2. Spheroids were then carefully washed once with PBS and fixed with paraformaldehyde (4%) at RT. Imaging was performed on the Operetta® High-content Imaging System (PerkinElmer, San Jose, CA, USA) (confocal mode, 10× objective magnification, 0.3 objective NA, 35 µm focus height) and processed by the Colombus™ (PerkinElmer, San Jose, CA, USA) analysis software.

4.5. Western Blotting

Protein lysate containing 20 µg of proteins was separated on a Bolt 4–12% Bis-Tris Gel (Novex™, ThermoFisher Scientific, Goteborg, Sweden) and transferred to a nitrocellulose membrane using the iBlot Gel Transfer Device (ThermoFisher Scientific, Goteborg, Sweden). Incubation with primary antibody (Cathepsin B (D1C7Y), Cell Signaling, Leiden, The Netherlands, Catalog no. 31718; Cathepsin D, BD Biosciences, San Jose, CA, USA, Catalog no. 610800; CDC42, Abcam, Cambridge, UK, Catalog no. ab155940; RhoA (67B89), Cell Signaling, Leiden, The Netherlands, Catalog no. 2117; PARP, Cell Signaling, Leiden, The Netherlands, Catalog no. 9542; Caspase 9, Bioss, Nordic BioSite, Stockholm, Sweden, Catalog no. bs-0049R; beta actin, Sigma-Aldrich, Stockholm, Sweden, Catalog no. A5441) diluted in TBST containing 3.5% bovine serum albumin (BSA) was done overnight at 4 °C. Secondary antibodies, goat anti-rabbit IgG HRP (Southern Biotech, Stockholm, Sweden Catalog no. 4030-05), or goat anti mouse IgG HRP (Southern Biotech, Stockholm, Sweden Catalog no. 1030-05) were incubated for 1 h. Membranes were developed using the AmershamTM ECLTM Start Western Blotting Detection Reagent

(GE Healthcare Life Sciences, Logan, UT, USA) and bands were visualized using the Bio-Rad Quantity One imaging system (Bio-Rad, Stockholm, Sweden). Images were quantified using ImageJ software.

4.6. Adhesion Assay

0.5×10^6 cells were seeded in 25 cm^2 flasks and incubated at 37 °C under 5% CO_2 24 h. Media was changed and cells were treated with 5 µM of compounds, after which floating cells were collected, centrifuged, and seeded at a density of 40,000 cells in 400 µL of fresh medium/well in a 24-well plate. The control cells were scrapped and seeded at the same density in 24-well plates. The cells were allowed to adhere to the surface of the plates. Cells were incubated at 37 °C, 5% CO_2 for 3 h, when 95% of the control cells adhered to the plate, after which they were fixed using 4% paraformaldehyde (PFA). The cells were further stained with 200 µL Coomassie blue staining solution (0.2% Coomassie Blue Brilliant R-250, 10% Acetic Acid and 40% Methanol) for 1 h at room temperature. The cells were then washed with PBS and further incubated for 1 h with 0.5 mL elution buffer (0.1 N NaOH and 50% Methanol). Furthermore, 0.5 mL of developing solution containing 10% Trichloroacetic acid (TCA) was added into the wells. Following this, 200 µL of the mix was transferred to a 96-well plate and further absorbance was read at 595 nm using the plate reader Infinite® M200 Pro, Tecan, Mannedorf, Switzerland.

4.7. Flow Cytometry

0.5×10^6 cells were seeded in 25 cm^2 flasks and allowed to attach for 24 h. After that, medium was replaced and cells were treated with the corresponding compounds or vehicle (DMSO) for 24 h. Cells were collected, washed with PBS-staining buffer (1% BSA, 0.01% NaN_3, 1% FBS), and stained for 30 min at 4 °C and darkness in 50 µL PBS-staining buffer with the corresponding antibody: CD29/integrin 1-β (FITC conjugate, clone MEM-101A, Life Technologies, Eugene, OR, USA), CD325/N-cadherin (PE conjugate, clone 8C11, Life Technologies, Eugene, OR, USA). Cells were washed once with PBS-staining buffer and resuspended in fixation buffer (PBS, 1% paraformaldehyde, 2% FBS) until being read in a BD FACSCalibur™ (BD Biosciences, San Jose, CA, USA).

4.8. Clonogenic Assay

0.5×10^6 cells were seeded in 25 cm^2 flasks and incubated at 37 °C under 5% CO_2 for 24 h. Media was changed and cells were treated with 5 µM of compounds for 24 h, after which floating cells were collected, centrifuged, and seeded at a density of 1000 cells in total volume of 2 mL/well in a six-well plate. The control cells were checked for colony formation for five days. A group of 50 cells were considered as one colony. The plates were later stained with crystal violet according to Franken et al. [50].

4.9. Chemical Synthesis

The NMR spectra (^{1}H and ^{13}C) were recorded on a Bruker 400 Ultrashield™ spectrometer (Rheinstetten, Germany) and are provided in the supplementary material. The samples were solved in $CDCl_3$ and TMS was used as an internal standard. IR spectra were obtained on a Thermo Nicolet FT-IR Nexus spectrophotometer (Thermo Nicolet, Madison, WI, USA) using KBr pellets for solids or NaCl plates for oil compounds. The HRMS spectra were recorded on a Thermo Scientific Q Exactive Focus mass spectrometer (Thermo Scientific™, Waltham, MA, USA) by direct infusion. For TLC assays, Alugram SIL G7UV254 sheets (Macherey-Nagel; Düren, Germany) were used. Column chromatography was performed with silica gel 60 (E. Merck KGaA, Darmstadt, Germany). Chemicals were purchased from E. Merck KGaA (Darmstadt, Germany), Panreac Química S.A. (Montcada i Reixac, Barcelona, Spain), Sigma-Aldrich Quimica, S.A. (Alcobendas, Madrid, Spain), and Acros Organics (Janssen Pharmaceuticalaan, Geel, Belgium).

4.9.1. Procedure for Compounds **1** and **2**

Compounds **1** and **2** were synthesized as described in our previous work [14], under the references **5** and **15**, respectively.

Procedure for Compounds **1a**, **2a**, **1b** and **2c**

The chemical synthesis was carried out following an already described procedure [51,52] with some modifications. Briefly, the corresponding carboxylic acid was chlorinated by a reaction with $SOCl_2$. Se powder reacted with $NaBH_4$ (1:2) in water or ethanol (1:1) and N_2 atmosphere to form NaHSe. The corresponding acyl chloride dissolved in *N*,*N*-dimethylformamide (2 mL) or chloroform (2 mL) was then added and the reaction was stirred at room temperature until the reaction took place (20 min–3.5 h). The reaction was followed by IR or TLC. The mixture was filtered and the intermediate was further alkylated with the corresponding halide until discoloration of the mixture. The product was extracted with methylene chloride and dried over Na_2SO_4. The solvent was eliminated under rotatory evaporation and the residue was purified through column chromatography.

Ethyl 3-Chlorothiophen-2-Carboselenoate (**1a**)

From 3-chlorothiophen-2-carboxylic acid (1.5 mmol), Se powder (1.5 mmol), $NaBH_4$ (3 mmol), and ethyl iodide (1.5 mmol). A yellow oil was obtained, which was further purified through column chromatography using methylene chloride as the eluent. Yield: 11%. ^1H NMR (400 MHz, $CDCl_3$): δ 1.52 (t, 3H, $–CH_3$, $J_{CH3\text{-}CH2}$ = 7.5 Hz), 3.11 (q, 2H, $–CH_2–$), 7.06 (d, 1H, H_4 $J_{4\text{-}5}$ = 5.3 Hz), 7.54 ppm (d, 1H, H_5). ^{13}C NMR (100 MHz, $CDCl_3$): δ 15.7 ($–CH_3$), 20.5 ($–CH_2–$), 128.0 (C_4), 130.6 (C_2), 131.0 (C_5), 137.7 (C_3), 184.3 ppm (–C=O). IR (KBr): ν 3105 (w, $C-H_{arom}$), 2962–2867 (s, $C-H_{aliph}$), 1649 cm^{-1} (s, −C=O). HRMS calculated for $C_7H_8ClOSSe$ (M + H): 254.91441, found: 254.91418.

Diethyl 2,5-Furandicarboselenoate (**2a**)

From 2,5-furandicarboxylic acid (1.74 mmol), Se powder (3.48 mmol), $NaBH_4$ (7.1 mmol), and ethyl iodide (3.48 mmol). Conditions: 45 min reaction with NaHSe and 2 h reaction with ethyl iodide. A yellow solid was obtained, which was purified through column chromatography using ethyl acetate/hexane (1:10) as the eluent. Yield: 10%; m.p.: 35–36 °C. ^1H NMR (400 MHz, $CDCl_3$): δ 1.5 (t, 6H, $2–CH_3$, $J_{CH2\text{-}CH3}$ = 7.5 Hz), 3.11 (q, 4H, $–CH_2–$), 7.17 ppm (s, 2H, $H_3 + H_4$). ^{13}C NMR (100 MHz, $CDCl_3$): δ 15.8 ($–CH_3$), 19.2 ($–CH_2–$), 114.7 ($C_3 + C_4$), 153.5 ($C_2 + C_5$), 183.5 ppm (–C=O). IR (KBr): ν 3143 (w, $C-H_{arom}$), 2961–2860 (s, $C-H_{aliph}$), 1649 cm^{-1} (s, −C=O). HRMS calculated for $C_{10}H_{13}O_3Se_2$ (M + H): 340.91896; found: 340.91891.

Pentyl 3-Chlorothiophen-2-Carboselenoate (**1b**)

From 3-chlorothiophen-2-carboxylic acid (2 mmol), Se powder (2 mmol), $NABH_4$ (2.15 mmol), and pentyl iodide (2.15 mmol). Under N_2 atmosphere, absolute ethanol (10 mL) was added to a mixture of $NaBH_4$ and selenium cooled by an ice bath, with magnetic stirring. After the formation of NaHSe was achieved, the ice bath was removed and the following reactions were carried out at room temperature. Before adding an excess of pentyl iodide, the mixture was filtered. Conditions: 20 min reaction with NaHSe and 20 min reaction with pentyl iodide. The solvent was eliminated under rotatory evaporation. The product was purified through column chromatography using a gradient elution of ethyl acetate: hexane. An orange oil was obtained. Yield: 53%. ^1H NMR (400 MHz, $CDCl_3$): δ 0.83 (t, 3H, $–CH_3$, $J_{CH3\text{-}CH2}$ = 7.1 Hz), 1.27–1.35 (m, 4H, γ + $δCH_2$), 1.66–1.77 (m, 2H, $ßCH_2$), 3.02 (t, 2H, $αCH_2$, $J_{CH2\text{-}CH2}$ = 7.4 Hz,), 6.96 (d, 1H, H_4, $J_{4\text{-}5}$ = $J_{5\text{-}4}$ = 5.3 Hz), 7.44 ppm (d, 1H, H_5). ^{13}C NMR (100 MHz, $CDCl_3$): δ 12.94 ($-CH_3$), 21.19 ($δCH_2$), 25.56 ($αCH_2$), 28.89 ($ßCH_2$), 31.18 ($γCH_2$), 126.82 (C_4), 129.50 (C_2), 129.76 (C_5), 136.56 (C_3), 183.18 ppm (−CO). IR (KBr): ν 2922 −2852 (s, $C-H_{alif}$), 1669 cm^{-1} (s, −C=O).

Dibenzyl 2,5-Furandicarboselenoate (**2c**)

From 2,5-furandicarboxylic acid (1.74 mmol), Se powder (3.48 mmol), $NABH_4$ (7.1 mmol), and benzyl bromide (3.48 mmol). Conditions: 1.5 h reaction with NaHSe and 3.5 h reaction with benzyl bromide. The product was extracted with methylene chloride, further washed with water, dried over Na_2SO_4. The solvent was eliminated under rotatory evaporation. A yellow oil was obtained, which was precipitated and washed with diethyl ether. A yellow solid was obtained. Yield: 25%; m.p.: 114–115 °C. ^1H NMR (400 MHz, $CDCl_3$): δ 4.34 (s, 4H, 2–CH_2–), 7.2 (s, 2H, $H_3 + H_4$), 7.22–7.35 ppm (m, 10 H, H_{arom}). ^{13}C NMR (100 MHz, $CDCl_3$): δ 28.5 (–CH_2–), 115.0 ($C_3 + C_4$), 127.3 ($C_{4'}$), 128.7 ($C_{2'} + C_{6'}$), 129.1($C_{3'} + C_{5'}$), 138.21 ($C_{1'}$), 153.2 ($C_2 + C_5$), 182.8 (−C=O). IR (KBr): ν 3123−3088 (s, C−H_{arom}), 1677 cm^{-1} (s, −C=O). HRMS $C_{20}H_{16}O_3Se_2Na$ ($M + Na^+$): calculated 486.9322; found 486.9430.

4.9.2. Procedure for Compound 3

Compound **3** was synthesized in a previous work [32], under the reference **3c.**

4.10. Timelapse

0.5×10^6 cells were seeded in 25 cm^2 flasks and incubated at 37 °C under 5% CO_2 24 h. Media was changed and cells were treated with 5 μM of compounds for 24 h, after which floating cells were collected, centrifuged, and seeded at a density of 50,000 cells in total volume of 100 μL/well in a 96-well plate. Post 48 h of treatment, the cells were imaged live for another 24 h in Operetta and images were captured every 5 min.

4.11. Confocal

Monolayer cultures were stained with CellTracker Red or Green (Invitrogen) for 1 h at 37 °C in the absence of serum. After this, 0.4×10^5 cells stained with each of the cell trackers were mixed (1:1) and seeded onto 25 cm^2 flasks for 24 h, followed by treatment with 5 μM of respective compounds for 18 h. Cells were imaged live using an LSM 800 confocal microscope (Zeiss, Oberkochen, Germany).

4.12. Statistical Analysis

One-way ANOVA followed by Dunnet's test was performed using GraphPad 6.01 (GraphPad Software, San Diego, CA, USA). (* $p < 0.05$, ** $p < 0.01$, *** $p < 0.001$).

Supplementary Materials: Supplementary materials can be found at http://www.mdpi.com/1422-0067/19/10/2849/s1.

Author Contributions: Conceptualization, A.P.F., C.S., P.K., and N.D.-A; Methodology, A.P.F., P.K., N.D.-A., and J.A.P.; Validation, A.P.F., P.K., and N.D.-A.; Formal Analysis, P.K and N.D.-A.; Investigation, P.K. and N.D.-A; Resources, A.P.F.; C.S., and J.A.P; Writing-Original Draft Preparation, N.D.-A. and P.K.; Writing-Review & Editing, A.P.F.; P.K., N.D.-A., and C.S.; Visualization, P.K. and N.D.-A; Supervision, A.P.F.; Project Administration, A.P.F.; Funding Acquisition, A.P.F.

Funding: This article has been financially supported by The Swedish Cancer Society (Cancerfonden). The research leading to these results has also received funding from "la Caixa" Banking Foundation through a grant to N.D.-A, who additionally received a mobility scholarship from Asociación de Amigos de la Universidad de Navarra.

Acknowledgments: We thank Pablo Garnica for his help with compound **1b**.

Conflicts of Interest: The authors declare no conflict of interest.

Abbreviations

BznSeH	Benzeneselenol
CatB	Cathepsin B
CatD	Cathepsin D
CD29	β1-integrin
CDC42	Cell division control protein 42 homolog
PARP	DNA damage-responsive enzymes poly(ADP-ribose) polymerase

MSA	Methylseleninic acid
MeSeCys	Methylselenocysteine
CH_3SeH	Methylselenol
Nrf2	nuclear factor erythroid 2 related factor 2
PDAC	Pancreatic ductal adenocarcinoma
PI	Propidium iodide
ROS	Reactive oxygen species
Se	Selenium

References

1. Siegel, R.; Ma, J.; Zou, Z.; Jemal, A. Cancer statistics, 2014. *CA Cancer J. Clin.* **2014**, *64*, 9–29. [CrossRef] [PubMed]
2. Rahib, L.; Smith, B.D.; Aizenberg, R.; Rosenzweig, A.B.; Fleshman, J.M.; Matrisian, L.M. Projecting cancer incidence and deaths to 2030: The unexpected burden of thyroid, liver, and pancreas cancers in the united states. *Cancer Res.* **2014**, *74*, 2913–2921. [CrossRef] [PubMed]
3. Bijlsma, M.F.; van Laarhoven, H.W.M. The conflicting roles of tumor stroma in pancreatic cancer and their contribution to the failure of clinical trials: A systematic review and critical appraisal. *Cancer Metastasis Rev.* **2015**, *34*, 97–114. [CrossRef] [PubMed]
4. Al Saati, T.; Clerc, P.; Hanoun, N.; Peuget, S.; Lulka, H.; Gigoux, V.; Capilla, F.; Béluchon, B.; Couvelard, A.; Selves, J.; et al. Oxidative Stress Induced by Inactivation of TP53INP1 Cooperates with KrasG12D to Initiate and Promote Pancreatic Carcinogenesis in the Murine Pancreas. *Am. J. Pathol.* **2013**, *182*, 1996–2004. [CrossRef] [PubMed]
5. Kong, B.; Qia, C.; Erkan, M.; Kleeff, J.; Michalski, C.W. Overview on how oncogenic Kras promotes pancreatic carcinogenesis by inducing low intracellular ROS levels. *Front. Physiol.* **2013**. [CrossRef] [PubMed]
6. Diehn, M.; Cho, R.W.; Lobo, N.A.; Kalisky, T.; Dorie, M.J.; Kulp, A.N.; Qian, D.; Lam, J.S.; Ailles, L.E.; Wong, M.; et al. Association of reactive oxygen species levels and radioresistance in cancer stem cells. *Nature* **2009**, *458*, 780–783. [CrossRef] [PubMed]
7. Gorrini, C.; Harris, I.S.; Mak, T.W. Modulation of oxidative stress as an anticancer strategy. *Nat. Rev. Drug Discov.* **2013**, *12*, 931–947. [CrossRef] [PubMed]
8. Cairns, R.A.; Harris, I.; Mccracken, S.; Mak, T.W. Cancer cell metabolism. *Cold Spring Harb. Symp. Quant. Biol.* **2011**. [CrossRef] [PubMed]
9. Cairns, R.; Harris, I.; Mak, T. Regulation of cancer cell metabolism. *Nat. Rev. Cancer* **2011**, *11*, 85–95. [CrossRef] [PubMed]
10. Sosa, V.; Moline, T.; Somoza, R.; Paciucci, R.; Kondoh, H.; Me, L.L. Oxidative stress and cancer: An overview. *Ageing Res. Rev.* **2013**, *12*, 376–390. [CrossRef] [PubMed]
11. Chaiswing, L.; St Clair, W.H.; St Clair, D.K. Redox Paradox: A novel approach to therapeutics-resistant cancer. *Antioxid. Redox Signal.* **2018**. [CrossRef] [PubMed]
12. Fernandes, A.P.; Gandin, V. Selenium compounds as therapeutic agents in cancer. *Biochim. Biophys. Acta* **2015**, *1850*, 1642–1660. [CrossRef] [PubMed]
13. Gandin, V.; Khalkar, P.; Braude, J.; Fernandes, A.P. Organic selenium compounds as potential chemotherapeutic agents for improved cancer treatment. *Free Radic. Biol. Med.* **2018**. [CrossRef] [PubMed]
14. Díaz-Argelich, N.; Encío, I.; Plano, D.; Fernandes, A.P.; Palop, J.A.; Sanmartín, C. Novel Methylselenoesters as Antiproliferative Agents. *Molecules* **2017**, *22*, 1288. [CrossRef] [PubMed]
15. Overholtzer, M.; Mailleux, A.A.; Mouneimne, G.; Normand, G.; Schnitt, S.J.; King, R.W.; Cibas, E.S.; Brugge, J.S. A Nonapoptotic Cell Death Process, Entosis, that Occurs by Cell-in-Cell Invasion. *Cell* **2007**, *131*, 966–979. [CrossRef] [PubMed]
16. Durgan, J.; Tseng, Y.Y.; Hamann, J.C.; Domart, M.C.; Collinson, L.; Hall, A.; Overholtzer, M.; Florey, O. Mitosis can drive cell cannibalism through entosis. *eLife* **2017**, *6*, 1–26. [CrossRef] [PubMed]
17. Garanina, A.S.; Kisurina-Evgenieva, O.P.; Erokhina, M.V.; Smirnova, E.A.; Factor, V.M.; Onishchenko, G.E. Consecutive entosis stages in human substrate-dependent cultured cells. *Sci. Rep.* **2017**, *7*, 1–12. [CrossRef] [PubMed]

18. Wan, Q.; Liu, J.; Zheng, Z.; Zhu, H.; Chu, X.; Dong, Z.; Huang, S.; Du, Q. Regulation of myosin activation during cell-cell contact formation by Par3-Lgl antagonism: Entosis without matrix detachment. *Mol. Biol. Cell* **2012**, *23*, 2076–2091. [CrossRef] [PubMed]
19. Hamann, J.C.; Surcel, A.; Chen, R.; Teragawa, C.; Albeck, J.G.; Robinson, D.N.; Overholtzer, M. Entosis Is Induced by Glucose Starvation. *Cell Rep.* **2017**, *20*, 201–210. [CrossRef] [PubMed]
20. Florey, O.; Kim, S.E.; Sandoval, C.P.; Haynes, C.M.; Overholtzer, M. Autophagy machinery mediates macroendocytic processing and entotic cell death by targeting single membranes. *Nat. Cell Biol.* **2011**, *13*, 1335–1343. [CrossRef] [PubMed]
21. Krishna, S.; Overholtzer, M. Mechanisms and consequences of entosis. *Cell. Mol. Life Sci.* **2016**, *73*, 2379–2386. [CrossRef] [PubMed]
22. Reymond, N.; Im, J.H.; Garg, R.; Vega, F.M.; Borda d'Agua, B.; Riou, P.; Cox, S.; Valderrama, F.; Muschel, R.J.; Ridley, A.J. Cdc42 promotes transendothelial migration of cancer cells through β1 integrin. *J. Cell Biol.* **2012**, *199*, 653–668. [CrossRef] [PubMed]
23. Longati, P.; Jia, X.; Eimer, J.; Wagman, A.; Witt, M.-R.; Rehnmark, S.; Verbeke, C.; Toftgård, R.; Löhr, M.; Heuchel, R.L. 3D pancreatic carcinoma spheroids induce a matrix-rich, chemoresistant phenotype offering a better model for drug testing. *BMC Cancer* **2013**, *13*, 95. [CrossRef] [PubMed]
24. Seguin, L.; Desgrosellier, J.S.; Weis, S.M.; Cheresh, D.A. Integrins and cancer: Regulators of cancer stemness, metastasis, and drug resistance. *Trends Cell Biol.* **2015**, *25*, 234–240. [CrossRef] [PubMed]
25. Van Roy, F. Beyond E-cadherin: Roles of other cadherin superfamily members in cancer. *Nat. Rev. Cancer* **2014**, *14*, 121–134. [CrossRef] [PubMed]
26. McGinnis, K.M.; Gnegy, M.E.; Park, Y.H.; Mukerjee, N.; Wang, K.K.W. Procaspase-3 and Poly(ADP)ribose Polymerase (PARP) Are Calpain Substrates. *Biochem. Biophys. Res. Commun.* **1999**, *263*, 94–99. [CrossRef] [PubMed]
27. Gobeil, S.; Boucher, C.C.; Nadeau, D.; Poirier, G.G. Characterization of the necrotic cleavage of poly(ADP-ribose) polymerase (PARP-1): Implication of lysosomal proteases. *Cell Death Differ.* **2001**, *8*, 588–594. [CrossRef] [PubMed]
28. Shalini, S.; Dorstyn, L.; Dawar, S.; Kumar, S. Old, new and emerging functions of caspases. *Cell Death Differ.* **2015**, *22*, 526–539. [CrossRef] [PubMed]
29. Chaitanya, G.; Alexander, J.S.; Babu, P. PARP-1 cleavage fragments: Signatures of cell-death proteases in neurodegeneration. *Cell Commun. Signal.* **2010**, *8*, 31. [CrossRef] [PubMed]
30. Lugini, L.; Matarrese, P.; Tinari, A.; Lozupone, F.; Federici, C.; Iessi, E.; Gentile, M.; Luciani, F.; Parmiani, G.; Rivoltini, L.; et al. C annibalism of live lymphocytes by human metastatic but not primary melanoma cells. *Cancer Res.* **2006**, *66*, 3629–3638. [CrossRef] [PubMed]
31. Khalkhali-Ellis, Z.; Goossens, W.; Margaryan, N.V.; Hendrix, M.J.C. Cleavage of histone 3 by cathepsin D in the involuting mammary gland. *PLoS ONE* **2014**, *9*, e103230. [CrossRef] [PubMed]
32. Moreno, E.; Plano, D.; Lamberto, I.; Font, M.; Encío, I.; Palop, J.A.; Sanmartín, C. Sulfur and selenium derivatives of quinazoline and pyrido[2,3-d]pyrimidine: Synthesis and study of their potential cytotoxic activity in vitro. *Eur. J. Med. Chem.* **2012**, *47*, 283–298. [CrossRef] [PubMed]
33. Ip, C.; Thompson, H.J.; Zhu, Z.; Ganther, H.E. In vitro and in vivo studies of methylseleninic acid: Evidence that a monomethylated selenium metabolite is critical for cancer chemoprevention. *Cancer Res.* **2000**, *60*, 2882–2886. [CrossRef] [PubMed]
34. Khalkar, P.; Ali, H.A.; Codó, P.; Argelich, N.D.; Martikainen, A.; Arzenani, M.K.; Lehmann, S.; Walfridsson, J.; Ungerstedt, J.; Fernandes, A.P. Selenite and methylseleninic acid epigenetically affects distinct gene sets in myeloid leukemia: A genome wide epigenetic analysis. *Free Radic. Biol. Med.* **2018**, *117*, 247–257. [CrossRef] [PubMed]
35. Yang, D.; Shi, J.; Fu, H.; Wei, Z.; Xu, J.; Hu, Z.; Zhang, Y.; Yan, R.; Cai, Q. Integrin B1 modulates tumour resistance to gemcitabine and serves as an independent prognostic factor in pancreatic adenocarcinomas. *Tumor Biol.* **2016**, *37*, 12315–12327. [CrossRef] [PubMed]
36. Grzesiak, J.J.; Cao, H.S.T.; Burton, D.W.; Kaushal, S.; Vargas, F.; Clopton, P.; Snyder, C.S.; Deftos, L.J.; Hoffman, R.M.; Bouvet, M. Knockdown of the β_1 integrin subunit reduces primary tumor growth and inhibits pancreatic cancer metastasis. *Int. J. Cancer* **2011**, *129*, 2905–2915. [CrossRef] [PubMed]

37. Straub, B.K.; Rickelt, S.; Zimbelmann, R.; Grund, C.; Kuhn, C.; Iken, M.; Ott, M.; Schirmacher, P.; Franke, W.W. E-N-cadherin heterodimers define novel adherens junctions connecting endoderm-derived cells. *J. Cell Biol.* **2011**, *195*, 873–887. [CrossRef] [PubMed]
38. Cano, C.E.; Sandí, M.J.; Hamidi, T.; Calvo, E.L.; Turrini, O.; Bartholin, L.; Loncle, C.; Secq, V.; Garcia, S.; Lomberk, G.; et al. Homotypic cell cannibalism, a cell-death process regulated by the nuclear protein 1, opposes to metastasis in pancreatic cancer. *EMBO Mol. Med.* **2012**, *4*, 964–979. [CrossRef] [PubMed]
39. Su, Y.; Li, J.; Shi, C.; Hruban, R.H.; Radice, G.L. N-cadherin functions as a growth suppressor in a model of K-ras-induced PanIN. *Oncogene* **2016**, *35*, 3335–3341. [CrossRef] [PubMed]
40. Camand, E.; Peglion, F.; Osmani, N.; Sanson, M.; Etienne-Manneville, S. N-cadherin expression level modulates integrin-mediated polarity and strongly impacts on the speed and directionality of glial cell migration. *J. Cell Sci.* **2012**, *125*, 844–857. [CrossRef] [PubMed]
41. Maldonado, M.D.M.; Dharmawardhane, S. Targeting Rac and Cdc42 GTPases in Cancer. *Cancer Res.* **2018**, *78*, 3101–3111. [CrossRef] [PubMed]
42. Ishikawa, F.; Ushida, K.; Mori, K.; Shibanuma, M. Loss of anchorage primarily induces non-apoptotic cell death in a human mammary epithelial cell line under atypical focal adhesion kinase signaling. *Cell Death Dis.* **2015**, *6*, e1619. [CrossRef] [PubMed]
43. Hah, Y.S.; Noh, H.S.; Ha, J.H.; Ahn, J.S.; Hahm, J.R.; Cho, H.Y.; Kim, D.R. Cathepsin D inhibits oxidative stress-induced cell death via activation of autophagy in cancer cells. *Cancer Lett.* **2012**, *323*, 208–214. [CrossRef] [PubMed]
44. Glondu, M.; Liaudet-Coopman, E.; Derocq, D.; Platet, N.; Rochefort, H.; Garcia, M. Down-regulation of cathepsin-D expression by antisense gene transfer inhibits tumor growth and experimental lung metastasis of human breast cancer cells. *Oncogene* **2002**, *21*, 5127–5134. [CrossRef] [PubMed]
45. Park, H.-D.; Kang, E.-S.; Kim, J.-W.; Lee, K.-T.; Lee, K.H.; Park, Y.S.; Park, J.-O.; Lee, J.; Heo, J.S.; Choi, S.H.; et al. Serum CA19-9, cathepsin D, and matrix metalloproteinase-7 as a diagnostic panel for pancreatic ductal adenocarcinoma. *Proteomics* **2012**, *12*, 3590–3597. [CrossRef] [PubMed]
46. Dumartin, L.; Whiteman, H.J.; Weeks, M.E.; Hariharan, D.; Dmitrovic, B.; Iacobuzio-Donahue, C.A.; Brentnall, T.A.; Bronner, M.P.; Feakins, R.M.; Timms, J.F.; et al. AGR2 is a novel surface antigen that promotes the dissemination of pancreatic cancer cells through regulation of cathepsins B and D. *Cancer Res.* **2011**, *71*, 7091–7102. [CrossRef] [PubMed]
47. Jiang, C.; Wang, Z.; Ganther, H.; Lu, J. Caspases as key executors of methyl selenium-induced apoptosis (anoikis) of DU-145 prostate cancer cells. *Cancer Res.* **2001**, *61*, 3062–3070. [PubMed]
48. Kim, A.; Oh, J.H.; Park, J.M.; Chung, A.S. Methylselenol generated from selenomethionine by methioninase downregulates integrin expression and induces caspase-mediated apoptosis of B16F10 melanoma cells. *J. Cell. Physiol.* **2007**, *212*, 386–400. [CrossRef] [PubMed]
49. Ibáñez, E.; Plano, D.; Font, M.; Calvo, A.; Prior, C.; Palop, J.A.; Sanmartín, C. Synthesis and antiproliferative activity of novel symmetrical alkylthio- and alkylseleno-imidocarbamates. *Eur. J. Med. Chem.* **2011**, *46*, 265–274. [CrossRef] [PubMed]
50. Franken, N.A.P.; Rodermond, H.M.; Stap, J.; Haveman, J.; van Bree, C. Clonogenic assay of cells in vitro. *Nat. Protoc.* **2006**, *1*, 2315–2319. [CrossRef] [PubMed]
51. Domínguez-Álvarez, E.; Plano, D.; Font, M.; Calvo, A.; Prior, C.; Jacob, C.; Palop, J.A.; Sanmartín, C. Synthesis and antiproliferative activity of novel selenoester derivatives. *Eur. J. Med. Chem.* **2014**, *73*, 153–166. [CrossRef] [PubMed]
52. Klayman, D.L.; Griffin, T.S. Reaction of Selenium with Sodium Borohydride in Protic Solvents. A Facile Method for the Introduction of Selenium into Organic Molecules. *J. Am. Chem. Soc.* **1973**, *2*, 197–199. [CrossRef]

© 2018 by the authors. Licensee MDPI, Basel, Switzerland. This article is an open access article distributed under the terms and conditions of the Creative Commons Attribution (CC BY) license (http://creativecommons.org/licenses/by/4.0/).

SUPPLEMENTARY MATERIAL

Supplementary figure 1

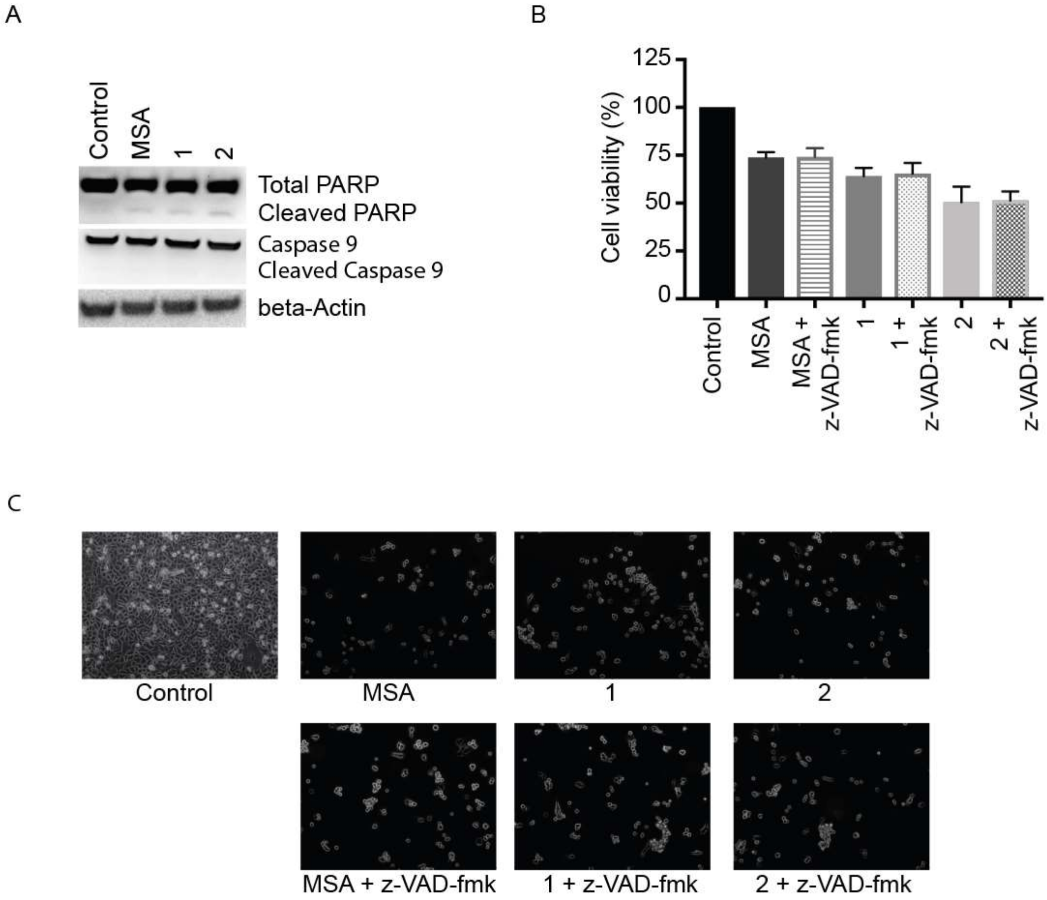

Supplementary Figure 1. MSA, compounds **1** and **2** induce a caspase-independent slight increase in cleaved PARP. (A) Western blot analysis of PARP and caspase 9 levels after 72 h and 48 h treatment with the compounds respectively. (B) Cell viability assessed by Trypan blue exclusion after treatment with the compounds in the presence of the pancaspase inhibitor z-vad-FMK at 72 h.

Supplementary videos. Post 24 h of seeding, Panc-1 cells were treated with **MSA** (**video 1**) or compound **1** (**video 2**) or compound **2** (**video 3**) for 48 h, after which the floating cells were plated at a density of 50000 cells per well of a 96 well plate pre-coated with polyhema. Timelapse microscopy showing the process of entosis, where upon treatment with respective compounds, one cell engulfs another cell further leading to its degradation.

SUPPLEMENTARY CHEMICAL INFORMATION

^{1}H NMR of compound **1a**

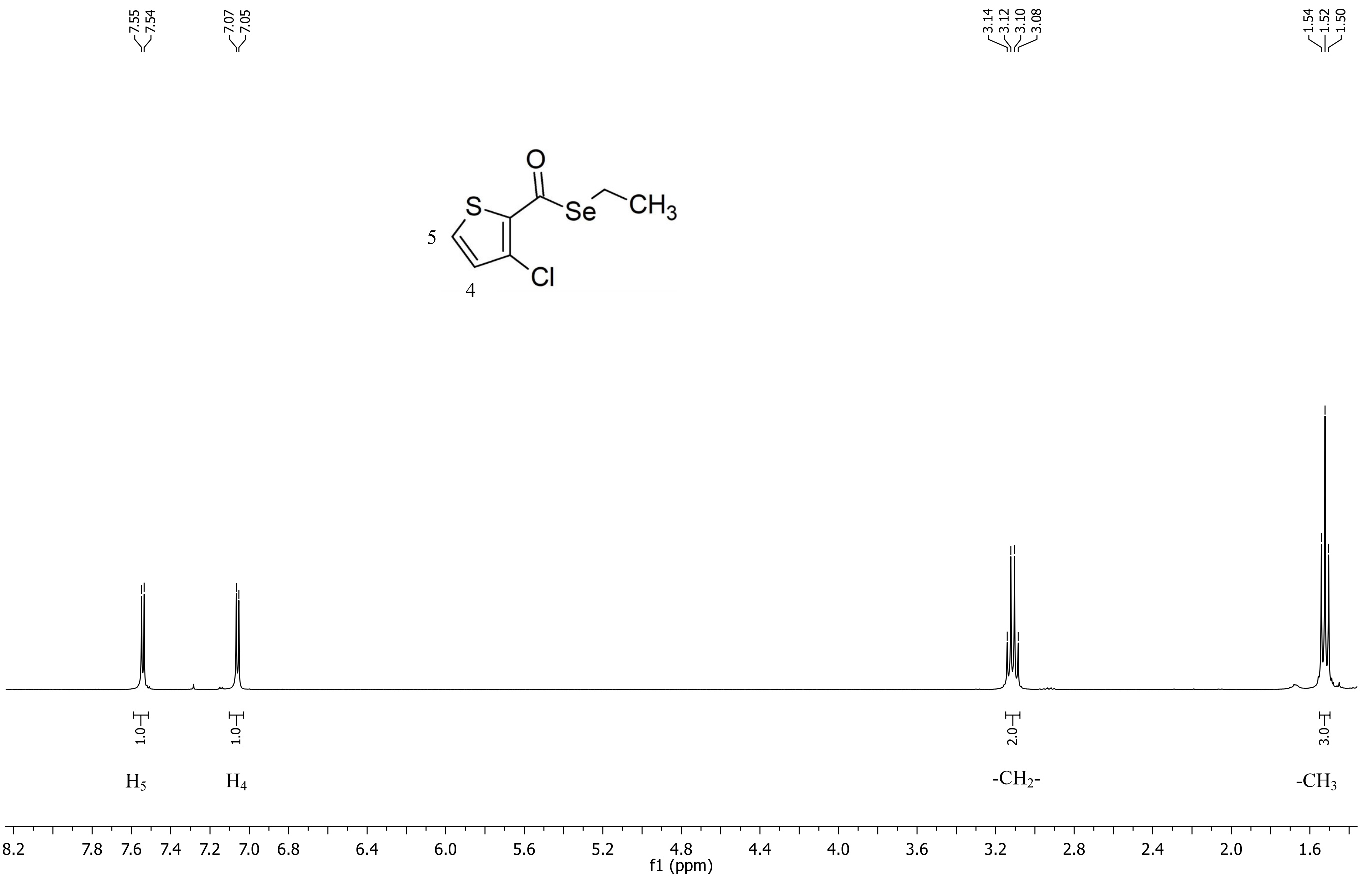

^{13}C NMR of compound **1a**

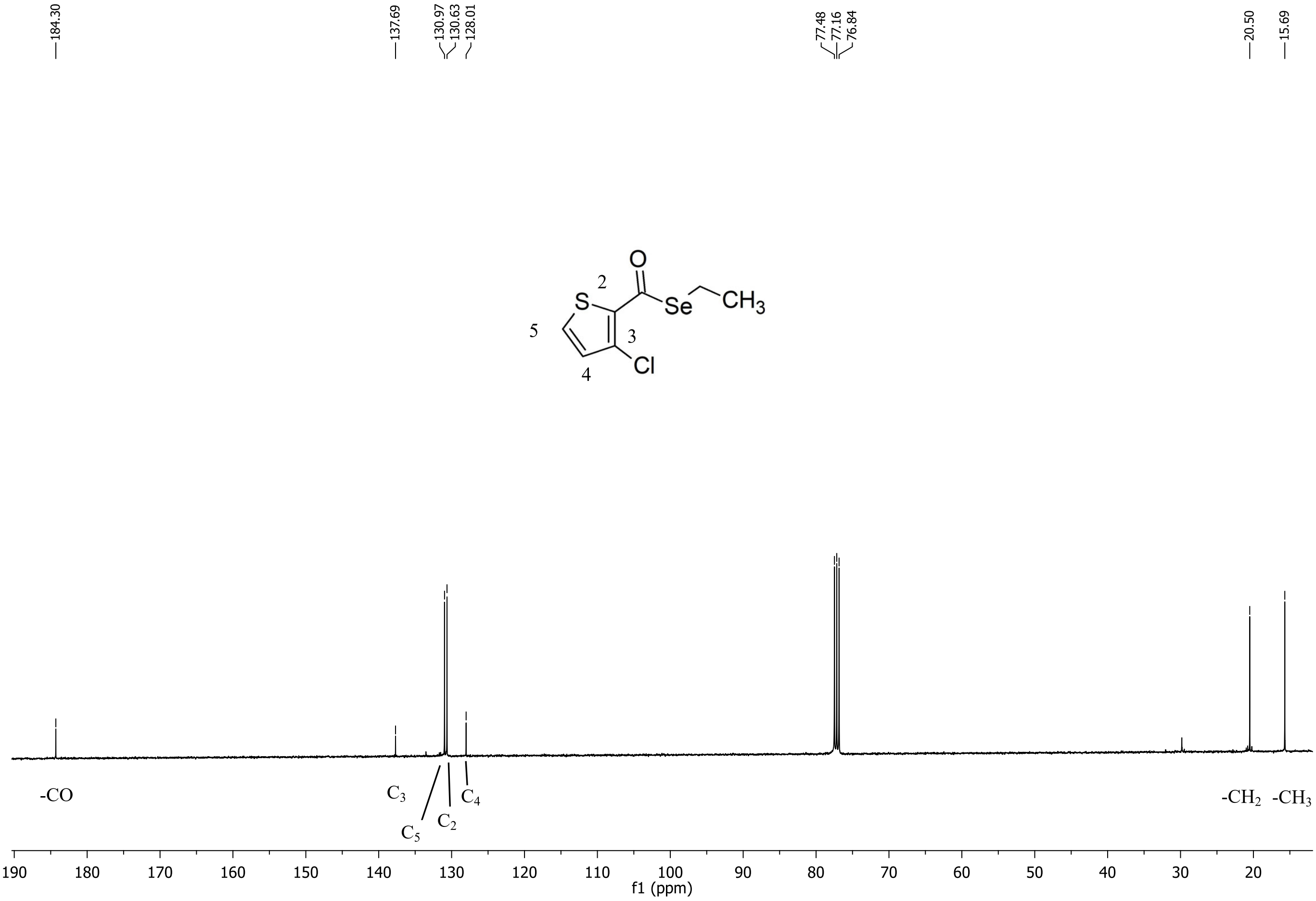

^{1}H NMR of compound **1b**

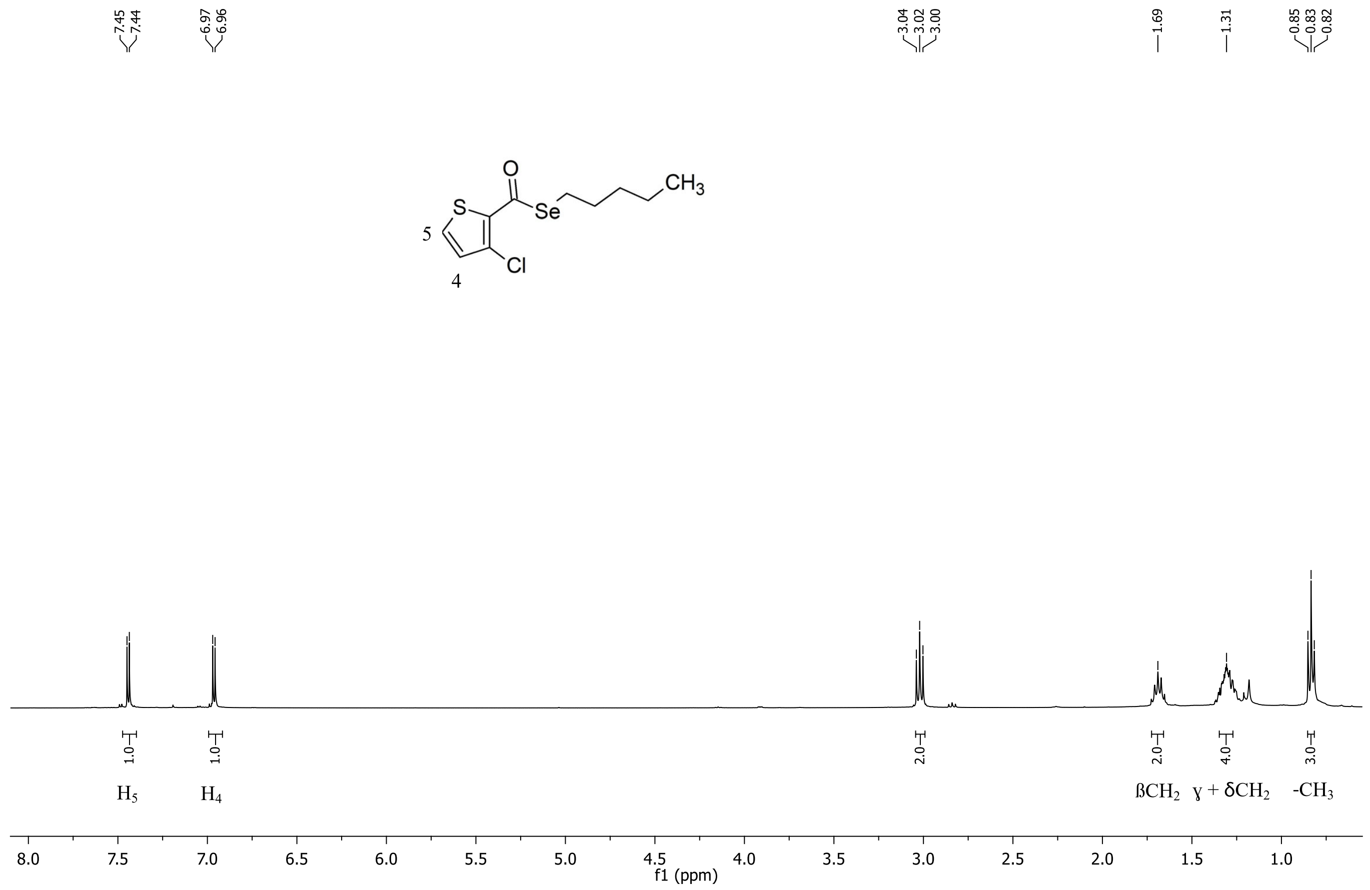

^{13}C NMR APT of compound **1b**

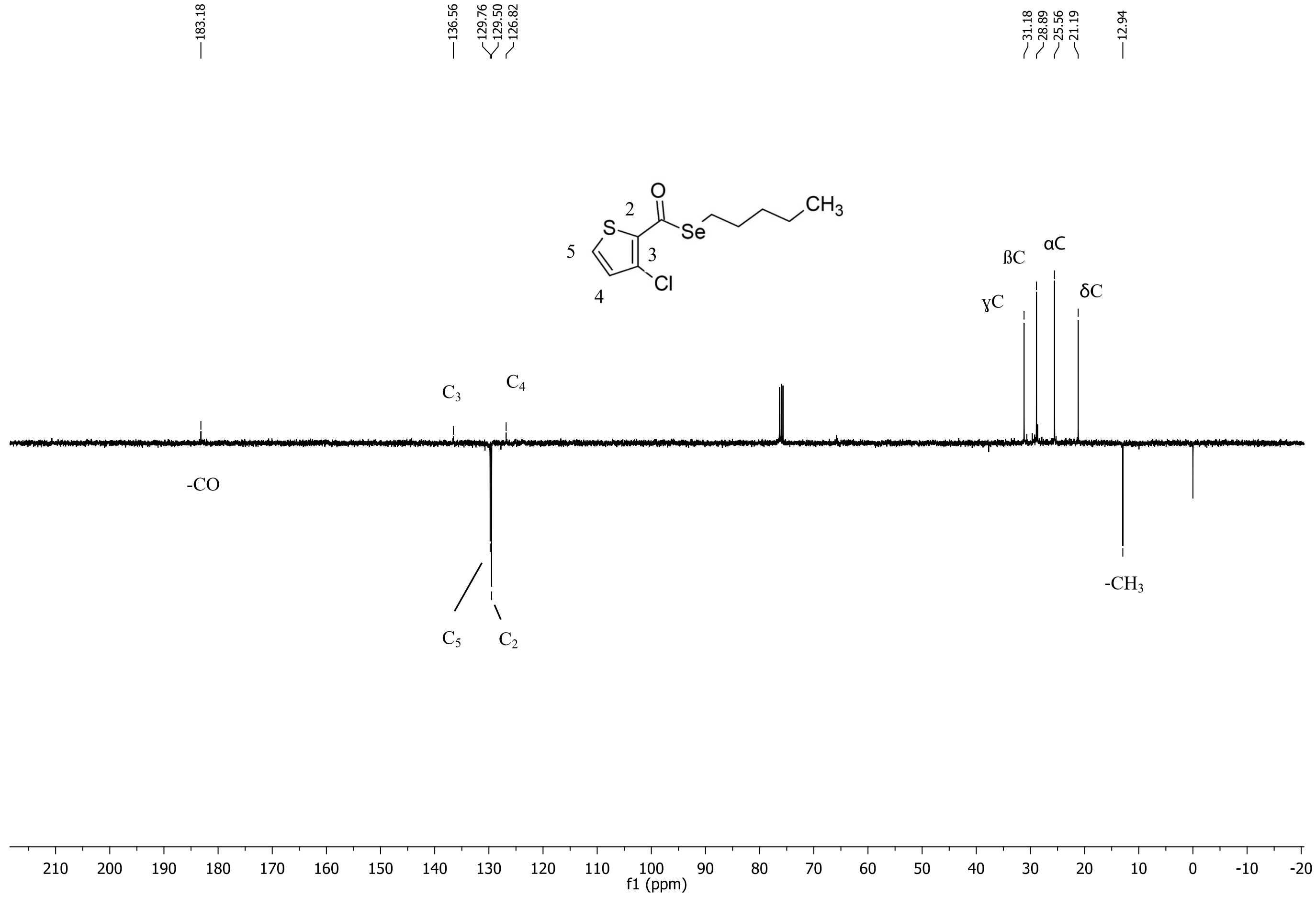

^{1}H NMR of compound **2a**

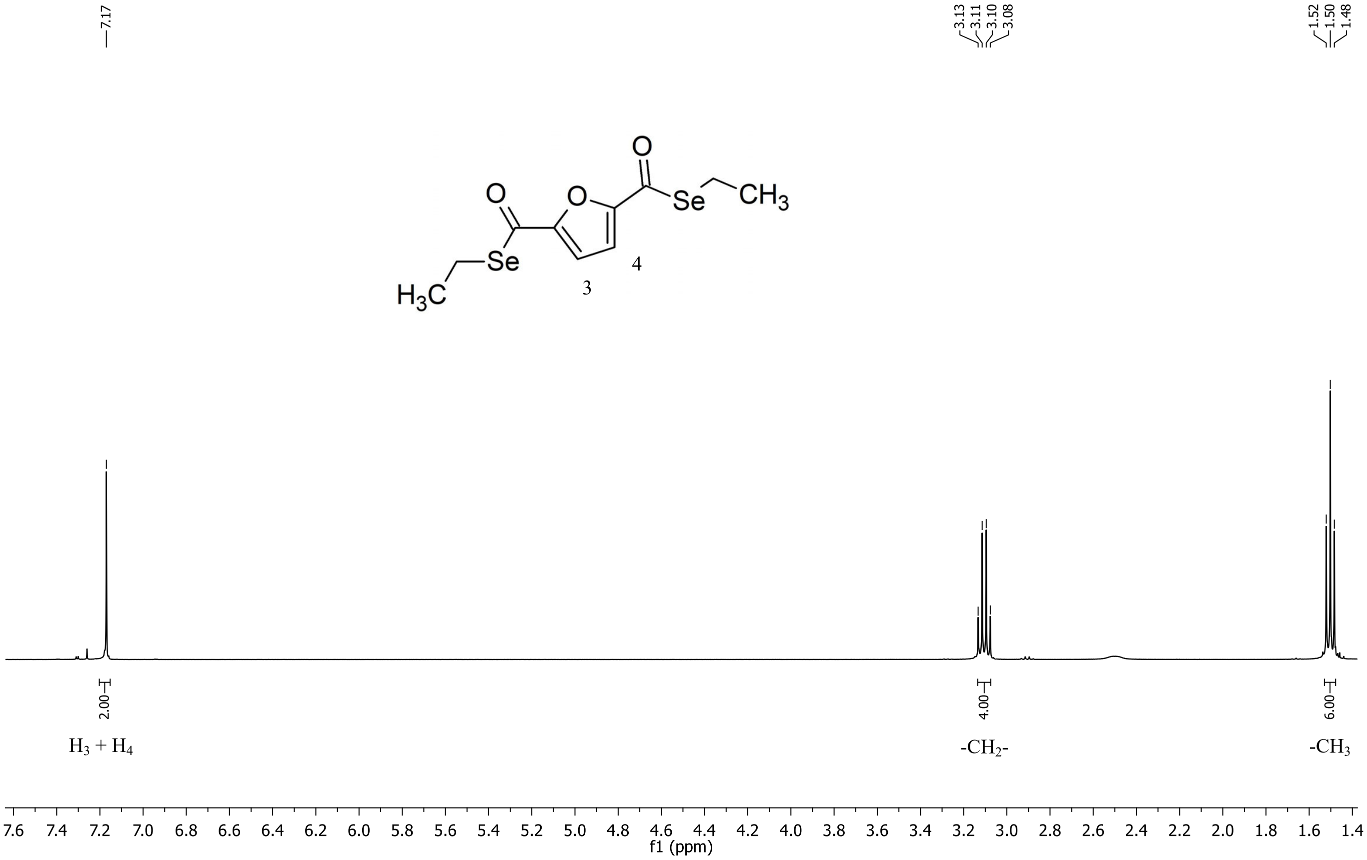

^{13}C NMR of Compound **2a**

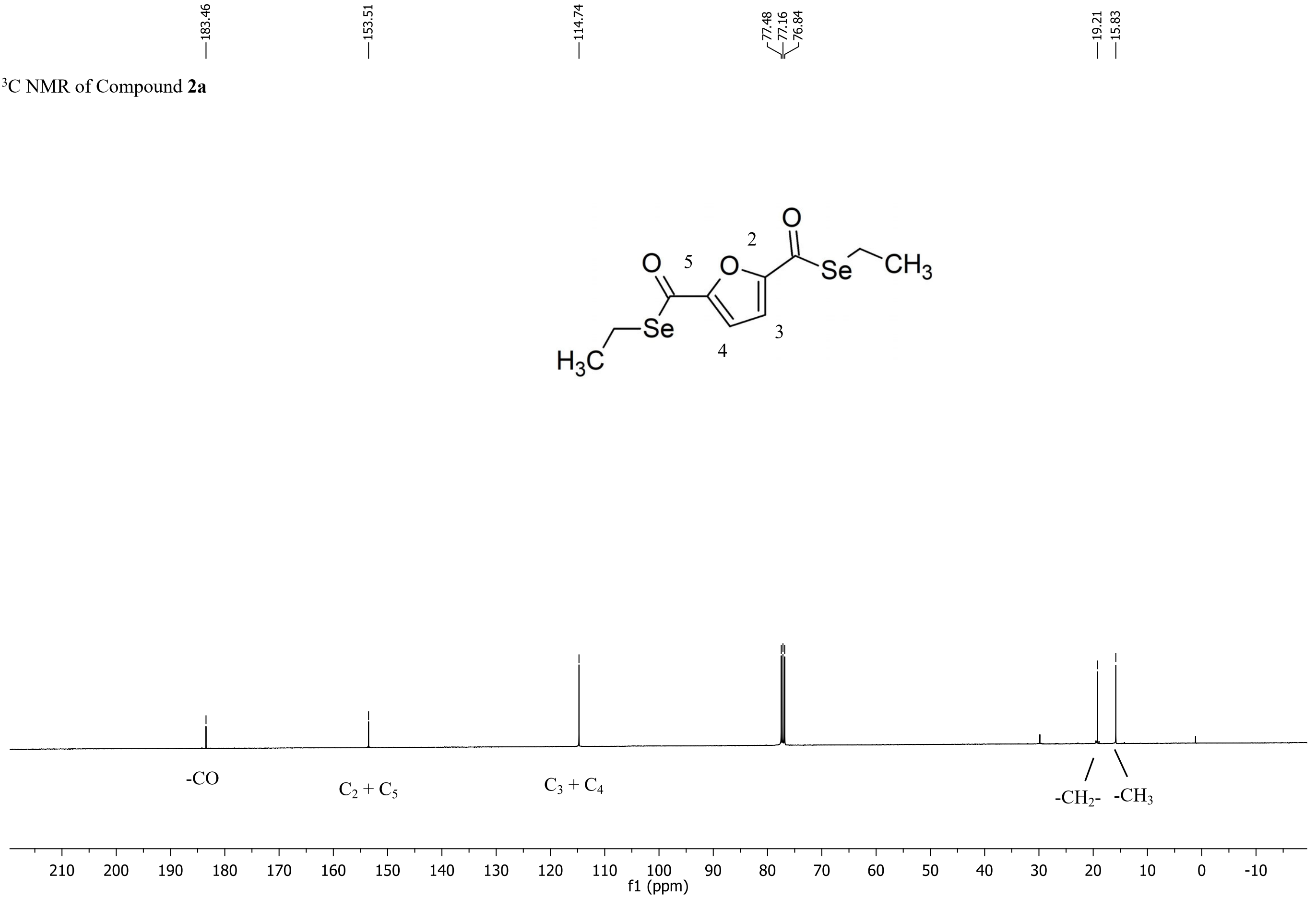

^{1}H NMR of compound **2c**

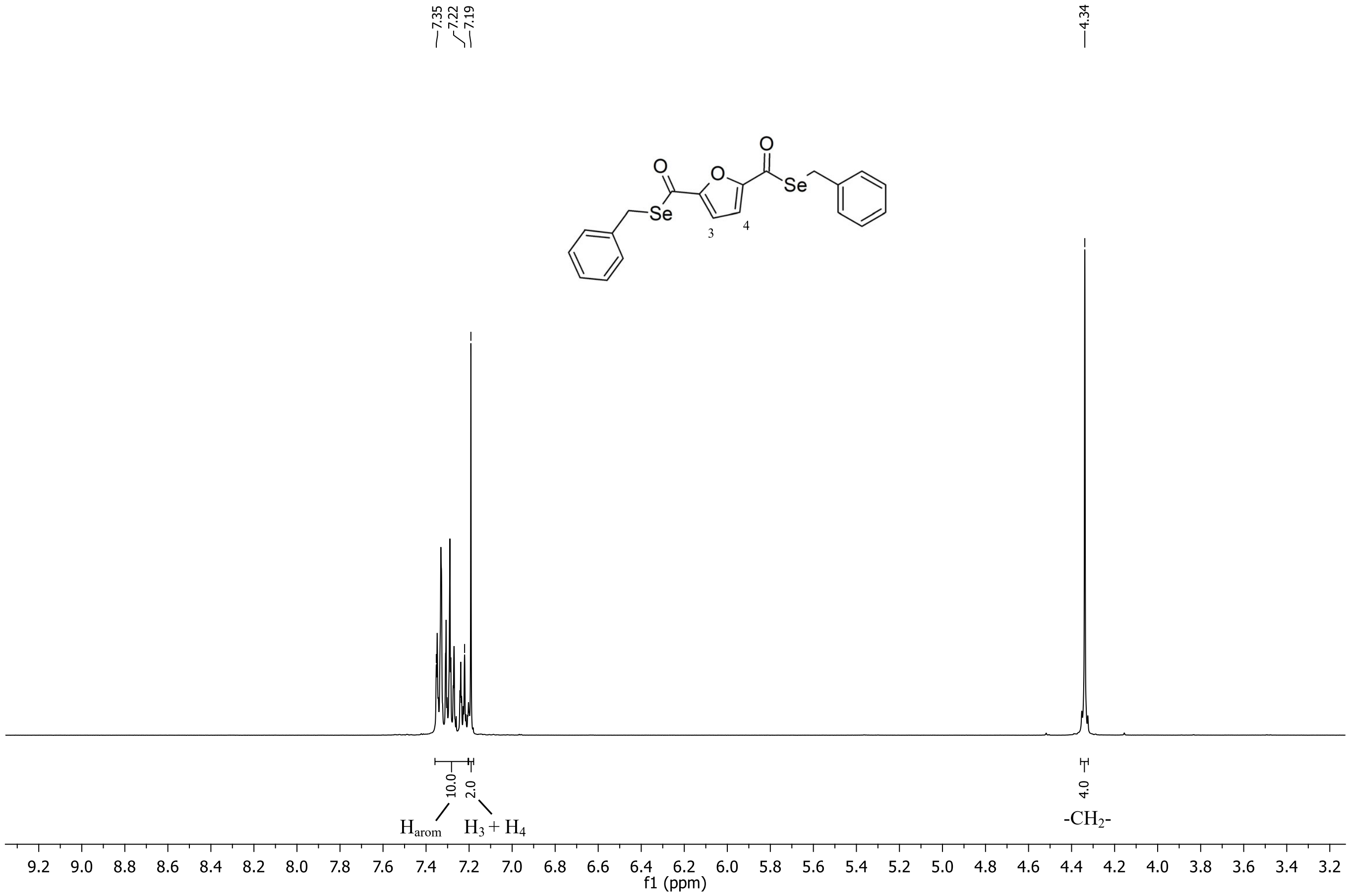

^{13}C NMR APT of compound **2c**

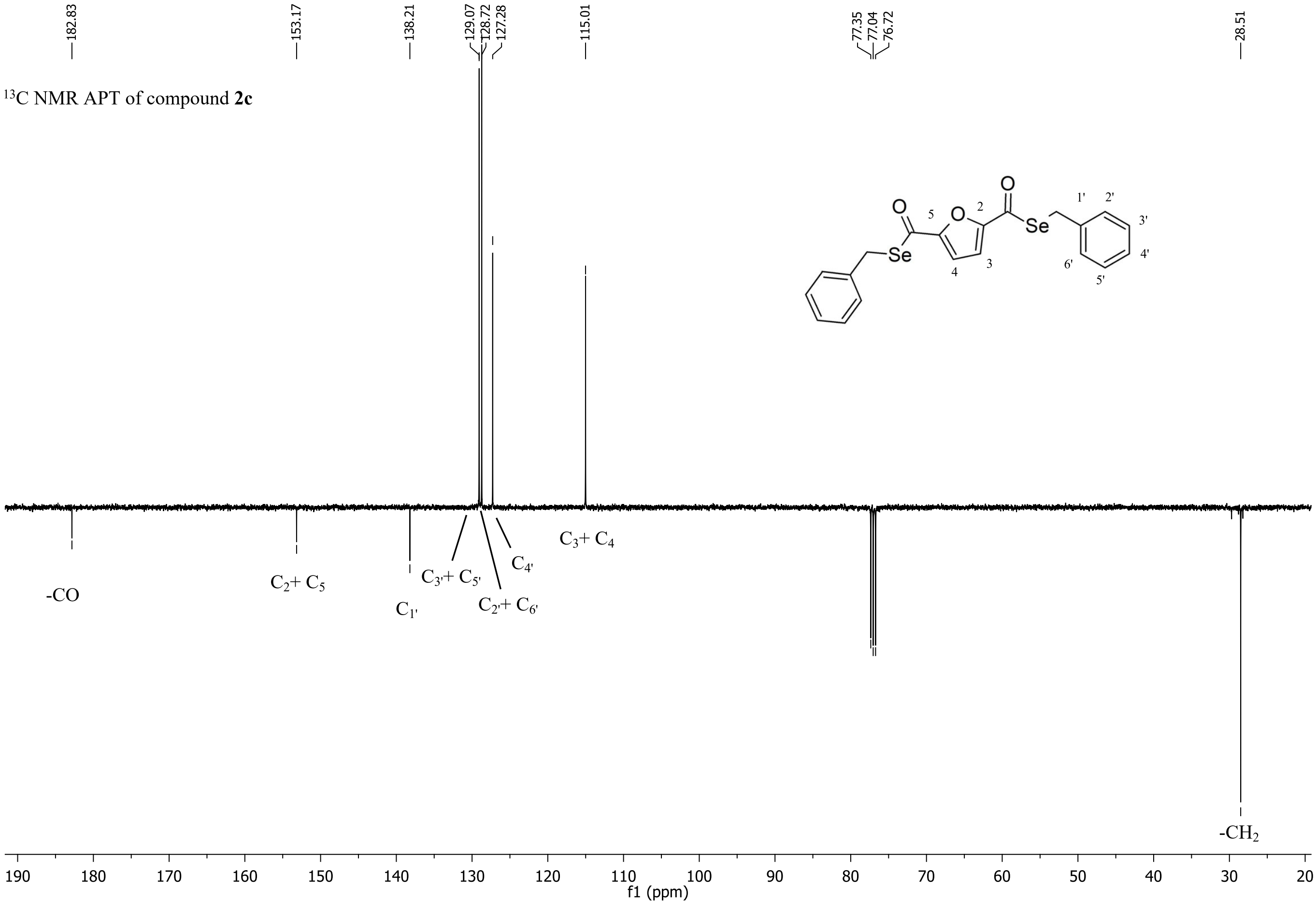

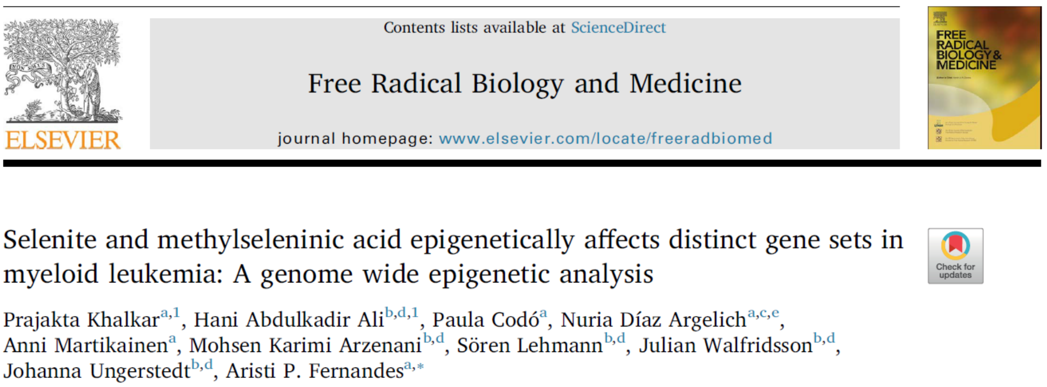

Free Radical Biology and Medicine 117 (2018) 247–257

Contents lists available at ScienceDirect

Free Radical Biology and Medicine

journal homepage: www.elsevier.com/locate/freeradbiomed

Selenite and methylseleninic acid epigenetically affects distinct gene sets in myeloid leukemia: A genome wide epigenetic analysis

Prajakta Khalkar[a,1], Hani Abdulkadir Ali[b,d,1], Paula Codó[a], Nuria Díaz Argelich[a,c,e], Anni Martikainen[a], Mohsen Karimi Arzenani[b,d], Sören Lehmann[b,d], Julian Walfridsson[b,d], Johanna Ungerstedt[b,d], Aristi P. Fernandes[a,*]

PUBLISHED

Free Radic Biol Med. 2018 Mar;117:247-257

PAPER 3

Khalkar P, et al. Selenite and methylseleninic acid epigenetically affects distinct gene sets in myeloid leukemia: A genome wide epigenetic analysis. Free Radical Biology and Medicine, 2018, 117:247-257. https://doi.org/10.1016/j.freeradbiomed.2018.02.014

Supplementary table 1

Biological Processes significantly affected for H3K4me3 by MSA (log2FC)

GO term	Description	P-value	FDR q-value
GO:0040011	locomotion	3.2E-5	3.6E-1
GO:0048870	cell motility	6.73E-5	3.78E-1
GO:0051222	positive regulation of protein transport	7.34E-5	2.75E-1
GO:0018243	protein O-linked glycosylation via threonine	9.27E-5	2.6E-1
GO:0007605	sensory perception of sound	1.09E-4	2.45E-1
GO:0050954	sensory perception of mechanical stimulus	1.35E-4	2.52E-1
GO:1904951	positive regulation of establishment of protein localization	1.35E-4	2.16E-1
GO:0034332	adherens junction organization	2.15E-4	3.01E-1
GO:0008589	regulation of smoothened signaling pathway	2.21E-4	2.75E-1
GO:0009154	purine ribonucleotide catabolic process	2.66E-4	2.99E-1
GO:0016477	cell migration	2.82E-4	2.88E-1
GO:0086019	cell-cell signaling involved in cardiac conduction	3.58E-4	3.35E-1
GO:0035136	forelimb morphogenesis	3.58E-4	3.09E-1
GO:0048496	maintenance of animal organ identity	4.72E-4	3.79E-1
GO:0071657	positive regulation of granulocyte colony-stimulating factor production	4.98E-4	3.73E-1
GO:0071655	regulation of granulocyte colony-stimulating factor production	4.98E-4	3.5E-1
GO:0071971	extracellular exosome assembly	4.98E-4	3.29E-1
GO:1900035	negative regulation of cellular response to heat	4.98E-4	3.11E-1
GO:1904238	pericyte cell differentiation	4.98E-4	2.95E-1
GO:1901258	positive regulation of macrophage colony-stimulating factor production	4.98E-4	2.8E-1
GO:0061042	vascular wound healing	4.98E-4	2.67E-1
GO:0003094	glomerular filtration	4.98E-4	2.54E-1
GO:0072209	metanephric mesangial cell differentiation	4.98E-4	2.43E-1
GO:0072254	metanephric glomerular mesangial cell differentiation	4.98E-4	2.33E-1
GO:0072007	mesangial cell differentiation	4.98E-4	2.24E-1
GO:0072008	glomerular mesangial cell differentiation	4.98E-4	2.15E-1
GO:0097205	renal filtration	4.98E-4	2.07E-1
GO:0035759	mesangial cell-matrix adhesion	4.98E-4	2E-1
GO:0009261	ribonucleotide catabolic process	5.36E-4	2.08E-1
GO:0051223	regulation of protein transport	5.52E-4	2.07E-1
GO:0032804	negative regulation of low-density lipoprotein particle receptor catabolic process	6.03E-4	2.18E-1
GO:0006195	purine nucleotide catabolic process	6.33E-4	2.22E-1
GO:0021794	thalamus development	6.52E-4	2.22E-1
GO:0050715	positive regulation of cytokine secretion	6.98E-4	2.31E-1
GO:0018242	protein O-linked glycosylation via serine	8.4E-4	2.69E-1
GO:0035107	appendage morphogenesis	9.07E-4	2.83E-1
GO:0035108	limb morphogenesis	9.07E-4	2.75E-1

Supplementary figure legend

Supplementary figure 1: Heat maps illustrating the largest changes in enrichment for A) H3K9me3 and B) H3K4me3 protein coding genes after MSA treatment compared to control and selenite. The one to the left is with logFC>2 and to the right logFC<-2.

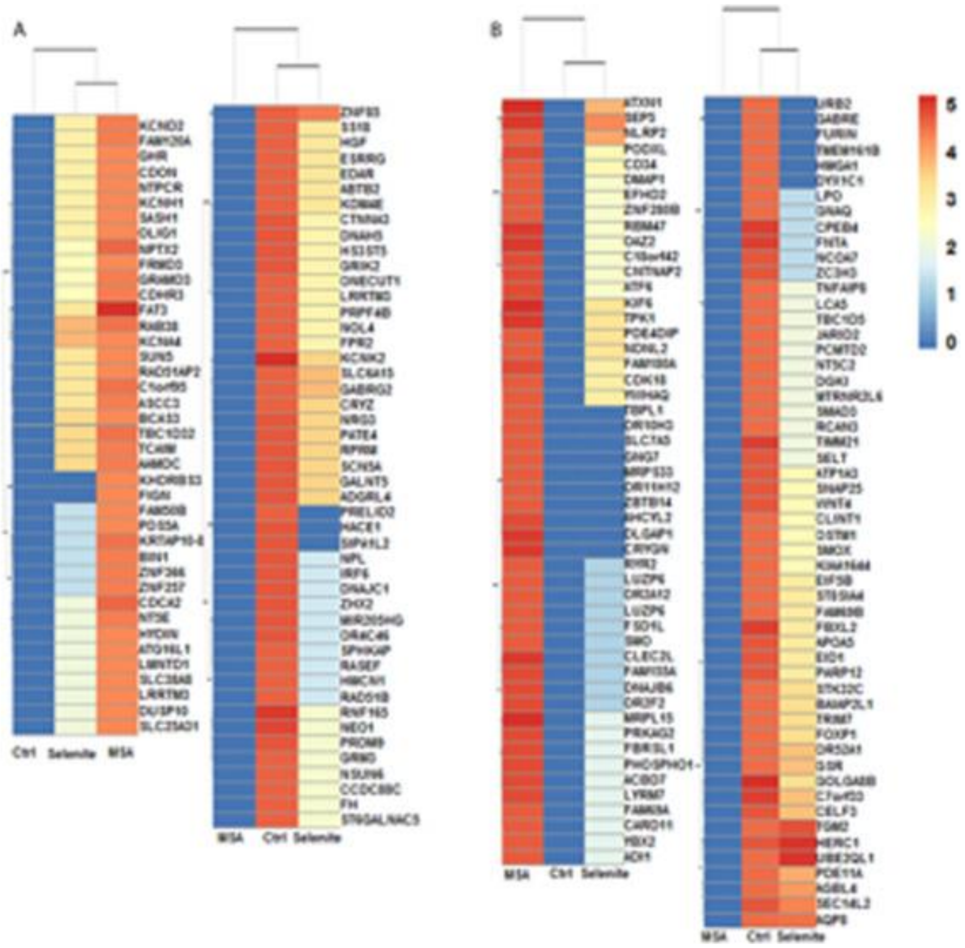

Supplementary information- Materials and Methods

Following is the list of primer sequences that were used for qPCR-

MET_fwd	5’-ACCTTTGATATAACTGTTTACTTGTTGCA-3’
MET_rev	5’-GCTTTAGGGTGCCAGCATTTT-3’
SDC1_fwd	5’-TCTGACAACTTCTCCGGCTC-3’
SDC1_rev	5’-CCACTTCTGGCAGGACTAC-3’
CD29_fwd	5’- GAAGGGTTGCCCCTCCAGA -3’
CD29_rev	5’- GCTTGAGCTTCTCTGCTGTT -3’

Additionally, following primers for qPCR were purchased from Qiagen, Stockholm, Sweden-

Hs_RICTOR_1_SG QuantiTect Primer Assay, Catalog QT00065793
Hs_DAB2_1_SG QuantiTect Primer Assay, Catalog QT00085582
Hs_ZEB1_1_SG QuantiTect Primer Assay, Catalog QT00020972
Hs_HIP1_1_SG QuantiTect Primer Assay, Catalog QT00042616
Hs_CD9_1_SG QuantiTect Primer Assay, Catalog QT00019096

Following is the list of primers used for ChIP-qPCR-

CD29_H3K9Ac enriched_fwd	5’-TAAACACGGGGAAGTGGACTG-3’
CD29_H3K9Ac enriched_rev	5’-GCCGGGTAGAAGTTGGCTTA-3’
CD29_non-enriched_fwd	5’-GCCACTGGTTGCTGACTTGA-3’
CD29_non-enriched_rev	5’-TGGTTTCTCGCAGCCATCTG-3’
HIP1_H3K9Ac enriched_fwd	5’-TCTGTGTCTCCTCCACGGTA-3’
HIP1_H3K9Ac enriched_rev	5’-CCAGGAGGGCTGTCAATCAC-3’
HIP1_non-enriched_fwd	5’- TCGAAAAGGGTGGCTCATGT-3’
HIP1_non-enriched_rev	5’ CCCCAACCTTGCTCCTTTAGT-3’
DAB2_H3K9Ac_fwd	5’- ACCGCTATGTTGACTGAGGC-3’
DAB2_H3K9Ac_rev	5’- GCTTGCCTGCCTGTTGTAAG-3’
DAB2_non-enriched_fwd	5’- GCCTGCCCCATTCACTTAGA-3’
DAB2_non-enriched_rev	5’-GAAGCAGCCTGGCAAGTTTT-3’

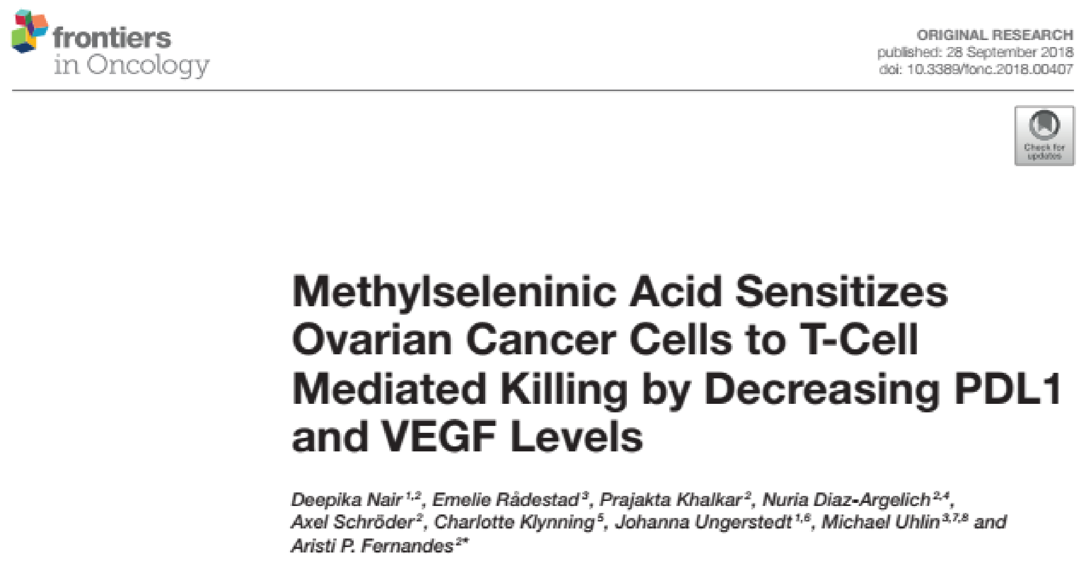

frontiers in Oncology

ORIGINAL RESEARCH
published: 28 September 2018
doi: 10.3389/fonc.2018.00407

Methylseleninic Acid Sensitizes Ovarian Cancer Cells to T-Cell Mediated Killing by Decreasing PDL1 and VEGF Levels

Deepika Nair[1,2], Emelie Rådestad[3], Prajakta Khalkar[2], Nuria Diaz-Argelich[2,4], Axel Schröder[2], Charlotte Klynning[5], Johanna Ungerstedt[1,6], Michael Uhlin[3,7,8] and Aristi P. Fernandes[2]*

PUBLISHED

Front Oncol. 2018 Sep 28;8:407

PAPER 4

frontiers
in Oncology

ORIGINAL RESEARCH
published: 28 September 2018
doi: 10.3389/fonc.2018.00407

Methylseleninic Acid Sensitizes Ovarian Cancer Cells to T-Cell Mediated Killing by Decreasing PDL1 and VEGF Levels

Deepika Nair [1,2], ***Emelie Rådestad*** [3], ***Prajakta Khalkar*** [2], ***Nuria Diaz-Argelich*** [2,4], ***Axel Schröder*** [2], ***Charlotte Klynning*** [5], ***Johanna Ungerstedt*** [1,6], ***Michael Uhlin*** [3,7,8] **and** ***Aristi P. Fernandes*** [2*]

[1] Department of Medicine Huddinge, Center for Hematology and Regenerative Medicine, Karolinska Institutet, Stockholm, Sweden, [2] Division of Biochemistry, Department of Medical Biochemistry and Biophysics, Karolinska Institutet, Stockholm, Sweden, [3] Department of Clinical Science, Intervention and Technology, Karolinska Institutet, Stockholm, Sweden, [4] Department of Organic and Pharmaceutical Chemistry, University of Navarra, Pamplona, Spain, [5] Department of Gynecological Oncology, Karolinska University Hospital, Stockholm, Sweden, [6] Hematology Center, Karolinska University Hospital, Stockholm, Sweden, [7] Department of Applied Physics, Royal Institute of Technology, Stockholm, Sweden, [8] Department of Clinical Immunology and Transfusion Medicine, Karolinska University Hospital, Stockholm, Sweden

OPEN ACCESS

Edited by:
Sarah-Maria Fendt,
VIB KU Leuven Center for Cancer Biology, Belgium

Reviewed by:
Pablo Sarobe,
Centro de Investigación Médica Aplicada (CIMA), Spain
Ping-Chih Ho,
Université de Lausanne, Switzerland

****Correspondence:***
Aristi P. Fernandes
aristi.fernandes@ki.se

Specialty section:
This article was submitted to Molecular and Cellular Oncology, a section of the journal Frontiers in Oncology

Received: *11 June 2018*
Accepted: *06 September 2018*
Published: *28 September 2018*

Citation:
Nair D, Rådestad E, Khalkar P, Diaz-Argelich N, Schröder A, Klynning C, Ungerstedt J, Uhlin M and Fernandes AP (2018) Methylseleninic Acid Sensitizes Ovarian Cancer Cells to T-Cell Mediated Killing by Decreasing PDL1 and VEGF Levels. Front. Oncol. 8:407. doi: 10.3389/fonc.2018.00407

Redox active selenium (Se) compounds at sub toxic doses act as pro-oxidants with cytotoxic effects on tumor cells and are promising future chemotherapeutic agents. However, little is known about how Se compounds affect immune cells in the tumor microenvironment. We demonstrate that the inorganic Se compound selenite and the organic methylseleninic acid (MSA) do not, despite their pro-oxidant function, influence the viability of immune cells, at doses that gives cytotoxic effects in ovarian cancer cell lines. Treatment of the ovarian cancer cell line A2780 with selenite and MSA increases NK cell mediated lysis, and enhances the cytolytic activity of T cells. Increased T cell function was observed after incubation of T cells in preconditioned media from tumor cells treated with MSA, an effect that was coupled to decreased levels of PDL1, HIF-1α, and VEGF. In conclusion, redox active selenium compounds do not kill or inactivate immune cells at doses required for anti-cancer treatment, and we demonstrate that MSA enhances T cell-mediated tumor cell killing via PDL1 and VEGF inhibition.

Keywords: selenium, methylseleninic acid, PDL1, VEGF, HIF-1α

INTRODUCTION

Cancer cells are known to have an aberrant metabolism that gives rise to increased production of endogenous reactive oxygen species (ROS). In order to cope with augmented stress caused by the increased ROS, cancer cells maximize their antioxidant capacity rendering them more vulnerable to additional ROS levels. Therefore, increasing ROS levels through redox modulation may be a therapeutic strategy to selectively kill cancer cells but not normal cells (1). Selenium (Se) has been demonstrated to possess anti-cancer activity in several clinical and experimental studies (2), and one of the most well-studied mechanisms by which Se targets cancer cells is by inducing the production of ROS.

Se compounds have been shown to be selectively toxic to malignant cells, particularly to chemotherapeutic drug resistant cells, compared to normal cells (3). They exert their biological activity via their redox active metabolites. Two well characterized and widely used Se compounds are methylseleninic acid (MSA; CH_3SeO_2H) and sodium selenite (Na_2SeO_3) (2). Selenite is readily reduced by thiols to the key metabolite selenide that can redox cycle with oxygen and generate superoxide (4, 5). MSA is metabolized to methylselenol (CH_3SeH) that is another important, redox active and central Se metabolite (1). Both compounds have shown anticancer properties, but with distinct modes.

Very little is known about the mechanistic effects of Se on the immune system, however Se compounds have been shown to influence the immune response by enhancing phagocytosis and inducing cytokine production (6). Treatment of tumor cells with selenite has been shown to result in loss of HLA-E expression thereby increasing susceptibility to CD94/NKG2A-positive natural killer (NK) cells mediated tumor cell killing (7). MSA has been reported to alter the expression of NKG2D ligands on cancer cells, thereby enhancing their recognition and elimination by NKG2D-expressing immune effector cells (8).

Immunosuppression is one of the major side effects in cancer patients treated with chemo and radiotherapy. The new frontier in anti-cancer treatment is the concept of stimulating endogenous immune response against tumor cells by removal of elements such as, influence of co-inhibitory receptors. Several strategies, like usage of immune checkpoint blockade with anti-PD-1/PD-L1 or CTLA-4 antibodies and cancer vaccines have been proposed in ovarian cancer to enhance immune cell response, especially of the T cells (9). The combination of chemo- and immunomodulatory treatment may benefit in both direct cytotoxic effects and the development of long-term antitumor immunity (10). These therapies might potentially enhance the susceptibility of tumor cells to T cell mediated tumor killing via different mechanisms.

In particular, suppression of regulatory T cells (Tregs) has been shown to aggravate the proliferation of implanted tumor cells in mice. Increased expression of programmed cell death ligand 1 (PDL1) on both tumor cells and dendritic cells (DCs), is known to cause T-cell exhaustion (11, 12). In ovarian cancer cell lines, treatment with various chemotherapeutic agents has been shown to upregulate PDL1 leading to suppression of antigen-specific T-cell function *in vitro*. In a mouse model of ovarian cancer, treatment with paclitaxel resulted in upregulated PDL1 expression. Treatment with a combination of paclitaxel and PDL1/PD-1 blockade resulted in longer survival compared with mice treated with paclitaxel alone (13). Moreover, factors produced in the tumor microenvironment have also been shown to cause exhaustion of T cells by up-regulation of PD-1 (14). Increased levels of vascular endothelial growth factor (VEGF) in the tumor microenvironment have for instance been shown to enhance the expression of PD-1 leading to CD8+ T cell exhaustion (15). VEGF can directly suppress activation of T cells isolated from ascites from ovarian cancer patients via the VEGF receptor-2 (16). Ovarian cancer cells have also been shown to act immunosuppressive as a mechanism of tumor immune escape and tolerance via increasing the infiltration and induction of Tregs, suppressing NK cell function, T cell activation, and T cell proliferation (17).

This study was primarily undertaken to investigate the effect of selenite and MSA on the immune system in terms of cell viability and activation at doses that are cytotoxic for the cancer cells. Furthermore, it also aimed to study the possible indirect immune modulatory mechanism of selenite and MSA through which they potentially exert by affecting tumor cells and/or the microenvironment. Based on the literature of the immunomodulatory effect of Se compounds, we thus hypothesize that selenite and MSA might alter the immune cells mediated tumor cytolytic activity.

MATERIALS AND METHODS

Sample Collection, Mononuclear Cell Isolation

Ascites was obtained from 4 ovarian cancer patients (International Federation of Gynecology and Obstetrics (FIGO) stage III or IV) at the Karolinska University Hospital, Solna, Sweden with written consent from donating patients and ethical approval granted by the Regional Ethical Review Board in Stockholm (Dnr 2013/2161-31). Heparin (5,000 IE/mL) was added upon collection during surgery. The ascites samples were centrifuged at 400 g for 7 min to remove excess liquid. Mononuclear cells were isolated from the samples by density gradient centrifugation using Lymphoprep (Fresenius Kabi) and centrifugation at 800 g for 20 min. The mononuclear cell fraction was washed twice in PBS (at 500 g for 10 min) and thereafter either cultured fresh or was frozen in complete 1640 RPMI medium (Thermo Fisher Scientific) containing 10% human AB serum (Karolinska University Hospital), 1 % PEST (100 U penicillin/mL and 100 μg streptomycin/mL, Thermo Fisher Scientific) and containing 10% DMSO (WAK-Chemie Medical GmbH). Frozen samples were stored at −192°C until usage.

Peripheral blood mononuclear cells (PBMCs) of healthy donors ($n = 15$) were isolated using density gradient separation (Lymphoprep-Lonza). NK cells (CD56 biotinylated) and T cells (CD45 RA, clone HI 100) were purified using MojoSort Streptavidin Nanobeads (BioLegend) by following manufacturer protocol. T cells were further FACS sorted in FACSVantage (BD Biosciences) using anti-human CD3 PE (Miltenyi Biotec).

Cell Culturing Conditions and Generation of Conditioned Media

The human ovarian cancer cell lines (A2780 and CP70), PBMCs as well as immune cells derived from ascites were maintained in RPMI 1640 media with ultraglutamine I (Lonza)

Abbreviations: DC, dendritic cells; GCLM, Gamma-glutamylcysteine synthetase; HIF-1α, Hypoxic inducing factor 1α; HOX1, Heme oxygenase-1; INFγ, Interferon gamma; MMPs, matrix metalloproteineases; MSA, Methylseleninic acid; NK cells, natural killer cells; Nrf2, Nuclear factor erythroid 2–related factor 2; PBMC, peripheral blood mononuclear cells; PDL1, Programed cell death ligand 1; ROS, reactive oxygen species; Se, selenium; VEGF, vascular endothelial growth factor.

supplemented with 10% fetal bovine serum (FBS) (GE Healthcare HYCLONE) and 2 mM glutamine (Gibco, Life Technologies); in 5% CO_2 at 37°C. To study the induction of hypoxia, cells were treated with selenite or MSA for 4 h and quickly lysed in cytoskeletol buffer (10 mM PIPES, 300 mM NaCl, 1 mM EDTA, 300 mM sucrose, 1 mM $MgCl_2$, 0.5% TritonX 100, Phosphatase inhibitor) supplemented with protease inhibitor cocktail (Roche) for protein extraction. Conditioned media was generated by culturing A2780 or CP70 cells as described above, exposing cells to 5 μM selenite (Sigma Aldrich) or MSA (Sigma Aldrich) for 24 h, where after the cell culture media was collected for further experiments. When indicated extra VEGF (PeproTech) (1 ng/ml) was added daily for 48 h where T cells were cultured in tumor conditioned media.

Quantification of Thiols

Free thiols in the culture medium were quantified using 300 μL of medium with final concentrations of 200 mM Tris-HCl (pH 8.0), 2 M guanidine hydrochloride, and 1 mM DTNB. Absorbance at 412 nm was measured using plate reader (SpectraMax 340PC, Molecular Devices).

Cell Viability

Cell viability was assessed in 96-well plates, either by crystal violet staining (Sigma-Aldrich), neutral red 40 μg/ml (Sigma -Aldrich), or by flow cytometry with 1:10 dilution of AnnexinV-FITC (BD Biosciences) and PI 5 μg/ml (Sigma Aldrich). The latter was analyzed on a BD FACS Callibur (BD Biosciences) and the data were analyzed using FlowJo V10 (BD Biosciences).

Western Blotting

40 μg of proteins were separated on a Bolt^{TM} 4–12% Bis-Tris Gel (Novex) and transferred to a nitrocellulose membrane using the iBlot Gel Transfer Device (Invitrogen). The membranes were then probed with rabbit monoclonal anti-human PDL1 (E1L3N, Cell signaling Technology), rabbit monoclonal anti-human HIF-1α (D2U3T, Cell signaling Technology)) and mouse monoclonal anti-human β-actin (A5441, Sigma- Aldrich). Incubation with primary antibody diluted in TBST containing 5% dry non-fat milk was done overnight at 4°C. Secondary antibodies (1:5,000 in TBST with 5% dry milk) were incubated for 1h at room temperature. Membranes were developed using the Amersham^{TM} ECL^{TM} Start Western Blotting Detection Reagent (GE Healthcare) and bands were visualized using the Bio-Rad Quantity One imaging system (Bio-Rad).

Cytolytic Assays

When indicated, recombinant human Interleukin-2 (IL-2) (PeproTech) was used for NK cell activation at a concentration of 1,000 IU/ml for 24 h prior to the lysis assay. T cells were stimulated with the human T cell-activator CD3/CD28 Dynabeads (Thermo Fischer Scientific) and 30 IU/mL IL-2 (PeproTech) for 96 h. Target cells were pre-labeled with fluorescent membrane staining PKH67 Green Fluorescent Cell Linker Mini Kit for General Cell Membrane Labeling (Sigma-Aldrich). Activated T cells and NK cells were co-incubated with target cells at different ratios, in a final volume of 420 μl for 3.5 h at 37°C and 5% CO_2. At the end of the assay, cells were stained with PI (Sigma-Aldrich) to determine apoptosis by flow cytometry using BD FACS Calibur (BD Biosciences) and analyzed with FlowJo V10 (BD Biosciences).

Multicolor Flow Cytometry

Multicolor flow cytometry was performed to identify T cells and NK cells in patient-derived ascites and analyze their expression of different surface activation markers. All antibodies were purchased from BD Biosciences and included FITC-conjugated anti-HLA-DR (G46-6), PE-conjugated anti-CD25 (M-A251), PE-conjugated anti-CD56 (MY31), PE-Cy7-conjugated anti-CD3 (SK7), Alexa700-conjugated anti-CD4 (RPA-T4), APC-Cy7-conjugated anti-CD69 (FN50) and V500-conjugated CD8 (RPA-T8). Cells were stained in a 96-well plate with titrated volumes of antibodies and incubated for 20 min at 4°C in the dark. After one wash with PBS, the cells were stained with 7AAD (BD Biosciences) for dead cell discrimination according to the manufacturer's instructions. After 10 min of incubation, PBS was added to all wells and the samples were acquired on BD FACSCanto I SORP (BD Biosciences) using FACSDiva V7 software (BD Biosciences). The data was analyzed using FlowJo V10 (BD Biosciences).

Quantitative Polymerase Chain Reaction (qPCR)

RNA was extracted using the RNeasy Plus Mini Kit (Qiagen) according to manufacturer's instructions and converted to cDNA using First strand cDNA synthesis Kit for RT-qPCR (Thermo Fischer Scientific). qPCR was performed in duplicates on 96-well plates using a PikoReal Real-Time PCR System (Thermo Fischer Scientific) and Luminaris Color HiGreen Master Mix (Thermo Fischer Scientific). Included primers were: HMOX (Forward-5′-CCGACAGCATGCCCCAGGATT-3′ and Reverse-5′-GTCT CGGGTCACCTGGCCCTT-3′) and GCLM (Forward- 5′-CAT TTACAGCCTTACTGGGAGG-3′ and Reverse-5′-ATGCAGTC AAATCTGGTGGCA-3′) (Integrated DNA Technologies), PDL1 (QuantiTect primer assay-QT00082775, Qiagen), MMP9, MMP13, MMP19 (Quantitech primer assay- QT00040040, QT00001764, QT00027286, Qiagen). Results were analyzed using the $2^{-\Delta\Delta C_T}$ method, and β-actin was used as endogenous control.

Enzyme-Linked Immunosorbent Assay (ELISA)

Tumor cells were harvested at 24 h and culture supernatant was analyzed for VEGF levels using an ELISA kit in accordance to the protocol provided by the manufacturer (Thermo Fischer Scientific and Mabtech). T cell culture supernatants were collected after 96 h of activation, and analyzed for Interferon gamma (IFNγ) and Granzyme B levels using an ELISA kit (Thermo Fischer Scientific) according to the manufacturer's instructions.

Luminex Assay

Media obtained from the co-culture of stimulated T cells and tumor pre-conditioned media were collected after 48 h.

This media was then analyzed for cytokines using a Luminex Magpix-based assay (Luminex Corporation). 17 different soluble analytes (GM-CSF, sCD137, IFNγ,sFas, sFasL,Granzyme A, Granzyme B, IL-2, IL-4, IL-5, IL-6, IL-10, IL-13, MIP-1α, MIP-1β, TNF-α, and Perforin from the Human High Sensitivity T-Cell panel (HCD8MAG15K-17,Merck Millipore) were analyzed. This assay was performed at Clinical Immunology, Karolinska University Hospital, Sweden using manufacturer's instructions.

Statistics

Statistical analyses were performed with GraphPad Prism (GraphPad). Student's *t*-test was applied on all the obtained data. Statistical significance was determined where *p*-value was <0.05.

RESULTS

Immune Cells Are More Resistant to Cytotoxic Effects of Selenite and MSA Compared to the Ovarian Cancer Cell Lines A2780 and CP70

To assess the cytotoxicity of selenite and MSA, ovarian cancer cell lines and immune cells were treated for 24 h with varying concentration of selenite and MSA. Viability assay showed that A2780 cells were resistant to sodium selenite treatment (EC_{50} approximately at 70 μM, data not shown) whereas their cisplatin resistant counterpart, the CP70 cell line, were more sensitive to selenite (EC_{50} approximately between 10 and 12.5 μM) (**Figure 1A**). Moreover, in accordance with previous studies (18) sensitivity to selenite was coupled to the amount of free extracellular thiols in the media produced by the particular cell line, which in turn has been shown to be directly connected to the uptake of selenite (**Figure 1B**). However both cell lines where equally sensitive to MSA treatment (**Figure 1A**). Neither selenite nor MSA were toxic to lymphocytes from ovarian cancer patient ascites and healthy control at similar doses (**Figure 1C**). Even after sorting and assessing cell viability of NK and T cells, no significant cytotoxicity was observed with neither of the treatments (**Figure 1D**). Taken together these results suggest that NK cells and T cells are resistant to selenite and MSA at doses that are toxic to ovarian cancer cells.

Resistance of Immune Cells to Selenite Is Associated With Upregulation of Nrf2 Pathway.

Nuclear factor erythroid 2–related factor 2 (Nrf2) is a transcription factor induced by oxidative stress and upregulates antioxidant defense systems like Heme oxygenase-1 and NAD(P)H quinone oxidoreductase 1(Nqo1). To test if the immune cell resistance to selenite or MSA is a consequence of Nrf2 activation, a qPCR was performed to analyze the expression of genes regulated by Nrf2. Selenite induced a significant increase in the expression of GCLM and HMOX upon 24 h treatment of ascites-derived immune cells, however treatment with MSA did not trigger any Nrf2 response (**Figure 1E**). This result suggests that survival of immune cells upon treatment with selenite may be due to activation of Nrf2 target genes.

Expression of Lymphocyte Activation Markers Upon Pretreatment With Selenite or MSA

To test the direct effect of Se compounds on immune cell activation, immune cells isolated from ascites of ovarian cancer patients were treated with selenite or MSA for 24 h, and expression of activation markers HLA-DR, CD69, and CD25 were analyzed by flow cytometry. A significant increase in the expression of HLA-DR in NK cells (CD3–/CD56+) and CD8+ T cells (CD3+/CD4–CD8+) was observed upon treatment with selenite and MSA (**Figure 2A**). However, no significant alteration in the expression of activation markers CD69 and CD25 was observed by the treatments (data not shown). To further examine any alteration in the distribution of cellular populations in immune cell compartment of ovarian cancer patient ascites, we analyzed the proportion of CD4+ (T helper cells) and CD8+ T-cells (T cytotoxic cells). Treatment with selenite and MSA caused no significant shift in the proportion of these populations (data not shown).

Pretreatment of Ovarian Cancer Cell Line A2780, With MSA Enhances NK Cell Mediated Tumor Cell Killing

To assess whether pretreatment of ovarian cancer cells with selenite or MSA results in increasing NK cell mediated tumor cell killing, A2780 cells were pretreated with selenite or MSA for 24 h. Pretreatment of A2780 cells with selenite for 24 h showed a trend of increased *in vitro* lysis efficiency of NK cells with approximately 10%, but not with MSA pretreatment (**Figure 2B**). Conventional NK cell activation with IL-2 (1,000 UI/ml, 24 h) prior to the lysis assay showed a trend for an even further enhanced effect with tumor cells pretreated with selenite even though not statistically significant. However, MSA pretreatment, in the IL-2 activated NK cells, had a significant increased lytic activity (**Figure 2B**). These results indicate that pretreatment of A2780 cells with MSA increases the lytic activity of NK cell.

Pretreatment of Ovarian Cancer Cell Line CP70, With Selenite or MSA Decreases the Expression of PDL1

We next wanted to examine the effects of selenite and MSA on tumor cells in more detail. Using western blotting, PDL1 expression was measured on the ovarian cancer cells, and in accordance with previous studies where A2780 expressed low levels of PDL1 (19), PDL1 was here below detection limit, while the cisplatin resistant CP70 cell line showed very high basal levels of PDL1. The PDL1 protein expression was significantly decreased upon treatment with selenite and MSA (**Figure 3A**). The downregulation of PDL1 however did not occur at the transcriptional level as the mRNA expression of PDL1 was

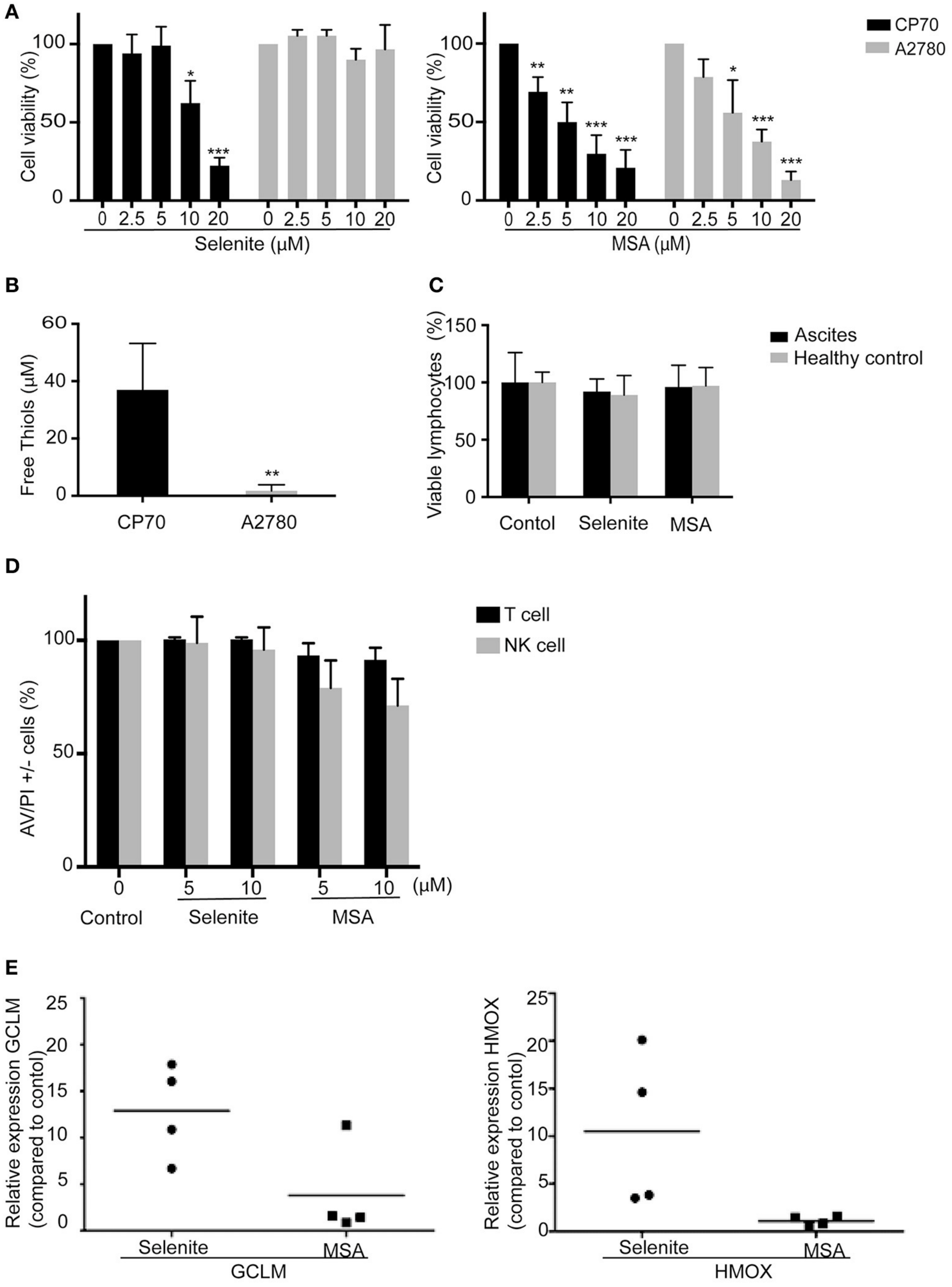

FIGURE 1 | Immune cells are resistant to Selenite and MSA treatment at cytotoxic doses for ovarian cancer cells. Cell viability of tumor cells, peripheral blood mononuclear cells (PBMCs) and immune cells (NK and T cells) were assessed after treatment with selenite and MSA at different concentrations for 24 h. **(A)** Cell viability in % of tumor cells. **(B)** Free thiols in media obtained from tumor cells. **(C)** Viability % of lymphocytes obtained from healthy controls and ascites from ovarian cancer patients after treatment with selenite and MSA (10 μM) ($n = 4$). **(D)** % viability of immune cells ($n = 4$). **(E)** The mRNA levels of Nrf2 response genes (HMOX1 and GCLM) after treatment with selenite/MSA compared to control and relative to actin ($n = 4$). (bars indicate *SD*, $^{*}p \leq 0.05$, $^{**}p \leq 0.01$, $^{***}p \leq 0.001$).

drastically increased upon MSA treatment (**Figure 3B**). To further understand the mechanism of PDL1 downregulation, the expression of matrix metalloproteineases (MMP9, MMP13, and MMP 19) were analyzed, as MMPs have been reported to degrade PDL1 (20). All the three MMP's were significantly upregulated in response to MSA (**Figure 3C**).

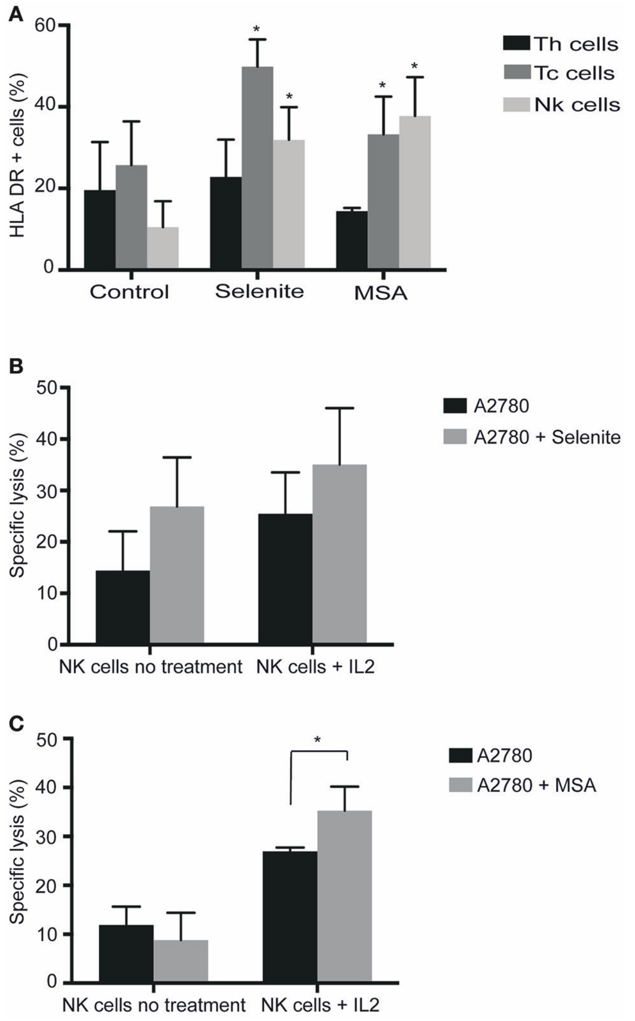

FIGURE 2 | Selenite and MSA sensitizes tumor cells to NK cell mediated killing**.** Direct effects on immune cells (activation, shift in population) assessed after 24 h treatment with selenite and MSA. **(A)** HLA-DR expression on immune cell subsets following treatment with selenite and MSA (10 μM) ($n = 3$). **(B,C)** Specific killing of tumor cells monitored after co incubation with non-activated or overnight IL-2 activated NK cells with A2780 cells pretreated with selenite or MSA (10 μM) ($n = 3$). Columns represent mean specific killing (%); bar indicates *SD*. MSA and/or selenite treated samples were compared to the control (*$p \leq 0.05$).

T Cell Activation and Increase in T-Cell Mediated Killing of Ovarian Tumor Cells by Selenite and MSA

T cells were activated for four days and several soluble markers were used to confirm the activation (**Supplementary Figure S1A**). As both IFN γ and granzyme B increased above the upper detection limit in the Luminex analysis, separate ELISAs were performed for these markers, and both demonstrated a drastic increase after activation (**Supplementary Figure S1B**). To further evaluate if the preconditioned media from tumor cells pretreated with selenite or MSA for 24 h might have an additional effect on the lytic activity of T cells, activated T cells were incubated with preconditioned media for 48 h prior to incubation with fresh tumor cells for 3.5 h. An increased cytolytic activity of T cell cultured in preconditioned media from A2780 and CP70 cells treated with selenite or MSA was observed in both cell lines (**Figure 4A**). The enhanced lytic activity correlated well with the significantly elevated levels of IFNγ and granzyme B for the MSA treatment (**Figures 4B,C**). The incubation however did not alter the proportion of CD4+/CD8+ T cell subsets (**Figure 4D**). These results suggest that treatment with especially MSA not only alters the expression of PDL1 on the tumors, but also enhances the T cell mediated killing of tumor cells.

MSA Alters the Levels of HIF-1α and VEGF, Thereby Increasing the T Cell Mediated Tumor Cell Killing

To explore the effect by which T cells gain increased cytolytic activity after incubation in preconditioned media, HIF-1α levels were determined under hypoxic conditions. MSA clearly suppressed the protein levels of HIF-1α, whereas selenite treatment did not (**Figure 5A**). As HIF-1α is known to regulate the expression of VEGF, and VEGF in turn is known to inhibit T cell function, VEGF levels were measured in the preconditioned media. A more than 4-fold decrease in VEGF was observed in both cell lines treated with MSA. Again, no such effect was seen using selenite pretreatment (**Figure 5B**).

To assess if the enhanced cytolytic activity of the T cells was truly mediated via decreased levels of VEGF, VEGF was added to the preconditioned media in an attempt to block the observed effect. On addition of VEGF (1 ng/ml) to the T cells incubated with tumor preconditioned media (with selenite or MSA), the lytic activity exerted by the T cells was reversed compared to T cell incubated in preconditioned media from MSA (**Figure 5C**). Conversely, as selenite pretreatment did not affect the VEGF levels which remained high, additional VEGF did not alter the specific lytic activity in a significant way. The addition of VEGF to the preconditioned media from tumor cells was also followed by a decrease in cytokine production (**Figures 5D,E**). These results demonstrate that changes in VEGF levels by MSA contribute to the T cell mediated tumor cell killing.

Effect of MSA on T cells

To further investigate the effect of the Se compounds on T cell cytotoxicity, stimulated T cells were cultured with pretreated (5 μM selenite or MSA for 24 h) tumor cells for 48 h. To maintain the low levels of PDL1, 1 μM treatment (both MSA and selenite) was added during the co-culturing for 48 h. There was an approximately 20% decrease in viability of tumor cells treated with MSA (**Figure 6A**). **Figure 6B** shows a graphical representation of the proposed mechanism for action of MSA in the tumor microenvironment.

DISCUSSION

Redox active compounds can readily form ROS and generate oxidative stress, which is generally believed to inhibit the immune

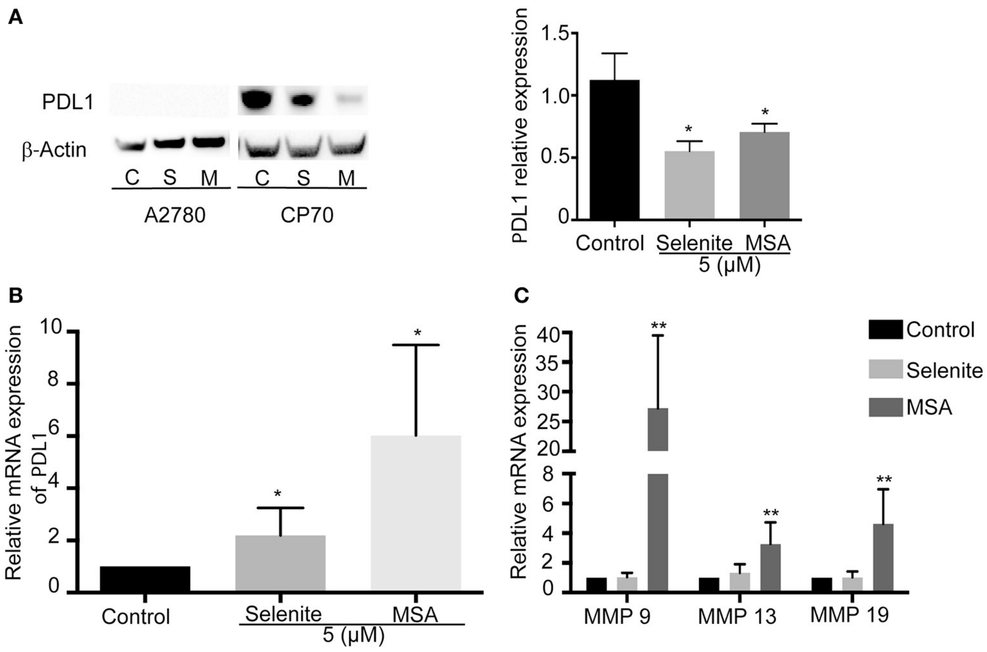

FIGURE 3 | MSA decreases the protein levels of PDL1. **(A)** Western blot analysis of PDL1 (approximately 50 kDa) after treatment (5 μM) with selenite (S) or MSA (M) for 24 h. Graph shows quantification of PDL1 proteins normalized by β-actin. **(B)** Relative mRNA expression of PDL1 on treatment with selenite and MSA compared to control. **(C)** Relative mRNA expression of MMPs after selenite and MSA treatment compared to control. Columns represent mean expression levels (%); bar indicates *SD* (*$p \leq 0.05$, **$p \leq 0.01$, ***$p \leq 0.001$).

system. This study demonstrates that the redox active selenium compounds selenite and MSA, at cytotoxic doses for ovarian cancer cells, does not inhibit or affect the viability of T cells and NK cells. To our knowledge, this is also the first time it has been demonstrated that enhancement of lytic activity by T cells on ovarian cancer cell lines can be mediated by MSA, through the inhibition of PDL1 and VEGF.

Our data suggests that selenite and MSA are selectively toxic to tumor cells, with the T cells and NK cells remaining unaffected by the treatments. Selenite is also known to be especially cytotoxic in drug resistant tumor cells (1). Concomitantly, in this study, a difference in the cytotoxicity of selenite was observed between A2780 and CP70 cell line where CP70 (Cisplatin resistant variant of A2780) was found to be more sensitive to selenite toxicity. Selenite's tumor specific killing (21–23), is mainly attributed to the redox cycling of selenide with oxygen generating superoxide, and eventually oxidative stress (24, 25). Selenite has however been reported to give rise to more systemic effects compared to organic selenium compounds like MSA. Xenograft mice models treated with MSA has for instance shown to reduce tumor growth without inducing any systemic toxicity or any other genotoxic side effects (26), and organic Se compounds have therefore been foreseen as more promising chemotherapeutic agents (2).

Selenite, known to induce intracellular oxidative stress, can trigger the Nrf2 transcriptional response, which is a central regulator of cellular defense against oxidative stress (27). Consistently, treatment of immune cells with selenite resulted in a strong upregulation of Nrf2 regulated genes, indicating a protective mechanism adopted by immune cells for survival. This might partly explain the survival of immune cells upon treatment with selenite. MSA has however been reported in several studies to act via redox modulatory effects that do not mainly cause oxidative stress to the cells (28). In line with these previous studies, MSA did not trigger any Nrf2 response, indicating that immune cell resistance to MSA is achieved by a different molecular mechanism, again illustrating the distinct effect encompassed by each separate selenium metabolite (29).

Several studies have described the correlation between selenium supplementation at supra-nutritional doses and immune responses, but studies on the effect of Se compounds at subtoxic doses on immune cell activation are scarce. One study showed indirect effect of selenite on NK cells, where selenite induced posttranscriptional inhibition of HLA-E and sensitized tumor cells to CD94/NKG2A positive NK cells (7). Herein, selenite showed the same trend, but did not significantly affect the ovarian cancer cell line. Similar results on NK cells have also been reported for MSA (8), and our data confirms this on ovarian cancer cells, as treatment of A2780 cells with MSA increases NK cell mediated lysis. This most likely occurs by the same mechanism as previously reported, with loss of the HLA-E antigen, since ovarian cancer cells also are known to possess DNAM-1 receptor (7), rendering the cells susceptible to NK cell mediated killing.

Sensitization of ovarian cancer cells to T cells via MSA could herein directly be linked to decreased levels of PDL1 in the CP70 cell line. Nevertheless, MSA does not seem to affect PDL1

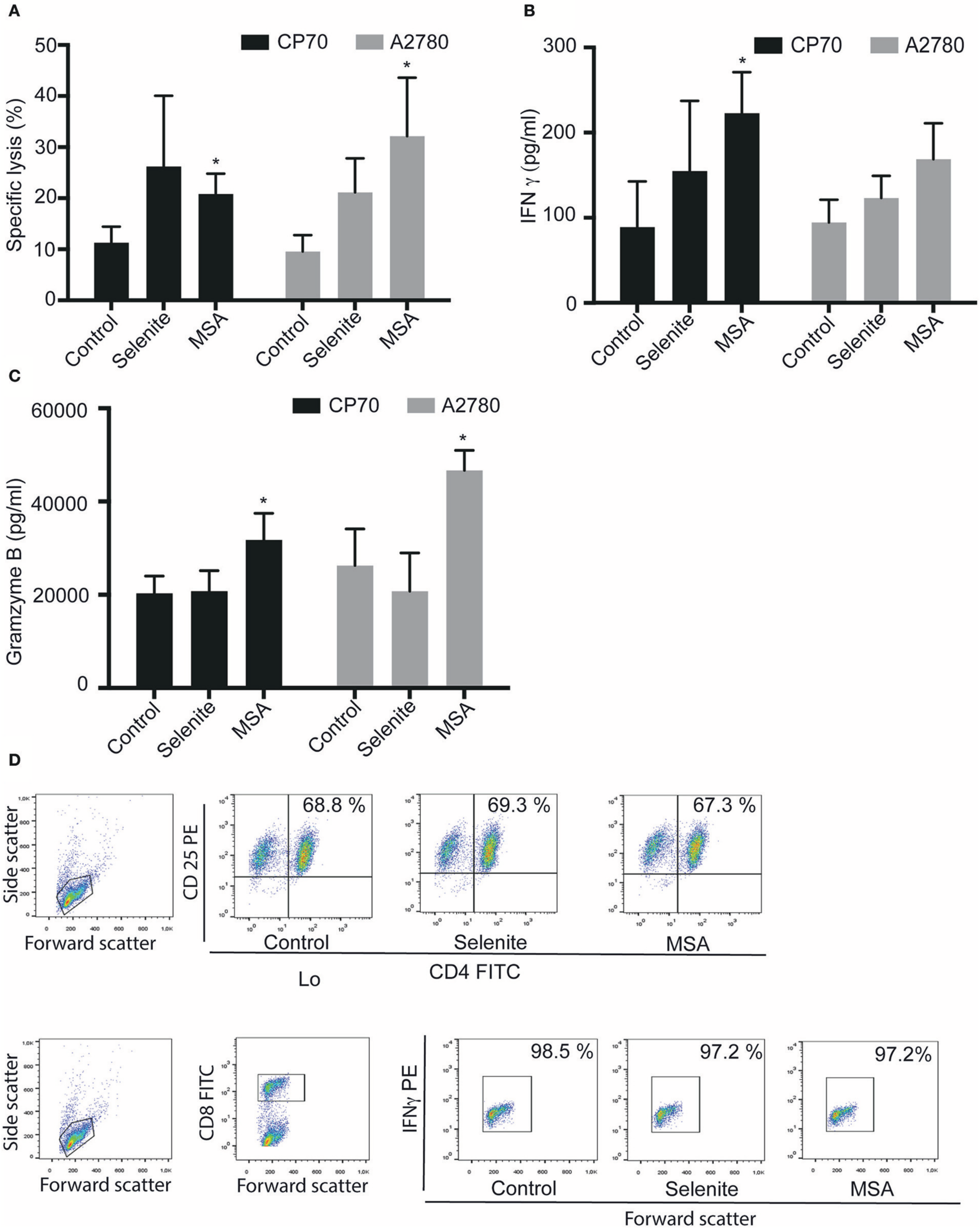

FIGURE 4 | Tumor preconditioned media increases cytolytic activity of T cells. Activated T cells cultured in preconditioned media for 48 h followed by cytolytic measurements after co-incubation with new target cells. **(A)** Specific T cell killing of tumor cells ($n = 3$). Columns represent mean specific killing (%); bar indicates *SD*. **(B)** IFNγ levels in cell supernatant after incubation with T cells for 48 h ($n = 3$). **(C)** Granzyme B levels in cell supernatant after incubation with T cells for 48 h ($n = 3$). Columns represent mean IFNγ and Granzyme B levels (pg/ml); bar indicates *SD*. **(D)** Representative plots form one experiment showing shift in T cell population. MSA and/or selenite treated samples were compared to control (*$p \leq 0.05$).

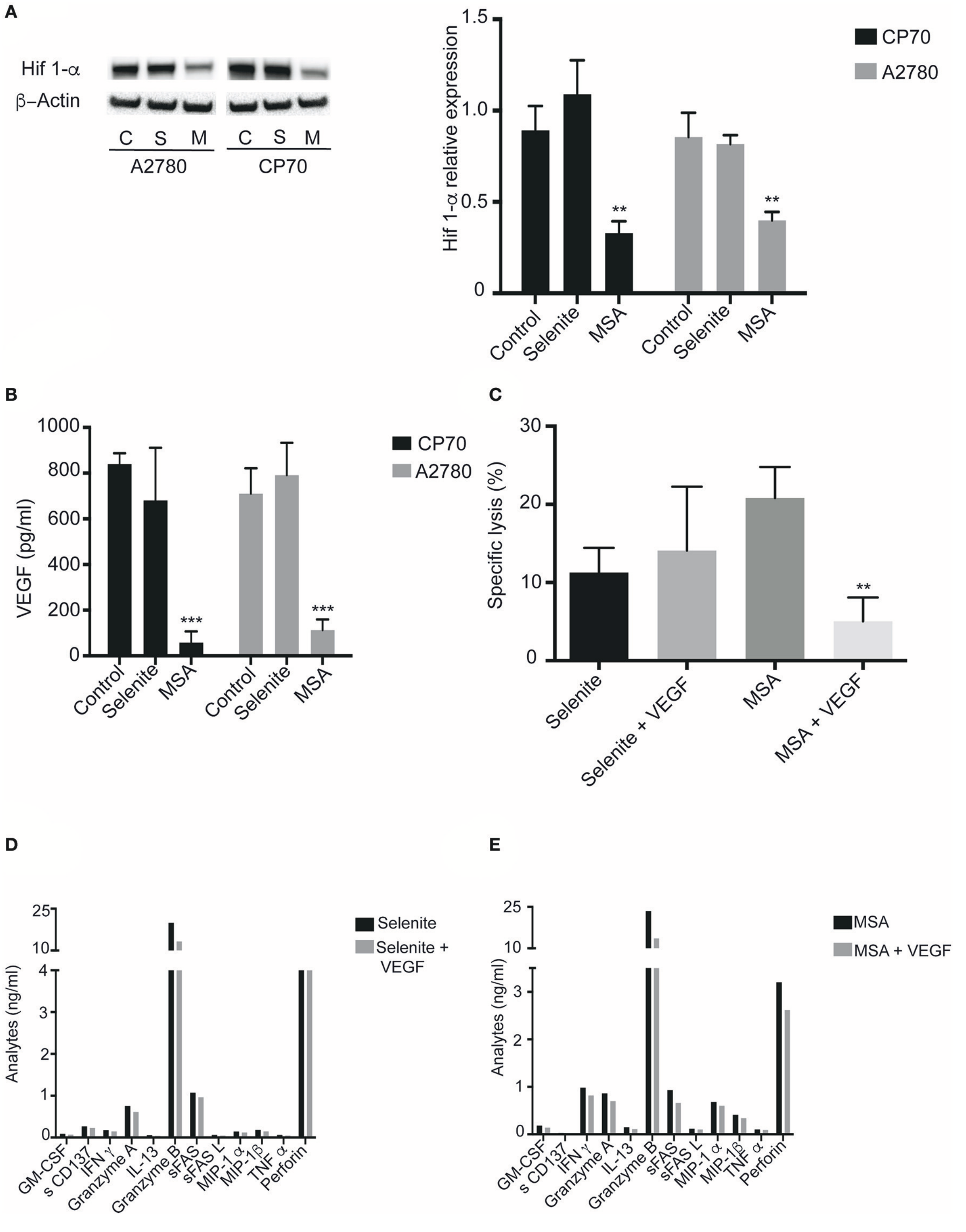

FIGURE 5 | MSA treatment Decreases HIF-1α **(A)** Cells were treated (5 μM) with selenite and MSA under hypoxic condition for 4 h. Western blot analysis of HIF 1-α for CP70 and A2780 cells (approximately 120 kDa). Graph shows quantification of HIF 1-α protein normalized to β-actin. **(B)** Activated T cells cultured in preconditioned media with or without VEGF for 48 h. Killing was monitored after coincubation with CP70 cells. **(B)** VEGF levels from CP70 and A2780 treated with 5 μM selenite/MSA for 24 h ($n = 3$). Columns represent mean VEGF levels (pg/ml); bar indicates *SD*. **(C)** Specific T cell (with or without VEGF in culture) killing of CP70 cells ($n = 3$). **(D)** Representative experiment of T cell specific analytes from Luminex assay on addition of VEGF (**$p \leq 0.01$, ***$p \leq 0.001$).

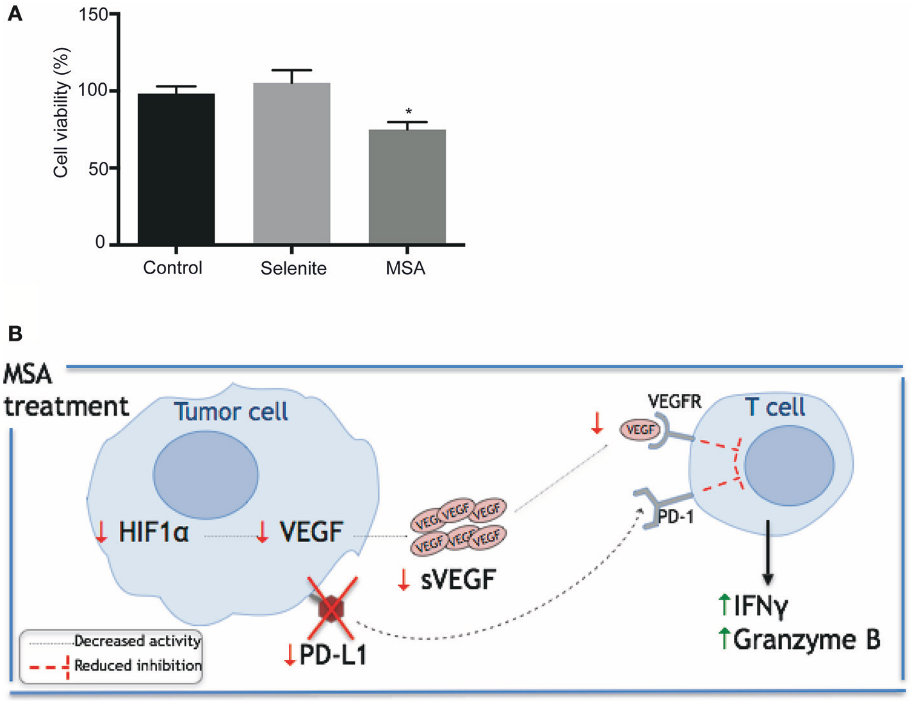

FIGURE 6 | Schematic illustration of proposed mechanism by which MSA sensitizes tumor cells to T cell mediated killing. **(A)** Relative tumor cell killing by T cells in pretreated tumor cells. Activated T cells were cultured in a 96 well plate with the pretreated (with selenite and MSA 5 μM for 24 h) CP70 cells in media containing 1 μM treatment for 48 h. Tumor cell viability was measured using neutral red. Tumor cell killing represents percentage reduction in number of tumor cells, relative to control cultures without T cells. All experiments were performed with three biological replicates per group **(B)** Schematic representation of proposed mechanism for MSA. MSA and/or selenite treated samples were compared to the control (*$p \leq 0.05$).

at the transcriptional level as the mRNA expression increased dramatically. This further indicates that the effect might be at a posttranscriptional level. We recently demonstrated that MSA affect a large set of genes involved in the loss of attachment of cells to the extracellular matrix. Among the many genes identified, several of the matrix metalloproteineases (MMPs) were found to be significantly upregulated in response to MSA (28). Methylselenol, the active metabolite of MSA, was also identified by Zeng and co-workers to activate MMP-2 and MMP-9 (30). Consistently our results also show an upregulation of MMP9, MMP13 and MMP19 in response to MSA. MMPs have recently been shown to degrade PDL1 (20), thus the decreased protein levels of PDL1 after MSA treatment of CP70 cells found in the current study, may likely be explained via the induction of MMPs that subsequently degrade PDL1. A further study is warranted to confirm if the mechanism by which MSA downregulates PDL1 is via MMPs.

MSA treated bone metastatic mammary cancer cells have been reported to decrease VEGF levels (31). MSA have also been reported to inhibit HIF-1α expression and VEGF secretion in lymphoma cell lines and in prostate cancer cells (32). In both studies, authors connected the beneficial effects observed of VEGF inhibition to its angiogenic properties. However, in addition to its angiogenic properties (33, 34), VEGF also encompasses immunosuppressive effects (35), and there are many proposed mechanisms by which VEGF is used by tumors to achieve immunosuppression (36, 37). VEGF has been shown to suppress the activation of T cells from ascites from ovarian cancer patients via VEGF receptor type 2 (16). Secretion of VEGF by tumor cells has also been reported to induce endothelial cells to upregulate prostaglandin E2 (PGE2) which led to the suppression of T cell functions (38). Herein, our results show that incubation of activated T cells in tumor preconditioned media with selenite or MSA indeed enhanced the T cells mediated killing of CP70 and A2780 cells. This enhanced tumor killing activity of T cells is also supported by increased levels of granzyme B and IFNγ in the media. HIF-1α and VEGF were identified as key players with significantly lowered levels upon MSA treatment, and upon addition of VEGF, the lytic activity of T cells was reduced. The increase in lytic activity by MSA treatment could hence at least partially be explained via inhibition of the tumor secreted factor VEGF expression (37). Interestingly this observation was only seen for MSA and not selenite. MSA may therefore not only have an effect on angiogenesis via VEGF inhibition as stated in previous studies, but may also contribute to the upregulation of a tumor specific immune response, and may ultimately contribute in blocking the immune escape and progression of tumors.

Several studies have demonstrated that increased VEGF, HIF-lα, and PTEN expression in ovarian cancer cells can be used as predictors of metastasis and prognosis (39), and that increased plasma VEGF levels in ovarian cancer patients correlate to advanced tumor stage and a poor outcome (40). Compounds inhibiting VEGF may therefore be beneficial in ovarian cancer. From the present study we now know that selenite and MSA do not adversely affect the viability of immune cells at concentrations cytotoxic to tumor cells. Furthermore, we report that MSA decreases the levels of PDL1, HIF-1α, and VEGF in ovarian cancer cell lines and thereby renders the tumor cell sensitive to T cells, turning MSA into an interesting candidate for combinational treatments. MSA may contribute in tumor killing by two possible modes; (1) downregulating the expression of PDL1 thus limiting the activation inhibiting PD-1/PDL1 pathway, resulting in increased T cell activation and killing; (2) by decreasing HIF-1α expression which in turn leads to reduced VEGF levels in the tumor microenvironment. The reduction in VEGF levels will consequently increase the ability of T cells to kill tumor cells. Although further experiments are warranted to confirm these findings and animal models are required, these results suggest a potential strategy to use selenium compounds in anticancer treatment to boost immune functions.

AUTHOR CONTRIBUTIONS

AF and DN: conception and design of the work; DN, ER, ND-A, AS, and PK: data collection; AF, DN, ER, ND-A, and PK: data analysis and interpretation; DN and AF: drafting the article; CK, PK, MU, JU, and ER: critical revision of the article; AF, MU, and JU: final approval of the version to be published.

ACKNOWLEDGMENTS

This article has been financially supported by The Swedish Cancer Society (Cancerfonden, Award number: CAN 2016/606), Stockholm Cancer Society and Marianne and Marcus Wallenbergs foundation. NDA received the pre-doctoral and mobility scholarship from Asociación de Amigos de la Universidad de Navarra.

SUPPLEMENTARY MATERIAL

The Supplementary Material for this article can be found online at: https://www.frontiersin.org/articles/10.3389/fonc.2018.00407/full#supplementary-material

REFERENCES

1. Fernandes AP, Gandin V. Selenium compounds as therapeutic agents in cancer. *Biochim Biophys Acta* (2015) 1850:1642–60. doi: 10.1016/j.bbagen.2014.10.008
2. Gandin V, Fernandes AP. Chapter 15 organoselenium compounds as cancer therapeutic agents. In: Jain VK, Priyadarsini KI, editors. *Organoselenium Compounds in Biology and Medicine: Synthesis, Biological and Therapeutic Treatments*. Royal Society of Chemistry (2018) p. 401–35. doi: 10.1039/9781788011907
3. Wang Y, Fang W, Huang Y, Hu F, Ying Q, Yang W, et al. Reduction of selenium-binding protein 1 sensitizes cancer cells to selenite via elevating extracellular glutathione: a novel mechanism of cancer-specific cytotoxicity of selenite. *Free Radical Biol Med.* (2015) 79:186–96. doi: 10.1016/j.freeradbiomed.2014.11.015
4. Wallenberg M, Olm E, Hebert C, Björnstedt M, Aristi Fernandes P. Selenium compounds are substrates for glutaredoxins: a novel pathway for selenium metabolism and a potential mechanism for selenium-mediated cytotoxicity. *Biochem J.* (2010) 429:85–93. doi: 10.1042/BJ20100368
5. Wallenberg M, Misra S, Wasik AM, Marzano C, Bjornstedt M, Gandin V, et al. Selenium induces a multi-targeted cell death process in addition to ROS formation. *J Cell Mol Med.* (2014) 18:671–84. doi: 10.1111/jcmm.12214
6. Safir N, Wendel A, Saile R, Chabraoui L. The effect of selenium on immune functions of J774.1 cells. *Clin Chem Lab Med.* (2003) 41:1005–11. doi: 10.1515/CCLM.2003.154
7. Enqvist M, Nilsonne G, Hammarfjord O, Wallin RPA, Björkström NK, Björnstedt M, et al. Selenite induces posttranscriptional blockade of HLA-E expression and sensitizes tumor cells to CD94/NKG2A-positive NK cells. *J Immunol.* (2011) 187:3546–54. doi: 10.4049/jimmunol.1100610
8. Hagemann-Jensen M, Uhlenbrock F, Kehlet S, Andresen L, Gabel-Jensen C, Ellgaard L, et al. The selenium metabolite methylselenol regulates the expression of ligands that trigger immune activation through the lymphocyte receptor NKG2D. *J Biol Chem.* (2014) 289:31576–90. doi: 10.1074/jbc.M114.591537
9. Rodriguez-Garcia A, Minutolo NG, Robinson JM, Powell DJ. T-cell target antigens across major gynecologic cancers. *Gynecol Oncol.* (2017) 145:426–35. doi: 10.1016/j.ygyno.2017.03.510
10. Zitvogel L, Tesniere A, Apetoh L, Ghiringhelli F, Kroemer G. [Immunological aspects of anticancer chemotherapy]. *Bull Acad Natl Med.* (2008) 192:1469–87. discussion 1487–1469.
11. Deng L, Liang H, Burnette B, Beckett M, Darga T, Weichselbaum RR, et al. Irradiation and anti-PD-L1 treatment synergistically promote antitumor immunity in mice. *J Clin Invest.* (2014) 124:687–95. doi: 10.1172/JCI67313
12. Shabason JE, Minn AJ. Radiation and immune checkpoint blockade: from bench to clinic. *Semin Radiat Oncol.* (2017) 27:289–98. doi: 10.1016/j.semradonc.2017.03.002
13. Peng J, Hamanishi J, Matsumura N, Abiko K, Murat K, Baba T, et al. Chemotherapy induces programmed cell death-ligand 1 overexpression via the nuclear factor-kappab to foster an immunosuppressive tumor microenvironment in ovarian cancer. *Cancer Res.* (2015) 75:5034–45. doi: 10.1158/0008-5472.CAN-14-3098
14. Baitsch L, Baumgaertner P, Devevre E, Raghav SK, Legat A, Barba L, et al. Exhaustion of tumor-specific CD8(+) T cells in metastases from melanoma patients. *J Clin Invest.* (2011) 121:2350–60. doi: 10.1172/JCI46102
15. Voron T, Colussi O, Marcheteau E, Pernot S, Nizard M, Pointet al, et al. VEGF-A modulates expression of inhibitory checkpoints on CD8+ T cells in tumors. *J Exp Med.* (2015) 212:139–48. doi: 10.1084/jem.20140559
16. Gavalas NG, Tsiatas M, Tsitsilonis O, Politi E, Ioannou K, Ziogas AC, et al. VEGF directly suppresses activation of T cells from ascites secondary to ovarian cancer via VEGF receptor type 2. *Br J Cancer* (2012) 107:1869–75. doi: 10.1038/bjc.2012.468
17. Latha TS, Panati K, Gowd DS, Reddy MC, Lomada D. Ovarian cancer biology and immunotherapy. *Int Rev Immunol.* (2014) 33:428–40. doi: 10.3109/08830185.2014.921161
18. Olm E, Fernandes AP, Hebert C, Rundlof AK, Larsen EH, Danielsson O, et al. Extracellular thiol-assisted selenium uptake dependent on the x(c)- cystine transporter explains the cancer-specific cytotoxicity of selenite. *Proc Natl Acad Sci USA.* (2009) 106:11400–5. doi: 10.1073/pnas.0902204106
19. Cacan E. Epigenetic-mediated immune suppression of positive co-stimulatory molecules in chemoresistant ovarian cancer cells. *Cell Biol Int.* (2017) 41:328–39. doi: 10.1002/cbin.10729
20. Hira-Miyazawa M, Nakamura H, Hirai M, Kobayashi Y, Kitahara H, Bou-Gharios G, et al. Regulation of programmed-death ligand in the human head and neck squamous cell carcinoma microenvironment is mediated through

matrix metalloproteinase-mediated proteolytic cleavage. *Int J Oncol* (2018) 52:379–88. doi: 10.3892/ijo.2017.4221

21. Bandura L, Drukala J, Wolnicka-Glubisz A, Björnstedt M, Korohoda W. Differential effects of selenite and selenate on human melanocytes, keratinocytes, and melanoma cells. *Biochem Cell Biol.* (2005) 83:196–211. doi: 10.1139/o04-130
22. Husbeck B, Nonn L, Peehl DM, Knox SJ. Tumor-selective killing by selenite in patient-matched pairs of normal and malignant prostate cells. *The Prostate* (2006) 66:218–25. doi: 10.1002/pros.20337
23. Kandaş NÖ, Randolph C, Bosland MC. Differential effects of selenium on benign and malignant prostate epithelial cells: stimulation of LNCaP cell growth by noncytotoxic, low selenite concentrations. *Nutr Cancer* (2009) 61:251–64. doi: 10.1080/01635580802398430
24. Olm E, Jönsson-Videsäter K, Ribera-Cortada I, Fernandes AP, Eriksson LC, Lehmann S, et al. Selenite is a potent cytotoxic agent for human primary AML cells. *Cancer Lett.* (2009) 282:116–23. doi: 10.1016/j.canlet.2009.03.010
25. Selenius M, Rundlof AK, Olm E, Fernandes AP, Bjornstedt M. Selenium and the selenoprotein thioredoxin reductase in the prevention, treatment and diagnostics of cancer. *Antioxid Redox Signal.* (2010) 12:867–80. doi: 10.1089/ars.2009.2884
26. Wang L, Bonorden MJ, Li GX, Lee HJ, Hu H, Zhang Y, et al. Methyl-selenium compounds inhibit prostate carcinogenesis in the transgenic adenocarcinoma of mouse prostate model with survival benefit. *Cancer Prev Res.* (2009) 2:484–95. doi: 10.1158/1940-6207.CAPR-08-0173
27. Tonelli C, Chio IIC, Tuveson DA. Transcriptional regulation by Nrf2. *Antioxid Redox Signal.* (2017) doi: 10.1089/ars.2017.7342
28. Khalkar P, Ali HA, Codo P, Argelich ND, Martikainen A, Arzenani MK, et al. Selenite and methylseleninic acid epigenetically affects distinct gene sets in myeloid leukemia: a genome wide epigenetic analysis. *Free Radical Biol Med.* (2018) 117:247–57. doi: 10.1016/j.freeradbiomed.2018.02.014
29. Jariwalla RJ, Gangapurkar B, Nakamura D. Differential sensitivity of various human tumour-derived cell types to apoptosis by organic derivatives of selenium. *Br J Nutr.* (2009) 101:182–9. doi: 10.1017/S0007114508998305
30. Zeng H, Briske-Anderson M, Idso JP, Hunt CD. The selenium metabolite methylselenol inhibits the migration and invasion potential of HT1080 tumor cells. *J Nutr.* (2006) 136:1528–32. doi: 10.1093/jn/136.6.1528
31. Wu X, Zhang Y, Pei Z, Chen S, Yang X, Chen Y, et al. Methylseleninic acid restricts tumor growth in nude mice model of metastatic breast cancer probably via inhibiting angiopoietin-2. *BMC Cancer* (2012) 12:192. doi: 10.1186/1471-2407-12-192
32. Sinha I, Null K, Wolter W, Suckow MA, King T, Pinto JT, et al. Methylseleninic acid downregulates hypoxia-inducible factor-1alpha in invasive prostate cancer. *Int J Cancer* (2012) 130:1430–9. doi: 10.1002/ijc.26141
33. Ferrara N, Kerbel RS. Angiogenesis as a therapeutic target. *Nature* (2005) 438:967–74. doi: 10.1038/nature04483
34. Spannuth WA, Nick AM, Jennings NB, Armaiz-Pena GN, Mangala LS, Danes CG, et al. Functional significance of VEGFR-2 on ovarian cancer cells. *Int J Cancer* (2009) 124:1045–53. doi: 10.1002/ijc.24028
35. Marigo I, Dolcetti L, Serafini P, Zanovello P, Bronte V. Tumor-induced tolerance and immune suppression by myeloid derived suppressor cells. *Immunol Rev.* (2008) 222:162–79. doi: 10.1111/j.1600-065X.2008.00602.x
36. Motz GT, Coukos G. The parallel lives of angiogenesis and immunosuppression: cancer and other tales. *Nat Rev Immunol.* (2011) 11:702–11. doi: 10.1038/nri3064
37. Lapeyre-Prost A, Terme M, Pernot S, Pointet al, Voron T, Tartour E, et al. Chapter Seven - Immunomodulatory Activity of VEGF in Cancer. *Int Rev Cell Mol Biol.* (2017) 330:295–342. doi: 10.1016/bs.ircmb.2016.09.007
38. Mulligan JK, Rosenzweig SA, Young MR. Tumor secretion of VEGF induces endothelial cells to suppress T cell functions through the production of PGE2. *J Immunother.* (2010) 33:126–35. doi: 10.1097/CJI.0b013e3181b91c9c
39. Shen W, Li HL, Liu L, Cheng JX. Expression levels of PTEN, HIF-1alpha, and VEGF as prognostic factors in ovarian cancer. *Eur Rev Med Pharmacol Sci.* (2017) 21:2596–603.
40. Caporarello N, Lupo G, Olivieri M, Cristaldi M, Cambria MT, Salmeri M, et al. Classical VEGF, Notch and Ang signalling in cancer angiogenesis, alternative approaches and future directions, (Review). *Mol Med Rep.* (2017) 16:4393–402. doi: 10.3892/mmr.2017.7179

Conflict of Interest Statement: The authors declare that the research was conducted in the absence of any commercial or financial relationships that could be construed as a potential conflict of interest.

Copyright © 2018 Nair, Rådestad, Khalkar, Diaz-Argelich, Schröder, Klynning, Ungerstedt, Uhlin and Fernandes. This is an open-access article distributed under the terms of the Creative Commons Attribution License (CC BY). The use, distribution or reproduction in other forums is permitted, provided the original author(s) and the copyright owner(s) are credited and that the original publication in this journal is cited, in accordance with accepted academic practice. No use, distribution or reproduction is permitted which does not comply with these terms.

Supplementary Material

Methylseleninic acid sensitizes ovarian cancer cells to T-cell mediated killing by decreasing PDL1 and VEGF levels

Deepika Nair*, Emelie Rådestad, Prajakta Khalkar, Nuria Diaz-Argelich, Axel Schröder, Charlotte Klynning, Johanna Ungerstedt, Michael Uhlin, Aristi P. Fernandes

Correspondence: Aristi Fernandes aristi.fernandes@ki.se.

1 Supplementary Data

Supplementary data includes one figure.

2 Supplementary Figures:

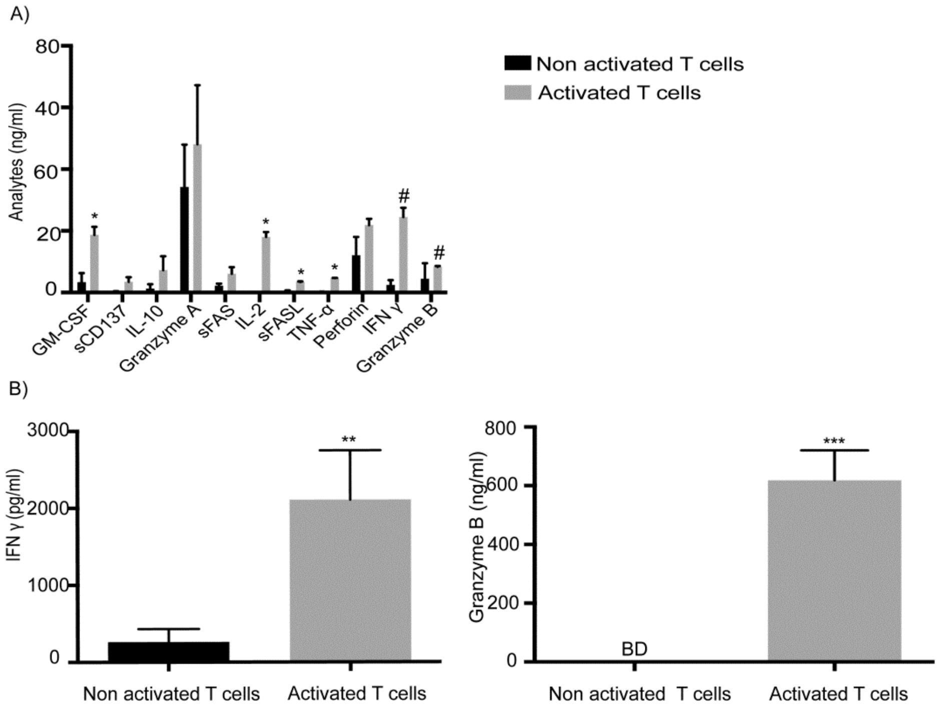

Supplementary Figure 1: Analysis of T cell activation

A) T cells were isolated and stimulated with anti-CD3/CD28 for 96h, and confirmation for activation of T cells was performed using Luminex assay. # represents the values that had to be extrapolated from the standard curve and BD represents values below detection levels. B) ELISA for IFN γ and Granzyme B. Columns represent mean analytes levels; bar indicates SD. (* $p \leq 0.05$, ** $p \leq 0.01$, *** $p \leq 0.001$)

DISCUSSION

DISCUSSION

Cancer is the second cause of death worldwide. Although early detection and treatment have improved, current chemotherapy is not entirely satisfactory due to side-effects and, occasionally, emerging resistances of cancer cells. Therefore, the development of new drugs is still an urgent need.

Se compounds, on the other hand, have gained substantial attention in the last decades due to their anticancerous properties. Although their biological activity depends greatly on the molecule, dose and system tested, Se compounds are highly versatile and affect several signaling pathways, thereby having a multi-targeting effect.

Notably, CH_3SeH is considered an essential Se metabolite in Se anticancer activity and has been extensively studied in the last decades.[147,154,181,182] Its chemical characteristics require *in situ* production or the use of precursors, which are considered the next-generation Se compounds.[127]

The primary aim of this work was the design, synthesis and biological evaluation of novel CH_3SeH precursors. Nevertheless, the research development required the synthesis of other selenoesters for Paper 2 and, besides, other selenium compounds were evaluated in Papers 3 and 4. To facilitate the reading, **Figure 17** summarizes all the compounds evaluated in this work and the paper wherein they are investigated. The references used in the discussion are depicted in bold.

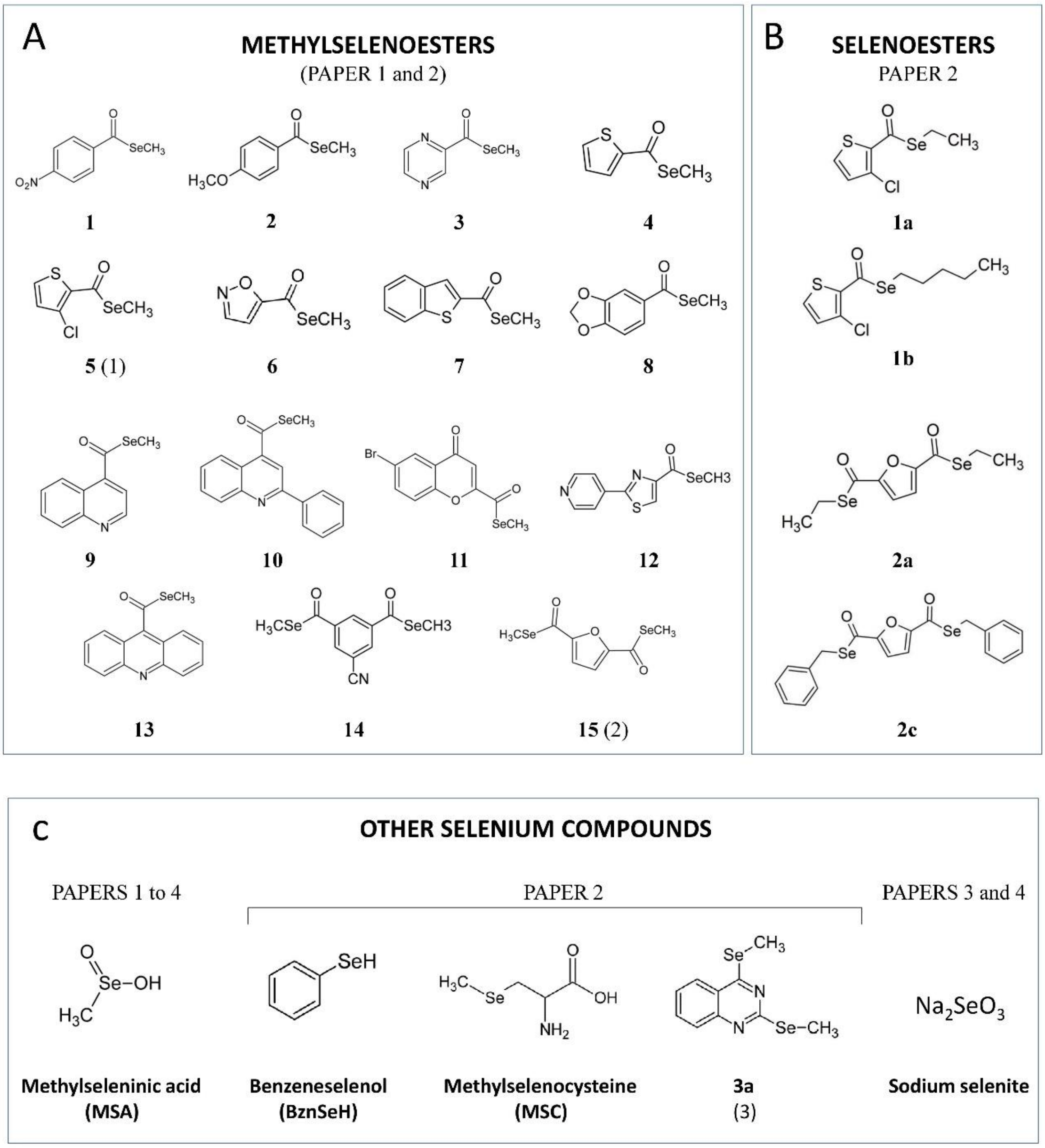
A
METHYLSELENOESTERS
(PAPER 1 and 2)
1
2
3
4
5 (1)
6
7
8
9
10
11
12
13
14
15 (2)
B
SELENOESTERS
PAPER 2
1a
1b
2a
2c
C
OTHER SELENIUM COMPOUNDS
PAPERS 1 to 4
PAPER 2
PAPERS 3 and 4
Na2SeO3
Methylseleninic acid (MSA)
Benzeneselenol (BznSeH)
Methylselenocysteine (MSC)
3a (3)
Sodium selenite

Figure 17. Summary of the studied compounds in this work. References depicted in bold are used in the discussion. **A**. Synthesized compounds for Papers 1 and 2. For compounds appearing in both papers, the reference used in Paper 2 is indicated in parentheses. **B**. Synthesized compounds for Paper 2. **C**. Studied compounds which were commercially available or synthesized in previous work (**3**/**3a**) from our group.[171] Compound **3** in Paper 2 is named **3a** in the discussion to distinguish it from compound **3** (pyrazine) in Paper 1.

An innovative series of methylselenoesters as CH_3SeH precursors was designed. The chemical characteristics of the carbonyl-selenium bond allow a nucleophilic attack that can render CH_3SeH. Different aromatic or heteroaromatic rings were selected with two main aims. First, to provide a synergic activity to CH_3SeH, according to a fragment-based design strategy. To this aim, we based our selection on previous studies from our group[170], supported by further extensive bibliographic research. Second, we hypothesized that the chemical variety provided by such different structures could modulate the lability of the carbonyl-selenium bond, therefore hindering or facilitating a nucleophilic attack, i.e., by water. Although water is a weak nucleophile, it is the primary component of the cell medium.

Fifteen new compounds were synthesized and structurally characterized through infrared spectroscopy, nuclear magnetic resonance (^{1}H-NMR and ^{13}C-NMR), mass spectrometry and/or HRMS. The chemical synthesis of the compounds was carried out in three or four steps and was time-efficient and economically affordable. Some of the compounds (**3**, **8**, **10** and **12**) were achieved with low yields (< 20%) due to a troublesome purification. Besides, the purity of all the compounds was assessed by thin-layer chromatography and elemental analysis.

We performed an *in silico* approach to evaluate the theoretical prediction of drug-likeness properties of the synthesized compounds. All the compounds fulfill Lipinski's Rule of Five, fit the range of $0 < \log P < 5$ and have good values of Polar Surface Area, predicting proper intestinal absorption. Concerning predicted toxicity, nine out of fifteen compounds are classified as non-toxic, although with low values. Importantly, thirteen out of fifteen compounds present better values than MSA, which is considered our reference compound. The general low values achieved might be due to the fact that Se is considered a hazardous compound by the program.

Selenium compounds can have a dual role both as antioxidants or pro-oxidants, depending on the dose, model, and cellular redox state. The antioxidant properties might be useful for cancer prevention, by abrogating oxidative damage in DNA and critical organelles, and therefore preventing cancer initiation. On the contrary, the pro-oxidant activity targets cancer cells which have increased oxidative stress *per se* and are less capable of dealing with small increases of ROS. In a preliminary characterization of the compounds, we evaluated their antioxidant activity. Except for compound **11**, none of the compounds can reduce the DPPH radical, ruling out their possible use as chemopreventive molecules. Interestingly, although compound **11** has antioxidant properties, it presented similar antiproliferative activity to the other compounds, as stated below.

We used the Ellman assay to verify our hypothesis of a differential CH_3SeH release among the compounds. Compounds **6** and **11** are fast releasers, being hydrolyzed within the first 2 h of incubation. CH_3SeH is released entirely from compound **3** at 24 h whereas a more sustained release corresponds, in this order, to compounds **15**, **1**, and **9**. In contrast, the remaining compounds are hardly hydrolyzed (< 15%) at 72 h, showing enhanced stability in these conditions.

From this experiment, it can be concluded that differences in CH_3SeH release correspond to different strengths of the carbonyl-selenium bond among the compounds, supporting our initial aim. However, it must be taken into account that the release rates in these conditions cannot be extrapolated to rates in the cell culture, due to multiple factors. For instance, hydrolysis is only one of the potential mechanisms for the production of CH_3SeH, besides others, and neither the pH or solvent components are the same. In addition to water, other nucleophiles might act. Cell uptake before hydrolysis and cell metabolism could also alter CH_3SeH release.

Our initial hypothesis suggested that the modulation of CH_3SeH release through hydrolysis could likewise regulate the biological activity. We tested the corresponding carboxylic acids in MCF7 and Panc-1 cells and found that were not toxic, indicating that the ultimate effector could be CH_3SeH. However, we cannot correlate differences in release with biological activity in the period studied (72 h).

All the compounds decrease cell proliferation. K562 is the most resistant line, where GI_{50} values greater than 10 μM were determined for all the compounds. By contrast, compounds **2**–**6**, **8**–**11** and **14** present GI_{50} values below 10 μM in PC-3, MCF7, HT-29, and HTB-54. However, considering the LC_{50} parameter, all the compounds exhibit similar moderate potencies. In fact, the compounds are more cytostatic than cytotoxic due to high LC_{50} values (>30 μM) in all cell lines.

We found that the inclusion of an electron-withdrawing substituent in the thiophene ring (compound **5**) improves the activity in MCF7 (LC_{50}= 89.6 μM, LC_{50} = 35.9 μM, respectively) and HT-29 (LC_{50} = 47.5 μM, LC_{50} = 8.9 μM, respectively) but not in PC-3 or HTB-54. The presence of two methylseleno moieties does not particularly enhance potency, as neither compound **14** nor **15** have significantly lower GI_{50}, TGI or LC_{50} values than the monofunctionalized molecules.

We also analyzed the selectivity of the compounds towards the nonmalignant human cell lines BEAS-2B (lung epithelial) and 184B5 (mammary epithelial). Unexpectedly, most of the compounds are not very selective, with similar toxicity in normal and cancer cells. MSA, the reference control, is also toxic but it has been extensively studied both *in vitro* and *in vivo*. Prompted by these data, we selected compounds **5** and **15** as promising candidates for further evaluation, due to their cytotoxic profile and similarity to MSA regarding selectivity.

As a first approach, we searched for potential enzymes that could metabolize these compounds. Metabolism is crucial for Se compounds, given that metabolites rather than original molecules are responsible for biological activity and redox-active enzymes have been reported to metabolize Se compounds. Consistently, we found that compounds **5** and **15**, along with MSA, are substrates for thioredoxin reductase but not for the glutathione-glutaredoxin system.

We also evaluated the modulation of cell cycle and cell death by these compounds through flow cytometry in the mammary carcinoma cell line MCF7. We found that both compounds induce a G_2-M arrest that is dose-dependent at 24 h. Cell death is dose-dependent for both compounds but time-dependent only for compound **15**. Besides, cell death is, at least partially, carried out by caspases, as concomitant treatment with z-vad-FMK partially prevented cell death.

Compounds **5** and **15** were also selected for further evaluation in Panc-1 cells. In these cells, we also used 3D cultures as an additional tool to assess their antiproliferative and/or cytotoxic properties. 3D cultures are thought to better resemble the *in vivo* characteristics of tumors than their 2D counterparts. They show a chemoresistant and matrix-rich phenotype, and differences in metabolism with respect to 2D cultures.[183] Most promising drugs that successfully pass high-throughput screenings, later fail *in vivo* or in clinical studies, a fact that argues for 3D cultures as a better tool to evaluate and discriminate between potential drugs.

MSA, compound **5** and **15** show IC_{50} values in the low micromolar range (< 4 μM) for 2D cultures. In accordance with previous reports, a higher dose was required to reduce cell proliferation in 3D cultures, indicating that cells growing in spheres are more resistant to chemotherapy than conventional 2D cultures. However, the compounds are still active and able to penetrate to the core of the spheroid and induce cell death, as demonstrated by PI staining.

Interestingly, MSA, compound **5** and **15** modify cell morphology and induce round, refringent floating cells, which are viable 24 h after treatment. Nevertheless, both the ability to re-adhere and the colony formation potential are significantly impaired after the treatment.

These results were in accordance with the results of the ChiP sequencing and gene ontology analyses exposed in Paper 3. In this study, we tested MSA and selenite in the leukemic cell line K562, wherein we explored Se-induced genome-wide epigenetic alterations. The ChiP sequencing revealed that both MSA and selenite induce histone modification but in a very different way. Further GO analysis uncovered that selenite induces significant enrichment of H3K9ac of genes within the GO terms for biological processes for oxygen response and hypoxia, whereas MSA is implicated in cell adhesion and glucocorticoid receptor binding. Selenite does not affect these genes, suggesting that adhesion disturbance might be a particular effect of MSA.

We found several dysregulated genes in K562 cells upon treatment with MSA. Amongst them, CD9, implicated in motility, adhesion and fertilization;

DAB2, which has a role in cell-cell and cell-fibrinogen contact, and cell proliferation, and has been described both as a tumor promoter and suppressor; and HIP1 and SDC1, which have been related to cancer progression. We focused on CD29 and verified through flow cytometry that the proteins levels are down-regulated after treatment with MSA. Besides, functional assays revealed that MSA-treated K562 cells show decreased attachment to fibronectin. The same results were obtained for primary AML cells obtained from patient samples.

In addition to K562 and the primary AML cells, MSA decreases CD29 in Panc-1 cells and profoundly impairs the reattachment abilities of the treated cells. This indicates that adhesion disturbance is a well-conserved effect not depending on cell type. Furthermore, CH_3SeH had previously been reported to decrease adhesiveness in melanoma[147]and prostate[148] cancers.

Congruently, we observed the same adhesion disturbance with the new methylselenoesters in Panc-1 cells. The fact that compounds **5** and **15** wholly detach the cells, behaving like MSA, suggests that CH_3SeH is the ultimate effector. To further verify if detachment properties are exclusive to CH_3SeH, we synthesized different analogs with selenoethyl (**1a**, **2a**), selenopentyl (**1b**) and selenobenzyl (**2c**) moieties. The same general synthetic procedure as with the methyl derivatives was followed for these compounds, but with the corresponding halides. All these molecules were conveniently characterized through ^1H and ^{13}C NMR, IR and HRMS.

In addition, we evaluated commercial BznSeH and MSC and a previously synthesized quinazoline bearing two methylseleno moieties (**3a**).[171] All the compounds can to reduce cell proliferation. However, a longer chain or the substitution with a benzyl residue impairs the cytostatic activity for the selenoesters. In general trends, and considering the 72-h time point, the potency to reduce proliferation decreases in the following order: methyl> ethyl> pentyl or benzyl. BznSeH and compound **3a** present the highest cytostatic potential, both of them inhibiting proliferation at 24 h of treatment. In terms of cytotoxicity, the same order is observed: methyl> ethyl> pentyl or benzyl. Compound **3a**, on the other hand, was the most potent compound, inducing cell death at 24 h treatment.

The methyl derivatives are more cytotoxic at 72 h than analogs with a longer alkyl chain or with the benzyl moiety. Almost all the compounds show similar activity at 24 and 48 h, with exception of compound **1b**, which is not cytotoxic. BznSeH, which is highly cytostatic, does not induce noteworthy cell death, with only 15% of dead cells at 72 h. MeSeCys, which has been reported to have similar activity to MSA in vivo, requires a considerably higher concentration to achieve similar cell death induction in vitro, due to the need for metabolic processing to release CH_3SeH, consistent with previous reports.

Significantly, results showed that additional methylated Se compounds (MSC and **3a**) completely detach cells from the culture plate. Nevertheless, we exclude that cell detachment is restricted to methylated forms of Se. The length of the alkyl chain decreases cell detachment, with the ethyl derivative **2a** detaching only 25% of cells. The ethyl and pentyl derivatives, **1a** and **1b** do not exhibit detaching abilities. The carboaromatic BznSeH has limited detaching potential (around 15%). On the contrary, the selenobenzyl derivative **2c** completely detaches all the cells. Importantly, consideration of the fact that not only methylseleno derivatives can induce cell detachment should be a critical milestone in further evaluation of organic Se compounds, as important mechanisms of action can be missed without considering the loss of attachment as a trigger.

Moreover, the fact that some Se compounds induce cell detachment without inducing cell death deserves further consideration. As evidenced by compound **2c**, it is clear that detachment *per se* does not trigger death signaling and it might be interesting to investigate the signaling pathways that the methyl and benzylseleno moieties are differentially able to activate.

Notably, the key finding of this work is that MSA and compounds **5** and **15**, after detachment, induce entosis. While down-regulation of CD29 and detachment from the culture plate are known effects of CH_3SeH[147,148], cell-in-cell formation has not been described for the time being for Se compounds. Therefore, this is a major contribution broadening the knowledge on the distinct mechanisms of action of Se compounds.

Cell-in-cell formation induced by these compounds is triggered upon cell detachment and was demonstrated by confocal microscopy and live time-lapse imaging. Detached cells show reduced expression of CD29 but increased levels of N-cadherin. Looking for upstream regulators, Cdc42 appeared as a compelling candidate to evaluate. It is a member of the Rho family of GTPases, which are highly implicated in entosis and has been reported to regulate CD29. In addition, Cdc42 also interacts with cadherins as it can down-regulate E-cadherin expression, targeting it for lysosomal degradation.[184] Besides, E-cadherin was shown to reduce Cdc42 and RhoA, another Rho-GTPase, activity in non-small cell lung cancer.[185]

We found decreased levels of Cdc42. Cdc42-depletion was reported to drive mitotic entosis whereas it did not have any effect on suspension cells.[186] However, its role in this particular setting is probably to allow cell-ECM detachment through CD29, and cadherin expression modification. Surprisingly, we did not find altered levels of RhoA, which has been described to mediate entosis.[31]

Entotic cell death usually depends on lysosomal degradation, although it can switch to apoptosis. Besides, in a floating population, different types of cell death can coexist.[187] We found slightly increased cleaved PARP levels but we ruled out caspase implications, as z-vad-fmk does not prevent cell death. Moreover, this pan-caspase inhibitor neither attenuates cell detachment, as previously reported in prostate cells.[148] In Paper 1, conversely, we found partial caspase implication. One limitation of this first paper is that we did not take cell detachment into account and only analyzed cell death, although the same phenotype of round, floating cells was observed. It could be interesting to study this in greater depth and verify if entosis has a role in treated MCF7. Further research could unveil why caspases are more implicated in MCF7 cell death and not in Panc-1 death.

PARP can be cleaved by other proteases such as calpains and cathepsins. As entosis relies on lysosomal degradation, we checked cathepsins B and D, which have been reported as playing a role in entosis.[31,188] Moreover, they have been described both as apoptotic response amplifiers[189] and bad prognosis factors.[190] As expected, MSA and compounds **5** and **15** upregulate cathepsin B (CatB), indicating lysosomal degradation, but surprisingly down-regulate cathepsin D(CatD) levels. In pancreatic cancer, increased levels of CatD have been reported to increase tumor dissemination and anchorage-independent proliferation. Thus, it is quite interesting that compounds inducing cell detachment concomitantly decrease CatD.

In Paper 4, the role of selenite and MSA on immune cells was evaluated. Immune cells were more resistant to these compounds than the ovarian cancer cells A2780 and the cisplatin-resistant CP70. For selenite, immune cell survival is mediated via overexpression of the Nrf2-regulated genes GCLM and HMOX. Oxidative stress induces Nrf2, which fosters the cell antioxidant defense. This is in accordance to results in Paper 2, where selenite was shown to regulate genes related to oxygen and oxidative stress. Moreover, MSA and selenite upregulate the lymphocyte activation marker HLA-DR in NK cells and CD8+ T cells isolated from ascites of ovarian cancer patients.

MSA and selenite decrease PDL1 expression. Moreover, MSA was found to upregulate MMP9, MMP13 and MMP19 and to down-regulate HIF-1α and VEGF in ovarian cancer cells. Through this mechanism, MSA sensitizes ovarian cancer cells to T cells; thus, MSA could be an interesting candidate for combinational treatments.

In summary, this work has led to the design, synthesis and biological evaluation of novel methylselenoesters with antiproliferative activity. Among them, compound **5** and **15,** along with MSA as a reference, present a novel mechanism of action: they induce entosis through down-regulation of Cdc42 and CD29 (therefore inducing cell detachment) and increase the expression of cadherins and cathepsin B.

To our knowledge, this is the first time that MSA and CH_3SeH precursors have been reported to induce cell-in-cell formation and lysosomal degradation. Although other Se derivatives can induce cell detachment, loss of adhesion signaling does not necessarily lead to cell death. Further research is needed to thoroughly dissect the complex properties of Se compounds to induce cell detachment and finally cell death, but the present results unveil an entirely new mechanism for these methylselenoesters and MSA.

Besides, this work has broadened the knowledge of selenite and MSA as epigenetic regulators targeting different gene sets and, particularly MSA, as modulators of the immune response to ovarian cancer cells.

CONCLUSIONS

CONCLUSIONS

This Ph.D. project leads to the following conclusions:

1. CH_3SeH release is differentially modulated through the organic fragments linked to the methylselenoester moiety. These substituents determine the lability of the carbonyl-selenium bound. Compounds **6** and **11** release CH_3SeH within the two first hours of incubation, whereas compound **3** is hydrolyzed entirely at 24 h. Compounds **15**, **1** and **9** have a more sustained release, and the remaining compounds are almost stable at 72 h.

2. The biological activity of the compounds does not correlate with the release of CH_3SeH in the Ellman's Assay at the studied time point. This fact is probably due to the different conditions of both experiments and the more complex biological matrix in the proliferation assays, where more processes occur apart from hydrolysis.

3. *In silico* approach to molecular descriptors indicated that all the compounds fulfill Lipinski's Rule of Five, fit the range of $0 < \log P < 5$ and have good values of Polar Surface Area, predicting proper intestinal absorption. Regarding predicted toxicity, nine out of fifteen compounds were classified as non-toxic, although with low values. This might be because the program considers Se as a hazardous element. Thirteen out of fifteen compounds presented better values than MSA, the reference compound.

4. All the synthesized compounds reduce cell proliferation, with compounds **2**–**6**, **8**–**11** and **14** presenting GI_{50} values below 10 μM in PC-3, MCF7, HT-29, and HTB-54. The bifunctionalized molecules **14** and **15** did not exhibit a better profile than the monofunctionalized compounds at the studied time point, probably due to enhanced resistance to hydrolysis of the second methylseleno group. All the compounds are more cytostatic than cytotoxic, due to their high LC_{50} values.

5. Compound **5** and **15** are substrates for TrxR but not for the glutathione-glutaredoxin system. Both of them induce G_2-M blockage of the cell cycle in the mammary MCF7 cell line in a dose- and time-dependent way. Ultimately, they induce partially caspase-dependent cell death, which is dose-dependent for both compounds and only time-dependent for compound **15**.

6. Only compound **11** has antioxidant properties and is capable of reducing the DPPH and ABTS radicals. Whereas at high concentrations, it exhibits the same efficacy as ascorbic acid, this does not happen at low concentrations.

7. MSA, compound **5** and **15** penetrate into the core of Panc-1 3D spheroids, reduce cell proliferation and induce cell death at higher concentrations than in traditional 2D cultures. These data suggest that 3D cultures are a better way to evaluate drugs due to significant resemblance to *in vivo* tumors.

8. MSA, compound **5** and **15** profoundly induce adhesive disturbance in Panc-1 cells, affecting both cell-ECM and cell-cell adhesion and changing cell morphology to a round, refringent phenotype. These compounds completely detach the cells, which remain viable at 24 h, although their ability to reattach is severely compromised, as well as the colony formation capacity.

9. MSA, compound **5** and **15** induce entosis after downregulating Cdc42 and its effector CD29, leading to temporary anchorage-independent conditions of Panc-1 cells. The increase in N-cadherin enables the formation of *adherens junctions* and ultimately, the invasion of the target cell and its degradation in the host cell. This degradation is lysosomal-driven by cathepsin B and occurs with a slight increase of cleaved PARP and concomitant downregulation of cathepsin D. Importantly, this is the first time that methylseleno derivatives are reported to induce entosis triggered after the loss of matrix adhesion signaling.

10. The ability to induce cell detachment is not restricted to methylated forms of selenium. Whereas detachment potential decreases both with the length of the alkyl chain and with aromatic selenols (as evidenced by benzeneselenol), the replacement of the methyl with a benzyl moiety does not affect the detachment abilities.

11. Importantly, the detachment potential does not correlate with the cytotoxicity of the compounds, as evidenced by compound **2c**. In general trends, cytotoxicity and the antiproliferative potential decrease in the following order: methyl > ethyl > pentyl or benzyl.

12. MSA and selenite distinctly affect histone modification. Selenite is implicated in genes related to oxygen and hypoxia responses whereas MSA modifies the expression of adhesion and migration-related genes. In particular, MSA down-regulates the expression of CD29, leading to decreased attachment to fibronectin both in K562 and primary AML cells.

13. MSA and selenite are not toxic to immune cells at toxic concentrations for ovarian cancer cells. Moreover, they increase NK cell-mediated lysis and enhance the cytolytic activity of T cells. MSA decreases HIF-1α and upregulates MMP9, MMP13 and MMP19, and enhances T cell function by decreasing PDL1 and VEGF expression on ovarian cancer cells, being therefore a compelling candidate for combination therapies.

14. CH_3SeH release is a useful strategy in different fields of cancer research.

REFERENCES

REFERENCES

1. Bray, F., Ferlay, J. & Soerjomataram, I. Global Cancer Statistics 2018 : GLOBOCAN Estimates of Incidence and Mortality Worldwide for 36 Cancers in 185 Countries. *CA Cancer J Clin* **00,** 1–31 (2018).
2. *World Cancer Report 2014*. International Agency for Research in Cancer, 2014.
3. www.who.int/cancer/en. Available at: www.who.int/cancer/en. (Accessed:: 15 September 2018)
4. *Las Cifras del Cáncer en España 2018*. Sociedad Española de Oncología Médica, 2018.
5. Hanahan, D. & Weinberg, R. A. Hallmarks of cancer: The next generation. *Cell* **144,** 646–674 (2011).
6. Pietras, K. & Östman, A. Hallmarks of cancer: Interactions with the tumor stroma. *Exp. Cell Res.* **316,** 1324–1331 (2010).
7. Sun, Y. Tumor microenvironment and cancer therapy resistance. *Cancer Lett.* **380,** 205–215 (2016).
8. Williams, G. H. & Stoeber, K. The cell cycle and cancer. *J. Pathol.* **226,** 352–364 (2012).
9. Asghar, U., Witkiewicz, A. K., Turner, N. C. & Knudsen, E. S. The history and future of targeting cyclin-dependent kinases in cancer therapy. *Nat. Rev. Drug Discov.* **14,** 130–146 (2015).
10. Gulei, D. *et al.* The 'good-cop bad-cop' TGF-beta role in breast cancer modulated by non-coding RNAs. *Biochim. Biophys. Acta - Gen. Subj.* **1861,** 1661–1675 (2017).
11. Seoane, J. & Gomis, R. R. TGF-ß Family Signaling in Tumor Suppression and Cancer Progression. *Cold Spring Harb. Perspect. Biol.* a022277 (2017).
12. Shay, J. W. Role of Telomeres and Telomerase in Aging and Cancer. *Cancer Discov.* **6,** (2016).
13. Jafri, M. A., Ansari, S. A., Alqahtani, M. H. & Shay, J. W. Roles of telomeres and telomerase in cancer, and advances in telomerase-targeted therapies. *Genome Med.* **8,** 69 (2016).
14. Low, K. C. & Tergaonkar, V. Telomerase: Central regulator of all of the hallmarks of cancer. *Trends Biochem. Sci.* **38,** 426–434 (2013).
15. Ronca, R., Benkheil, M., Mitola, S., Struyf, S. & Liekens, S. Tumor angiogenesis revisited: Regulators and clinical implications. *Med. Res. Rev.* 1–44 (2017).
16. Labernadie, A. *et al.* A mechanically active heterotypic E-cadherin/N-

cadherin adhesion enables fibroblasts to drive cancer cell invasion. *Nat. Cell Biol.* **19,** 224–237 (2017).

17. Liao, T.-T. & Yang, M.-H. Revisiting epithelial-mesenchymal transition in cancer metastasis: the connection between epithelial plasticity and stemness. *Mol. Oncol.* **2,** 1–13 (2017).

18. Racané, L. *et al.* Novel 2-Thienyl- and 2-Benzothienyl-Substituted 6-(2-Imidazolinyl)Benzothiazoles: Synthesis; in vitro Evaluation of Antitumor Effects and Assessment of Mitochondrial Toxicity. *Anticancer. Agents Med. Chem.* **17 (1),** 57–66 (2017).

19. Muenst, S. *et al.* The immune system and cancer evasion strategies: therapeutic concepts. *J. Intern. Med.* **279,** 541–562 (2016).

20. Galluzzi, L. *et al.* Molecular definitions of cell death subroutines: recommendations of the Nomenclature Committee on Cell Death 2012. *Cell Death Differ.* **19,** 107–120 (2011).

21. Fuchs, Y. & Steller, H. Live to die another way: modes of programmed cell death and the signals emanating from dying cells. *Nat. Publ. Gr.* **16,** (2015).

22. Ichim, G. & G Tait, S. W. A fate worse than death: apoptosis as an oncogenic process. *Nat. Publ. Gr.* **16,** (2016).

23. Galluzzi, L. *et al.* Essential versus accessory aspects of cell death: recommendations of the NCCD 2015. *Cell Death Differ.* 1–16 (2014).

24. Taatjes, D. J., Sobel, B. E. & Budd, R. C. Morphological and cytochemical determination of cell death by apoptosis. *Histochem. Cell Biol.* **129,** 33–43 (2008).

25. Kroemer, G. & Levine, B. Autophagic cell death: the story of a misnomer. *Nat. Rev. Mol. Cell Biol.* (2008). doi:10.1038/nrm2529

26. Kroemer, G. *et al.* Classification of cell death: recommendations of the Nomenclature Committee on Cell Death 2009. *Cell Death Differ* **16,** 3–11 (2009).

27. Yao, D. *et al.* Deconvoluting the relationships between autophagy and metastasis for potential cancer therapy. *Apoptosis* **21,** 683–698 (2016).

28. Fung, C. *et al.* Induction of autophagy during extracellular matrix detachment promotes cell survival. *Mol. Biol. Cell* **19,** 797–806 (2008).

29. Anding, A. L. & Baehrecke, E. H. Autophagy in Cell Life and Cell Death. *Curr Top Dev Biol.* **114,** 67–91 (2015).

30. Kaur, J. & Debnath, J. Autophagy at the crossroads of catabolism and anabolism. *Nat. Rev. Mol. Cell Biol.* **16,** 461–472 (2015).

31. Overholtzer, M. *et al.* A Nonapoptotic Cell Death Process, Entosis, that Occurs by Cell-in-Cell Invasion. *Cell* **131,** 966–979 (2007).

32. Cano, C. E. *et al.* Homotypic cell cannibalism, a cell-death process regulated by the nuclear protein 1, opposes to metastasis in pancreatic cancer. *EMBO Mol. Med.* **4,** 964–979 (2012).

33. Schwegler, M. *et al.* Prognostic Value of Homotypic Cell Internalization by Nonprofessional Phagocytic Cancer Cells. *Biomed Res. Int.* **2015,** (2015).

34. Krishna, S. & Overholtzer, M. Mechanisms and consequences of entosis. *Cell. Mol. Life Sci.* **73,** 2379–2386 (2016).

35. Hamann, J. C. & Overholtzer, M. Entosis enables a population response to starvation. *Oncotarget* **8,** 57934–57935 (2017).

36. Florey, O., Kim, S. E., Sandoval, C. P., Haynes, C. M. & Overholtzer, M. Autophagy machinery mediates macroendocytic processing and entotic cell death by targeting single membranes. *Nat. Cell Biol.* **13,** 1335–1343 (2011).

37. Wan, Q. *et al.* Regulation of myosin activation during cell-cell contact formation by Par3-Lgl antagonism: entosis without matrix detachment. *Mol. Biol. Cell* **23,** 2076–2091 (2012).

38. Vitale, I., Galluzzi, L., Castedo, M. & Kroemer, G. Mitotic catastrophe: a mechanism for avoiding genomic instability. *Nat. Rev. Mol. Cell Biol.* **12,** 385–392 (2011).

39. Denisenko, T. V., Sorokina, I. V., Gogvadze, V. & Zhivotovsky, B. Mitotic catastrophe and cancer drug resistance: A link that must to be broken. *Drug Resist. Updat.* **24,** 1–12 (2016).

40. Seguin, L., Desgrosellier, J. S., Weis, S. M. & Cheresh, D. A. Integrins and cancer: Regulators of cancer stemness, metastasis, and drug resistance. *Trends Cell Biol.* **25,** 234–240 (2015).

41. Zhong, X. & Rescorla, F. J. Cell surface adhesion molecules and adhesion-initiated signaling: Understanding of anoikis resistance mechanisms and therapeutic opportunities. *Cell. Signal.* **24,** 393–401 (2012).

42. Naci, D., Vuori, K. & Aoudjit, F. Alpha2beta1 integrin in cancer development and chemoresistance. *Semin. Cancer Biol.* **35,** 145–153 (2015).

43. Zhong, X. & Rescorla, F. J. Cell surface adhesion molecules and adhesion-initiated signaling : Understanding of anoikis resistance mechanisms and therapeutic opportunities. *Cell. Signal.* **24,** 393–401 (2012).

44. Desgrosellier, J. S. & Cheresh, D. Integrins in cancer: biological implications and therapeutic opportunities. *Nat. Rev. Cancer* **10,** 9–22 (2010).

45. Guadamillas, M. C., Cerezo, A. & del Pozo, M. A. Overcoming anoikis - pathways to anchorage-independent growth in cancer. *J. Cell Sci.* **124,** 3189–3197 (2011).

46. Schooley, A. M., Andrews, N. M., Zhao, H. & Addison, C. L. beta1 integrin is required for anchorage-independent growth and invasion of tumor cells in a context dependent manner. *Cancer Lett.* **316,** 157–167 (2012).

47. Cagnet, S. *et al.* Signaling events mediated by α3β1 integrin are essential for mammary tumorigenesis. *Oncogene* **33,** 4286–4295 (2014).

48. Huang, C. *et al.* B1 Integrin Mediates an Alternative Survival Pathway in Breast Cancer Cells Resistant To Lapatinib. *Breast Cancer Res.* **13,** R84 (2011).

49. Lovitt, C. J., Shelper, T. B. & Avery, V. M. Doxorubicin resistance in breast cancer cells is mediated by extracellular matrix proteins. *BMC Cancer* **18,** 41 (2018).

50. Kanda, R. *et al.* Erlotinib resistance in lung cancer cells mediated by integrin β1/Src/Akt-driven bypass signaling. *Cancer Res.* **73,** 6243–6253 (2013).

51. Fukata, M. & Kaibuchi, K. Rho-family GTPases in cadherin-mediated cell — cell adhesion. *Nat. Rev. Mol. Cell Biol.* **2,** 887–897 (2001).

52. Leckband, D. E. & De Rooij, J. Cadherin Adhesion and Mechanotransduction. *Annu. Rev. Cell Dev. Biol* **30,** 291–315 (2014).

53. Igarashi, T., Araki, K., Yokobori, T. & Altan, B. Association of RAB5 overexpression in pancreatic cancer with cancer progression and poor prognosis via E-cadherin suppression. **8,** 12290–12300 (2017).

54. Gan, W.-J. *et al.* RAR?-induced E-cadherin downregulation promotes hepatocellular carcinoma invasion and metastasis. *J. Exp. Clin. Cancer Res.* **35,** 164 (2016).

55. Zhou, Z. *et al.* Loss of TET1 facilitates DLD1 colon cancer cell migration via H3K27me3-mediated down-regulation of E-cadherin. *J. Cell. Physiol.* 1–11 (2017). doi:10.1002/jcp.26012

56. Canel, M., Serrels, A., Frame, M. C. & Brunton, V. G. E-cadherin – integrin crosstalk in cancer invasion and metastasis. (2013). doi:10.1242/jcs.100115

57. Rodriguez, F. J., Lewis-Tuffin, L. J. & Anastasiadis, P. Z. E-cadherin's dark side: possible role in tumor progression. *Biochim. Biophys. Acta* **1826,** 23–31 (2012).

58. Hu, Q. P., Kuang, J. Y., Yang, Q. K., Bian, X. W. & Yu, S. C. Beyond a tumor suppressor: Soluble E-cadherin promotes the progression of

cancer. *Int. J. Cancer* **138,** 2804–2812 (2016).

59. Roy, F. Van. Beyond E-cadherin: roles of other cadherin superfamily members in cancer. *Nat. Publ. Gr.* **14,** 121–134 (2014).

60. Straub, B. K. *et al.* E-N-cadherin heterodimers define novel adherens junctions connecting endoderm-derived cells. *J. Cell Biol.* **195,** 873–887 (2011).

61. Tanaka, H. *et al.* Monoclonal antibody targeting of N-cadherin inhibits prostate cancer growth, metastasis and castration resistance. *Nat. Med.* **16,** 1414–1420 (2010).

62. Mrozik, K. M. *et al.* Therapeutic targeting of N-cadherin is an effective treatment for multiple myeloma. *Br. J. Haematol.* **171,** 387–399 (2015).

63. Monaghan-Benson, E. & Burridge, K. Mutant B-RAF regulates a Rac-dependent cadherin switch in melanoma. *Oncogene* **32,** 4836–4844 (2013).

64. Klymenko, Y. *et al.* Cadherin composition and multicellular aggregate invasion in organotypic models of epithelial ovarian cancer intraperitoneal metastasis. *Oncogene* 1–12 (2017).

65. Zhan, D. Q. *et al.* Reduced N-cadherin expression is associated with metastatic potential and poor surgical outcomes of hepatocellular carcinoma. *J. Gastroenterol. Hepatol.* **27,** 173–180 (2012).

66. Lammens, T. *et al.* N-cadherin in neuroblastoma disease: expression and clinical significance. *PLoS One* **7,** e31206 (2012).

67. Su, Y., Li, J., Shi, C., Hruban, R. H. & Radice, G. L. N-cadherin functions as a growth suppressor in a model of K-ras-induced PanIN. *Oncogene* **35,** 3335–3341 (2016).

68. Su, Y. *et al.* N-cadherin haploinsufficiency increases survival in a mouse model of pancreatic cancer. *Oncogene* **31,** 4484–4489 (2012).

69. Cavallaro, U. & Christofori, G. Cell adhesion and signalling by cadherins and Ig-CAMs in cancer. *Nat. Rev. Cancer* **4,** 118–132 (2004).

70. McCormack, J., Welsh, N. J. & Braga, V. M. M. Cycling around cell–cell adhesion with Rho GTPase regulators. *J. Cell Sci.* **126,** (2013).

71. Mui, K. L., Chen, C. S. & Assoian, R. K. The mechanical regulation of integrin-cadherin crosstalk organizes cells, signaling and forces. *J. Cell Sci.* **129,** 1093–1100 (2016).

72. Collins, C. & Nelson, W. J. Running with neighbors : coordinating cell migration and cell – cell adhesion. *Curr. Opin. Cell Biol.* **36,** 62–70 (2015).

73. https://www.cancer.org/treatment/treatments-and-side-effects.html. Available at: https://www.cancer.org/treatment/treatments-and-side-

effects.html. (Accessed: 18 January 2018)

74. Puyo, S., Montaudon, D. & Pourquier, P. From old alkylating agents to new minor groove binders. *Crit. Rev. Oncol. Hematol.* **89,** 43–61 (2014).

75. https://www.cancer.org/treatment/treatments-and-side-effects/treatment-types/immunotherapy/what-is-immunotherapy.html. Available at: https://www.cancer.org/treatment/treatments-and-side-effects/treatment-types/immunotherapy/what-is-immunotherapy.html. (Accessed: 17 January 2018)

76. Weekley, C. M. & Harris, H. H. Which form is that? The importance of selenium speciation and metabolism in the prevention and treatment of disease. *Chem. Soc. Rev.* **42,** 8870–8894 (2013).

77. Vinceti, M. *et al.* The epidemiology of selenium and human cancer. Selenium: Its Molecular Biology and Role in Human Health, Fourth Edition **136,** (Elsevier Inc., 2016).

78. Bartolini, D. *et al.* Selenocompounds in Cancer Therapy: An Overview. **136,** 259–302 (2017).

79. Labunskyy, V. M., Hatfield, D. L. & Gladyshev, V. N. Selenoproteins: Molecular Pathways and Physiological Roles. *Physiol. Rev.* **94,** (2014).

80. Benstoem, C. *et al.* Selenium and its supplementation in cardiovascular disease—what do we know? *Nutrients* **7,** 3094–3118 (2015).

81. Rayman, M. P. Selenium and human health. *Lancet* **379,** 1256–1268 (2012).

82. Loscalzo, J. Keshan Disease, Selenium Deficiency, and the Selenoproteome. *N. Engl. J. Med.* **370,** 1756–1760 (2014).

83. Wang, X., Ning, Y., Yang, L., Yu, F. & Guo, X. Zinc: the Other Suspected Environmental Factor in Kashin-Beck Disease in Addition to Selenium. *Biol. Trace Elem. Res.* (2017).

84. Schomburg, L. Selenium, selenoproteins and the thyroid gland: interactions in health and disease. *Nat. Publ. Gr.* **8,** (2011).

85. Mistry, H. D., Broughton Pipkin, F., Redman, C. W. G. & Poston, L. Selenium in reproductive health. *Am. J. Obstet. Gynecol.* **206,** 21–30 (2012).

86. Steinbrenner, H., Al-Quraishy, S., Dkhil, M. A., Wunderlich, F. & Sies, H. Dietary selenium in adjuvant therapy of viral and bacterial infections. *Adv. Nutr.* **6,** 73–82 (2015).

87. Steinbrenner, H. & Sies, H. Selenium homeostasis and antioxidant selenoproteins in brain: Implications for disorders in the central nervous system. *Archives of Biochemistry and Biophysics* **536,** 152–157 (2013).

88. de Wilde, M. C., Vellas, B., Girault, E., Yavuz, A. C. & Sijben, J. W. Lower

brain and blood nutrient status in Alzheimer's disease: Results from meta-analyses. *Alzheimer's Dement. Transl. Res. Clin. Interv.* **3,** 416–431 (2017).

89. Kudin, A. P. *et al.* Homozygous mutation in TXNRD1 is associated with genetic generalized epilepsy. *Free Radic. Biol. Med.* **106,** 270–277 (2017).
90. Pillai, R., Uyehara-Lock, J. H. & Bellinger, F. P. Selenium and selenoprotein function in brain disorders. *IUBMB Life* **66,** 229–239 (2014).
91. Zhang, Z.-H. *et al.* Selenomethionine Mitigates Cognitive Decline by Targeting Both Tau Hyperphosphorylation and Autophagic Clearance in an Alzheimer's Disease Mouse Model. *J. Neurosci.* **37,** 2449–2462 (2017).
92. Song, G. *et al.* Selenomethionine ameliorates cognitive decline, reduces tau hyperphosphorylation, and reverses synaptic deficit in the triple transgenic mouse model of alzheimer's disease. *J. Alzheimer's Dis.* **41,** 85–99 (2014).
93. Xie, Y., Tan, Y., Zheng, Y., Du, X. & Liu, Q. Ebselen ameliorates β-amyloid pathology, tau pathology, and cognitive impairment in triple-transgenic Alzheimer's disease mice. *J. Biol. Inorg. Chem.* **22,** 851–865 (2017).
94. Jin, N. *et al.* Sodium selenate activated Wnt/β-catenin signaling and repressed amyloid-β formation in a triple transgenic mouse model of Alzheimer's disease. *Exp. Neurol.* **297,** 36–49 (2017).
95. Liu, S. J. *et al.* Sodium selenate retards epileptogenesis in acquired epilepsy models reversing changes in protein phosphatase 2A and hyperphosphorylated tau. *Brain* **139,** 1919–1938 (2016).
96. Sampaio, T. B., Pinton, S., da Rocha, J. T., Gai, B. M. & Nogueira, C. W. Involvement of BDNF/TrkB signaling in the effect of diphenyl diselenide on motor function in a Parkinson's disease rat model. *Eur. J. Pharmacol.* **795,** 28–35 (2017).
97. Yu, S. Y. *et al.* A preliminary report on the intervention trials of primary liver cancer in high-risk populations with nutritional supplementation of selenium in China. *Biol. Trace Elem. Res.* **29,** 289–94 (1991).
98. Yu, S. Y., Zhu, Y. J. & Li, W. G. Protective role of selenium against hepatitis B virus and primary liver cancer in Qidong. *Biol. Trace Elem. Res.* **56,** 117–24 (1997).
99. Clark, L. C. *et al.* Effects of selenium supplementation for cancer prevention in patients with carcinoma of the skin. A randomized controlled trial. Nutritional Prevention of Cancer Study Group. *JAMA* **276,** 1957–63 (1996).
100. Combs, G. F., Clark, L. C. & Turnbull, B. W. Reduction of cancer risk with

an oral supplement of selenium. *Biomed. Environ. Sci.* **10,** 227–34 (1997).

101. Clark, L. C. *et al.* Decreased incidence of prostate cancer with selenium supplementation: results of a double-blind cancer prevention trial. *Br. J. Urol.* **81,** 730–4 (1998).

102. Duffield-Lillico, A. J. *et al.* Baseline characteristics and the effect of selenium supplementation on cancer incidence in a randomized clinical trial: a summary report of the Nutritional Prevention of Cancer Trial. *Cancer Epidemiol. Biomarkers Prev.* **11,** 630–9 (2002).

103. Duffield-Lillico, A. J. *et al.* Selenium supplementation, baseline plasma selenium status and incidence of prostate cancer: an analysis of the complete treatment period of the Nutritional Prevention of Cancer Trial. *BJU Int.* **91,** 608–12 (2003).

104. Lippman, S. M. *et al.* Designing the Selenium and Vitamin E Cancer Prevention Trial (SELECT). *JNCI J. Natl. Cancer Inst.* **97,** 94–102 (2005).

105. Lippman, S. M. *et al.* Effect of Selenium and Vitamin E on Risk of Prostate Cancer and Other Cancers. *JAMA* **301,** 39 (2009).

106. Fernandes, A. P. & Gandin, V. Selenium compounds as therapeutic agents in cancer. *Biochim. Biophys. Acta - Gen. Subj.* **1850,** 1642–1660 (2015).

107. Misra, S., Boylan, M., Selvam, A., Spallholz, J. E. & Björnstedt, M. Redox-active selenium compounds—from toxicity and cell death to cancer treatment. *Nutrients* **7,** 3536–3556 (2015).

108. Ganyc, D. & Self, W. T. High affinity selenium uptake in a keratinocyte model. *FEBS Lett.* **582,** 299–304 (2008).

109. Olm, E. *et al.* Extracellular thiol-assisted selenium uptake dependent on the xc- cystine transporter explains the cancer-specific cytotoxicity of selenite. *Proc. Natl. Acad. Sci.* **106,** 11400–11405 (2009).

110. McDermott, J. R. *et al.* Zinc- and bicarbonate-dependent ZIP8 transporter mediates selenite uptake. *Oncotarget* **7,** 35327–35340 (2016).

111. Marciel, M. P. & Hoffmann, P. R. *Selenoproteins and Metastasis*. *Advances in Cancer Research* **136,** (Elsevier Inc., 2017).

112. Ip, C. & Ganther, H. E. Activity of Methylated Forms of Selenium in Cancer Prevention. *Cancer Res.* **50,** 1206–1211 (1990).

113. Ip, C., Hayes, C. & Marie Budnick, R. Chemical Form of Selenium, Critical Metabolites, and Cancer Prevention. *Cancer Res.* **51,** 595–600 (1991).

114. Ip, C., Thompson, H. J., Zhu, Z. & Ganther, H. E. In vitro and in vivo studies of methylseleninic acid: Evidence that a monomethylated selenium metabolite is critical for cancer chemoprevention. *Cancer Res.* **60,** 2882–2886 (2000).

115. Ip, C. Lessons from basic research in selenium and cancer prevention. *J. Nutr.* **128,** 1845–54 (1998).

116. Short, S. P. & Williams, C. S. Selenoproteins in Tumorigenesis and Cancer Progression. Advances in Cancer Research **136,** (Elsevier Inc., 2017).

117. Arnér, E. S. J. Targeting the Selenoprotein Thioredoxin Reductase 1 for Anticancer Therapy. *Adv. Cancer Res.* **136,** 139–151 (2017).

118. Lu, Y. P. *et al.* Enhanced skin carcinogenesis in transgenic mice with high expression of glutathione peroxidase or both glutathione peroxidase and superoxide dismutase. *Cancer Res.* **57,** 1468–74 (1997).

119. Kipp, A. P. *Selenium-Dependent Glutathione Peroxidases During Tumor Development*. *Advances in Cancer Research* **136,** (Elsevier Inc., 2017).

120. Barrett, C. W. *et al.* Tumor suppressor function of the plasma glutathione peroxidase Gpx3 in colitis-associated carcinoma. *Cancer Res.* **73,** 1245–1255 (2013).

121. Varlamova, E. G. & Cheremushkina, I. V. Contribution of mammalian selenocysteine-containing proteins to carcinogenesis. *Journal of Trace Elements in Medicine and Biology* **39,** 76–85 (2017).

122. Azad, G. K. & Tomar, R. S. Ebselen, a promising antioxidant drug: Mechanisms of action and targets of biological pathways. *Molecular Biology Reports* **41,** 4865–4879 (2014).

123. Yamaguchi, T. *et al.* Ebselen in acute ischemic stroke: a placebo-controlled, double-blind clinical trial. Ebselen Study Group. *Stroke* **29,** 12–7 (1998).

124. Kil, J. *et al.* Safety and efficacy of ebselen for the prevention of noise-induced hearing loss: a randomised, double-blind, placebo-controlled, phase 2 trial. *Lancet* **390,** 969–979 (2017).

125. Brodin, O. *et al.* Pharmacokinetics and toxicity of sodium selenite in the treatment of patients with carcinoma in a phase I clinical trial: The SECAR study. *Nutrients* **7,** 4978–4994 (2015).

126. https://clinicaltrials.gov/ct2/show/NCT02166242.

127. Lü, J. *et al.* Cancer chemoprevention research with selenium in the post-SELECT era: Promises and challenges. *Nutr. Cancer* **68,** 1–17 (2016).

128. Liu, Y. *et al.* Methylselenocysteine preventing castration-resistant progression of prostate cancer. *Prostate* **75,** 1001–1008 (2015).

129. Cao, S., Durrani, F. A., Tóth, K. & Rustum, Y. M. Se-methylselenocysteine offers selective protection against toxicity and potentiates the antitumour activity of anticancer drugs in preclinical animal models. *Br. J. Cancer* **110,** 1733–1743 (2014).

130. Wang, L. *et al.* Methylseleninic acid superactivates p53-senescence cancer progression barrier in prostate lesions of pten-knockout mouse. *Cancer Prev. Res.* **9,** 35–42 (2016).

131. Park, J.-M., Kim, D.-H., Na, H.-K. & Surh, Y.-J. Methylseleninic acid induces NAD(P)H:quinone oxidoreductase-1 expression through activation of NF-E2-related factor 2 in Chang liver cells. *Oncotarget* (2016). doi:10.18632/oncotarget.10289

132. Tarrado-Castellarnau, M. *et al.* Methylseleninic acid promotes antitumour effects via nuclear FOXO3a translocation through Akt inhibition. *Pharmacol. Res.* **102,** 218–234 (2015).

133. Wang, L. *et al.* Methylseleninic Acid Suppresses Pancreatic Cancer Growth Involving Multiple Pathways. *Nutr. Cancer* **66,** 295–307 (2014).

134. Lu, Z. *et al.* Se-methylselenocysteine suppresses the growth of prostate cancer cell DU145 through connexin 43-induced apoptosis. *J. Cancer Res. Ther.* **11,** 840 (2015).

135. Zeng, H., Cheng, W. H. & Johnson, L. K. Methylselenol, a selenium metabolite, modulates p53 pathway and inhibits the growth of colon cancer xenografts in Balb/c mice. *J. Nutr. Biochem.* **24,** 776–780 (2013).

136. Wu, X. *et al.* Methylseleninic acid restricts tumor growth in nude mice model of metastatic breast cancer probably via inhibiting angiopoietin-2. *BMC Cancer* **12,** 192–200 (2012).

137. Jiang, W. *et al.* In vivo molecular mediators of cancer growth suppression and apoptosis by selenium in mammary and prostate models: lack of involvement of gadd genes. *Mol. Cancer Ther.* **8,** 682–691 (2009).

138. Zeng, H., Wu, M. & Botnen, J. H. Methylselenol, a selenium metabolite, induces cell cycle arrest in G1 phase and apoptosis via the extracellular-regulated kinase 1/2 pathway and other cancer signaling genes. *J. Nutr.* **139,** 1613–1618 (2009).

139. Zhu, Z., Jiang, W., Ganther, H. E. & Thompson, H. J. Mechanisms of Cell Cycle Arrest by Methylseleninic Acid. *Cancer Res* **62,** 156–164 (2002).

140. Yin, S. *et al.* Methylseleninic acid potentiates multiple types of cancer cells to ABT-737-induced apoptosis by targeting Mcl-1 and Bad. *Apoptosis* **17,** 388–399 (2012).

141. Kassam, S. *et al.* Methylseleninic acid inhibits HDAC activity in diffuse large B-cell lymphoma cell lines. *Cancer Chemother. Pharmacol.* **68,** 815–821 (2011).

142. Sinha, I. *et al.* Methylseleninic acid downregulates hypoxia-inducible factor-1α in invasive prostate cancer. *Int. J. Cancer* **130,** 1430–1439 (2012).

143. Li, W. *et al.* Selenium Induces an Anti-tumor Effect Via Inhibiting Intratumoral Angiogenesis in a Mouse Model of Transplanted Canine Mammary Tumor Cells. *Biol. Trace Elem. Res.* **171,** 371–379 (2016).

144. Wu, X. *et al.* Methylseleninic acid restricts tumor growth in nude mice model of metastatic breast cancer probably via inhibiting angiopoietin-2. *BMC Cancer* **12,** 192–200 (2012).

145. Cai, Z. *et al.* Methylseleninic Acid Provided at Nutritional Selenium Levels Inhibits Angiogenesis by Down-regulating Integrin β3 Signaling. *Sci. Rep.* **7,** 9445 (2017).

146. Zeng, H., Briske-Anderson, M., Wu, M. & Moyer, M. P. Methylselenol, a selenium metabolite, plays common and different roles in cancerous colon HCT116 cell and noncancerous NCM460 colon cell proliferation. *Nutr. Cancer* **64,** 128–35 (2012).

147. Kim, A., Oh, J. H., Park, J. M. & Chung, A. S. Methylselenol generated from selenomethionine by methioninase downregulates integrin expression and induces caspase-mediated apoptosis of B16F10 melanoma cells. *J. Cell. Physiol.* **212,** 386–400 (2007).

148. Jiang, C., Wang, Z., Ganther, H. & Lu, J. Caspases as key executors of methyl selenium-induced apoptosis (anoikis) of DU-145 prostate cancer cells. *Cancer Res.* **61,** 3062–3070 (2001).

149. Kim. Long exposure of non-cytotoxic concentrations of methylselenol suppresses the invasive potential of B16F10 melanoma. *Oncol. Rep.* (1994). doi:10.3892/or_00000042

150. Zeng, H., Briske-Anderson, M., Idso, J. P. & Hunt, C. D. The selenium metabolite methylselenol inhibits the migration and invasion potential of HT1080 tumor cells. *J. Nutr.* **136,** 1528–32 (2006).

151. Jiang, C., Ganther, H. & Lu, J. Monomethyl selenium-specific inhibition of MMP-2 and VEGF expression: Implications for angiogenic switch regulation. *Mol. Carcinog.* **29,** 236–250 (2000).

152. Yan, L. & Combs, G. F. Consumption of a high-fat diet abrogates inhibitory effects of methylseleninic acid on spontaneous metastasis of Lewis lung carcinoma in mice. *Carcinogenesis* **35,** 2308–2313 (2014).

153. Lennicke, C. *et al.* Modulation of MHC class I surface expression in B16F10 melanoma cells by methylseleninic acid. *Oncoimmunology* **6,** e1259049 (2017).

154. Hagemann-Jensen, M. *et al.* The selenium metabolite methylselenol regulates the expression of ligands that trigger immune activation through the lymphocyte receptor NKG2D. *J. Biol. Chem.* **289,** 31576–31590 (2014).

155. Chen, Y.-C. *et al.* Selenium modifies the osteoblast inflammatory stress response to bone metastatic breast cancer. *Carcinogenesis* **30,** 1941–1948 (2009).

156. Zeng, H. & Wu, M. The Inhibitory Efficacy of Methylseleninic Acid Against Colon Cancer Xenografts in C57BL/6 Mice. *Nutr. Cancer* **67,** 831–838 (2015).

157. Hu, C. *et al.* Upregulation of KLF4 by methylseleninic acid in human esophageal squamous cell carcinoma cells: Modification of histone H3 acetylation through HAT/HDAC interplay. *Mol. Carcinog.* **54,** 1051–1059 (2015).

158. Tarrado-Castellarnau, M. *et al.* Methylseleninic acid promotes antitumour effects via nuclear FOXO3a translocation through Akt inhibition. *Pharmacol. Res.* **102,** 218–234 (2015).

159. Jüliger, S., Goenaga-Infante, H., Lister, T. A., Fitzgibbon, J. & Joel, S. P. Chemosensitization of B-Cell Lymphomas by Methylseleninic Acid Involves Nuclear Factor-κB Inhibition and the Rapid Generation of Other Selenium Species. *Cancer Res.* **67,** 10984–92 (2007).

160. Qi, Y. *et al.* Methylseleninic acid enhances paclitaxel efficacy for the treatment of triple-negative breast cancer. *PLoS One* **7,** e31539 (2012).

161. Hu, H. *et al.* Methylseleninic acid enhances taxane drug efficacy against human prostate cancer and down-regulates antiapoptotic proteins Bcl-XL and survivin. *Clin. Cancer Res.* **14,** 1150–1158 (2008).

162. Gonzalez-Moreno, O. *et al.* Methylseleninic acid enhances the effect of etoposide to inhibit prostate cancer growth in vivo. *Int. J. Cancer* **121,** 1197–1204 (2007).

163. Tzeng, T. J., Cao, L., Fu, Y., Zeng, H. & Cheng, W.-H. Methylseleninic Acid Sensitizes Notch3-Activated OVCA429 Ovarian Cancer Cells to Carboplatin. *PLoS One* **9,** e101664 (2014).

164. Zhang, Y. *et al.* Synergistic Induction of Apoptosis by Methylseleninic Acid and Cisplatin, The Role of ROS-ERK/AKT-p53 Pathway. *Mol. Pharm.* **11,** 1282–1293 (2014).

165. Kassam, S., Juliger, S., Jia, L. & Joel, S. P. Methylseleninic acid antagonizes the cytotoxic effect of bortezomib in mantle cell lymphoma cell lines through modulation of Bcl-2 family proteins. *Br. J. Haematol.* **156,** 286–289 (2012).

166. Saifo, M. S., Rempinski Jr, D. R., Rustum, Y. M. & Azrak, R. G. Targeting the oncogenic protein beta-catenin to enhance chemotherapy outcome against solid human cancers. doi:10.1186/1476-4598-9-310

167. Park, J.-M., Kim, D.-H., Na, H.-K. & Surh, Y.-J. Methylseleninic acid induces NAD(P)H:quinone oxidoreductase-1 expression through activation of NF-E2-related factor 2 in Chang liver cells. *Oncotarget* (2016). doi:10.18632/oncotarget.10289

168. Liu, M. *et al.* Methylseleninic acid activates Keap1/Nrf2 pathway via up-regulating miR-200a in human oesophageal squamous cell carcinoma cells. *Biosci. Rep* (2015). doi:10.1042/BSR20150092

169. Wang, L. *et al.* Methylseleninic Acid Superactivates p53- Senescence Cancer Progression Barrier in Prostate Lesions of Pten-Knockout Mouse. *Cancer Prev Res* **9,** 35–42 (2016).

170. Ibáñez, E. *et al.* Synthesis and antiproliferative activity of novel symmetrical alkylthio- and alkylseleno-imidocarbamates. *Eur. J. Med. Chem.* **46,** 265–274 (2011).

171. Moreno, E. *et al.* Sulfur and selenium derivatives of quinazoline and pyrido[2,3-d]pyrimidine: Synthesis and study of their potential cytotoxic activity in vitro. *Eur. J. Med. Chem.* **47,** 283–298 (2012).

172. Domínguez-Álvarez, E. *et al.* Synthesis and antiproliferative activity of novel selenoester derivatives. *Eur. J. Med. Chem.* **73,** 153–166 (2014).

173. Romano, B., Font, M., Encío, I., Palop, J. A. & Sanmartín, C. Synthesis and antiproliferative activity of novel methylselenocarbamates. *Eur. J. Med. Chem.* **83,** 674–684 (2014).

174. Romano, B., Plano, D., Encío, I., Palop, J. A. & Sanmartín, C. In vitro radical scavenging and cytotoxic activities of novel hybrid selenocarbamates. *Bioorganic Med. Chem.* **23,** 1716–1727 (2015).

175. Alcolea, V. *et al.* Chalcogen containing heterocyclic scaffolds: New hybrids with antitumoral activity. *Eur. J. Med. Chem.* **123,** 407–418 (2016).

176. Plano, D. *et al.* Synthesis and in vitro Anticancer Activities of some Selenadiazole Derivatives. *Arch. Pharm. (Weinheim).* **343,** 680–691 (2010).

177. Plano, D. *et al.* Novel potent organoselenium compounds as cytotoxic agents in prostate cancer cells. *Bioorganic Med. Chem. Lett.* **17,** 6853–6859 (2007).

178. Ibáñez, E. *et al.* The quinoline imidoselenocarbamate EI201 blocks the AKT/mTOR pathway and targets cancer stem cells leading to a strong antitumor activity. *Curr. Med. Chem.* **19,** 3031–3043 (2012).

179. Lamberto, I. *et al.* Bisacylimidoselenocarbamates cause G2/M arrest associated with the modulation of CDK1 and Chk2 in human breast cancer MCF-7 cells. *Curr. Med. Chem.* **20,** 1609–1619 (2013).

180. Zuazo, A. *et al.* Cytotoxic and proapototic activities of

imidoselenocarbamate derivatives are dependent on the release of methylselenol. *Chem. Res. Toxicol.* **25,** 2479–2489 (2012).

181. Fernandes, A. P. *et al.* Methylselenol Formed by Spontaneous Methylation of Selenide Is a Superior Selenium Substrate to the Thioredoxin and Glutaredoxin Systems. *PLoS One* **7,** e50727 (2012).

182. Wang, Z., Jiang, C. & Lü, J. Induction of caspase-mediated apoptosis and cell-cycle G1 arrest by selenium metabolite methylselenol. *Mol. Carcinog.* **34,** 113–120 (2002).

183. Longati, P. *et al.* 3D pancreatic carcinoma spheroids induce a matrix-rich, chemoresistant phenotype offering a better model for drug testing. *BMC Cancer* **13,** 95 (2013).

184. Reymond, N. *et al.* Cdc42 promotes transendothelial migration of cancer cells through β1 integrin. *J. Cell Biol.* **199,** 653–68 (2012).

185. Asnaghi, L. *et al.* E-cadherin negatively regulates neoplastic growth in non-small cell lung cancer: Role of Rho GTPases. *Oncogene* **29,** 2760–2771 (2010).

186. Durgan, J. *et al.* Mitosis can drive cell cannibalism through entosis. *Elife* **6,** 1–26 (2017).

187. Ishikawa, F., Ushida, K., Mori, K. & Shibanuma, M. Loss of anchorage primarily induces non-apoptotic cell death in a human mammary epithelial cell line under atypical focal adhesion kinase signaling. *Cell Death Dis.* **6,** e1619 (2015).

188. Khalkhali-Ellis, Z., Goossens, W., Margaryan, N. V. & Hendrix, M. J. C. Cleavage of histone 3 by cathepsin D in the involuting mammary gland. *PLoS One* **9,** 1–9 (2014).

189. Repnik, U., Stoka, V., Turk, V. & Turk, B. Lysosomes and lysosomal cathepsins in cell death. *Biochim. Biophys. Acta - Proteins Proteomics* **1824,** 22–33 (2012).

190. Shin, I. Y. *et al.* The Expression of Multiple Proteins as Prognostic Factors in Colorectal Cancer: Cathepsin D, p53, COX-2, Epidermal Growth Factor Receptor, C-erbB-2, and Ki-67. *Gut Liver* **8,** 13–23 (2014).

191. Fairweather-Tait, S. J. *et al.* Selenium in Human Health and Disease. *Antioxid. Redox Signal.* **14,** 1337–1383 (2011).

192. Vinceti, M., Crespi, C. M., Malagoli, C., Del Giovane, C. & Krogh, V. Friend or foe? The current epidemiologic evidence on selenium and human cancer risk. *J. Environ. Sci. Heal. - Part C Environ. Carcinog. Ecotoxicol. Rev.* **31,** 305–341 (2013).

APPENDIX

SYNTHESIZED COMPOUNDS

SERIES I: Methylselenoesters

Reference	Name	Structure
1	*Methyl 4-nitrobenzoselenoate*	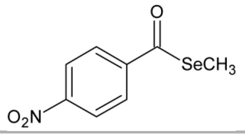
2	*Methyl 4-methoxybenzoselenoate*	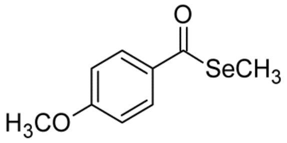
3	*Methyl pyrazinecarboselenoate*	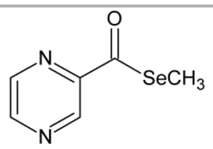
4	*Methyl 2-thiophencarboselenoate*	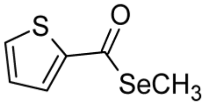
5 (1)*	*Methyl 3-chlorothiophen-2-carboselenoate*	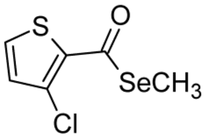
6	*Methyl 5-isoxazolecarboselenoate*	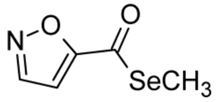
7	*Methyl benzo[b]thiophene-2-carboselenoate*	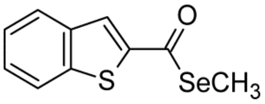
8	*Methyl 1,3-benzodioxole-5-carboselenoate*	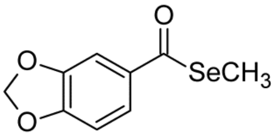
9	*Methyl 3-quinolinecarboselenoate*	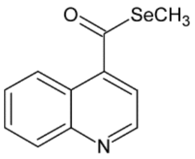
10	*Methyl 2-phenyl-4-quinolinecarboselenoate*	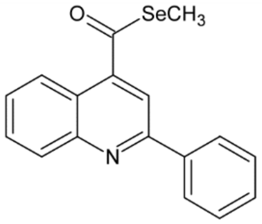

11	*Methyl 6-bromochromone-2-carboselenoate*	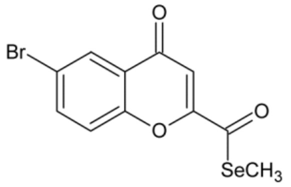
12	*Methyl 2-(4-pyridyl)thiazole-4-carboselenoate*	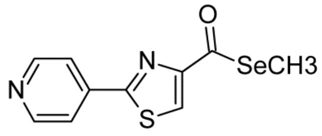
13	*Methyl 9-acridinecarboselenoate*	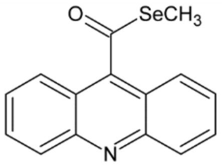
14	*Dimethyl 5-cyano-1,3-benzenedicarboselenoate*	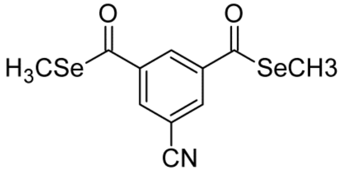
15 (2)*	*Dimethyl 2,5-furandicarboselenoate*	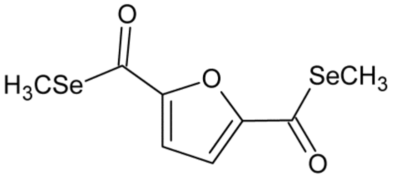

*The number in parentheses indicates the reference used in Paper 2.

SERIES II: Other selenoesters

Reference	Name	Structure
1a	*Ethyl 3-chlorothiophen-2-carboselenoate*	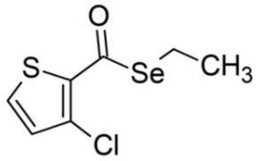
1b	*Pentyl 3-chlorothiophen-2-carboselenoate*	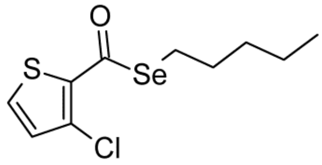
2a	*Diethyl 2,5-furandicarboselenoate*	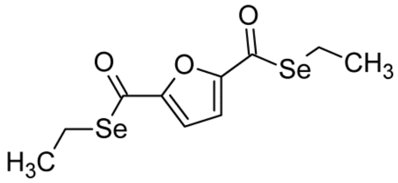

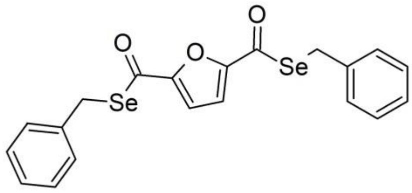2c	*Dibenzyl 2,5-furandicarboselenoate*